Acta Morphologica et Anthropologica 30 (3–4)

Prof. Marin Drinov Publishing House
of Bulgarian Academy of Sciences

Acta Morphologica et Anthropologica
is the continuation of Acta cytobiologica et morphologica

Indexed in:

BIOSIS databases
Life sciences and biomedical literature on Web of Science

WEB OF SCIENCE

WorldCat®

NCBI
NLM Catalog

ISSN INTERNATIONAL STANDARD SERIAL NUMBER INTERNATIONAL CENTRE

ZDB ZEITSCHRIFTEN DATENBANK

Editorial Correspondence

Institute of Experimental Morphology, Pathology and Anthropology with Museum
Bulgarian Academy of Sciences
Acta Morphologica et Anthropologica
Acad. Georgi Bonchev Str., Bl. 25
1113 Sofia, Bulgaria

E-mail: ama.journal@iempam.bas.bg; yordanka.gluhcheva@iempam.bas.bg;
ygluhcheva@hotmail.com

Tel.: +359 2 979 2344

Издаването на настоящия том 30, книжки 3 и 4 е осъществено с финансовата подкрепа на Фонд „Научни изследвания“

Prof. Marin Drinov Publishing House of Bulgarian Academy of Sciences
Bulgaria, 1113 Sofia, Acad. Georgi Bonchev Str., Bl. 6

Graphic designer Veronika Tomcheva.

Format 70×100/16 Printed sheets 11,50

Printing Office of Prof. Marin Drinov Publishing House of Bulgarian Academy of Sciences
Bulgaria, 1113 Sofia, Acad. Georgi Bonchev Str., Bl. 5

Acta Morphologica et Anthropologica

ISSN 1311-8773 (print)
ISSN 2535-0811 (online)

Acta Morphologica et Anthropologica

30
(3-4)

30 (3-4) ● Sofia ● 2023
Institute of Experimental Morphology, Pathology and Anthropology with Museum
Bulgarian Anatomical Society

Contents

MORPHOLOGY 30 (3)

Original Articles

Original Articles

Review Articles

Institute of Experimental Morphology, Pathology and Anthropology with Museum
Bulgarian Anatomical Society

Acta Morphologica et Anthropologica, 30 (3-4)
Sofia ● 2023

MORPHOLOGY 30 (3)

Original Articles

Evaluation of Different Staining Methods and Image Analyses of the Results from a Comet Assay in Human Colorectal Cancer Cells Treated with Hydrogen Peroxide

Inna Sulikovska[1], Vera Djeliova[2], Ludmil Kirazov[1], Ivaylo Ivanov[3], Mashenka Dimitrova[1]*

[1] *Institute of Experimental Morphology, Pathology and Anthropology with Museum, Bulgarian Academy of Sciences, Sofia, Bulgaria*
[2] *Institute* of *Molecular Biology "Acad. R. Tsanev", Bulgarian Academy* of *Sciences, Sofia, Bulgaria*
[3] *Department of Bioorganic Chemistry and Biochemistry, Medical University, of Sofia, Bulgaria*

*Corresponding author e-mail: inna_sulikovska@ukr.net

In the present study we applied comet assay to cultured *in vitro* human colorectal carcinoma cell line HT-29 in order to optimize the approach for staining and analysis of the comets after treatment with hydrogen peroxide as a DNA damaging agent. Two staining methods (fluorescent – ethidium bromide and non-fluorescent – silver staining) as well as two types of software for the analysis were evaluated. Additionally, the comets were scored visually after both types of staining. In general, we concluded that the silver staining can replace the ethidium bromide fluorescent dye, which is toxic and requires special equipment for the examination.

Key words: comet assay, ethidium bromide, silver staining, HT29 cells, DNA damage

Introduction

Oxidative DNA damage has been widely recognized as a major risk for developing deferent diseases. Hydrogen peroxide (H_2O_2) is known to produce reactive oxygen species (ROS) which are responsible for oxidative DNA lesions in animal models [1], resulting in induction and progress of neoplasms [10]. The DNA damage induced by H_2O_2 is presented by both DNA strand breaks (SBs) and alkali labile sites (ALS) which intensity is clearly dose-dependent [15]. It has been shown that under alkaline conditions, DNA loops containing breaks lose supercoiling, unwind, and are released from the nucleus to form a "comet tail" after gel electrophoresis. By applying a DNA dye, DNA SBs can be visualized and quantified by computer analysis or by visual grading [13]. Ethidium bromide (EtBr) is commonly used as a fluorescent intercalating dye that binds more efficiently to double-stranded DNA than to single stranded DNA [4]. Another possibility is the silver staining of comets. The comet assay can detect thousands lesions per cell. However, the actual percentage of tail DNA depends on the assay conditions [5]. Additionally, the methods of comet analyses can also influence the results.

The main problem in all genotoxic assays is cell death since it is also associated with degradation of DNA and so, adds to the DNA damage caused directly by the genotoxic exposure. Thus, the genotoxic agent dose should be adapted to the level of its cytotoxicity. Thresholds of cytotoxicity and cell death for comet assay reported in the literature are usually between 20% and 30%. However, the practice shows that the effect of cytotoxicity on comet assay endpoints should be assessed by a case-by-case approach rather than by adopting a predetermined threshold. Another potential source of error is the attribution of a particular tail shape to apoptosis or necrosis. For example, it has been previously accepted that the so-called "hedgehog" comets represent apoptotic cells [4]. Recently, a number of objections to this assumption are indicated [5].

There are numerous software packages to choose from, that can compute fluorescence parameters for comets selected by the operator. The most commonly used parameters are tail length, relative fluorescence intensity of head, percentage of DNA in tail and tail moment [4]. Analysis of at least 50 comets per slide has been recommended. The percentage of DNA in the comet tail represents the frequency of DNA SBs and is measured by image analysis. It is also possible to compute DNA damage from comets without sophisticated image analysis programs. The human eye is easily trained to discriminate degrees of damage according to comet appearance. The 5 classes, from 0 (no tail) to 4 (almost all DNA in tail) give sufficient resolution. If 100 comets are scored, and each comet assigned a value of 0 to 4 according to its class, the total score for the sample gel will be between 0 and 400 "arbitrary units." Visual scoring is rapid as well as simple and should appeal to scientists exploring the usefulness of the technique without wanting to invest in expensive analytical equipment [4].

Image analysis from comet assays represents a significant challenge to researchers. A number of authors have compared different comet staining techniques and image analysis software to find the most optimal option for their model systems [see e.g 3, 6, 7, 9, 11].

The aim of the present study is to specify the most convenient methods for staining and analyzing the comets obtained in human colorectal carcinoma cell line HT-29 cells after the application of H_2O_2 as an inducer of oxidative DNA damage.

Materials and Methods

Hydrogen peroxide H_2O_2 (30% w/w solution in water), was purchased from Sigma-Aldrich (Merck KGaA, Darmstadt, Germany) and diluted in phosphate-buffered saline (PBS, pH=7) immediately before use.

Cell culture. The HT-29 cells (human colorectal carcinoma) (ATCC, Manassas, Virginia, USA)) were cultured in Dulbecco's Modified Eagle's medium – high glucose (DMEM 4,5 g/l glucose), supplied with 10% fetal bovine serum and antibiotics in usual concentrations in a humidified atmosphere with 5% CO_2 at 37.5ºC until 90% confluence. The cells were routinely grown as monolayers in 25 cm^2 tissue culture flasks (Biologix™). Cells were detached by trypsinization (Trypsin-0.25 % EDTA).

H_2O_2 treatment. The cells were treated directly on the prepared agarose slides with encapsulated cells with 70 µl 150 µM H_2O_2 applied for 3 minutes in the dark at 4ºC by coverslips. The coverslips were removed carefully and the slides were immersed in standard lysis solution for at least 1 h in a Coplin jar at 4°C in dark.

Alkaline Comet Assay. This was performed according to a previously described procedure [5]. The slides were immersed briefly in 1% (wt/vol) LMP (low melting point) agarose, their backs were wiped and they were left on a plate overnight at room temperature (RT). The cell suspensions were counted using an automatic cell counter (Countess®, Invitrogen) and centrifuged at ~150–300g for 5 min at 4°C, washed with ice-cold PBS (phosphate buffered saline), and centrifuged again. The 45 µl of the cell suspension in PBS (~1×10^6cells/ml) were mixed with 105 µl 0.7% LMP agarose. Two drops (40–75µl) of the mixture were transferred to pre-coated microscope slides. The gels were covered with coverslips and kept for 5 min at 4°C in dark. The coverslips were then removed and the slides were placed in standard lysis solution (89 ml lysis stock solution: 2.5M NaCl, 100mM EDTA, 10mM Tris base, pH 10-10.5, freshly added 10 ml DMSO and 1 ml Triton X-100) for at least 1 h in a Coplin jar at 4°C in dark. The slides were transferred directly to the electrophoresis tank containing cold (4°C) solution (0.3M NaOH and 1mM Na_2EDTA, pH>13) and incubated in electrophoresis solution for 20–40 min avoiding direct light. Electrophoresis was performed at 25V (~1 V/cm) for 30 min, pH>13 at 4 °C.

The gels were neutralized by washing in cold neutralizing solution (400 mM Tris–HCl, pH 7.5) three times for 5 min. Slides were washed for 10 min in cold (4°C)

dH_2O. The gels were air-dried overnight. All steps were performed avoiding direct light.

Fluorescence staining. For staining with EtBr, 10 µg/mL aqueous solutions were added to 20–40 µL staining solution and applied to each gel. The excess EtBr was washed out by immersing the slides in 0.4 M Tris/HCl, pH 7.5 before covering them with coverslips. Stained gels can be stored overnight in the dark at RT and hydrated before scoring with 20 µL dH_2O. Comets were studied under a fluorescence microscope Leica DM 5000B (Leica microscope, Wetzlar, Germany) using appropriate filters.

Silver staining. The silver staining was performed according to the procedure [12]. The gels were fixed for 10 min in a fixing solution, containing 15% w/v trichloroacetic acid, 5% w/v zinc sulfate, and 5% glycerol. After fixation, the slides were washed three times in deionized water and dried for approximately 5 h at RT. Before silver staining, the gels were re-hydrated for 5 min in deionized water. The staining solution was prepared just before use as follows: 34 ml of the solution B (0.2% w/v ammonium nitrate, 0.2% w/v silver nitrate, 0.5% w/v tungstosilicic acid, 0.15% v/v formaldehyde) were added to 66 ml of the solution A (5% sodium carbonate). The slides were immersed for 20 – 30 min, 37°C (approximately the time required to obtain a light gray color) and placed in a shaker in small glass boxes covered with aluminum foil. After staining, the slides were washed in deionized water. The staining was stopped by immersing the slides for 5 min in 1% acetic acid solution, followed by two washes in deionized water, and were air-dried. All the glass materials used for the silver staining were pretreated with 50% nitric acid and then washed with detergents and several times with deionized water. The slides were observed and photographed using a microscope Leica DM 5000B (Leica microscope, Wetzlar, Germany).

Classification and measurement of comet parameters. For the measurement of fluorescently stained comets' parameters, the free Internet software OpenComet was used [7]. Counting of comets was done automatically. The analysis of the results was made according to the values proposed by Norozi et al. [13]. The OpenComet program allows analysis of a large number of comets, but the results were equalized to 100.

For the measurement of silver stained comets' parameters the free Internet software CaspLab was used. The comets were marked manually. For protocol validated by the parameter '% DNA in tail' in silver stained comets, we used the classification proposed by Norozi et al. [13]: 0 class (no damage) – 1-5%; 1 class (low damage) – 5–25%; 2 class (medium damage) – >25–45%; 3 class (high damage) – >45–70%; 4 class (very high damage) – >70%.

About 100 cells were evaluated per sample in visual scoring. In this system, comets are visually classified in 5 categories according to the intensity of the comet tail and head. Each comet was given a value between 0 and 4; 0 for undamaged comets and 4 for the comets with almost all DNA in their tails. DNA damage index was calculated using the following equation:

DNA damage index = 0x(n) +1x(n) +2x(n) +3x(n) +4x(n)

n = number of cells in each category

Consequently, the total score was in the range from 0 to 400 arbitrary units [2].

Statistical analysis of the results. Data were analyzed using One-way ANOVA followed by Bonferroni's post hoc test; $p < 0.05$ was accepted as the lowest level of statistical significance. The distribution of the result was checked for normality utilizing Kolmogorov-Smirnov test (GraphPad Prism software package). The data obtained were average from three independent experiments ± SD.

Results and Discussion

Presently, comet assay is widely used to evaluate the DNA damage after application of a genotoxic agent to cell cultures. It has been shown that the test can detect between ~50 and ~10,000 lesions per cell. However, the results depend substantially on the assay conditions and the method chosen for analyzing the comets. Recently, we obtained a pronounced cytotoxicity in HT-29 human tumor cell line after application of extracts from different medicinal plants endemic for our country [8, 14]. Before analyzing the possible genotoxicity of those extracts, we had to standardize the comet assay for this type of cells. For the purpose, we performed the comet assay of HT-29 cells after application of a known agent inducing oxidative DNA damage, i.e. the hydrogen peroxide. Since it was essential to apply a sub-cytotoxic concentration of H_2O_2, we used a previously recommended method for the agent application [5, 7]. We tested two types of staining – a fluorescent with EtBr and a non-fluorescent with silver nitrate. Additionally, we applied three types of analyzers – OpenComet for EtBr staining, Casplab for silver staining and also the visual analyses.

Microphotographs of EtBr and silver stained DNA of HT-29 cells for alkaline Comet assay are presented on **Fig. 1**.

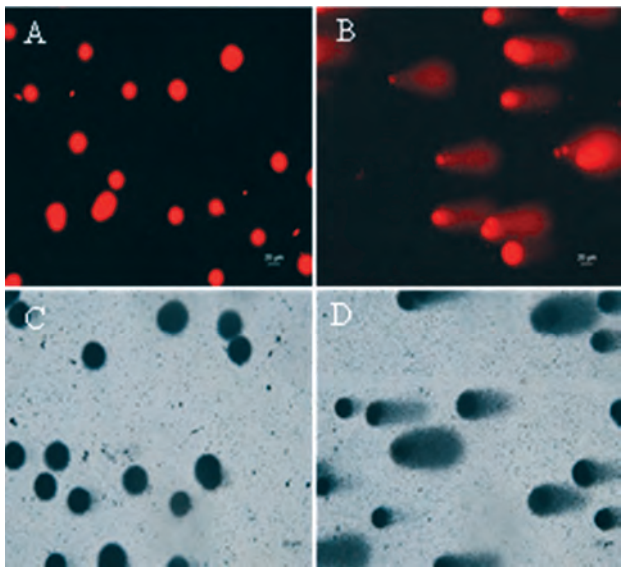

Fig. 1. Microphotographs of the stained DNA comets of HT-29 cells for alkaline Comet assay: A, B – EtBr stained non-treated cells (A) and cells treated with H_2O_2 (B); C, D – Silver stained non-treated cells (C) and cells treated with H_2O_2 (D). × 400

Typical images of the five types of comet categories obtained with the two types of staining are shown in the **Fig. 2**.

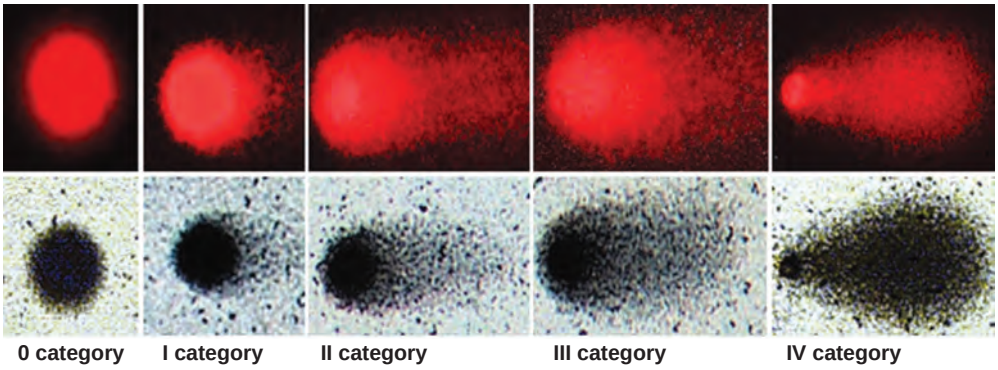

Fig. 2. Classification of the comets. Comet categories are defined by the size of the head (nucleus) and the length and intensity of the tail. 0 category – no DNA damage, I category – low DNA damage, II category – medium damage, III category – high damage, IV category – very high damage. EtBr-stained comets are represented in the top panels and silver-stained in the bottom panels.

The results obtained for DNA damage index are shown in **Fig. 3**. Data are presented as the number of cells counted in a given category/class during the visual assessment and software analysis in the range from 0 to 400 arbitrary units. In the analysis with the programs OpenComet and CaspLab, categorization of comets is

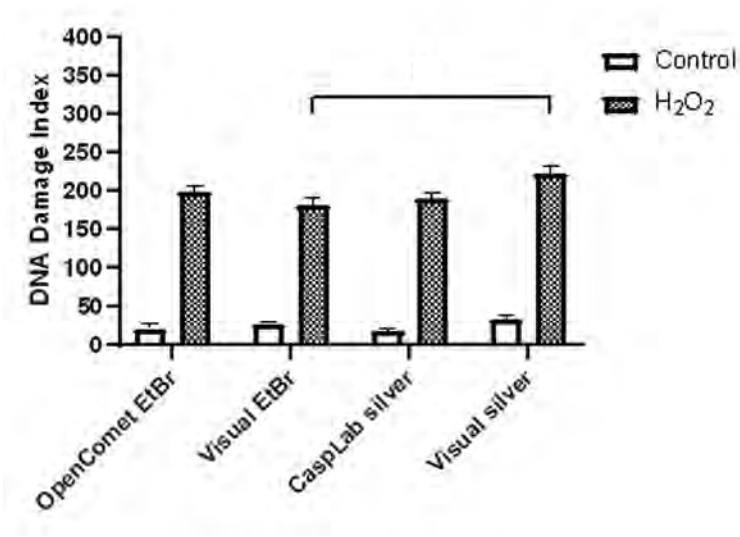

Fig. 3. Relations between the subjective visual scoring and percentage of DNA in the tail by two image analysis – CaspLab and OpenComet and the visual scoring. Each point represents the mean (± SD) of three independent counts of 100 comets.

used according to the values obtained as ‚% DNA in tail' according to the scale in [13] and calculations by the equation above [2] as explained in "Materials and methods". Statistical examination of the results are given in the figure to show that only the visual count of comets obtained after EtBr staining and the visual count of comets obtained after silver staining have a statistically significant difference (*).

The results of percentage of DNA in tail for different categories of comets are presented in **Table 1**. The obtained mean values and their deviations for each class of comets after analysis with the respective programs are presented. The table gives information about the distribution of cells in the corresponding category as a level of DNA damage.

Table 1. Percentage of DNA in tail for different categories of comets

Category	Range	OpenComet – EtBr staining		Casplab – Silver staining	
		Control	H_2O_2	Control	H_2O_2
0	<5%	2.03±1.1	3.5±1.4	0.5±0.9	0.5±0.3
I	5-25%	6.4±1.7	13.3±5.8	9.6±3.9	20.3±4.1
II	25-45%	0	35.2±6.3	0	34.9±5.1
III	45-70%	47.4±3.8	56.5±7.4	0	48.2±2.1
IV	>70%	0	85.4±8.3	0	0

The OpenComet program [7] has been developed only for the analysis of fluorescently stained comets. According to our results, it recognized perfectly the class IV (very high DNA damage) comets (**Table 1**) in this type of H_2O_2-induced DNA damage of HT-29 cells. It also classified well the comets between class III and class IV.

The CaspLab software analysis [9] performed significantly better for silver staining. The CaspLab software, compared to the other two types of analysis, has difficulty in the measuring of class IV comets (hedgehog comets – very high DNA damage) (**Table 1**) in this type of DNA damage (H_2O_2) and therefore, the results were underestimated. The program classifies comets between class II and class III very well (**Table 1**).

Visual counting is fully accepted by all researchers as one of the most accurate analyzers [4]. In the visual counting of the silver-stained preparations, the greatest degree of presence of DNA damage was obtained. This can be explained by the fact that in this type of analysis comets of type IV (very high DNA damage) are easy to classify since they have a large tail almost without a head (**Fig. 2**). However, in visual counting, the classification of comets between II and III degrees is the most subjective.

By visual counting, it is possible to make a very quick assessment of comet classes and calculate the DNA damage Index, but no more accurate data can be given regarding more detailed parameters of comet types such as: HeadArea, TailArea, HeadDNA, TailDNA, HeadDNA%, TailDNA%, HeadRadius, TailLength, CometLength, HeadMeanX, TailMeanX, TailMoment and OliveTailMoment.

A comparison between the two types of staining of preparations used in our experiments is given in **Table 2**.

Table 2. Comparison of the two staining methods: advantages and disadvantages

Staining method	Advantages	Disadvantages
EtBr Staining	Relatively fast staining, after staining with EtBr a silver staining can also be made	Toxic, requires special equipment - florescence microscope, non-permanent staining, must be analyzed within 24 hours
Silver staining	Non-toxic and requires a light microscope for analysis, permanent preparations, stained slides can be stored for years	Multi-step, slower, strong background is possible, after this staining other stainings cannot be performed

Our results for colon cancer HT-29 cells correlate well with those obtained with similar staining comparisons and assay approaches in the comet assay in previous studies with other cell types, different conditions and other agents inducing DNA damage [3, 6, 11], as well as with the same agent used by us – H_2O_2 [7, 13].

Conclusions

It can be concluded that for the analysis of DNA damage in HT-29 cells by the comet assay, both stains of the slides could be used. We can perform a faster analysis after the fluorescence staining with OpenComet, and then the same slides can be stained with silver and analyzed with the CaspLab software or by visual counting. In general, we concluded that the silver staining can replace the ethidium bromide staining, which is toxic and requires special equipment for the examination.

Acknowledgement: This work is financially supported by the National Science Fund of the Bulgarian Ministry of Education and Science, Grant Nr KP-06-N31/1.

References

1. Andreoli, C., P. Leopardi, S. Rossi, R. Crebelli. Processing of DNA damage induced by hydrogen peroxide and methyl methane sulfonate in human lymphocytes: analysis by alkaline single gel electrophoresis and cytogenetic methods. – *Mutagenesis*, **14**, 1999, 497-503.

2. Azqueta, A., S. A. S. Langie, E. Boutet-Robinet, S. Duthie, C. Ladeira, P. Møller, A. R. Collins, R. W. L. Godschalk. DNA repair as a human biomonitoring tool: Comet assay approaches. – *Mutat. Res. Rev. Mutat. Res*, **781**, 2019, 71-87.

3. Christofoletti, C. A., J. A. David, C. S. Fontanetti. Application of the comet assay in erythrocytes of Oreochromis niloticus (Pisces): A methodological comparison. – *Genet. Mol. Biol.*, **32(1)**, 2009, 155-158.
4. Collins, A. R. The comet assay for DNA damage and repair. – *Mol. Biotechnol*., **26**, 2004, 249-261.
5. Collins A., P. Møller, G. Gajski, S. Vodenková, A. Abdulwahed, et al. Measuring DNA modifications with the comet assay: a compendium of protocols. – *Nat. Protoc.*, **18(3)**, 2023, 929-989.
6. Garcia O., I. Romero, J. E. González, T. Mandina. Measurements of DNA damage on silver stained comets using free Internet software. – *Mutation Research/Genetic Toxicology and Environmental Mutagenesis*, **627(2)**, 2007, 186-190.
7. Gyori, B. M., G. Venkatachalam, P. S. Thiagarajan, D. Hsu, M.-V. Clement. OpenComet: An automated tool for comet assay image analysis. – *Redox Biology*, **2**, 2014, 457-465.
8. Iliev, I., I. Ivanov, K. Todorova, D. Tasheva, M. Dimitrova. *Cotinus coggygria* non-volatile fraction affects the survival of human cultured cells. – *Acta Morphol. Anthropol*., **28(1-2)**, 2021, 19-27.
9. Konca, K., A. Lankoff, A. Banasik, H. Lisowska, T. Kuszewski, et al. A cross platform public domain PC image-analysis program for the comet assay. – *Mutat. Res.*, **534**, 2003, 15-20.
10. Kumar, N., A. Yadav, R. Gupta, N. Aggarwal. Antigenotoxic effect of *Withania somnifera* (Ashwagandha) extract against DNA damage induced by hydrogen peroxide in cultured human peripheral blood lymphocytes. – *Int. J. Curr. Microbiol. Appl. Sci.*, **5(4)**, 2016, 713-719.
11. Kyoya, T., R. Iwamoto, Y. Shimanura, M.i Terada, S. Masuda. The effect of different methods and image analyzers on the results of the in vivo comet assay. – *Genes and Environ*ment, **40**, 2018, Article Number 4.
12. Nadin, S. B., L. M. Vargas-Roig, D. R. Ciocca. A silver staining method for single-cell gel assay. – *J. Histochem Cytochem.*, **49(9),** 2001 1183-1186.
13. Noroozi, M., W. J. Angerson, M .E. J. Lean. Effects of flavonoids and Vitamin C on oxidative DNA damage to human lymphocytes. – *Am. J. Clin. Nutr.*, **67**, 1998, 1210-1218.
14. Sulikovska, I., E. Ivanova, I. Ivanov, D. Tasheva, M. Dimitrova, B. Nikolova, I. Iliev. Study on the phototoxicity and antitumor activity of plant extracts from *Tanacetum vulgare* L., *Epilobium parviflorum* Schreb., and *Geranium sanguineum* L. – *Int. J. BIOautomation*, **27(1)**, 2023, 39-50.
15. Valverde, M., J. Lozano-Salgado, P. Fortini, M.-A. Rodriguez-Sastre, E. Rojas, E. Dogliotti. Hydrogen peroxide-induced DNA damage repair through the differentiation of human adipose-derived mesenchymal stem cells. – *Stem Cells International*, **2018**, 2018, Article ID 1615497.

Institute of Experimental Morphology, Pathology and Anthropology with Museum
Bulgarian Anatomical Society

Acta Morphologica et Anthropologica, 30 (3-4)
Sofia ● 2023

Comparison between Whole-Mount Preparations and Paraffin-Embedded Sections in the Study of the Myenteric Plexus

Nikolay Genov[1], Nikola Tomov[2], Nikolay Dimitrov[1], Nikolai Lazarov[3,4], Dimitrinka Atanasova[1,3]*

[1] *Department of Anatomy, Faculty of Medicine, Trakia University, Stara Zagora, Bulgaria*
[2] *Institute of Anatomy, University of Bern, Bern, Switzerland*
[3] *Institute of Neurobiology, Bulgarian Academy of Sciences, Sofia, Bulgaria*
[4] *Department of Anatomy and Histology, Medical University of Sofia, Sofia, Bulgaria*

**Corresponding author e-mail: nikolay.genov@trakia-uni.bg*

The present study aimes to compare the whole-mount preparation of the colorectal region with the paraffin-embedded sections of the same area for histology studies. It focuses on analyzing the sectional area of myenteric ganglia and the sectional area of neuronal perikarya in the colorectal region of the rat. 82% of the ganglia obtained by cross-sectional cut had sectional area sizes ranging from 500 μm^2 to 4500 μm^2. Conversely, 72% of the ganglia observed by tangential cut ranged from 4500 μm^2 to 10500 μm^2. In whole-mount prepared slides, 40% of them were in the range of 10500 μm^2 to 20500 μm^2 while 80% of perikarya in the cross-sectional cut paraffin-embedded slides had a sectional area within 50 μm^2 to 150 μm^2. In tangential cut, 70% of the neuronal bodies had similar sectional sizes. Neuronal somata ranging from 200 μm^2 to 450 μm^2 were observed more frequently (57%) in whole-mount preparations.

Key words: morphometry, colon, rectum, myenteric plexus, myenteric ganglion

Introduction

The enteric nervous system is composed of a considerable number of cells which provide the independent innervation of the gastrointestinal (GI) tract, including smooth muscles of its wall, the epithelial tissues, blood vessels and endocrine cells associated with it [2, 5]. Enteric neurons are arranged in interconnected ganglia, thus forming a complex meshwork described as a polysynaptic circuit [10]. According to

current knowledge, the total number of enteric neurons is around 500 million, that is almost equal to the number of neurons in the spinal cord [2]. The ganglia between the longitudinal and circular muscle layers form the myenteric plexus. Enteric neurons and closely associated glial cells are compressed between muscle layers which can change their dimensions when observed by the longitudinal or the transverse axis [3].

The overall shape of the myenteric plexus is three-dimensional, which makes standard methods such as cryosections and paraffin-embedded sections not suitable for examination of the whole nerve plexus because only a fraction of it could be observed [5, 6]. Due to its specific shape, the usage of cross-sectional cut compared with tangential sectioning could bring a much more comprehensive information about the size of neuronal perikarya in the myenteric plexus [3].

On the other hand, whole-mount (WM) preparations have been used by many authors to provide a three-dimensional view of the meshwork of enteric ganglia and to give a much better ability for examination of the myenteric plexus and evaluation of the maximal size of the neuronal soma [2, 3, 6, 7, 9].

The present study aimed to measure the cross-sectional area of myenteric ganglia and the cross-sectional area of neuronal perikarya obtained by paraffin-embedded tissue (PET) at the light microscope level, and the subsequent cutting of cross-sectional (CS) and tangential sections (TS) and to compare them with whole-mounted preparations.

Material and Methods

The study was performed on six adult (18-month-old) male Wistar rats with an average weight 350-400 g. The animals have been delivered from the vivarium of the Faculty of Medicine at Trakia University-Stara Zagora. The housing of the animals has been conducted under an artificial 12-h light/dark cycle and at a temperature of 22 °C. Water and food pellets have been given *ad libitum*. The experimental procedure was approved by the Commission for Ethical Treatment of Animals at the Bulgarian Food Safety Agency and all experiments were carried out in full agreement with the Directive 2010/63/EU on the protection of animals used for scientific purposes. For the morphometric analyses, all rats were anaesthetized with 87 mg ketamine/kg of body weight and 13 mg xylazine/kg after simultaneous intraperitoneal injection and then transcardially perfused first with cold 0.05 M phosphate-buffered saline (PBS) and after that with cold 4% paraformaldehyde (PFA) in 0.1 M phosphate buffer (PB), pH 7.36. Three tissue segments were collected from the proximal colon, distal colon, and rectum. For the PET (CS) and the PET (TS) sections the tissue samples were postfixed in the same fixative for 24 h and subsequently washed first in tap water, followed by distilled water, dehydrated, and embedded in paraffin. Paraffin blocks were cut into 6 μm tissue sections and mounted on chrome-gelatinized glass slides and then processed for hematoxylin and eosin staining.

We used colonic tissue fixed with 4% PFA in 0.1M PB for the whole-mount preparations. It was dissected into the following segments: caecum, proximal colon,

distal colon, and rectum. Each of the samples was cut into separate pieces with a length of roughly 2 cm. During the whole mount preparation, the samples were held in cold PBS. The separation of the myenteric plexus from the mucosa and the circular muscle layer was done under a stereoscopic microscope (ZEISS OPTON 47 50 57) with microdissection tools. A research microscope Leica DM1000 equipped with a digital camera Leica DFC 290 was used to obtain images of objects in the slides. All images were processed with Adobe Photoshop CC software.

The graphic analysis, as well as the measurement of the sectional area of the myenteric ganglia and neurons, were performed with the software ImageJ (National Institutes of Health, Bethesda, MD, USA). Statistical analysis was performed by GraphPad Prism®6 software (San Diego, CA, USA) and Kruskal-Wallis One Way Analysis of Variance by Ranks test. Statistically significant differences were considered if *p*-values were <0.05.

Results

In this study, we have measured the sectional area of the ganglia and the neuronal perikarya in the myenteric plexus located at the colorectal region. The sections used in the measuring were from PET (CS), PET (TS) and whole-mount preparations (**Fig. 1**). The examined segments were collected from the proximal colon, distal colon and rectum and routinely stained with the haematoxylin and eosin staining technique. This staining method allowed us to observe in detail the ganglia and the perikarya from the myenteric plexus by fully delineating it from the nearby structures thus permitting us to measure it more precisely. For statistical purposes, we performed the non-parametric Kruskal–Wallis test to study the sectional area of the myenteric ganglia and the perikarya in cross-sectional, tangential and whole-mount preparations.

The measurements of the sectional area of the myenteric ganglia showed statically significant differences in the three examined methods proven by the non-

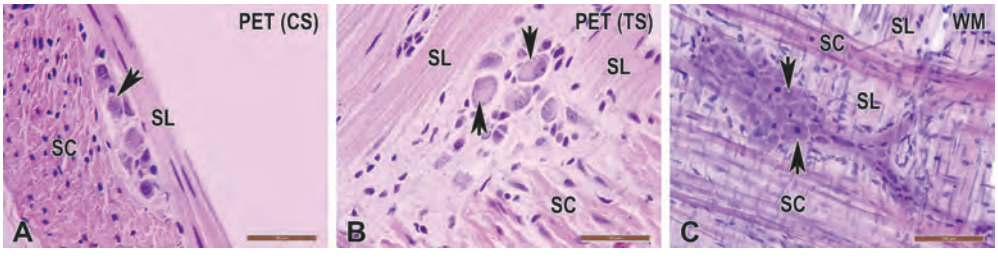

Fig. 1. Hematoxylin and eosin-stained sections visualizing the myenteric ganglia and the neuronal perikarya obtained by paraffin-embedded tissue (PET) and the subsequent cutting of cross-sectional (CS) **(A)** and tangential sections (TS) **(B)** and whole-mounted preparation **(C)**. Arrows point out neurons. SC, stratum cyrculare; SL, stratum longitudinale. Scale bars: 50 µm.

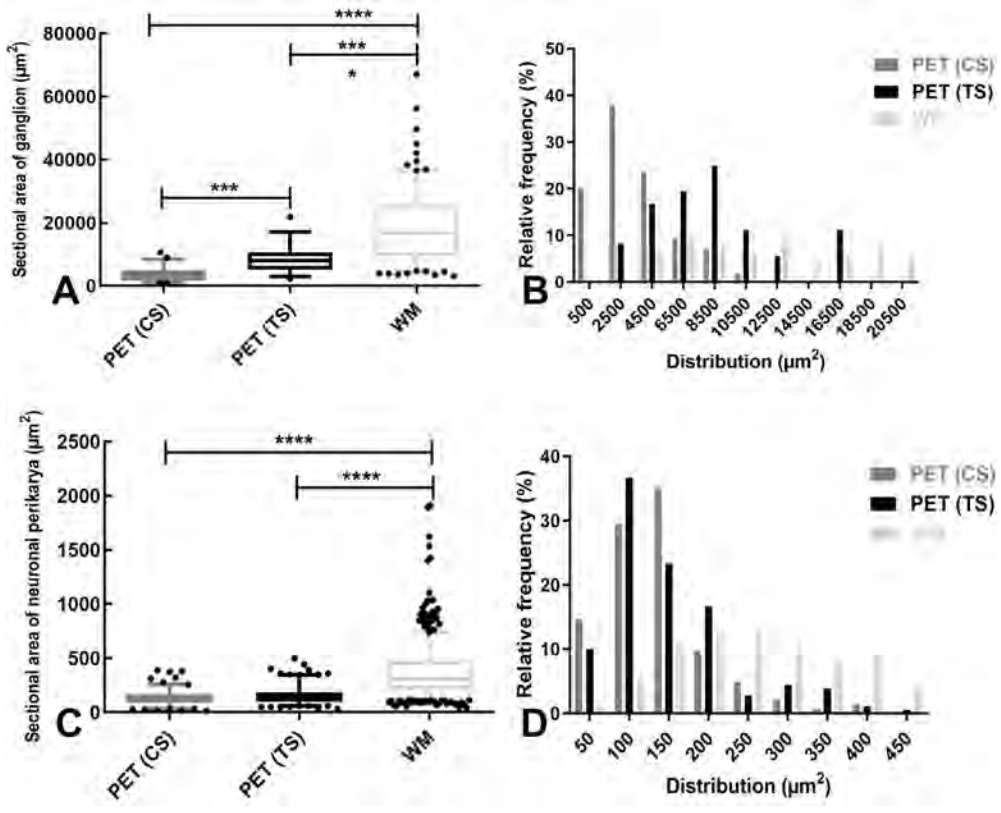

Fig. 2. Box plot diagrams showing statistical comparison of the sectional area of ganglia **(A)** and the sectional area of neuronal perikarya **(C)** in paraffin-embedded tissue (PET) and the subsequent cutting of cross-sectional PET (CS), tangential section PET (TS) and whole-mount (WM) preparations from the rat myenteric plexus. The data are presented as box plots, where the line within the box represents the median and the boxes represent the second and third quartiles (25–75%). Individual points are the corresponding values. The data compared using the Kruskal-Wallis test, where p*** < 0.001, p**** < 0.0001. Histograms showing the relative frequency in percent of a distribution of values for the cross-sectional area of ganglia **(B)** and cross-sectional area of neuronal perikarya **(D)**.

parametric Kruskal-Wallis test H(2)=127.3, p<0.0001 (**Fig. 2A**). Difference of the median (Med) of the ganglia obtained by the three methods applied for preparation of the large intestine was presented [paraffin-embedded tissue cross-sectional cut (Med = 3222 µm^2), paraffin-embedded tissue tangential section (Med = 8010 µm^2) and whole-mount preparations (Med = 16847 µm^2)]. Cross-sectional cut revealed that 82% of the myenteric ganglia had sectional area sizes in the field of 500 µm^2 to 4500 µm^2. In tangential cut, the sectional area in 72% of the ganglia ranged from 4500 µm^2 to 10500 µm^2, and 40% of the whole-mount it varied between 10500 µm^2 to 20500 µm^2 (**Fig. 2B**). The sectional area of the neuronal perikarya measured by the three

methods also showed statically significant differences determined by the same test $H(2)=352.6$, $p<0.0001$. The medians of the perikarya obtained by the three cutting techniques was different: PET (CS) (128.5 μm^2), PET (TS) (132.8 μm^2), and whole-mount preparations (309.7 μm^2) (**Fig. 2C, D**). The total number (n) of the examined ganglia was 272, and the number of the examined neuronal bodies was 991.

Discussion

In the present study, we compared tissue preparations to examine the morphological differences of the Auerbach's plexus by three cutting directions (transversal, tangential and whole-mount preparations). Our results showed a statistically significant difference between the ganglia area and neuronal perikarya obtained by paraffin-embedded sections and whole-mount prepared slides. The three dimensions of the network forming the myenteric plexus do not allow us to thoroughly study its complexity by the standard methods of preparations, a conclusion drawn by many authors [5, 6].

Previous studies have reported that the most common neuron soma area ranges from 200 to 400 μm^2 [8]. By using whole mount preparations, we obtained similar data demonstrating that in 57% of the neuronal perikarya the surface area varies from 200 μm^2 to 450 μm^2. On the contrary, in the transverse and tangential plane sections, more than 70% of the neuronal cell bodies have sectional areas ranging from 50 μm^2 to 150 μm^2. Therefore, whole-mount preparation slides could give much more accurate results in terms of surface morphology. However, the procedure is more time-consuming, it requires a specific preparation technique and trained investigators with good microdissection skills to achieve reliable results. Last but not least, a greater number of experimental animals is needed contrary to animals used in the 3R principles. As reported by other researchers, during whole-mount preparations, it is not a rare occurrence to rupture the longitudinal muscle layer and even to damage the myenteric plexus [4, 5]. We have faced that problem many times in the tissue preparations. In contrast, standard techniques with paraffin embedding are well established and they can be performed on a routine basis. However, they generally tend to demonstrate the neuronal cell bodies and ganglia with sectional areas far smaller than the those in whole-mount slides.

Conclusions

The present study shows that the whole mount preparation technique allows a more precise measurement of myenteric ganglia and their connectivity. On the other hand, the paraffin-sectioning procedure could be a practical solution, which reduces the number of experimental animals and allows for multiple histological processing of the same tissue. One has to keep in mind the possible pitfalls of underestimating

neuronal and ganglion sizes when using paraffin sectioning procedure. A stereological approach is justified when accurate and precise measurements are needed.

Acknowledgements: This research is supported by the Bulgarian Ministry of Education and Science under the National Program "Young Scientists and Postdoctoral Students-2", by the Faculty of Medicine at Trakia University – Stara Zagora (Grant No. 8 /2023) and by the Bulgarian Ministry of Education and Science within the framework of the National Recovery and Resilience Plan of Bulgaria, Component "Innovative Bulgaria", project No. BG-RRP-2.004-0006-C02 "Development of research and innovation at Trakia University in service of health and sustainable well-being".

References

1. Costa, M., R. Buffa, J. B. Furness, E. Solcia. Immunohistochemical localization of polypeptides in peripheral autonomic nerves using whole mount preparations. – *Histochemistry*, **65**(2), 1980, 157-165.

2. Furness, J. B. The enteric nervous system and neurogastroenterology. – *Nat. Rev. Gastroenterol. Hepatol*., **9**(5), 2012, 286-294.

3. Gabella, G., P. Trigg. Size of neurons and glial cells in the enteric ganglia of mice, guinea-pigs, rabbits and sheep. – *J. Neurocytol*., **13**(1), 1984, 49-71.

4. Grundmann, D., M. Klotz, H. Rabe, M. Glanemann, K. H. Schäfer. Isolation of high-purity myenteric plexus from adult human and mouse gastrointestinal tract. – *Sci. Rep.*, **5**(1), 2015, 9226.

5. Huang, Z., L. Liao, Z. Wang, Y. Lu, W. Yan, H. Cao, B. Tan. An efficient approach for wholemount preparation of the myenteric plexus of rat colon. – *J. Neurosci. Methods*, **348**, 2021, 109012.

6. Krammer, H. J., S. T. Karahan, W. Sigge, W. Kühnel. Immunohistochemistry of markers of the enteric nervous system in whole-mount preparations of the human colon. – *Eur. J. Pediatr. Surg.*, **4**(5), 1994, 274-278.

7. Mandhan, P., B. Q. Qi, J. I. Keenan, S. Ismail, S. W. Beasley, M. J. Sullivan (2006). Counterstaining improves visualization of the myenteric plexus in immunolabelled whole-mount preparations. – J. Fluoresc., **16**(5), 655-658.

8. Santer, R. M., D. M. Baker. Enteric neuron numbers and sizes in Auerbach's plexus in the small and large intestine of adult and aged rats. – *J. Auton. Nerv. Syst*., **25**(1), 1988, 59-67.

9. Wester, T., S. O'Briain, P. Puri. Morphometric aspects of the submucous plexus in whole-mount preparations of normal human distal colon. – *J. Pediatr. Surg.*, **33**(4), 1998, 619-622.

10. Wood, J. D. Enteric nervous system: reflexes, pattern generators and motility. – *Curr. Opin. Gastroenterol*., **24**(2), 2008, 149-158.

Institute of Experimental Morphology, Pathology and Anthropology with Museum
Bulgarian Anatomical Society

Acta Morphologica et Anthropologica, 30 (3-4)
Sofia ● 2023

Bone-Cement Implantation Syndrome – Postmortem Morphological Findings

Gergana Trenova[1], Maria Koleva[2,3], Emral Kyosebekirov[4], Angelina Mollova[2,3]*

[1] Medical University - Plovdiv, Plovdiv, Bulgaria
[2] Department of General and Clinical Pathology, Medical University – Plovdiv, Plovdiv, Bulgaria
[3] Department of General and Clinical Pathology, St. George University Hospital, Plovdiv, Bulgaria
[4] Department of Anesthesiology and Intensive Care Medicine, Medical University – Plovdiv, Bulgaria

*Corresponding author e-mail: gergana.trenova@gmail.com

Cement implantation syndrome is a potentially fatal rapidly developing intraoperative complication which pathogenesis and methods of prevention are obscure. It presents with acute circulatory collapse and respiratory failure. We present a case of 85-year-old woman with closed fracture of the femoral neck, scheduled for a biarticular hip endoprosthesis replacement. Right after the cement implantation the patient goes into cardiac arrest. Despite to early initiation of cardio-pulmonal resuscitation, the patient died. Post-mortem findings showed massive pulmonary emboli, composed of bone marrow elements. Histopathological pulmonary findings, confirm the occurred intraoperative complication. Better knowledge of the pathophysiology and the ability for identification of high-risk patients could prevent the development of the syndrome and would help to reduce the mortality.

Key words: bone-cement, implantation syndrome, pulmonary emboli

Introduction

Bone-cement implantation syndrome (BCIS) is a poorly defined, rare and potentially fatal intra-operative complication that occurs within minutes of polymethyl methacrylate (PMMA) insertion, also known as bone cement in patients undergoing cemented orthopedic surgeries [1, 2, 4]. This syndrome is characterized by hypoxia, systemic hypotension, pulmonary hypertension, arrhythmias, loss of consciousness, and cardiac arrest or a combination of these, leading to death in 0.6-1% of patients [1, 3]. It should be noted that BCIS can also happen in the postoperative period, in a milder form [4].

Most of the case reports of BCIS are generally supported by clinical findings with no histological evidence. We report a case of BCIS confirmed by autopsy and histological examination.

Case report

We present a rare case of BCIS, as a severe complication of hip endoprosthesis replacement. The patient is an 85-year-old woman with closed fracture of the femoral neck, scheduled for a biarticular hip endoprosthesis replacement. Shortly after the cement implantation, the condition of the patient sharply deteriorates with the manifestation of severe bradycardia, hypotension, loss of consciousness and apnea. Despite the early initiation of cardiopulmonary resuscitation, the patient dies. The diagnosis is confirmed and supported by the autopsy.

Macroscopically, the lungs are enlarged, with dark-red color. On cut section, the parenchyma appears with dense consistency and after pressure is applied – profuse amount of blood leaks. Dilatation of the right ventricle is observed.

Microscopically, the alveolar spaces are diffusely filled by homogenous pink liquid – a severe pulmonary edema (**Fig. 1**). We observe massive emboli composed of bone marrow elements and adipose tissue which are pathognomonical for the final diagnosis (**Fig. 2A, B**). The rest of the organs are comparably unremarkable.

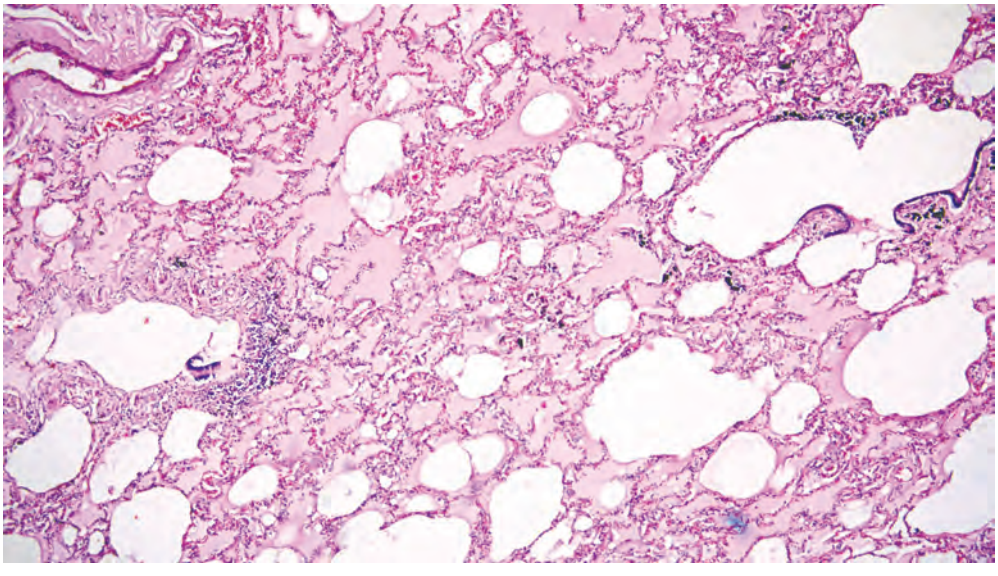

Fig. 1. Alveolar spaces filled by homogenous pink liquid – severe pulmonary edema. Haematoxylin-eosin, ×100

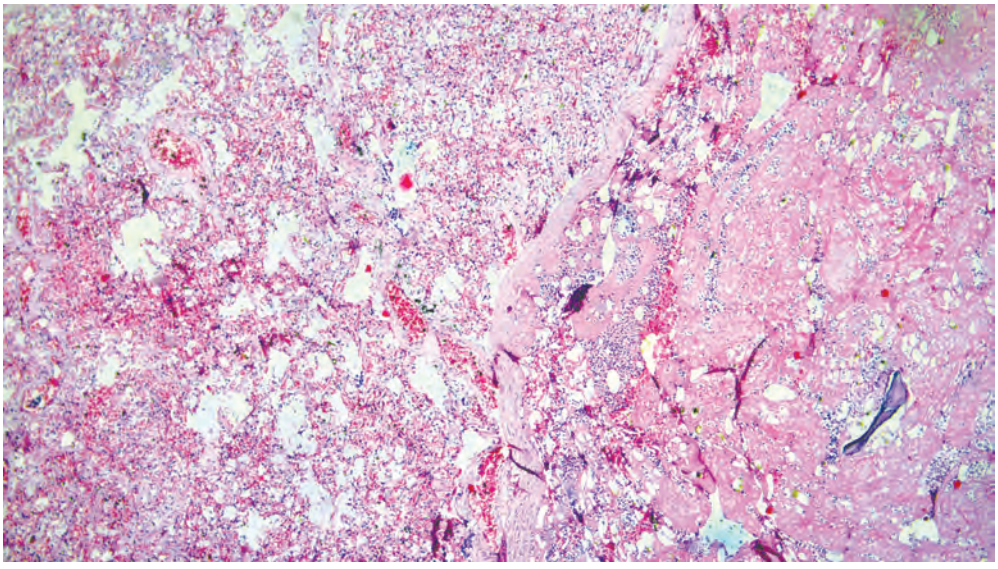

Fig. 2A. Massive emboli in the lungs composed of bone marrow elements and adipose tissue. Haematoxylin-eosin, ×100

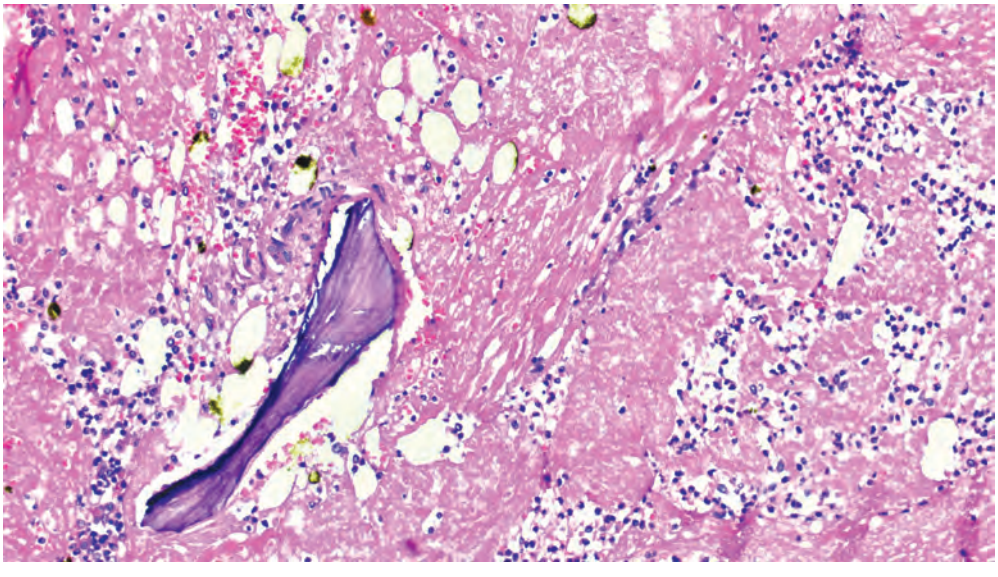

Fig. 2B. Bone marrow elements, adipose tissue, and a fragment of bone, forming the pulmonary emboli. Haematoxylin-eosin, ×200

Discussion

Bone-cement implantation syndrome is a condition with incompletely clarified etiology and pathophysiology. Many theories have been discussed, but the most recent ones focus on the releasing of polymethyl methacrylate monomer into the circulation, and emboli formation during cementation which result in right ventricular failure [5].

Several mechanisms such as histamine release, complement activation, and endogenous cannabinoid-mediated vasodilatation have also been proposed [6]. Based on clinical observations, most researchers favor the theory that a combination of diverse mechanisms operates in any individual developing BCIS [2].

Numerous risk factors related to the patients have been discussed in the genesis of BCIS including old age, poor preexisting physical reserve, impaired cardio-pulmonary function, preexisting pulmonary hypertension, osteoporosis, bone metastases, and concomitant hip fractures, particularly pathological or intertrochanteric fractures [6]. The majority of the cases, described in the literature are females with various indications for cemented arthroplasty including osteoarthrosis, rheumatoid arthritis of fractures [7]. However, there is no certain evidence that gender is a risk factor for occurrence of cement embolism [8].

In the presented case the patient is a high-risk candidate for bone-cementation as she is elderly (85-year-old) with a history of tuberculosis infection in the past, cardiac diseases, and previous hospitalizations for fractures. Minutes after the cement implantation the patient demonstrates the classical clinical findings of BCIS: cardiac arrhythmia (in this case presented by relapsing high frequency atrial fibrillation), decrease in respiratory function, hemodynamic collapse, and cardiac arrest.

The cause of death in this case is the right-sided heart failure secondary to massive pulmonary embolism composed by bone marrow elements.

Conclusion

In conclusion, better knowledge of the pathophysiology and the ability for identification of high-risk patients could prevent the development of the syndrome and will help in the reduction the mortality.

References

1. **Arora D., P. Govil, N. Kakar.** Bone cement implantation syndrome: a report of four cases. – *Indian J. Anaesth.,* **53**(2), 2009, 214-218.
2. **Bonetti, L., S. de Froidmont, M. del Mar., C. Palmiere, R. Villaverde.** Postmortem findings in bone cement implantation syndrome-related deaths. – *The American Journal of Forensic Medicine and Pathology,* **35**(3), 206-211.
3. **Donaldson, A., N. Harper, N. Kenny, H. Thomson.** Bone cement implantation syndrome. – *British Journal of Anaesthesia,* **102**(1), 2009, 12-22.
4. **Effat, O., M. Miswan, R. Razuin, M. Shahidan, D. Shama.** Bone cement implantation syndrome. – *Malaysian J. Pathol.,* **35**(1), 2013, 87-90.

5. **Houltz, E., F. Olsen, S-E. Ricksten, M. Segerstad, B. Nellgard.** The role of bone cement for the development of intraoperative hypotension and hypoxia and its impact on mortality in hemiarthroplasty for femoral neck fractures. – *Acta Orthop.,* **91**(3), 293–298.
6. **Hseinat, L., L.Husinat, B. Jouryyeh, A. Jurieh, Z. Modanat, S. Sharie, G. Varrassi.** Bone cement and its anesthetic complications: a narrative review. – *J. Clin. Med.,* **12**(6), 2023, 2105.
7. **Lehto, K., P. Paavolainen, H. Pitiilii, P. Rokkanen.** Posterior approach for total hip arthroplasty – *Orthop. Trauma Surg.,* **102,** 1984, 225-229.
8. **Mudgalkar, N., K. Ramesh.** Bone cement implantation syndrome: a rare catastrophe. – *Anesthesia: Essays and Researches,* **5**(2), 2011,240–242.

Institute of Experimental Morphology, Pathology and Anthropology with Museum
Bulgarian Anatomical Society

Acta Morphologica et Anthropologica, 30 (3-4)
Sofia ● 2023

Evaluation of COVID-19 Vertical Maternal Transmission with Respect to Foetal Visceral Maturation

Divia Paul Aricatt[1], Banushree Chandrasekhar Srinivasamurthy,[2] Shankaranarayan Subramanyan Ramakrishna[3], Ashwini Prabhu[4], Manisha Rajanand Gaikwad[5]

[1] Department of Anatomy, Fr Muller Medical College, Kankanady, Mangalore, Karnataka, India
[2] Department of Pathology, Indira Gandhi Medical college and Research Institute, Kathirkamam, Puducherry, India
[3] Lifenity International Laboratory, Abudhabi, U.A.E.
[4] Yenepoya Research Centre, Yenepoya (Deemed to be University), University Road, Deralakatte, Mangalore, Karnataka, India
[5] Department of Anatomy, All India Institute of Medical Sciences, Bhubaneswar, Odisha State, India

* Corresponding author e-mail: divia_manoj@yahoo.com

Novel corona virus infection could be transmitted from an infected pregnant woman to her infant, a process termed vertical infection. The study aimed to find the relationship between the SARSCoV-2 virus invasion and infection occurring during pregnancy and the nature and extent of impaired organ maturation in foetus. An observational, descriptive pilot study was conducted with 4 still born foetuses and their thymus, spleen, lungs and kidneys were processed. The microscopic examinations were done to evaluate the degree of visceral impairment. Our results revealed that mothers affected with COVID-19 infection during the first trimester of pregnancy exhibited impaired maturation for foetus of 33 weeks and 37 weeks compared to the viral disease during the last trimester of pregnancy of foetus of 38 weeks and 27 weeks. The study helps us to find out the possible mechanisms behind it as well as the nature of the maternal and foetal response to COVID-19 occurring during pregnancy.

Key words: Maternal infection, SARS-CoV-2, impaired fetal organ maturation, vertical transmission

Introduction

Following the identification of an outbreak of novel coronavirus infection (SARS-CoV-2), in Wuhan, China, in December 2019, there was concern for the potential

effects of the illness on pregnant women which impair the visceral maturation of foetus by vertical infection [3, 22]. In recent times, the histology of the embryological development of various organs has been studied and helps to correlate with the gestational age (GA). Histological examination of fetal viscera show marked qualitative or quantitative changes during development and marked as relevant [18]. Thymus is a lymphoepithelial organ and the key regulator of cellular immunity of the body [1]. Meanwhile, largest accumulation of lymphoid tissues in the body in spleen serves as defense against microorganisms that penetrate the circulation [10]. The human kidney develops through a complex process termed as 'branching' morphogenesis between 22 and 36 gestational weeks. This creates a radial glomerular pattern [8]. The histology of lung can also be a reliable parameter, [11] and radial alveolar count requires a pleural section parallel to the bronchiolar tree. The radial alveolar count described by Emery and Mithal is the number of alveoli crossed by an imaginary straight line drawn from the center of a terminal bronchiole to the nearest pleural surface [13]. Gestational age was calculated based on maternal data (last menses: Naegele's rule) [15]. Ultrasound data were obtained from the medical records department and possible genetic abnormalities were excluded and causes of death were identified as in utero death or spontaneous.

In viral defense mechanisms during pregnancy, syncytiotrophoblast of placenta possesses high rates of basal autophagy [5, 7]. This has critical role in the maternal-fetal interface and the destruction of the trophoblast may serve as a potential mechanism for a pathogenic virus to penetrate the chorionic villi. This reaches the fetal circulation which results in a programmed cell death [7]. The information on the effects of SARS-CoV-2 infection in pregnancy is limited [3, 12]. Thymic microstructure has specialized anatomical organization which is directly proportional to their function [4]. The medulla represents a site where each single positive thymocytes accumulate prior to their exit into the periphery. Subsets of medullary thymic epithelial cells are involved in multiple aspects of T-cell development and thymic migration. Medullary heterogeneity provides a better understanding of the mechanisms controlling α and β T-cell development especially in innate and adaptive immune systems [6, 17]. In severe chronic forms of viral diseases splenic tissue exhibits white pulp atrophy, to the degree that secondary lymphoid follicles completely disappear [9]. Changes in the structure of the spleen with splenic or lymphoid stromal hyperplasia, may be followed by lymphoid atrophy and disorganized compartments of the spleen. The development of human kidney is a complex process. The definitive and morphologically distinctive sequential developmental pattern of the glomerulus, commencing as early as 7^{th}–8^{th} week of gestation and continuing up to 35–36^{th} week of gestation, makes the fetal kidneys excellent viscera for estimation of period of gestation [8]. The histology of lung can also be a reliable parameter and radial alveolar count requires a pleural section parallel to the bronchiolar tree [11, 13]. Development of lung is a continuous process till 8 years and by 20^{th} week there is differentiation of the type 1 pneumocytes. Pneumocytes when infected early, can led to recruitment of leukocytes into the pulmonary interstitium, production of pro-inflammatory cytokines, injury to

parenchymal cells, collapse of the alveolar space which compromise of gas exchange and could cause hypercapnia [16].Thymus and spleen completes its embryological development by first trimester whereas kidney by third trimester and lung by 8th year of life, so that we can understand the effect of viral load during the development of these organs despite of the period of SARS-CoV-2 infection in pregnancy. Histological examination of the kidney has the advantage of revealing clearly visible structural changes that are still recognizable in cases of advanced necrosis, which is frequently encountered in forensic practice. The lung was also a reliable parameter in cases of putrefactive changes due to infections. Considering other organs for estimating gestational age, reports in the literature have shown that many pathological conditions can modify the histological examination e.g. pancreas, genital organs, and liver [18]. The case series aimed to find the relationship between the SARSCoV-2 virus invasion and infection occurring during pregnancy and the nature and extent of impaired organ maturation in foetus. Objectives under consideration were to characterize the foetal organ pathology findings in neonates infected by transplacental transmission arising from maternal infection with COVID-19 and to identify pathological risk factors for foetal infection.

Case series

Four different histological samples namely, thymus, spleen, lungs and kidneys were processed. All samples were fixed in 10% formalin and embedded in paraffin; 5 μm sections were stained with hematoxylin-eosin for light microscopy. The microscopic examinations were done to evaluate the degree of visceral maturation based on knowledge of the developmental chronology of foetal tissue. The GA with histological development of the foetal thymus maturation and spleen were noted. For the kidneys, gestational age were estimated by counting the rows of glomeruli between two well-oriented columns of Bertin running from the arcuate artery to the nephrogenic zone or with sequential development of glomerulus by counting the average radial glomerular count in cortical zones. Lung development was determined by the different stages of development based on the maturation.

History of COVID-19 infection was during the first trimester of pregnancy for mothers of foetus number 1 aged 33 weeks (wks) and foetus number 4 aged 37 wks whereas it was during the last trimester for mothers of foetus number 2 aged 38 wks and foetus number 3 aged 27 wks. We took written informed consent.

Foetus No.1 of 33 weeks weighted 1.26 kg had the following features that the kidney section studied from first image showed radial glomerular count (RGC) of 15. Second image showed 17 and third image showed single glomeruli. Thymus section show thymic parenchyma with well-formed trabeculae. Parenchyma composed of loosely arranged mesenchymal cells and lymphocytes. Cortex and medulla cannot be distinguished. No Hassall's corpuscles seen. Spleen section showed predominantly red pulp and indistinct white pulp. No trabeculae or capsule noted. Lung section showed extensive area of haemorrhage with small foci and congested blood vessels,

which are suggestive of intravascular coagulation. Lungs are in saccular stage of lung development (**Fig. 1**)

Foetus No.2 of 38 weeks weighed 2.5 kg had the following features that the kidney section studied from first image showed RGC of 2. Second image show 27 and third image is not showing any glomeruli. Thymus had well-form ed capsule and trabeculae dividing into lobules composed of lymphocytes. Two Hassall's corpuscles were noted. Spleen showed well-formed trabeculae with red pulp. White pulps not seen in the image provided. Lungs were in alveolar stage of lung development. There was no hyaline membrane in alveoli (**Fig. 1**).

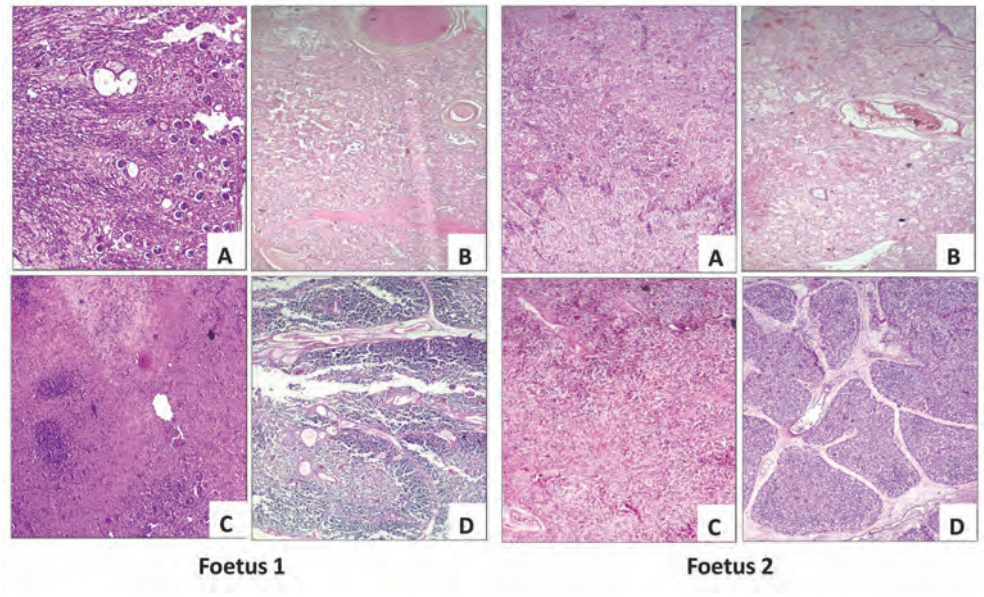

Fig. 1. Foetus 1(33 Wks) and Foetus 2 (38 Wks) : A-Kidney (Kidney average RGC is 11 corresponding to 24 weeks of gestation of foetus 1 and Kidney RGC is 14.5 corresponding to 28 weeks of gestation of foetus 2)**, B-Lung (**Lung shows primitive alveoli form corresponding to 26-32 weeks of gestation of foetus 1and Lung shows primitive alveoli form corresponds to 32-38 weeks of gestation of foetus 2)**, C-Spleen** (Spleen group IV corresponding to 18-24 weeks for both foetus 1 and 2)**, D-Thymus** (Thymus group IV corresponding to 18-24 weeks of foetus 1 and Thymus groups corresponds to 25-38(group V) weeks of gestation of foetus 2).

Foetus No.3 of 27 weeks weighted 900g had the following features that the kidney section studied from first image showed RGC of 17. Second image RGC is 3. Thymus had thin capsule and trabeculae dividing lymphocytes into lobules. No Hassall's corpuscles were noted. Spleen showed trabeculae with red pulp. No white pulp seen. Lungs are in saccular stage of lung development (**Fig. 2**).

Foetus No.4 of 37 weeks weighted 2 kg had the following features that the kidney section studied from first image showed RGC of 27 and second image showed 0. Thymus had thin capsule and trabeculae dividing lymphocytes into lobules. No Hassall's corpuscles were noted. Spleen showed trabeculae with red pulp. No white

pulp seen. Lung section showed extensive area of haemorrhage with small foci and congested blood vessels, which are suggestive of intravascular coagulation. Lungs were in saccular stage of lung development (**Fig. 2**).

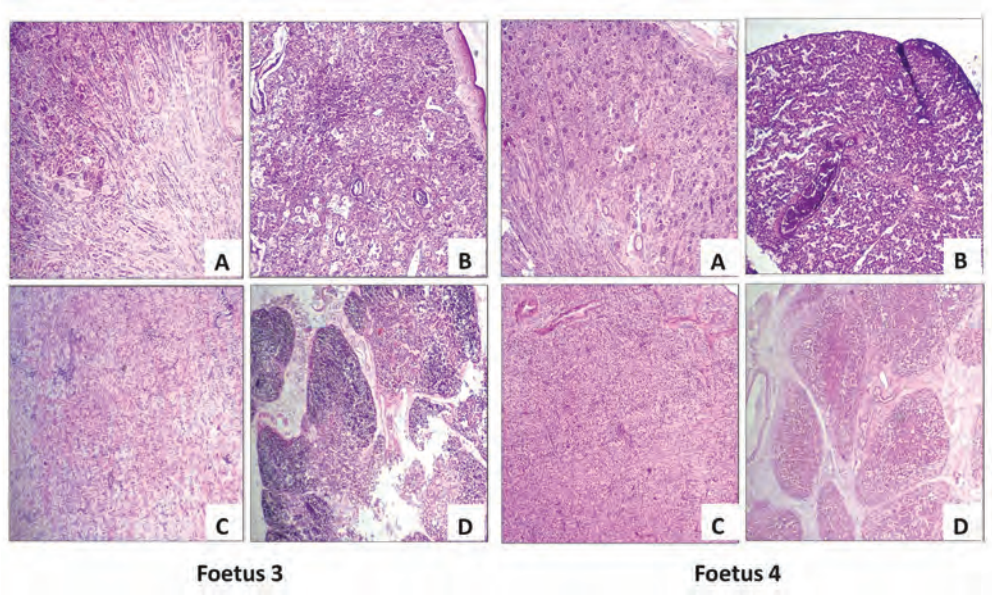

Fig. 2. Foetus 3 (27 Wks) and Foetus 4 (37 Wks) : A-Kidney (Kidney average RGC is 10 corresponding to 22 weeks of gestation of foetus 3 and Kidney RGC is 13.5 corresponding to 27 weeks of gestation of foetus 4)**, B-Lung (**Lung shows primitive alveoli form corresponding to 26-32 weeks of gestation for both foetus 3 and 4)**, C-Spleen** (Spleen group IV corresponding to 18-24 weeks for both foetus 3 and 4)**, D-Thymus** (Thymus group IV corresponding to 18-24 weeks for both foetus 3 and 4).

Discussion

Congenital transmission of SARS-CoV-2 was detected during the first trimester in the placental cells, amniotic fluid and also in the fetal membrane. However, the evidences were inadequate to establish foetal tissue involvement due to lack of samples for autopsy to study the virus particles [20]. In the present case series, we had two still birth foetus from the mothers diagnosed with SARS-CoV-2 during the first trimester of pregnancy. All organs which were studied showed delayed maturation which implies that the disease during the first trimester is causing more developmental issues on foetus as it is a period of organogenesis. The hypoxia induced on mothers due to the disease can also have an impact on foetoplacental circulation. However an extensive study with more number of samples is needed to draw a conclusion. Fetal tissues like the liver, heart, lungs and hematopoietic cells also express ACE2 which indicates that the presence of the virus in the amniotic fluid will cause the fetal infection [14]. In the present case series we had two fetuses obtained from mothers

who were affected by SARS-CoV-2 during the last trimester. It has been noticed that lung and thymus development appeared to be normal when the infection was in the last trimester, where spleen and kidney development was impaired irrespective of trimester of pregnancy and viral infection.

The thymus is an organ commonly targeted by infectious pathogens such as viruses, bacteria, and fungi. Alterations of proliferation, secretion, migration, differentiation and death of thymocytes can be induced by these infections due to phenotypic and functional changes within the thymus. The behavior of mature, peripheral T-lymphocytes can be equally affected [2]. In the present case series, two samples were from mother diagnosed with SARS-CoV-2 during the first trimester of pregnancy showed delayed maturation of thymus, which implies that the disease during the first trimester is causing more developmental issues on foetus as it is a period of organogenesis.

Irrespective of the trimester all cases had impaired growth in the spleen in the present case series. Splenic tissue of human fetuses develops at 14^{th} to 24^{th} week of gestation. The function of spleen in the foetus is hematopoietic and it continues from the fetal period till the child birth. So the red and white pulp attains maturation throughout the embryonic period though the maturation is complete. The viruses must have caused impaired function of the splenic cords due to hypoxia induced to the mother. Mild to moderate disorganization of the white pulp with indistinct regions and severe congestion and hemorrhage, and proliferation of megakaryocytes of red pulp was observed in the case series. An obvious distinction between white and red pulp is not always proper and several plasma cell aggregates replace the populations of normal resident cell of the red pulp observed [19].

Kidneys have the advantage of revealing clearly visible structural changes. The count of the glomerular zone extends from the top of the superficial definitive glomerulus to the bottom of the deepest glomerulus, at the junction with the medulla which is still recognizable in cases of advanced necrosis and frequently encountered in forensic practice [21]. In the case series all the samples have delayed and impaired glomerulogenesis. This indicates SARS-CoV-2 can cross the placental barrier as the viral RNA was detected in the amniotic fluid and the S proteins were detected in the fetal membrane [20].

Development of lung is a continuous process till 8 years and by 20^{th} week there is differentiation of the type 1 pneumocytes. The histopathological changes we observed in the infected lungs of K18-hACE2 mice correlate with the impaired pulmonary function [16]. It has been noticed in the case series that lung development appeared to be normal when the infection was in the last trimester. The pseudoglandular period in which most of the lung elements develop except alveoli must have likely to be affected by the viral disease which resulted in impaired growth of lungs of foetus born from mothers affected with COVID-19 infection during the first trimester.

Conclusion

The case series outlooks the impaired maturation of foetal vital viscera as can be related to SARS-CoV-2 virus invasion and infection during the pregnancy. This can prove the vertical transmission of infection through placenta and impaired organ development irrespective of the trimester of COVID-19 infection. The report helps us to find out the possible mechanisms behind it as well as the nature of the maternal and fetal response to COVID-19 infection occurring during pregnancy.

Limitations

We couldn't perform a placental or viseral immunohistochemical study with SARS-CoV-2 nucleocapsid-specific or cytokeratin-7 specific monoclonal antibody to detect SARS-CoV-2 antigen.

Acknowledgements: All authors appreciate the great effort of histology lab technicians of Yenepoya Medical College, Mangalore for their timely help and assistance in the conduction of this study.

References

1. **Ajita, R.K., T. N. Singh, Y. I. Singh, L. C. Singh.** An insight into the structure of the thymus in human foetus-a histological approach. – *J. Anat. Soc. India*., **55**(1), 2006, 45-49.
2. **Albano, F., E. Vecchio, M. Renna, E. Iaccino, S. Mimmi, C. Caiazza, A. Arcucci, A. Avagliano, V. Pagliara, G. C. Donato.** Palmieri. Insights into thymus development and viral thymic infections. – *Viruses*, 11(9), 2019, 836.
3. **Allotey, J., S. Fernandez, M. Bonet, E. Stallings, M. Yap, T. Kew., D. Zhou, D. Coomar, J. Sheikh, H. Lawson, K. Ansari.** Clinical manifestations, risk factors, and maternal and perinatal outcomes of coronavirus disease 2019 in pregnancy: living systematic review and meta-analysis. – *BM Journal*., 2020, *370*.
4. **Alves, N. L., Y. Takahama, I. Ohigashi, A. R. Ribeiro, S. Baik, G. Anderson, W. E. Jenkinson.** Serial progression of cortical and medullary thymic epithelial microenvironments. – *European Journal of Immunology*, **44**(1), 2014, 16-22.
5. **Ander, S.E., M. S. Diamond, C. B. Coyne.** Immune responses at the maternal-fetal interface. – *Science Immunology*, **4**(31), 2019,eaat6114.
6. **Anderson, G. and Y. Takahama.** Thymic epithelial cells: working class heroes for T cell development and repertoire selection. – *Trends in Immunology*, **33**(6), 2012, 256-263.
7. **Cornish, E.F., I. Filipovic, F. Åsenius, D. J. Williams, T. McDonnell.** Innate immune responses to acute viral infection during pregnancy. – *Frontiers in Immunology*, **11**, 2020, 2404.
8. **Daković-Bjelaković, M.Z., S. R. Vlajković, R. E. Čukuranović, S. Antić, G. B. Bjelaković, D. Mitić.** Quantitative analysis of the nephron during human fetal kidney development. – *Vojnosanitetski Pregled*, **62**(4), 2005, 281-286.
9. **Djokic, V., L. Akoolo, N. Parveen.** Babesia microti infection changes host spleen architecture and is cleared by a Th1 immune response. – *Frontiers in Microbiology*, **9**, 2018, 85.
10. **Dubey, A., S. L. Jethani, D. Singh.** Gestational age estimation in human fetuses from histogenesis of the spleen. – *SRHU Medical Journal*, **1**(2), 2018, 76-79.

11. Emery, J .L. and A. Mithal. The number of alveoli in the terminal respiratory unit of man during late intrauterine life and childhood. – *Archives of Disease in Childhood*., **35**(184), 1960, 544-547.
12. Gajbhiye, R.K., D. N. Modi, S. D. Mahale. Pregnancy outcomes, Newborn complications and Maternal-Fetal Transmission of SARS-CoV-2 in women with COVID-19: A systematic review. – *MedRxiv*, 2020, 2020-04.
13. Gaultier, C. L. Physiologie et physiopathologie du developpement et ´ de la maturation du poumon antenatal. - *Rev Mal Resp*., **5**, 1988, 213–22. [in French]
14. Li, M., L. Chen, J. Zhang, C. Xiong, X. The SARS-CoV-2 receptor ACE2 expression of maternal-fetal interface and fetal organs by single-cell transcriptome study. – *PloS One*, **15**(4), 2020, p.e0230295.
15. Loytved, C. A L. and V. Fleming. Naegele's rule revisited. – *Sexual & Reproductive Healthcare*, **8**, 2016, 100-101.
16. Pan, F., T. Ye, P. Sun, S. Gui, B. Liang, L. Li, D. Zheng, J. Wang, R. L. Hesketh, L. Yang, C. Zheng. Time course of lung changes at chest CT during recovery from coronavirus disease 2019(COVID-19). – *Radiology*, **295**(3), 2020, 715-721.
17. Perry, J. S., C. W. J. Lio, A. L. Kau, K. Nutsch, Z. Yang, J. I. Gordon, K. M. Murphy, C. S. Hsieh. Distinct contributions of Aire and antigen-presenting-cell subsets to the generation of self-tolerance in the thymus. – *Immunity*, **41**(3), 2014, 414-426.
18. Piercecchi-Marti, M. D., P. Adalian, A. Liprandi, D. Figarella-Branger, O. Dutour, G. Leonetti. Fetal visceral maturation: a useful contribution to gestational age estimation in human fetuses. – *Journal of Forensic Sciences*, **49**(5), 2004, 912-917.
19. Santos, S. O., J. L. Fontes, D. F. Laranjeira, J. Vassallo, S. M. Barrouin-Melo, W. L. Dos-Santos. A minimally invasive approach to spleen histopathology in dogs: A new method for follow-up studies of spleen changes in the course of Leishmania infantum infection. – *Comparative Immunology, Microbiology and Infectious Diseases*, **48**, 2016, 87-92.
20. Shende, P., P. Gaikwad, M. Gandhewar, P. Ukey, A. Bhide, V. Patel, S. Bhagat, V. Bhor, S. Mahale, R, Gajbhiye, D. Modi. Persistence of SARS-CoV-2 in the first trimester placenta leading to transplacental transmission and fetal demise from an asymptomatic mother. – *Human Reproduction*, **36**(4), 2021, 899-906.
21. Singer, D. B., C. J. Sung, J. S. Wigglesworth. Fetal growth and maturation: with standards for body and organ development. In: *Textbook of fetal and perinatal pathology* (Eds. J. S. Wigglesworth and C. J. Sung), Cambridge, Blackwell Scientific, 1991, 11–47.
22. Yang, X., Y. Yu, J. Xu, H, Shu, H. Liu, Y. Wu, L. Zhang, Z. Yu, M. Fang, T. Yu, Y. Wang. Clinical course and outcomes of critically ill patients with SARS-CoV-2 pneumonia in Wuhan, China: a single-centered, retrospective, observational study. – *The Lancet Respiratory Medicine*, **8**(5), 2020, 475-481.

Institute of Experimental Morphology, Pathology and Anthropology with Museum
Bulgarian Anatomical Society

Acta Morphologica et Anthropologica, 30 (3-4)
Sofia ● 2023

Cause of Death: Forensic Approach in Case of Fall with Fatal Blunt Force Trauma Combined with Electrocution.

Plamena Dineva[1,2], Pavel Timonov[1,2], Ivan Tsranchev[1,2], Mirena Sotirova[2], Kristina Hadzhieva[1,2], Antoaneta Fasova[3]*

[1] Department of Forensic medicine and Deontology, Medical University of Plovdiv, Plovdiv, Bulgaria
[2] Department of Forensic medicine at UMBAL "St. Georgi" EAD, Plovdiv, Bulgaria
[3] Department of Anatomy, Histology and Embryology, Medical University of Plovdiv, Plovdiv, Bulgaria

*Corresponding author e-mail: plamdineva@gmail.com

Industrial fallings from height as cases raise practical dilemma about the exact cause and the mechanism of death by forensic expert point of view. A 51-year-old man was subjected to a medico-legal autopsy at University Hospital St. George, Plovdiv, Bulgaria. An eye witness had seen the person sustaining injuries after a fall from a height from 3rd floor of construction building (around height of 10 meters). During the corpse examination a combination of two types of different trauma – electrical trauma and blunt force trauma, was stated. Such cases are extremely rare in the routine forensic practice and there usually is a serious diagnostic forensic dilemma about the exact cause and the exact mechanism of death. New forensic approach over the corpse tries to give conclusion about these categories and tries to fix these problematic points in the given case.

Key words: cause of death, diagnostic dilemma, fatal trauma, fall, electrocution

Introduction

Electrocution is defined as death or severe injury caused by electric shock from the action of electricity going through body tissues and organs [9]. The word is derived from "electro" and "execution" and this term is usually used for fatal cases of accidents related to the general action of current over body. Deaths due to electric shock are significantly increasing despite different modern preventive strategies. These shocks are a leading cause of death especially amongst construction workers [8]. Established severe internal injuries at autopsy in such cases could be associated either with the

blast of the electrical discharge or with the secondary fall [10]. Falling from a height can be defined as the movement of the body to a lower level than the state it is on by different reasons leading to severe complex of life-threatening injuries. Contact with electricity, depending on the voltage, may produce contraction of muscle groups leading to rotating of arms, extending of feet, straightening of hips and knees, that can propel an individual forward or backward with additional initial falling from height [4]. Such cases raise practical dilemma about the exact cause and mechanism of death by forensic expert point of view.

Case report: A 51-year-old man was subjected to a medico legal autopsy at the Department of forensic medicine, St. George Hospital, Plovdiv. An eye witness had seen him sustain injuries after a fall from a height from 3rd floor of construction building (around height of 10 meters). At the crime scene a dead body was fixed lying on his face with blood collection around the face near a construction building. During the examination of the body on the scene additional electrical marks over upper limbs and lower right limb were established, in combination with additional burns over the working clothes of the body.

During the external examination of the corpse were found numerous lacerated wounds, bruises, and abrasions on the skin of the face over prominent parts, abrasions on the front site of the chest and abdomen, bruises, and abrasions over the upper and lower limbs. Electrical burns with different dimensions and shapes over the palms of the hands tips of the fingers (**Fig.1**) and sole of the right foot were also fixed. Lesions had yellowish to black discoloration of the burn site with raised borders and central crater.

Fig. 1. Electrical burns over the palms

On the internal examination was found blunt force trauma on the head, chest, and abdomen. Trauma of the head was presented with fractures of the skull – frontal bone and base of the skull, subarachnoid hematoma, brain edema, soft tissues hemorrhage over the frontal area of the head. Chest trauma was manifested with serial fractures of ribs on both sides by anterior and middle axillary lines, fracture of the left clavicula, rupture of the lungs in the area of main bronchi near the bifurcation of trachea, contusions of both lungs, bilateral hemothorax – 1800 ml, rupture of pericardium and right atrium of the heart. Abdominal trauma was manifested with rupture of the spleen, handle-bucket tear of the mesentery and hematoma of the capsule of left kidney, in combination with blood collection inside peritoneal cavity with amount of 300 ml.

An additional microscopic examination of samples from the skin in the area electrical burns was performed and it showed a Swiss cheese appearance of epidermis. Routine toxicologic analysis of blood and urine samples collected from the body did not confirm evidence for any drug and alcohol concentrations.

The microscopic examination of the skin showed that nuclei of epidermis specifically these of the basal layer were elongated and with pyknotic appearance. Some of the hair follicles also showed nuclear streaming with loss of epidermis in combination with intraepidermal and subcorneal separation (**Figs. 2, 3**).

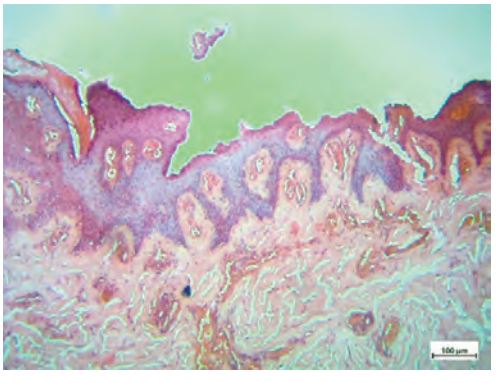

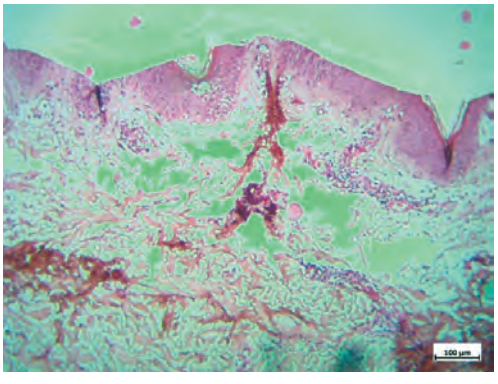

Fig. 2 and **Fig. 3.** Microscopic view of the skin – elongated nuclei of epidermis specifically these of the basal layer with pyknotic appearance in combination with intraepidermal and subcorneal separation. ×20

Hematoxylin-Eosin staining of lung tissues reveals diffuse intra-alveolar hemorrhages with alveolar disruption in combination with hemorrhagic changes inside interstitium. Sudan staining showed well seen orange-red fat globules, some of them with elongated shape, in the pulmonary parenchyma (**Figs. 3, 4**). In forensic expert practice confirmed predictor for vitality of trauma described by many authors is the presence of fat embolism that confirms active heart pump function and blood circulation.

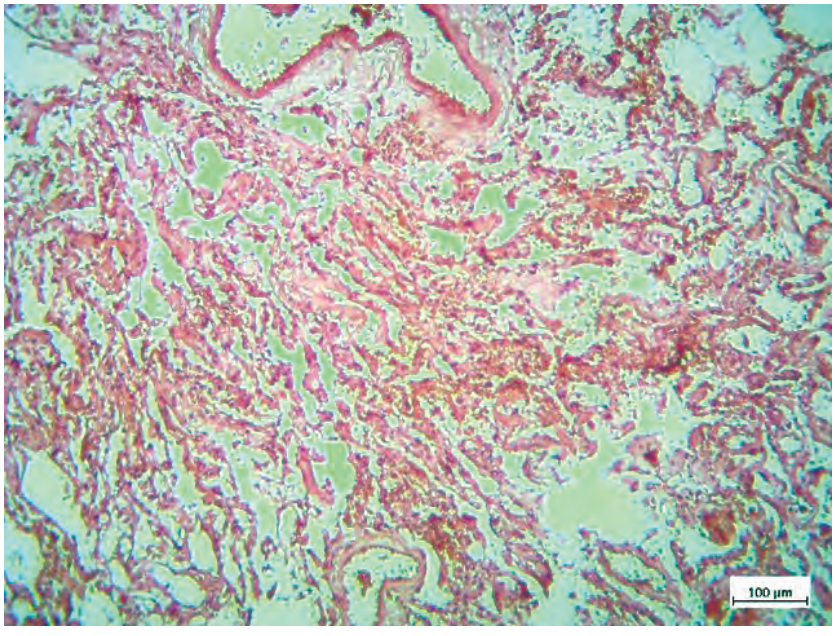

Fig. 4. Hematoxylin-Eosin staining showing diffuse intra-alveolar hemorrhages with alveolar disruption in combination with hemorrhagic changes inside interstitium. ×20.

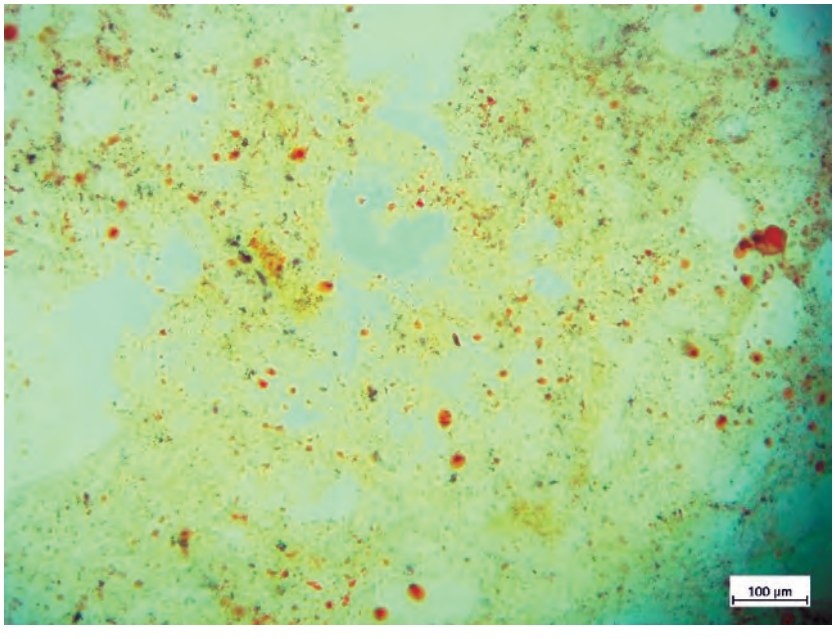

Fig. 5. Sudan staining showing well seen orange-red fat globules, some of them with elongated shape, in the pulmonary parenchyma. ×20

Discussion

Fatal accidents after electric trauma are related to increased risk to the life and health of people who are working in different industrial spheres of labour. Accidents during transport, exposures to harmful agents and falls represent the majority of fatal cases in this construction industry. This group of accidents includes all cases of electrical trauma, thermal trauma, chemical trauma, and radiation trauma. Fatalities due to electric trauma represent the majority of cases in this group of accidents [3, 7]. In Bulgaria almost all cases of electric trauma undergo investigation for different legal reasons [5].

Nevertheless, construction industry fatal accidents with combination of electrocution and falling from height are extremely rare. Electric trauma usually has accidental manner and it occurs in domestic settlings. Electrical burns are associated with higher morbidity and mortality with mechanism of direct damage to the tissues and organs. In such cases electrical marks could be the only external evidence proving the trauma, while during the internal examination of the corpse evidence proving this type of traumatism is usually lacking [15].

In fatal cases of electrocution, the mechanism of death usually is related to ventricular fibrillation. In this ventricular fibrillation consciousness may not be lost immediately [17]. This is because of the fact that the brain has approximately 10-15 s of oxygen reserve, irrespective of the heart. Thus, an individual can remain conscious for 10-15 s after cessation of the heart as a pumping organ [4]. In this situation the individual can sustain injury from falls and other associated trauma. Victims of electric shock may be thrown from a height that may lead to fractures and serious life-threatening injuries, even to death [14]. Usually, injuries by falling from height are divided into two main groups by mechanism of production: 1. injuries produced by initial impact of the body with the ground; 2. Secondary injuries. Severity and appearance of the traumatic complex depends on the height and the type of falling [1, 6, 11, 12, 13, 18].

In the present case all traumatic injuries are with characteristics of vitally achieved trauma and with characteristics of trauma, having inertial origin. The amount of blood inside chest cavity – 1800 ml is evidence for active heart pump function in the moment of trauma and confirms time of survival around several seconds. Around the fractures of all the bones well seen bruising of tissues was seen during the forensic examination of the corpse. Same finding was confirmed also by microscopic examination of muscle tissue taken from areas of injuries. An adequate heart pump function in combination with blunt force are the main factors, associated with the appearance and manifestation of injuries in the recent case – the presence of bilateral hemothorax, of hemoperitoneum, manifestation of contusions to the soft tissues and organs (especially the lungs) and fat embolism to the lungs.

The second most common cause of death in clear electrocution cases is from respiratory arrest from paralysis of the intercostal muscles and diaphragm. In each of these mechanisms of death in cases of electrical trauma during the autopsy should be

seen evidence of external and internal morphologic features of sudden, unexpected death - pinpoint hemorrhages, congestion and cyanosis of the face and the skin, cyanosis, and stasis of blood inside internal organs. In recent case autopsy findings are indicating different mechanism of the death - combination of severe internal blood loss with multiorgan disfunction due to mechanic destruction of tissues, confirming the exact cause of death.

Conclusion

Accidents involving electrocution or falling from height are one of the most common reasons for morbidity and mortality in industry workers. When patients survive the initial trauma, they become serious therapeutic and diagnostic challenges to healthcare workers in emergency and intensive care units [2, 16]. The combination of these two types of traumas is extremely rare. In such cases there is a serious diagnostic forensic dilemma about the exact cause and the mechanism of death. A detailed examination of the crime scene involving forensic pathologist, a comprehensive forensic examination of the corpse and a detailed microscopic and laboratory examination are necessary for determination the mechanism, the cause, and the manner of death in such cases. A thorough study of the cases, including combination of electrocution and falls from a height in construction workers, would help prevent such injuries. This case also raises additional questions about the implementation of new strategies for preventing this type of traumatism.

References

1. **Abder-Rahman, H.,** M. **Jaber, S. Al-Sabaileh.** Injuries sustained in falling fatalities in relation to different distances of falls. – *Journal of Forensic and Legal Medicine*, **54**, 2018, 69-73.
2. **Atliev, K., R. Kostadinov.** Emergency department challenges related to the medical support in case of mass casualty incidents, disasters, accidents and crises. – *Knowledge for Sustainability - International Journal*, **41**, 2020, 619-624.
3. **Colaki, B., N. Etiler, U. Bicer.** Fatal occupational injuries in the construction sector in Kocaeli, Turkey, 1990-2001. – *Ind. Health*, 42, 2004, 424-430.
4. **DiMaio, V. J., D. DiMaio.** *Forensic pathology*, 2nd ed. Book 2 New York, NY: CRC Press, 2001, p. 411-412.
5. **Dokov, W., K. Dokava.** Epidemiology and diagnostic problems of electrical injury in forensic medicine. In: *Forensic medicine – from old problems to new challenges*, (Ed. D. N. Vieira), Rijeka, Croatia, InTech, 2011, pp.121-136.
6. **Evans, J. A., K. J. P. van Wessem, D. McDougall, K. A. Lee, T. Lyons, Z. J. Balogh.** Epidemiology of traumatic deaths: comprehensive population – based assessment. – *World J. Surg.*, **34**, 2010, 158-163.
7. **Janicak, C.** Occupational fatalities due to electrocutions in the construction industry. – *Journal of Safety Research*, **39**, 2008, 617-621.
8. **Jayanth, S. H., B. P. Hugar, Y. P. Chandra, A. G. Krishnan.** Fatal head injury: a sequelae to electricshock – a case report. – *Medico-Legal Journal*, **83**, 2015, 47-50.

9. Makhchoune, M., O. Benhayoun, A. Laaidi, M. Y. Haouas, A. Naja, A. Lakhdar. Extra dural hematoma following a high voltage electrocution accident: A case report. – *Annals of Medicine and Surgery*, **73**, 2022, 103157, p.1-4.
10. Moar, J. J., J. B.Hunt. Death from electrical arc flash burns. A case report of two cases. – *S. Afr. Med. J.*, **71**, 1987, 181-182.
11. Rowbotham, S. K., S. Blau, J. Hislop-Jambrich, V. Francis. Skeletal trauma resulting from fatal low (≤3 m) free falls: an analysis of fracture patterns and morphologies. – *Journal of Forensic Sciences*, **63**, 2018, 1010-1020.
12. Rowbotham, S. K., S. Blau, J. Hislop-Jambrich, V. Francis. An assessment of the skeletal fracture patterns resulting from fatal high (>3 m) free falls. – *Journal of Forensic Sciences*, **64**, 2019, 58-68.
13. Rowbotham, S. K., S. Blau. Skeletal fractures resulting from fatal falls: A review of the literature. – *Forensic Science International*, **266**, 2016, 582.e1-582.e15.
14. Saukko, P., B. Knight. *Knight's forensic pathology*, 3rd ed. London, Arnold Publication, 2004, pp. 326-338.
15. Shetty, B., T. Kanchan, J. Acharya, R. Naik. Cardiac pathology in fatal electrocution. – *Burns*, **40**, 2014, e45-e46.
16. Shopov, D., T. Stoeva, K. Atliev. Reality in the primary medical care. – *General Medicin*e, **23**, 2021, 19-25.
17. Somogyi, E, C. G. Tedeschi. Injury by electrical force. – In: *Forensic medicine* (Eds. C. G. Tedeschi, W. G. Eckert and L. G. Tedeschi) Vol. I. Philadelphia, WB, Saunders, 1977, pp. 645-676.
18. Türkoğlu, A., K. Sehlikoğlu, M. Tokdemir. A study of fatal falls from height. – *Journal of Forensic and Legal Medicine*, **61**, 2019, 17- 21.

Institute of Experimental Morphology, Pathology and Anthropology with Museum
Bulgarian Anatomical Society

Acta Morphologica et Anthropologica, 30 (3-4)
Sofia ● 2023

Atrophic Age-Related Changes in Cerebral Hemispheres: Euclidean Geometry Based Morphometry of MRI Brain Scans

Nataliia Maryenko, Oleksandr Stepanenko*

Department of Histology, Cytology and Embryology, Kharkiv National Medical University, Kharkiv, Ukraine

*Corresponding author e-mail: maryenko.n@gmail.com, ni.marienko@knmu.edu.ua

The aim of the present study was to conduct a comprehensive morphometric analysis of two-dimensional MRI brain images and determine the simple morphometric parameters of the cerebral hemispheres that best characterize quantitatively brain atrophic changes in normal aging. This study analyzed MRI brain scans from 100 apparently healthy individuals (44 males and 56 females) aged 18 to 86 years (mean age 41.72±1.58 years). For each brain investigation, five tomographic sections were selected, including four coronal and one axial. The perimeter, area values, and their derivative indices were determined. The study has shown that the parameter most sensitive to aging changes was the ratio of two area values: the area corresponding specifically to cerebral tissue and the area that captures the cerebral tissue and the sulcal content. The results of the present study can be used in clinical practice for the quantitative assessment of age-related atrophic changes in cerebral hemispheres.

Key words: aging, brain, cerebral hemispheres, morphometry, neuroimaging

Introduction

Throughout an individual's lifespan, atrophic changes may occur in various brain structures. Age-related alterations in cerebral hemispheres encompass the smoothing of the cerebral surface, the widening and deepening of sulci, a reduction in overall size, and the simplification of gyral shape [1-3, 5, 8, 9, 11, 13]. Atrophic brain changes can result from either normal or pathological aging processes. Notably, changes arising from neurodegenerative conditions, including Alzheimer's disease, can closely resemble those observed in the process of normal brain aging [4, 6, 7, 12]. Consequently, the ability to differentiate between normal and pathological brain aging holds considerable significance in clinical practice.

Currently, in clinical neuroimaging, the detection and characterization of brain atrophic changes are primarily descriptive and subjective. To enhance objectivity and facilitate the quantitative characterization of identified atrophic changes, various morphometric methods are employed, often drawn from classical morphology. In studies aiming to characterize atrophic changes in cerebral hemispheres quantitatively, the following parameters were utilized: volumes of gray and white matter [1-3, 8, 9, 11, 13], cortical thickness [3, 5, 8, 13], gyrification index (defined as the ratio of the total area of the cortical sulcal surface to the superficially exposed area of the cerebral hemispheres) [3, 5, 13], sulcal depth [3, 13], folding area [3], and fractal dimension [3-5, 8]. The morphometric determination of these parameters (except for fractal dimension) derives from Euclidean (traditional) geometry.

However, most of these parameters were determined using the analysis of three-dimensional magnetic resonance imaging (MRI) brain models. In clinical practice, two-dimensional MRI images are assessed for diagnostic purposes, and constructing three-dimensional brain models is not always feasible or practical. Therefore, simplified morphometric approaches are still required for their easy integration into clinical practice. Given this, our aim was to conduct a comprehensive morphometric analysis of two-dimensional MRI brain images and determine the simple morphometric parameters of the cerebral hemispheres that best characterize quantitatively brain atrophic changes in normal aging.

Material and Methods

This study analyzed MRI brain scans from 100 apparently healthy individuals (44 males and 56 females) aged 18 to 86 years (mean age 41.72±1.58 years). The participants of the study underwent diagnostic MRI brain scanning. The inclusion criterion was age 18 years and older. The patients with the presence of pathological structural changes in the brain and surrounding tissues were excluded from the study. Therefore, MRI data from patients who showed no evident brain pathology upon examination were considered relatively normal and were used in the present study. The study was conducted in accordance with the Declaration of Helsinki, and approved by the Commission on Ethics and Bioethics of Kharkiv National Medical University (No. 10 of Nov. 7, 2018) for studies involving humans. Written informed consent has been obtained from the participants of the study.

The MRI images were obtained using a Siemens Magnetom Symphony magnetic resonance scanner with a 1.5 Tesla magnetic induction and a 5 mm section thickness. Both T2 and FLAIR modes were employed. The digital MRI images had a spatial resolution of 72 pixels per inch, with an absolute image scale of 3 pixels = 1 mm.

For each brain investigation, we selected five tomographic sections, comprising four in the coronal (frontal) projection and one in the axial (horizontal) projection. These sections were chosen based on easy identification through anatomical landmarks and their correspondence to various regions of the cerebral hemispheres. The first coronal tomographic section (coronal 1) was located at the level of the anterior points

of the temporal lobes. The second (coronal 2) was at the level of the mammillary bodies. The third (coronal 3) was positioned at the level of the quadrigeminal plate. Due to the section thickness of 5 mm, coronal sections often captured both rostral and caudal colliculi; in cases where different tomographic sections captured either the rostral or caudal colliculi, the section with the well-recognizable rostral colliculi was selected. The fourth (coronal 4) section was located at the level of the splenium of the corpus callosum. The axial section was located at the level of the thalamus. Importantly, these sections corresponded to frequently observed sites of pathological changes in neurodegenerative diseases, including Alzheimer's disease [4].

After the selection of the tomographic sections, we provided morphometry using Adobe Photoshop CS5 software. In each image, we determined the perimeter (P), area (A), and derived indices based on them. To determine the perimeter and area, we employed the "selection" and "analysis" tools. We determined these values in two different ways (**Fig. 1A** and **B**). In the first approach (**Fig. 1A**), we outlined the tomographic sections based on their external (visible) surface, disregarding the sulci. This resulted in the perimeter (P_A), which corresponded to the contour of the visible surface of the cerebral hemispheres, and the area (A_A), representing the overall brain tissue, including the sulci content.

In the second approach (**Fig. 1B**), we outlined the entire pial surface on the tomographic sections, taking the sulci into account. This yielded the perimeter (P_B), corresponding to the contour of the pial surface of the cerebral hemispheres (including the contour inside sulci), and the area (A_B), representing the overall brain tissue (excluding the sulci content).

In addition, we computed several derived indices. Based on the perimeter and area values obtained using two different approaches, we calculated perimeter-to-area ratios (P_A/A_A and P_B/A_B) and shape factors (SF_A and SF_B). The shape factor was determined using the formula: $SF = (4\pi \times A)/P^2$ [10]. Furthermore, we computed the ratio of perimeter values (P_B/P_A) and the ratio of area values (A_B/A_A). The ratio of the two perimeters (P_B/P_A) can be considered a two-dimensional analogue of the gyrification index, as it quantifies the ratio of the total contour length of the cerebral hemispheres' surface to the length of the contour of their superficially exposed surface.

Statistical data processing was performed using Microsoft Excel 2016. Data underwent variation statistics analysis, calculating arithmetic mean (M), standard error (m), minimum (min), and maximum (max) values. The significance of statistical differences between morphometric parameters determined in different tomographic sections was assessed using the Kruskal–Wallis H test and post-hoc Dunn's test with Bonferroni adjustment for multiple comparisons. Interrelationships of the values of the morphometric parameters were assessed using the Pearson correlation coefficient (r) and its significance was evaluated using the Student T test. The significance level for all results was accepted as $p < 0.05$.

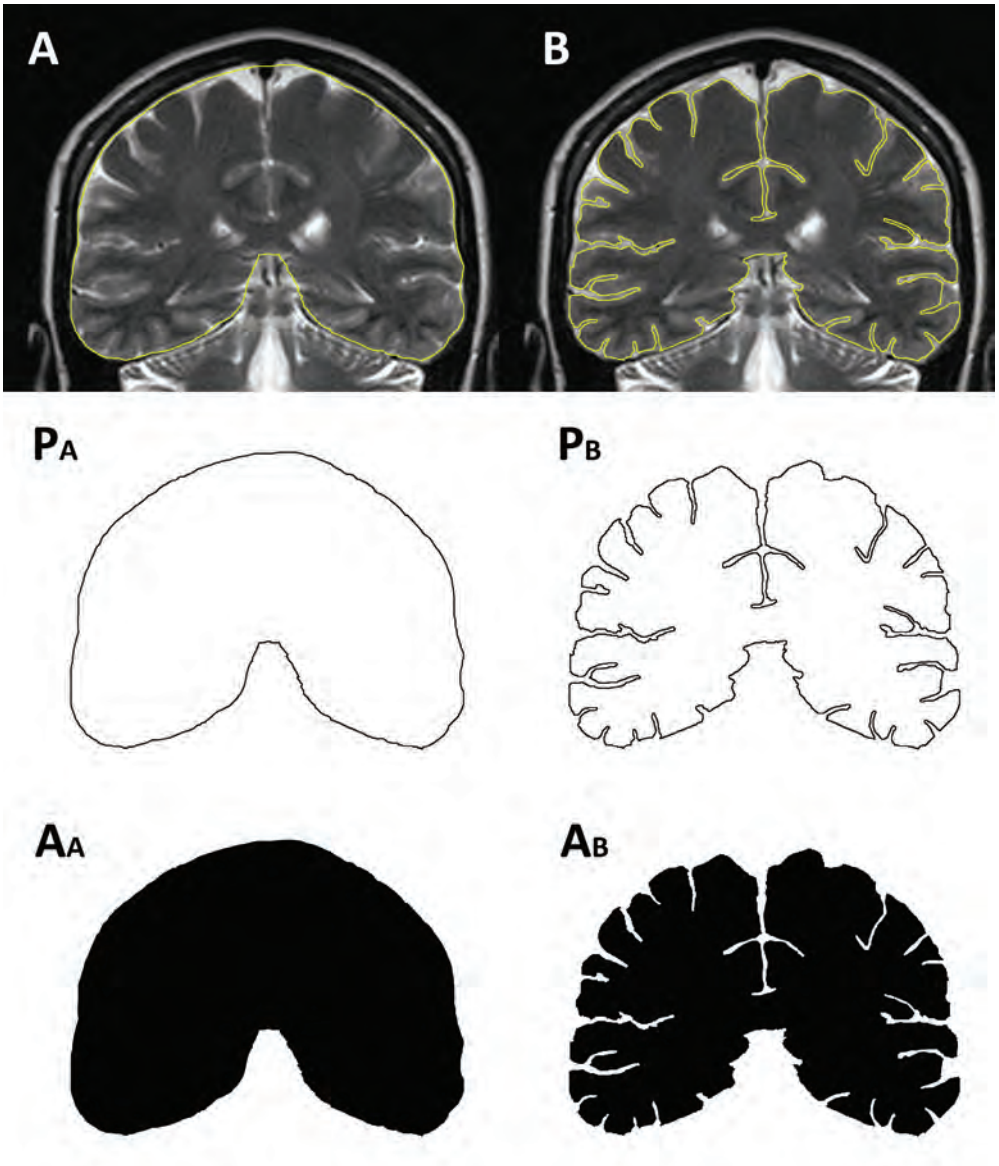

Fig. 1. MRI brain scan of 32 years old female individual, 3rd coronal section. Euclidean geometry based morphometry of cerebral hemispheres: determining area (A_A and A_B) and perimeter (P_A and P_B) values

Results

The descriptive statistics of the morphometric parameters are presented in **Table 1**. When comparing the values determined in different tomographic sections, it was found that the values of all parameters (except for the ratio of perimeters, P_B/P_A) differed

significantly, $p < 0.05$. The post-hoc test has shown that values of the morphometric parameters for the 2nd, 3rd, and 4th coronal sections did not differ significantly from each other. Meanwhile, the values of the 1st coronal section and axial section differed from the values of the 2nd-4th coronal sections. The difference between the values of the 1st coronal and axial sections was significant for all studied parameters except for the shape factor (SF_A) and the ratio of perimeters (P_B/P_A) – these values in the mentioned tomographic sections showed no significant difference. To reveal the peculiarities influencing the values of morphometric parameters, the correlation analysis was provided (**Fig. 2, Fig. 3, Table 2**).

Table 1. The values of the cerebral morphometric parameters

Morphometric parameter		Value	Tomographic section					
			Coronal 1	**Coronal 2**	**Coronal 3**	**Coronal 4**	**Axial**	**Average value**
P_A	Perimeter, cm	M	30.74	45.56	46.26	45.17	57.02	44.95
		m	0.14	0.21	0.20	0.19	0.42	0.17
		min	27.83	41.33	41.73	40.33	50.20	41.16
		max	34.40	50.83	51.90	50.50	72.30	49.49
A_A	Area, cm^2	M	57.24	103.59	103.81	102.17	196.98	112.76
		m	0.62	0.78	0.77	0.79	2.59	0.81
		min	44.97	87.06	87.24	85.31	155.23	93.34
		max	76.56	124.66	128.14	122.24	288.71	131.47
P_A/A_A	Ratio of perimeter and area	M	0.541	0.441	0.447	0.443	0.292	0.433
		m	0.004	0.002	0.002	0.002	0.002	0.002
		min	0.446	0.402	0.378	0.395	0.241	0.390
		max	0.668	0.501	0.502	0.500	0.327	0.479
SF_A	Shape Factor	M	0.760	0.627	0.610	0.629	0.760	0.677
		m	0.004	0.003	0.003	0.002	0.004	0.002
		min	0.605	0.556	0.527	0.565	0.644	0.599
		max	0.824	0.695	0.685	0.675	0.834	0.710
P_B	Perimeter, cm	M	85.69	124.47	128.03	122.64	158.95	123.96
		m	0.93	1.13	1.10	0.98	2.37	0.91
		min	68.67	99.63	107.17	92.07	118.43	102.51
		max	114.07	154.63	153.50	151.83	230.17	149.54

A_B	Area, cm^2	M	47.76	90.17	90.48	90.32	182.85	100.32
		m	0.59	0.77	0.71	0.73	2.35	0.75
		min	36.51	74.10	71.61	73.69	142.69	80.76
		max	65.22	109.88	108.95	109.41	265.36	117.24
P_B/A_B	Ratio of perimeter and area	M	1.809	1.387	1.421	1.363	0.876	1.371
		m	0.020	0.014	0.014	0.012	0.013	0.010
		min	1.379	1.083	1.111	1.088	0.613	1.143
		max	2.286	1.905	1.854	1.792	1.382	1.640
SF_B	Shape Factor	M	0.083	0.075	0.071	0.077	0.095	0.080
		m	0.002	0.001	0.001	0.001	0.002	0.001
		min	0.052	0.046	0.046	0.046	0.046	0.058
		max	0.129	0.112	0.103	0.125	0.163	0.106
P_B/P_A	Ratio of perimeter values (2D gyrification index)	M	2.785	2.732	2.767	2.715	2.788	2.757
		m	0.024	0.022	0.021	0.018	0.035	0.015
		min	2.279	2.211	2.359	2.238	2.148	2.443
		max	3.583	3.464	3.246	3.318	3.881	3.203
A_B/A_A	Ratio of area values	M	0.834	0.870	0.872	0.884	0.929	0.878
		m	0.004	0.003	0.003	0.003	0.002	0.003
		min	0.688	0.755	0.753	0.797	0.821	0.779
		max	0.911	0.923	0.927	0.934	0.955	0.925

The correlation analysis has shown that the values of the morphometric parameters had significant positive correlations when analyzing different tomographic sections (**Fig. 2**). The strongest correlation relationships were observed between adjacent coronal tomographic sections: the 1st and 2nd, 2nd and 3rd, and 3rd and 4th sections. The axial section had moderate to weak relationships with the values of the coronal sections. Considering that morphometric parameters primarily characterize the structural features of the brain, similar anatomical characteristics may influence values in the neighboring regions of the cerebral hemispheres. The parameters that showed the strongest correlations between different tomographic sections were the values of area (A_A and A_B) and their ratio (A_B/A_A).

When analyzing the relationships between different morphometric parameters (**Fig. 3**), it was found that both perimeter values (P_A and P_B), as well as both area values (A_A and A_B), had significant positive correlation relationships with each other in all the studied sections. The values of both perimeter-to-area ratios (P_A/A_A and P_B/A_B), while interrelated by a positive correlation, had negative relationships with most of the studied parameters. The shape factor values (SF_A and SF_B) had weak positive relationships with each other and mainly weak negative relationships with other parameters. The ratio of two perimeters (P_B/P_A), or two-dimensional gyrification index, showed the strongest

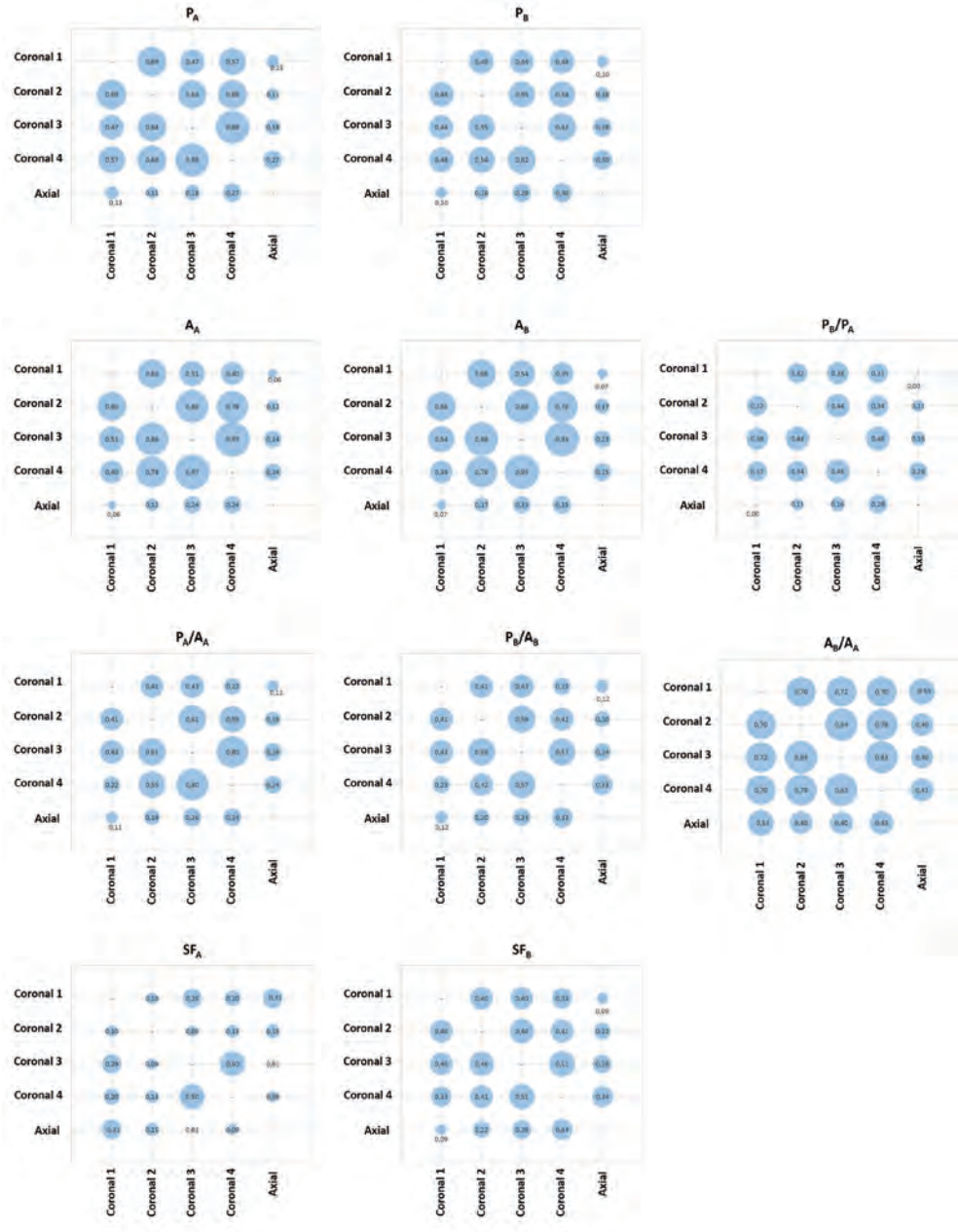

Fig. 2. Correlation relationships of cerebral morphometric parameters of different tomographic sections; the correlation matrix displays the Pearson correlation coefficient (r) values.

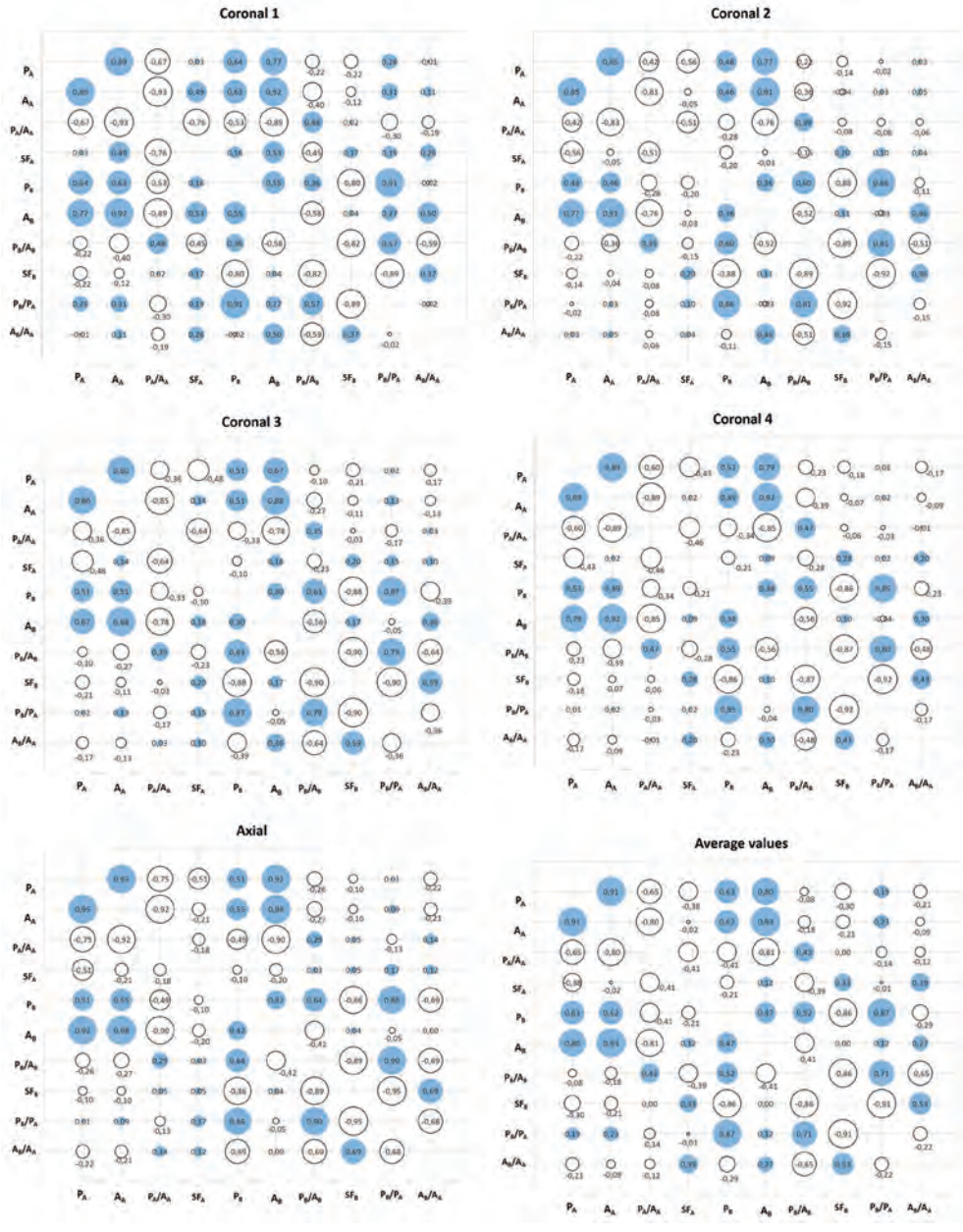

Fig. 3. Correlation relationships of cerebral morphometric parameters; the correlation matrix displays the Pearson correlation coefficient (r) values

relationships with perimeter P_B and the value of P_B/A_B. The ratio of two areas (A_B/A_A) exhibited diverse correlations with other studied parameters.

To identify the parameter that most accurately describes age-related changes, we calculated correlation coefficients between the values of the studied parameters and age (**Table 2**).

Table 2. Correlation coefficients (r) characterizing relationships between cerebral morphometric parameters and age

		Tomographic section					
		Coronal 1	**Coronal 2**	**Coronal 3**	**Coronal 4**	**Axial**	**Average value**
P_A	Perimeter, cm	-0.164	-0.036	0.130	0.090	-0.067	-0.020
A_A	Area, cm^2	-0.191	-0.159	-0.053	0.013	-0.141	-0.159
P_A/A_A	Perimeter-to-area ratio	0.199*	0.247*	0.195	0.058	0.217*	0.260**
SF_A	Shape Factor	-0.111	-0.194	-0.293**	-0.171	-0.180	-0.316**
P_B	Perimeter, cm	-0.232*	-0.171	0.000	-0.104	0.016	-0.104
A_B	Area, cm^2	-0.396***	-0.385***	-0.347***	-0.197*	-0.219*	-0.382***
P_B/A_B	Perimeter-to-area ratio	0.234*	0.172	0.281**	0.088	0.205*	0.290**
SF_B	Shape Factor	-0.027	-0.031	-0.190	-0.030	-0.143	-0.133
P_B/P_A	Ratio of perimeter values (2D gyrification index)	-0.196*	-0.174	-0.073	-0.173	0.065	-0.143
A_B/A_A	Ratio of area values	-0.567***	-0.582***	-0.630***	-0.536***	-0.378***	-0.645***

Note: * – $p<0.05$; ** – $p<0.01$; *** – $p<0.001$

Most of the studied parameters exhibited negative correlation relationships with age, except for both perimeter-to-area ratios (P_A/A_A and P_B/A_B), which showed weak positive correlation relationships. Both perimeter values, as well as both area values, slightly decreased with age, reflecting an overall decrease in brain size during aging. Both shape factor values had weak relationships with age, indicating that the cerebral

shape did not change significantly. An interesting finding is that the two-dimensional gyrification index (P_B/P_A) was not significantly affected by age-related changes.

The strongest negative relationships with age were exhibited by the ratio of area values (A_B/A_A), and these relationships exceeded the relationships exhibited by the area values separately. Considering that the area value A_B has shown a more intensive decrease than the A_A value, we can conclude that the difference between these two areas increases with age. The A_A value captures the entire area of the hemispheres, while the A_B value does not capture the area corresponding to the sulcal content. With the widening and deepening of the sulci during aging, the area occupied by sulcal content increases, and the difference between area values (A_A and A_B) increases in turn. Thus, age-related brain atrophic changes result in a decrease in the space in the cranial cavity filled by the cerebral tissue. Based on this, we can conclude that the ratio of two areas was the most accurate and sensitive parameter among those studied to characterize quantitatively age-related atrophic changes in cerebral hemispheres. We calculated confidence intervals for the A_B/A_A values (**Fig. 4**), which can be used as norm criteria for the assessment of the results of brain morphometry.

Discussion

In this study, we have conducted a comprehensive morphometric analysis focused on selecting the most sensitive parameter for detecting age-related changes. The morphometric assessment of age-related changes in cerebral hemispheres utilizing the morphometric approaches deriving from Euclidean geometry was employed in number of studies. The studies closest to the present one included analyses of the cerebral surface [5, 13] and analyses based on the volumetric indices [1, 2, 8, 9, 11, 13].

The study of F. Zheng et al. [13] has shown age-related decrease in the cortical thickness and local gyrification index as well as a decrease in the gray and white matter volumes ($r^2 > 0.16$). In the study by C.R. Madan and E.A. Kensinger [5], it was noted that certain morphometric parameters exhibited negative correlations with age: mean cortical thickness ($r = – 0.603$) and gyrification index ($r = – 0.494$). Thus, in these studies, it was revealed that the three-dimensional gyrification index decreased with age, while our study has shown weak correlations between age and the two-dimensional gyrification index. This difference in findings can be explained by differences in methodologies: the three-dimensional determination of the gyrification index captures the entire cerebral surface, while the two-dimensional variant characterizes individual tomographic sections.

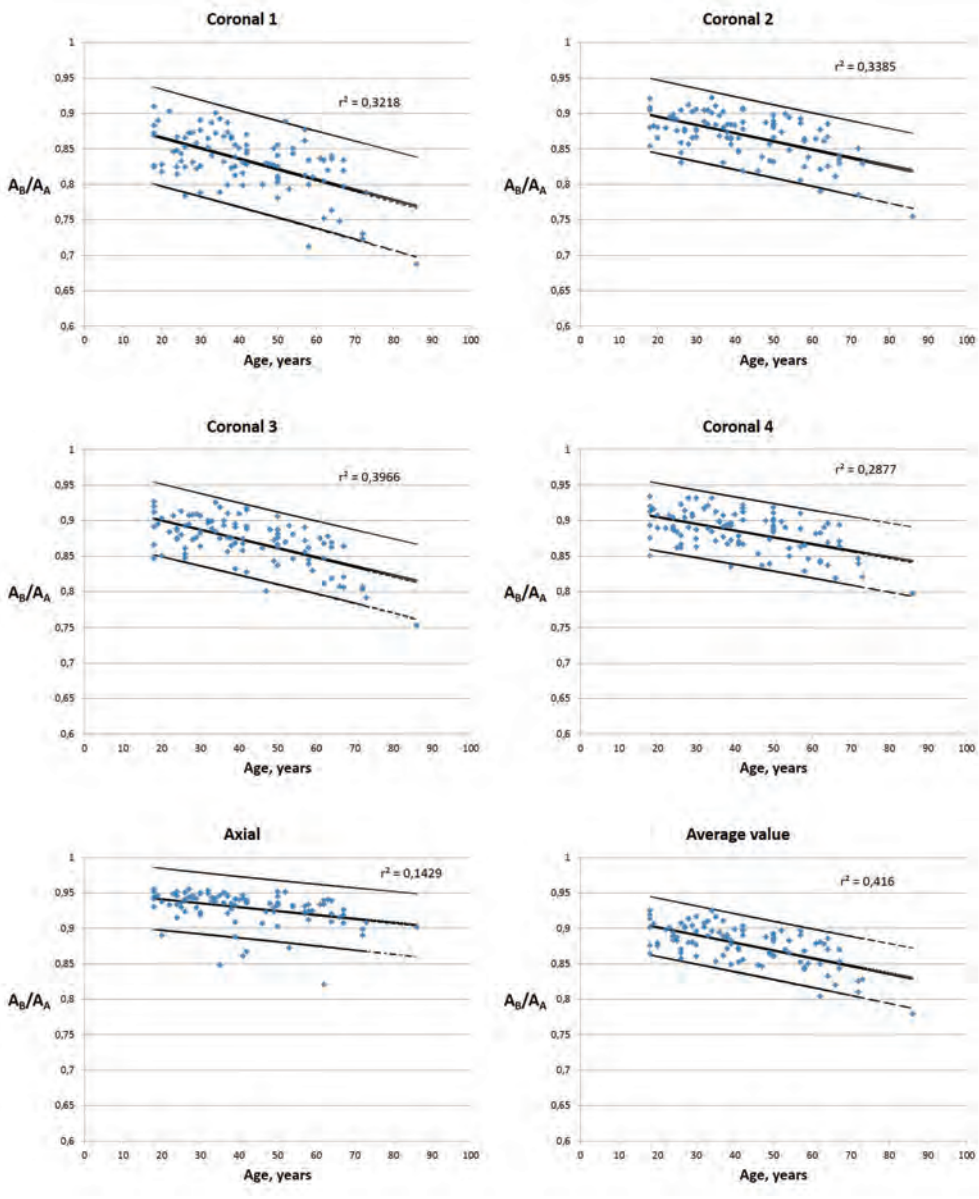

Fig. 4. Age dynamics and confidence intervals of the A_B/A_A values (ratio of area B and area A values)

The studies of Y. Ge et al. [1], R. Riello et al [9], and K. B. Walhovd et al. [11] have demonstrated age-related decrease in the volumes of gray and white matter. The study by P. Podgórski et al. [8] also demonstrated decrease in volumes of total gray matter and white matter; additionally, the study describes decrease in cortical thickness, gyrification index, and increase in the volume of cerebrospinal fluid as

well as sulcal depth. Another volumetric study by C. D. Good et al. [2] demonstrated a significant decrease in gray matter volume ($r^2 = 0.489$), while the decline in white matter volume was considered insignificant by the authors ($r^2 = 0.326$). The authors also revealed an increase in the volume of cerebrospinal fluid ($r^2 = 0.377$).

We did not find in the accessible literature the application of a parameter similar to the ratio of two areas used in the present study. Given that the difference between two area values and their ratio depends mainly on sulcal depth and width, the deepening and widening of sulci in aging lead to an increase in the area ratio (as described in our study), as well as an increase in the volume of cerebrospinal fluid filling the sulci [2, 8]. Thus, the age-related changes in area ratio A_B/A_A correspond to the changes in the volume of cerebrospinal fluid; moreover, both parameters exhibited close values of the correlation coefficient characterizing the relationships with age ($r^2 = 0.416$ and $r^2 = 0.377$ [2], respectively). Therefore, this parameter introduced in the present study may become a useful additional parameter for the quantitative assessment of the atrophic changes in cerebral hemispheres.

Conclusions

The study has shown that the parameter most sensitive to aging changes was the ratio of two area values: the area corresponding to cerebral tissue and the area that captures the sulcal content. The results of the present study can be used in clinical practice for the quantitative assessment of age-related atrophic changes in cerebral hemispheres.

References

1. **Ge, Y., R. I. Grossman, J. S. Babb, M. L. Rabin, L. J. Mannon, D. L. Kolson.** Age-related total gray matter and white matter changes in normal adult brain. Part I: volumetric MR imaging analysis. – *AJNR Am. J. Neuroradiol.*, **23**(8), 2002, 1327-1333.
2. **Good, C. D., I. S. Johnsrude, J. Ashburner, R. N. Henson, K. J. Friston, R. S. Frackowiak.** A voxel-based morphometric study of ageing in 465 normal adult human brains. – *NeuroImage*, **14**(1 Pt 1), 2001, 21–36.
3. **Im, K., J. M. Lee, U. Yoon, Y. W. Shin, S. B. Hong, I. Y. Kim, J. S. Kwon, S. I. Kim.** Fractal dimension in human cortical surface: multiple regression analysis with cortical thickness, sulcal depth, and folding area. – *Hum. Brain Mapp.*, **27**(12), 2006, 994-1003.
4. **King, R. D., A. T. George, T. Jeon, L. S. Hynan, T. S. Youn, D. N. Kennedy, B; the Alzheimer's Disease Neuroimaging Initiative.** Characterization of Atrophic Changes in the Cerebral Cortex Using Fractal Dimensional Analysis. – *Brain Imaging Behav.*, **3**(2), 2009, 154-166.
5. **Madan, C. R., E. A. Kensinger.** Cortical complexity as a measure of age-related brain atrophy. – *Neuroimage*, **134**, 2016, 617-629.
6. **Matsuda, H.** MRI morphometry in Alzheimer's disease. – *Ageing Res. Rev.*, **30**, 2016, 17-24.
7. **Pini, L., M. Pievani, M. Bocchetta, D. Altomare, P. Bosco, E. Cavedo, S. Galluzzi, M. Marizzoni, G. B. Frisoni.** Brain atrophy in Alzheimer's Disease and aging. – *Ageing Res. Rev.*, **30**, 2016, 25-48.

8. **Podgórski, P., J. Bladowska, M. Sasiadek, A. Zimny.** Novel Volumetric and Surface-Based Magnetic Resonance Indices of the Aging Brain - Does Male and Female Brain Age in the Same Way? – *Front. Neurol.,* **12**, 2021, 645729.
9. **Riello, R., F. Sabattoli, A. Beltramello, M. Bonetti, G. Bono, A. Falini, G. Magnani, G. Minonzio, E. Piovan, G. Alaimo, M. Ettori, S. Galluzzi, E. Locatelli, M. Noiszewska, C. Testa, G. B. Frisoni.** Brain volumes in healthy adults aged 40 years and over: a voxel-based morphometry study. – *Aging Clin. Exp. Res.,* **17**(4), 2005, 329-336.
10. **Underwood, E. E.** *Quantitative Stereology.* London: Addison-Wesley; 1970.
11. **Walhovd KB, A. M. Fjell, I. Reinvang, A. Lundervold, A. M. Dale, D. E. Eilertsen, B. T. Quinn, D. Salat, N. Makris, B. Fischl.** Effects of age on volumes of cortex, white matter and subcortical structures. – *Neurobiol. Aging*, **26**(9), 2005, 1261-1270; discussion 1275-1278.
12. **Whitwell, J. L.** Alzheimer's disease neuroimaging. – *Curr. Opin. Neurol.*, **31**(4), 2018, 396-404.
13. **Zheng, F., Y. Liu, Z. Yuan, X. Gao, Y. He, X. Liu, D. Cui, R. Qi, T. Chen, J. Qiu.** Age-related changes in cortical and subcortical structures of healthy adult brains: A surface-based morphometry study. – *J. Magn. Reson. Imaging*, **49**(1), 2019, 152-163.

Institute of Experimental Morphology, Pathology and Anthropology with Museum
Bulgarian Anatomical Society

Acta Morphologica et Anthropologica, 30 (3-4)
Sofia ● 2023

ANTHROPOLOGY AND ANATOMY 30 (4)

Original Articles

Comparative Assessment of Basic Anthropometric Features in Normal and Low Birth Weight Newborns (preliminary results)

Yanitsa Zhecheva[1], Ivaila Yankova Ivanova – Pandourska[1], Albena Dimitrova[1], Racho Stoev[1], Boyan Kirilov[1], Rayna Georgieva[2]*

[1] Institute of Experimental Morphology, Pathology and Anthropology with Museum, Bulgarian Academy of Sciences, Sofia, Bulgaria
[2] Institute of Information and Communication Technologies, Bulgarian Academy of Sciences, Bulgaria

*Corresponding author e-mail: janicca@gmail.com

The aim is to characterize the anthropometric and nutritional status of Bulgarian neonates with normal and low birth weight and to assess sexual differences. The data of 3086 neonates (1587 boys, 1499 girls) born in 2010 are gathered from the birth registry of Ist Obstetrics and Gynecology Hospital "St. Sofia" in Sofia. Newborns are classified as Normal Birth Weight (birth weight ≥ 2500 g to 4499 g) and Low Birth Weight (birth weight from 1500 g to 2499 g). Data of birth weight, length and BMI are analyzed, sexual differences in both groups are assessed. The neonates with NBW have significantly higher values of investigated features compared to LBW newborns. Sexual differences in LBW group are slightly expressed while in NBW group they are statistically significant. The results are valuable and could serve as a basis for development of national sex specific reference values for weight, length and BMI at birth in NBW and LBW newborns.

Key words: newborns, normal birth weight, low birth weight, birth length, sex differences

Introduction

Newborn sizes reflect fetal growth and development and are predictor of health throughout its life course [6]. Impaired fetal growth is associated with structural and functional anomalies that predispose individuals to cardiovascular and metabolic diseases at different stages of postnatal life [5, 13]. The assessment of weight and length as indicators of the health status of the newborn is essential for planning appropriate, timely interventions especially in neonates born preterm or with low birth weight. Preterm and low birth weight infants have a 2- to 10-fold higher risk of mortality than infants born at term and with normal birth weight [15]. In our country investigations of newborns are scarce and very rare they include data about low birth weight infants. The **aim** of the study is to characterize the anthropometric and nutritional status of Bulgarian neonates with normal and low birth weight and to assess sexual differences.

Material and Methods

The data used are gathered from the birth registry of First Obstetrics and Gynecology Hospital "St. Sofia" on the territory of Sofia and include all life births in the hospital for 2010. The birth weight and length are measured immediately after birth by professional obstetrics.

Data about 3086 newborns (1587 boys and 1499 girls) are included in the analysis. According to their birth weight newborns are classified as Normal Birth Weight (NBW) – weight range from 2500 g to 4499 g and Low Birth Weight (LBW) – 1500 g – 2499 g.

We exclude infants with very low (under 1500 g), extremely low (under 1000 g) and high birth weight (over 4500 g), newborns from multiple pregnancies and infants with syndromic and congenital anomalies affecting in utero growth (**Table 1**).

Table 1. Characteristic of the sample before the analysis

Sex	Newborns from multiple pregnancies*	Extremely low birth weight*	Very low birth weight*	Low birth weight	Normal birth weight	High birth weight*
		< 1000g	1000-1500g	1500-2499g	2500-4499g	≥ 4500g
Male	67	2	1	97	1490	10
Female	60	2	4	119	1380	3
Total	127	4	5	216	2870	13

*Data excluded from the analysis

BMI is calculated by the formula: BMI = weight (kg) ÷ height^2 (meters)

The sexual differences are evaluated in absolute differences and in relative index units (IU) by the formula of Wolanski for inter-group comparisons, called for the purposes of this study Index of Sexual Differences (ISD):

$$ISD = \frac{2 \times (\text{mean boys} - \text{mean girls})}{(\text{mean boys} + \text{mean girls})} \times 100$$

The index gives a quantitative assessment of the sexual differences, allowing comparisons between features of different dimensions, such as body weight (kg) and body length (cm). Sexual differences are assessed in index units (IU), which positive values show priority for boys and negative ones – priority for girls.

The statistical analyses are performed using SPSS 16.0. The significance of absolute sexual differences is assessed by Student's t-test ($p \leq 0.05$).

The study was conducted in accordance with the principles of Declaration of Helzinki (World Medical Association, Declaration of Helsinki. Ethical Principles for Medical Research Involving Human Subjects.WMJ. 2008; 54(4):122-125.) and after approval by the Ethical Committee of Institute of Experimental Morphology, Pathology and Anthropology with Museum – Bulgarian Academy of Sciences.

Results and Discussion

The anthropometric characteristic of NBW and LBW newborns from Sofia is made on the basis of three main anthropometric variables (body weight, body length and BMI), assessing their physical development and nutritional status. Differences between NBW and LBW newborns are discussed as well as sexual differences in both investigated groups.

Differences in anthropometric characteristic of NBW and LBW newborns

Values of investigated features in NBW and LBW newborns are presented on Table 2. As expected, means are significantly lower in LBW than those in NBW ($p \leq 0.05$). Normal birth weight male and female infants are heavier with 1039.3 g and 921.4 g, compared to low birth weight male and female infants. Similar results are established in regard to birth length, which mean values are higher in male and female newborns from NBW group, compared to those of LBW infants with/by 4.5 cm and 3.9 cm, respectively (**Table 2; Fig. 1**).

It is interesting to be noted that differences in birth weight and length between LBW and NBW male infants are quite bigger than that established between girls from different weight groups. This could be related to the reported in other studies evidences that male LBW newborns are less stable after birth and are more vulnerable to perinatal and postnatal mortality and morbidity [11, 2].

Table 2. Statistical data of investigated features in neonates with normal and low birth weight

Sex	Normal birth weight (2499-4999g)					Low birth weight (1500-2499g)					Differences NBW/LBW	
											Male	Female
Birth weight (g)												
	N	mean	SD	min	max	N	mean	SD	min	max		
Male	1490	3326.9	381.8	2550.0	4550.0	97	2287.6	225.6	1550	2490	1039.3*	921.4*
Female	1380	3228.1	369.8	2500.0	4450.0	119	2306.7	208.4	1650	2480		
Birth length (cm)												
Male	1490	50.1	1.7	45.0	57.0	97	45.6	2.2	34	50	4.5*	3.9*
Female	1380	49.6	1.6	45.0	55.0	119	45.7	1.7	40	51		
BMI (kg/m^2)												
Male	1490	13.2	1.0	10.0	17.2	97	11.0	1.0	8.1	13.8	2.2	2.1
Female	1380	13.1	1.0	10.6	16.5	119	11.0	0.9	8.5	12.8		

*Statistically significant differences at p≤0.05; NBW – normal birth weight; LBW – low birth weight

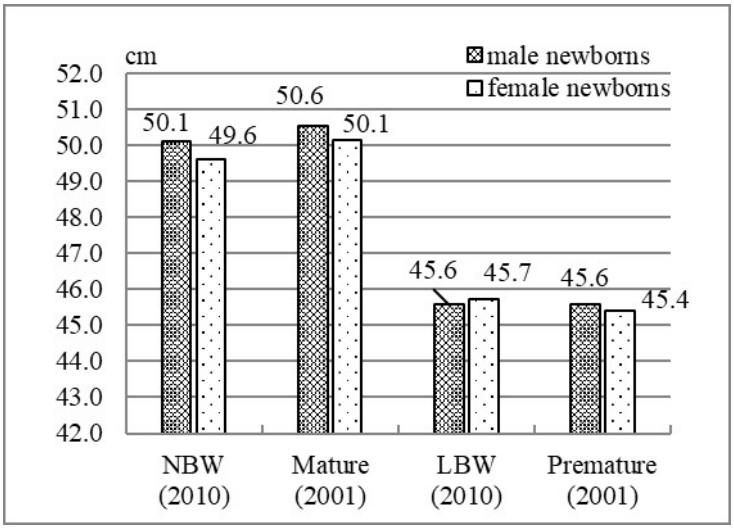

Fig. 1. Birth length in neonates with normal and low birth weight – comparison with 2001 data

Assessing the relationship between birth weight and length, BMI is accepted as appropriate measure of the nutritional status and adiposity during pediatric years [14, 12].

BMI mean values are very similar in both sexes, also showing significantly higher values (with 2 kg/m^2) for NBW infants than LBW ones. Significantly higher

values in NBW newborns compared to LBW newborns are also reported by other authors [7, 8, 17].

Table 3. Sex differences in neonates with normal and low birth weight

	Normal birth weight (2499-4999g)		**Low birth weight (1500-2499g)**	
	Absolute differences	ISD (IU)	Absolute differences	ISD (IU)
Birth weight	98.8g*	3.0	19.10g	-0.8
Birth length	0.5cm*	1.0	0.1cm	-0.2
BMI	0.1 kg/m^2	0.8	0.0 kg/m^2	-0.1

*Statistically significant differences at p≤0.05

Sexual differences in NBW and LBW groups – comparative assessment

In NBW newborns sexual differences are clearly expressed both in body weight and body length and are statistically significant (p≤0.05) as male infants show priority over girls. Concerning body nutritional status assessed by the BMI, statistically significant differences are not established, the mean of the index is 13.2 kg/m^2 and 13.1 kg/m^2 in male and female newborns respectively (**Table 3, Figs. 1, 2, 3**). Our results are similar to those reported by other authors in national and international studies [3, 16]. A study of Bulgarian newborns from Smolyan shows no significant differences depending on sex in body length and body weight at birth [10].

In LBW group sexual differences are slightly expressed and are not statistically significant for all three examined variables. The smallest differences are established for BMI.

While in NBW group the values of the anthropometric features are significantly greater in male newborns, in the LBW group, although small, the established differences are found to be with priority for girls (**Table 3, Figs. 1, 2, 3**). Similar results were found in an earlier study of newborns from Sofia [16], which demonstrated minimal priority of LBW female neonates for body weight, BMI, as well as in a number of other investigated anthropometric features. Data about body length shows that LBW male newborns are slightly, insignificantly longer than LBW females.

Most of the studies in the specialized literature do not establish similar advantage of the female sex in LBW infants [1, 4], which could be due to the use of different classification of neonates at birth – on gestational age or on birth weight. Both are considered to be helpful for counseling, clinical management and research [9], but the use of different classification makes the comparison between studies difficult and even impossible giving not accurate, biased results.

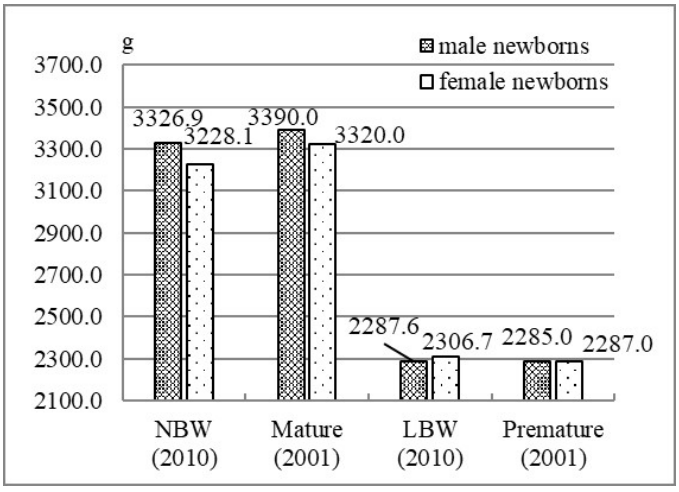

Fig. 2. Birth weight in neonates with normal and low birth weight – comparison with 2001 data

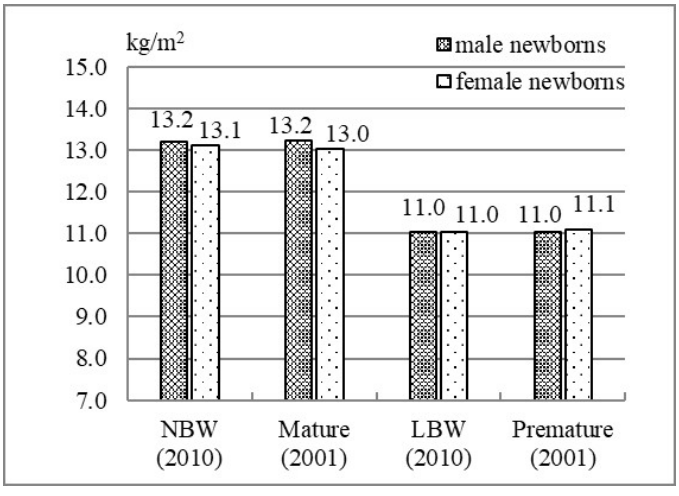

Fig. 3. BMI in neonates with normal and low birth weight – comparison with 2001 data

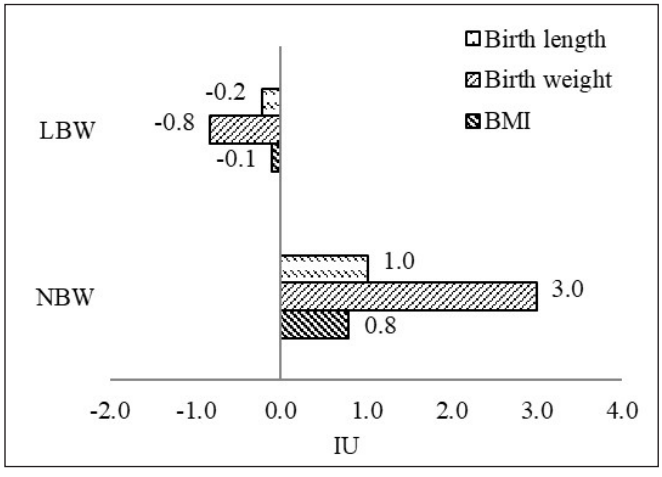

Fig. 4. Sex differences assessed by the ISD

The use of the ISD allows the comparison between the three investigated features, and expresses sexual differences in IU. Data are presented on **Fig. 4**. It is clearly observed that in both examined groups – NBW and LBW, differences between sexes are most pronounced in birth weight, followed by birth length and in the least extent sex is related to the BMI (**Table 3, Fig. 4**).

We compared our results with results from a study of newborns conducted in 2001 in Sofia [16], which used the same methodic and births are classified according to body weight as "preterm" (birth weight < 2500 g) and "mature" (birth weight ≥ 2500 g) corresponding to LBW and NBW groups respectively in our study. The comparison between NBW group in present study and "mature" newborns from 2001 as well as between LBW group and premature newborns study demonstrates similar means of the investigated features. However it should be noted that in NBW (mature) group mean values of birth weight and birth length in 2010 born neonates are lower. Male and female newborns are lighter with 63,1 g and with 91,9 g, respectively and shorter with 0,5 cm.

Lower values of birth weight are also observed in LBW (premature) neonates born in 2010 but the difference is insignificant (2,6 g in boys and 19,7 g in girls). Concerning length at birth, a minimal change of -0.3 cm is found, only in female newborns.

Mean values of BMI are similar in both investigated years – approximately 13.0 кg/m^2 in NBW (mature) group and 11.0 кg/m^2 in LBW (premature) group.

Conclusion

The data presented characterize anthropometrically the physical development and nutritional status of neonates with NBW and LBW born in 2010. NBW infants have significantly higher values of investigated features compared to LBW newborns. Sex specific differences in anthropometric characteristic in both NBW and LBW groups are established. Sexual differences in neonates with low birth weight are slightly expressed while in NBW newborns they are statistically significant. The peculiarities of LBW newborns are described adding a new knowledge about this specific population group.

Compared to mature and premature neonates born in 2001, mean values of the three investigated variables are lower in NBW neonates born in 2010, in LBW group differences are not observed. The results obtained are valuable and could serve as a basis for development of national sex specific reference values for weight, length and BMI at birth in NBW and LBW newborns.

Acknowledgements: The work was supported by the Bulgarian National Science Fund (Grant No КП-06-Н51/7 – 11.11.2021).

Refferences

1. **Azcorra, H., F. Dickinson, N. Mendez-Dominguez, R. Mumm, G. Valentín.** Development of birthweight and length for gestational age and sex references in Yucatan, Mexico. – *Am. J. Hum. Biol*., **34**(6), 2022, e23732. doi: 10.1002/ajhb.23732.
2. **Brothwood, M., D. Wolke, H. Gamsu, J. Benson, D. Cooper.** Prognosis of the very low birthweight baby in relation to gender. – *Arch. Dis. Child*, **61**, 1986, 559-564.
3. **Cole, T. J., M. C. Bellizzi, K .M. Flegal, W. H. Dietz.** Establishing a standard definition for child overweight and obesity worldwide: international survey. – *BMJ*, **320** (7244), 2000, 1240-1243.
4. **Fenton, T. R., J. H. Kim.** A systematic review and meta-analysis to revise the Fenton growth chart for preterm infants. – *BMC Pediatrics*, **13**, 2013, 59. doi.org/10.1186/1471-2431-13-59.
5. **Gluckman, P., M. Hanson, C. Cooper, K. Thornburg.** Effect of in utero and early-life conditions on adult health and disease. - *New England Journal of Medicine*, **359** (1), 2008, 61-73.
6. **Hack, M., D. J. Flannery, M. Schluchter, L. Cartar, E. Borawski, N. Klein.** Outcomes in Young Adulthood for Very-Low-Birth-Weight Infants, - *N. Engl. J. Med.*, **346**, 2002, 149-157.
7. **Hilaire, M., X. D. Andrianou, A. Lenglet, C. Ariti, K. Charles, S. Buitenhuis, D. Van Brusselen, H. Roggeveen, E. Ledger, R. S. Denat, L. Bryson.** Growth and neurodevelopment in low birth weight versus normal birth weight infants from birth to 24 months, born in an obstetric emergency hospital in Haiti, a prospective cohort study. – *BMC Pediatr.*, **21**, 2021.
8. **Kamburova, M.** Risk factors for prematurity birth and their impact on health and social needs in the development of children up to 3 – years. *PhD thesis*, Medical University – Pleven, 2014, p. 189. [in Bulgarian]
9. **Karnati, S., S. Kollikonda, J. Abu-Shaweesh.** Late preterm infants - Changing trends and continuing challenges. – *Int. J. Pediatr. Adolesc. Med.*, **7**(1), 2020, 36-44.
10. **Mladenova, S.** Anthropological characteristics of growth and development processes in Smolyan childrenand adolescents in contemporary living conditions. *PhD thesis*, Plovdiv University Paisii Hilendarski, 2003, p. 193.
11. **Stevenson, D. K., J. Verter, A. A. Fanaroff, W. Oh, R. A. Ehrenkranz, S. Shankaran, E. F. Donovan, L. L. Wright, J. A. Lemons, J. E. Tyson, S. B. Korones, C. R. Bauer, B. J. Stoll, L. A. Papile.** Sex differences in outcomes of very low birthweight infants: the newborn male disadvantage. – *Arch. Dis. Child Fetal Neonatal. Ed.*, **83**, 2000, 182-185.
12. **Tanaka, T., A. Matsuzaki, R. Kuromaru, N. Kinukawa, Y. Nose, T. Matsumoto, T. Tara**. Association between birth weight and body mass index at 3 years of age. – *Pediatr. Int.*, **43**, 2001, 641-646.
13. **Thornburg, K.** The programming of cardiovascular disease. - *Journal of Developmental Origins of Health and Disease*, **6**(5), 2015, 366-349.
14. **Van't Hof, M. A., F. Haschke.** Euro-Growth references for body mass index and weight for length. Euro-Growth Study Group. – *J. Pediatr. Gastroenterol. Nutr.*, **31** Supl. 1, 2000, 48-59.
15. WHO recommendations for care of the preterm or low birth weight infant. Geneva: World Health Organization; 2022, p. 75. Licence: CC BY-NC-SA 3.0 IGO
16. **Yankova, I.** Anthropological characteristics of newborn infants in Sofia at the beginning of the XXI Century. *PhD thesis*, Institute of Experimental Morphology and Anthropology with Museum, BAS, 2005, p. 199. [in Bulgarian]
17. **Yankova, I., E. Hristova, A. Nacheva.** Anthropometric characteristics and intersexual differences in full-term and preterm newborns – *Acta Morphol. Anthropol.*, **11**, 2006, 91-97.

Institute of Experimental Morphology, Pathology and Anthropology with Museum
Bulgarian Anatomical Society

Acta Morphologica et Anthropologica, 30 (3-4)
Sofia ● 2023

Association Between Foot Arch Index and Other Morphometric Indices

Meglena Angelova, Desislava Marinova, Veselina Zhekova, Stoyan Pavlov*

Dept. Anatomy and cell biology, Medical University "Prof. Dr. P. Stoyanov" – Varna, Bulgaria

*Corresponding author e-mail: angelovameglena@gmail.com

The foot morphology is crucial for the normal functioning of the locomotor system. Footprints of randomly selected 150 Bulgarians aged 18 to 60 years were collected. We examined the morphological features of each foot by measuring the arch index, the Clarke angle and the Chippaux-Smirak index. Our results showed a greater incidence of high arched foot versus low arched foot. The study of the arch index once again confirmed the association of the Morton's toe foot with a high medial arch. In the group with high arched foot, BMI was lower than that in the other groups. Further investigation of the relations between BMI and arch index found no significant correlation between them. We found a particularly well-expressed correlation between the arch index and Chippaux-Smirak index. Our findings gave us reason to assume that the measurement of Chippaux-Smirak index can successfully replace the measurement of arch index.

Key words: foot, foot indices, arch index

Introduction

The human foot is characterized by unique features. These features have evolved over time to allow humans to stand upright and walk bipedally [10]. In the different phases of this gait, the foot changes its biomechanics and turns from a flexible structure that adapts to the surface into a rigid lever. This is possible because of the arches of the foot. They not only redistribute the weight of the body, but also ensure the different mobility of the individual parts of the foot [2].

The importance of the two longitudinal arches and the transverse arch is well known and generally recognized. The study of these arches has led to the identification of three main types of human foot – normal, high-arched and low-arched foot. The assessment of foot morphology most often relies on clinical observation and

different measurement methods. The classic method for studying foot morphology is through footprints (plantograms) and the measurement of various morphometric indices. This methodology is the basis of the development of digital methods, such as the podoscope, as well as the basis of dynamic studies of the foot and its 3D reconstructions [5].

Materials and Methods

Footprints (plantograms) of randomly selected 150 Bulgarian men and women, without malformations, surgery or traumas of the foot, aged 18 to 60 years were collected after their written consent. The female participants were 86, and the male ones – 64. The study was approved by the Research Ethics Committee at the Medical University "Prof. Dr. P. Stoyanov" with protocol No 140/01.07.2021. All participants filled out a survey in which they also noted their height and weight. The body Mass Index (BMI) was calculated based on these data. BMI between 22-25 was considered as normal, below 22 – as low and above 25 – as high. Each plantogram was studied using different measurements – Clarke angle, the Chippaux-Smirak index and the arch index.

Clarke's angle is the angle between the tangent line joining the medial edges of the first metatarsal head and the heel, and the second line that connects the first metatarsal head and the innermost point of the medial longitudinal arch concavity. If the Clarke's angle value is between 42° and 54° the foot is normal. High-arched foot presents with Clarke's angle more than 54° and the low-arched one with Clarke's angle value less than 41° (**Fig. 1A**).

Chippaux-Smirak index was measured as follows: 1) the distance between the outermost point of the first metatarsal in the medial and the outermost point of the fifth metatarsal was measured (maximum metatarsal foot width); 2) at the narrowest point of the foot arch the width was measured using a line parallel to the first one; 3) Chippaux-Smirak index was defined as a ratio between these two lines. In the cases with Chippaux-Smirak index between 25% and 45% the foot was considered as normal. If the Chippaux-Smirak index was more than 45% the foot was described as flat or low-arched foot (pes planus) and when the index was less than 25% - as high arched foot (**Fig. 1B**).

The arch index is the ratio of the area of the middle third of the foot to the whole footprint area with toes excluded. This was calculated as follows: 1) a line was drawn between the heel center and the base of the second toe; 2) the footprint was divided into three equal parts via lines perpendicular to the first one; 3) the area of the middle part and the area of the entire footprint were measured with ImageJ software; 4) the arch index was calculated **(Fig. 1C)**. The normal foot was defined by arch index scores between 0,21 and 0,28. The high-arched foot had arch index value less than 0,21, and the low-arched foot – more than 0,28 [6].

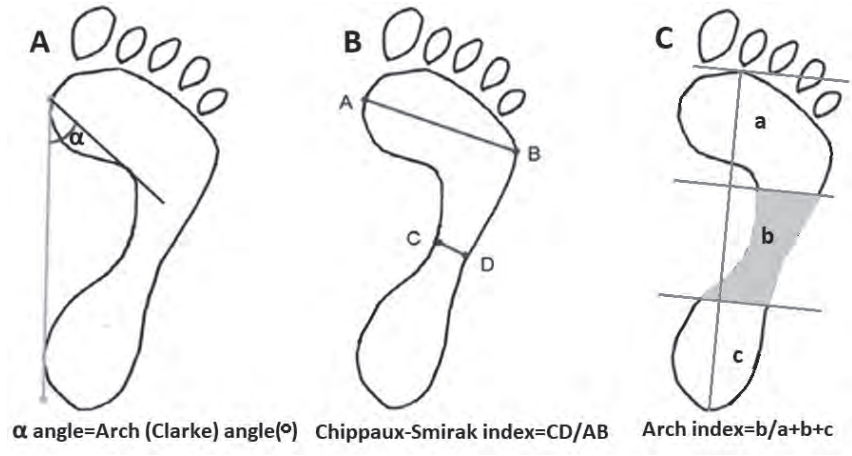

Fig. 1. A. Clarke's (arch) angle; **B**. Chippaux-Smirak index = CD/AB; **C.** Arch index=b/a+b+c

Results

According to the arch index values, the plantograms of 90 of the participants fell into the group with normal foot. Other 17 of them were classified as flat and 43 – with high-arched foot. The percentage distribution among the three groups was as follows: 60% were with normal; 11% – with flat; 29% with high-arched foot (**Fig. 2A**). We compared the BMI values of the participants distributed in the groups that were formed (**Fig. 2B**). The data analysis showed a statistically significant difference between the BMI values of people with high- and those with low-arched foot (**Fig. 2C**). When we compared the arch index values in the groups with low, with normal and with high BMI, there were no significant difference (data not shown).

Fig. 2A

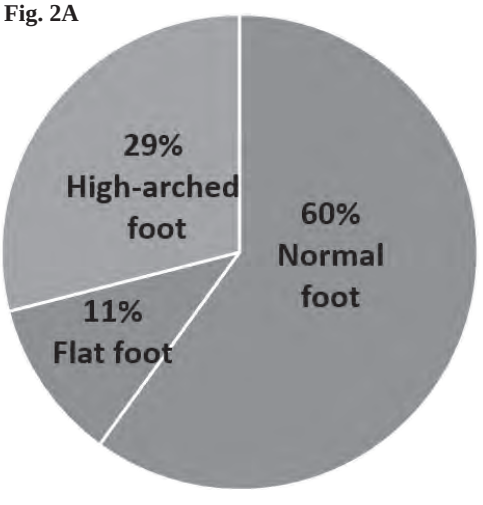

Fig. 2B

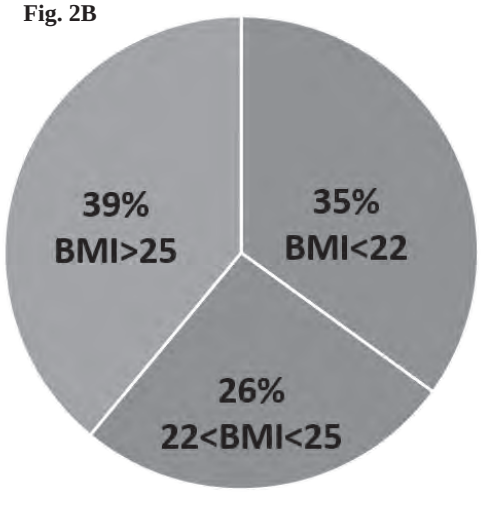

Fig. 2. A. Incidence of the foot types according to arch index values; **B.** Distribution of participants according to BMI;

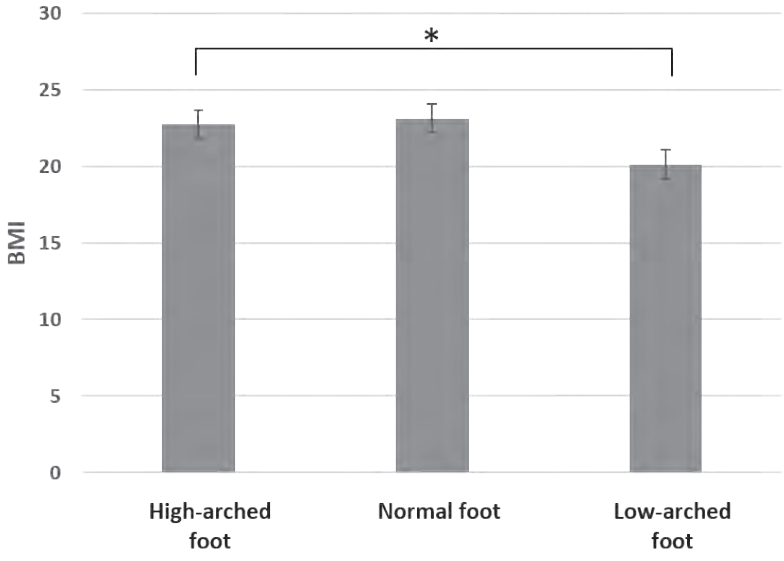

Fig. 2. C. BMI values in participants with different foot types. * - p≤0.05, BMI – body mass index

We analyzed the results obtained from arch index calculations in people with Morton's toe and those without it. The participants with longer second toe (Morton's toe) were 40 % of all, or 59 people out of 150. The arch index values in the group with Morton's toe were significantly lower with mean value 0,209. The mean value in the other group was 0,235 (**Fig. 3A**). The t-test confirmed this difference with p< 0,05.

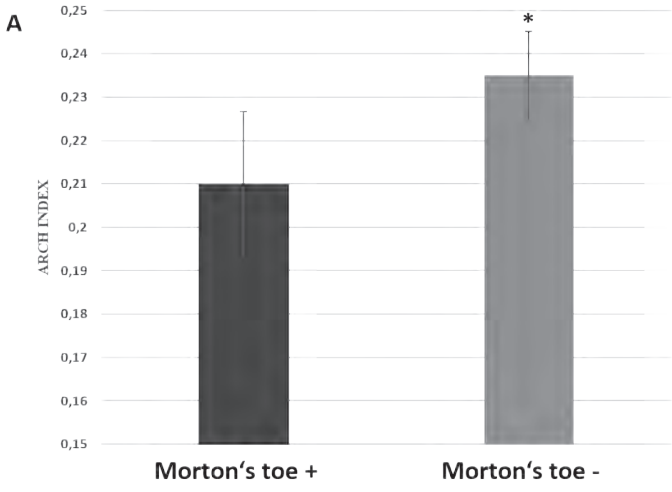

Fig.3. A. Arch index values in Morton's toe positive group and Morton's toe negative group

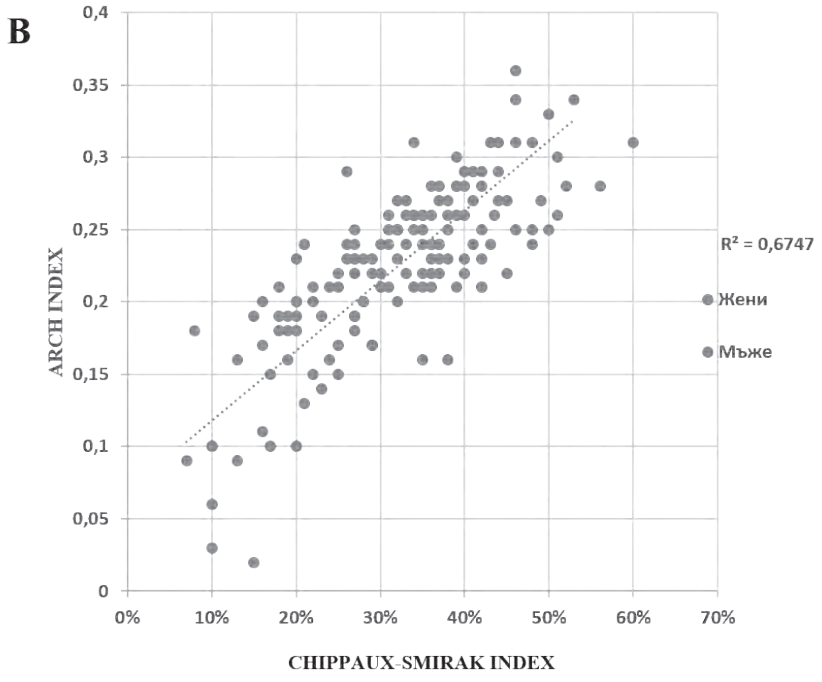

Fig.3. B. Correlation between arch index and Chippaux-Smirak index

We investigated the correlation between the arch index, Clarke's angle and Chippaux-Smirak index. Statistical analysis showed no correlation between Clarke's angle and Chippaux-Smirak index (r = -0,528), and no correlation between Clarke's angle and arch index (r = -0,399). We found very high, positive correlation between arch index and Chippaux-Smirak index with r = 0,777 (**Fig. 3B**).

Discussion

The type of foot is associated with various features of the biomechanics of the entire lower limb and body. A low-arched foot and a high-arched foot redistribute the weight of the body differently. This leads to uneven stress on different structures, which could lead to different manifestations of problems such as calluses, ulcerations, muscle-tendon strains and even stress fractures [1, 9]. That's why the type of foot should be evaluated in the medical practice of a wide range of specialists. The use of footprints is a simple, available, inexpensive and reliable method that does not require any equipment. Measuring more than one morphometric index increases reliability many times [8]. Arch index is both generally accepted as particularly reliable and relatively time consuming to use as it requires more calculations. The correlation between it and Chippaux-Smirak index allows its replacement by the easier-to-perform morphometric analysis.

Morton‘s toe is a condition that disrupts the biomechanics of the foot [7]. It is associated and accepted as a risk factor for the development of hallux valgus, plantar fasciitis, flat feet, stress fractures of the 2nd and 3rd metatarsal bones [3]. Literature data show that complications of Morton‘s toe occur and increase with advancing age [4, 7]. Our results for the co-existence of Morton‘s toe and high-arched foot can be interpreted in relation to the younger age of the participants, as a compensatory mechanism to overcome the instability of the first ray of the foot and as an additional risk for foot instability.

The obtained data show that BMI does not influence the arch index values. Lower BMI in people with a high-arched foot are most likely a result of constitutional features. At the same time, an even distribution of foot types is observed in the groups with different BMI.

Conclusions

1. The arch index values are not affected by BMI.
2. The measurement of Chippaux-Smirak index can replace the study of arch index in the assessment of foot type.

Acknowledgements: We thank the colleagues from the Medical Center for Rehabilitation and Sports Medicine -1, Varna for the opportunity to use their base.

References

1. Buldt, A. K., S. Forghany, K. Landorf, G. Murley, P. Levinger, H. Menz. Centre of pressure characteristics in normal, planus and cavus feet. – *Journal of Foot and Ankle Research,* **11**, 2018, 3.

2. Donatelli, R.. Normal biomechanics of the foot and ankle. – *The Journal of Orthopaedic and Sports Physical Therapy*, **3**, 1985, 91-95.

3. Glasoe, W., H. Yack, C. Saltzman. Anatomy and biomechanics of the first ray. – *Physical Therapy*, **79**, 1999, (9), 854-859.

4. Hallinan, J., S. Statum, B. Huang, H. Bezerra, D. Garcia, G. Bydder, C. Chung. High-resolution MRI of the first metatarsophalangeal joint: gross anatomy and injury characterization. - *RadioGraphics*, **40**, 2020, (4), 1107-1124.

5. Jung, D., K. Mun, S. Yoo, H. Jung, J. Kim. A Study on the contribution of medial and lateral longitudinal foot arch to human gait. – *IEEE Engineering in Medicine and Biology Society. Annual International Conference*, 2021, 4559-4565.

6. Menz, H., M. Fotoohabadi, E. Wee, M. Spink. Visual categorization of the arch index: a simplified measure of foot posture in older people. – *Journal of Foot and Ankle Research,* **5**, 2012, 1-10.

7. Morton, J. Structural factors in static disorders of the foot. – *The American Journal of Surgery*, **9**, 1930, (2), 315–328.

8. Papaliodis, D., M.Vanushkina, N. Richardson, J. DiPreta. The foot and ankle examination. – *The Medical Clinics of North America,* **98**, 2014, (2), 181-204.

9. Tong, J., P. Kong. Association between foot type and lower extremity injuries: systematic literature review with meta-analysis. – *Journal of Orthopaedic and Sports Physical Therapy,* **43,** 2013, (10), 700-714.

10. Ward, C., W. Kimbel, D. Johanson. Complete fourth metatarsal and arches in the foot of australopithecus afarensis. – *Science,* **331**, 2011, (6018), 750-753.

Institute of Experimental Morphology, Pathology and Anthropology with Museum
Bulgarian Anatomical Society

Acta Morphologica et Anthropologica, 30 (3-4)
Sofia ● 2023

Early Middle Age Surgeons – Two Trepanned Skulls from the Necropolis near the village Nedan, Bulgaria

Victoria Russeva[1], Emilia Evtimova[2], Nedyalka Krasteva[3]

[1] Institute of Experimental Morphology, Pathology and Anthropology with Museum, Bulgarian Academy of Sciences, Sofia, Bulgaria
[2] National Institute of Archaeology with Museum, Bulgarian Academy of Sciences, Sofia, Bulgaria
[3] Bulgariacurator-archaeologist Historical Museum Dimitrovgrad, Bulgaria

*Corresponding author e-mail: victoria_russeva@yahoo.com

Archaeological excavations near the village Nedan, Pavlikeni district, Bulgaria, revealed Middle Age cemetery with 26 graves, dated from the 9th and first decades of the 10th c CE. Burial ritual, follows in generally Christian practice. However, many deviations from the strict ritual are registered – most of the complexes contain animal bones; present traces of burning; posthumous intervention in the anatomical skeleton position is observed. In the complexes are found various materials, some being parts of the clothing of the buried, other could have been laid as offerings. Skulls from graves # 7 (child ca. 3-4 years) and # 23 (female, ca. 50-60 up to 65 years) present specific defects. The one from grave # 23 identifies as survived cranial trepanation. The defects on the skull from grave # 7 are more complex for interpretation. Skulls or the postcranial skeletal fragments don't present clues for possible reasons for the performed intentional manipulations.

Key words: Early Middle Age, trepanation

During rescue archaeological excavations in the site "Kovanlaka", near the village Nedan, Pavlikeni district, Bulgaria, a Middle Age cemetery with 26 graves is studied. Burials are performed by inhumation, burial ritual in generally follows Christian practice by laying the death in supine position, with orientation of West (head) to the East direction. In most cases, which allow registration, upper limbs had been laid on the chest or abdomen area. However many deviations from the strict Christian ritual are registered – most of the complexes contain animal bones; present traces of burning, possibly performed after the laying of the body, as the charcoal pieces are registered in the fill of the grave pits; in some cases, including one of the discussed

below, registers a posthumous intervention in the anatomical skeleton position, or ritual mutilations, connected in some periods with defusing a dangerous dead. In the complexes are found various materials, as glass beads, bronze and silver ear rings, buttons, some of which being parts of the clothing of the buried, other, after their location in the complexes, could have been laid as offerings during the burials [32]. Some planning of the necropolis is visible, in which graves of children present clustering. After the found material, which has vast dispersal in the territory of North and Central Bulgaria and North from the Danube River, the cemetery dates from the 9th and first decades of the 10th c CE, or it falls in the chronological and territorial limits of the First Bulgarian Kingdom [11, 21, 34]. No ceramic vessels, or coins are found. Even most of the graves present no tombstone markings, no super-positions are registered. It supposes relatively short period of functioning of the burial site, possibly of 40-50 years, in which light markings and memory had been active.

Material and Methods

The anthropological analysis of the material aimed registration of the skeletal remains on field and recognition of burial ritual and different practices on the area of the necropolis, identification of age, sex, anthropological features and signs of different pathological changes.

The osteometrical study is performed after the standard methods [19]. In achievement of age of buried are used scales for identification of dental development [33, 39], lengths of long bones, compared to the tables of Maresh [17], mean timings of epiphyseal fusion [4, 6, 31], results for cranial sutures' obliteration after the methods of Olivier-Simpson [5], simphyseal surface relief after Todd's scale [31]. The sex in adults is identified after the methods, summarized in Acsádi and Nemeskéri [3] with a priority of features of pelvic bones, after features on the cranial fragments [35] and the obtained measurements after a correlation to standard tables [4, 6, 16]. Stature reconstruction is performed using formulae of Pearson and Lee and Trotter and Gleser for Caucasian population [4].

Results

Still on field ascertains the presence of one individual in each grave complex, or in total, skeletal remains from 26 individuals are studied. In some complexes is observed an intentional disturbance of primary anatomical position of skeletons, performed some period after the burial, possibly after the decomposition of the soft tissue, most affected being the complexes with female skeletal identification. At the preliminary stage of investigation the age and sex identification is achieved, as well as recognition of some pathological changes on bone fragments. Absence of individuals under 2 – 3 years of age at death is visible in the age distribution of the material. It may be explained with discrimination in the burial ritual of these dead and their deposition in

a different place. There remains, however, a possibility the lack of these individuals to be caused by relatively small studied area of the necropolis, or by their destruction. Individuals in the age between 20 and 40 years of age prevail in the demographic distribution (**Table 1**). In sex distribution a prevalence of identified as females in comparison to males 7:10, respectively is registered.

Table 1. Age and sex distribution of buried. *Inf I – infants, 0-6 years of age; Inf II – infants 7-14 years of age; Ad – adults, 18/20-40 years of age; Mat – matures, 40-60 years of age; Sen – elderly, over 60 years of age*

Age	**Inf I**	**Inf II**	**Ad**		**Mat**		**Sen**	
Sex			M	F	M	F	F	Tt
N	7	2	4	6	3	3	1	26
%	26.92	7.69	15.38	23.08	11.54	11.54	3.85	100.00

On skulls from two individuals, from graves # 7, identified as a child at about 3-4 years at death, and # 23, a female, at about 50-60 up to 65 years at death are found specific defects. Skeleton from grave # 7 is highly fragmented. After the situation of the left femur, both tibiae and fibulae and remains from both iliac bones, found in initial position (**Fig. 1**) the body should have been laid on the back with extended lower limbs. From the skull, the mandible and fragments from skull vault remained in initial position. The other found skeletal parts are disturbed and moved from their primary anatomical position, most of the skeletal parts are missing. A fragment from the frontal bone, with a round perforation locates moved, near to the skull on the left side of the skeleton (**Fig. 1, arrow**). The age of this individual ascertains after the dental development of ca. 4 years at death. However the length of only measured femur (**Table 2**) is closer to the mean values for children at lower age of 3-3 ½ years after used methods.

Fig. 1. Grave # 7, situation on terrain. Position of the frontal bone fragment with trepanation, arrow; detail – fragment with trepanation B *in situ*

On a fragment from the frontal bone of the individual from grave # 7, on its left side, are found two defects. They are parts of two round openings, with reconstructed diameters of about 20÷25 *mm* (**Fig. 2**). The edge of both fragments presents slightly oblique walls, with inner diameter slightly smaller (at ca. 4 mm). While the better preserved part of the opening B (**Fig. 2, arrow B**) presents visible traces from a sharp pointed tool in radial direction (**Figs. 2, 3, arrows**), the small preserved detail of the other one presents smooth edge, but a thick layer of carbonate covers its surface (**Fig. 2, A**). On spots of the surface of the cut cranial bone on the place of better preserved opening (**Fig. 2, B**) are visible traces from the diploe layer, but the cuts from the used tool are smoothened. No other pathological changes are identified so far on the remaining bone fragments from the cranial vault and the postcranial skeleton of this individual.

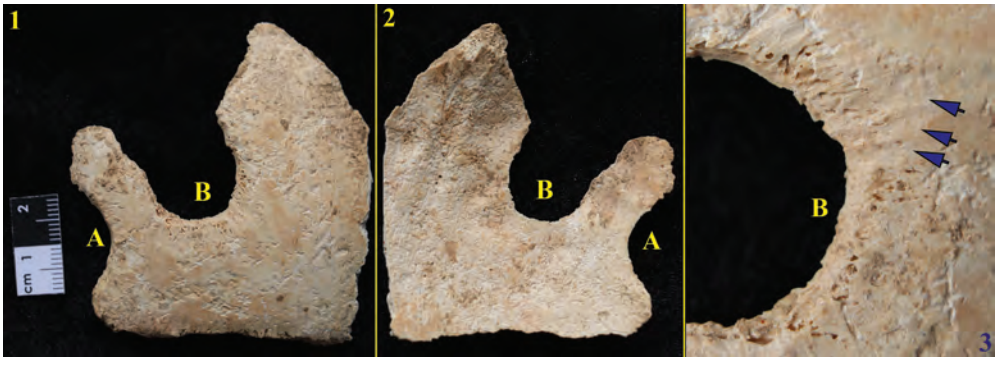

Fig. 2. Grave # 7, frontal bone fragment with trepanation defects, A and B. 2.1. Ectocranial surface (view of the outer tble). 2.2. Endocranial surface (view from the inner table. 2.3. Defect B, detail, ectocranial surface; traces from tool, arrows

Table 2. Dimensions of long bones and stature reconstruction. Gr. # - grave number; D – diameter of the head; B – bi-condylar breadth; L – biggest length; T-G – reconstruction of stature in *cm* after the Trotter-Glaeser formula; P-L – reconstruction of stature in *cm* after the Pearson-Lee formula; dx – right; sn – left

Gr. #	Bone	D	B	L	T-G	P-L
7	*Femur sn*			20,2	-	-
23	*Femur dx*	4,15	6,94	40	152,65 (148,93÷156,37)	150,45
	Femur sn	4,15	6,81	39,8		

Skeletal remains from grave # 23 are in better preservation. On the field are observed no post-inhumation disturbances and some fragmentation and missing fragments are to be explained with natural destruction in the deposition

environment (**Fig. 3**). The cranial skeleton is disturbed and fragmented after the contemporary construction works. The body has been laid on the back with extended lower and upper limbs, from the latter the left one has been laid on the grave pit's floor near the body, while the remains from the right one are found on the right pelvic bone. The sex of the individual is achieved after the reconstructed pelvic girdle and confirmed after the achieved dimensions of limb bones (**Table 2**). The age identifies after the advanced obliteration of the cranial sutures in the end of the mature group and beginning of the senile age. The stature of the individual reconstructs to have reached 152.65 *cm* after the Trotter and Glaeser formula and 150.45 *cm* after the Pearson and Lee formula, or after both used methods it categorizes as short.

Fig. 3. Grave # 23, situation on terrain.

On a fragment from right parietal bone of the skull from grave # 23, located on its relative center, ascertains a defect, a pit, with irregular, rounded form and biggest diameter of ca. 4÷4,5 *cm* (**Fig. 4.1**). On its relative center a perforation with irregular triangular form with bigger breadth of 2,2 *cm* and length of 4 *cm* is observed. The walls of the opening are in oblique direction to its center, from outer to inner table of the parietal bone. The diploe layer is well covered with callus bone formation with no exposition of diploe and smooth surface. No traces from the mechanical forces, or tool, which caused the opening are visible. At places of the opening is seen a post-mortal, taphonomical destruction.

Fig. 4. Grave # 23, right parietal bone trepanation defect in its approximate center. 4.1. Ectocranial surface (view of the outer tble). 4.2. Endocranial surface (viewof the perforation from the inner table).

Discussion

Both cases, the openings on the skulls from graves # 7 and 23, are to be interpreted as intentional manipulations on skulls. They present different situation on both individuals. In case of the child from the grave # 7 the round opening B had not been survived for long. The traces of the mechanical forces, observed on the preserved fragments present technique of their formation with a sharp, pointed tool, which had been used in radial direction to extract a relatively round bone fragment in the opening. The fragment from the opening A (**Fig. 2, A**) is smaller, and difficult for examination due to a thick layer of carbonate, which covers its surface. It could be supposed, that at the time of intentional disturbance of the skeletal remains of the child, after some period of time had elapsed after the inhumation, the manipulation on the skull had also happened, during which is extracted, a relatively square fragment, which preserves partially both openings, moved and left near to the skeletal remains. Skeletal remains don't present any clues about the cause of death of the individual, neither the cause of the posthumous treatment of the skull.

The skull from the female from grave # 23 presents a different situation. Walls of the opening present smooth undisturbed callus layer, proving long time of survival after the manipulation. The method used in obtaining the opening should be reconstructed as scrapping the bone plates, by use of sharp blade, resulting thinning of the bone up to 2 *mm*. In the relative center of the pit, on the thinnest bone, the perforation occurs as an irregular triangular opening. The very thin bone at place does not allow to be rejected also the hypothesis, that when performed, the whole retained a thin layer of bone and the perforation itself occurred post mortem. In concordance with the case from grave # 7, relatively completely preserved skeletal remains from the individual from grave # 23, do not present any data about the reason of performing the observed manipulation, neither the cause of death, a relatively long period after the manipulation took place.

Intentional manipulations on skull bones are evident on material from many cultures in vast territorial and chronological limits. From the anthropological material, studied from contemporary Bulgarian territory, such are known from the Eneolithic period [9, 16], during the sequent periods [8, 27] and in the Middle Ages [28, 29, 30, 37, 38, 15]. All these manipulations present different types, possible aims, and results for the individuals, whose skulls have been affected, during life or after death. Trepanations from Nedan are performed with the most often used methods in paleo populations – one by scraping a plate from outer cranial surface. In it with application of an oblique force, the performer aims a perforation of the cranial bone with maximal control, so not to harm the structures under the trepanned bone. The other technique aims to create a perforation by using consecutive oblique piercing forces in radial direction. Again, a high control on the force is looked for, in order to prevent disturbance of the structures under the cranial bones. Both techniques are used in the Middle ages, and even found consequently applied on one place, on a skull from Anhialos from 11th c. CE [28]. Here on the place of the manipulation (parietal bones, on the sagittal suture) first had been removed outer plate of the bone by scrapping from two opposite directions, performed with sharp blade, similar to the case of the skull from grave # 23, Nedan, and after it, perforation itself had been achieved by a radial forces with pointed tool. This operation had been survived from the individual, as the one observed on the skull from grave # 23, Nedan. Other skull from Anchialos presents a type of incomplete trepanation in which the skull bone is thinned at specific places without being perforated [28]. Most skulls with similar defects and case with most similar defects on one skull are found in the necropolis by the village of Odartsi, dated in the 11th c. CE [38]. For technique used in these cases is proposed cauterization, scrapping or combination of both. Defects, which could be connected with cauterization are smaller in diameter.

Some light on the practices of trepanation in Old world shed historical sources. This manipulation is described still in the “On Head Wounds” ascribed with some uncertainty to Hippocrates [12, 18, 24]. As the work title admits, the manipulation is recommended in the treatment of head injuries. In the ancient world the medical tradition is followed in works of Galen [26] and later from early medieval medicals

as Paul of Aegina and the Holy Abbas. Later the manipulation is accepted also in the Arab medical tradition in work of Avicenna (Ibn Sina), "Canon of Medicine" [1].

In spite of the historical evidences and recommendations of medical authors, evidences for the use of trepanation for purposes other than treatment of traumatic conditions in Roman Empire, and later, are evident in the anthropological investigations. In some of these cases the trepanation is used in treatment of evident pathological conditions, detected on the skeletal remains [10, 20]. Later sources describe cases of use of trepanation in medical conditions, described as neurological disturbances, as migraine and epilepsy. Such are used by crusaders, and later from the Ottoman medicals Ibrahim ibn Abdulah and Serefeddin Sabuncuoglu [2, 10, 13, 22] from 11-12th to the 15–16th c CE. The anthropological investigations of material from Roman period and Early Middle Ages from England and Germany in many cases finds big portion of cases of applied head trepanations on skeletal remains, which don't present any pathological changes, as the Bulgarian ones [23, 25, 36]. In England and Ireland most used technique is the scrapping [23, 25].

Cases of peri-mortem or posthumous manipulations on cranial bones, first ones, known as not survived trepanations, and the latter, as post-mortal trepanations are much rare finds in the discussed period. One case is a finding from Serdica, from Late Antiquity [8,], performed on an adult female, who is supposed to have died during the manipulation. The other case is with closer dating and cultural context to the studied from grave # 7, ascertained on a skull from the Middle Age necropolis # 2 near the village of Odartsi, dated in the 11th c CE [38]. Here the manipulation is also performed on a skull of a child, using similar technique. It is supposed that the child had not survived the manipulation. Most cases of posthumous manipulations, aiming the obtaining of a bone fragment, and artefacts made from human skulls, later preserved in settlement context are known from much earlier period in Bulgaria [7, 9, 14]. Nevertheless such are found again on vast territorial and temporal limits.

Conclusions

On both skulls, from graves # 7 and 23, are detected intentional manipulations. On the skull from the grave N 23 the manipulation is performed during life and survived long time before death. As in many other published findings from Ancient and Medieval Europe and Near East no medical reason for the manipulation is ascertained. Nevertheless the find falls in the group of similar evidences for medical skills and tradition, passed through long period of time between cultures from vast territory of the Eurasia. With the trepanation from grave # 23 from Medieval cemetery near village Nedan enlarges the source material for reconstruction of level of medical knowledge and religious believes of population of Medieval Bulgaria.

The case from the grave # 7 is more difficult for interpretation. The interpretation of the detail from opening A is difficult because of post-mortal destruction and carbonate layer. The opening B had not been survived for long. It is possible that one of the openings had been made short before death and the other peri-mortem

or after death. Clear evidence of posthumous disturbance on the skeleton, in which the skull had been also involved, and features of the opening detail and the skull fragment, render the possibility that the posthumous manipulation aimed obtaining of a bone fragment for some other purposes. It remains unclear if the missing skull fragments are taken away in this act with the bone plate, which left the opening on the frontal bone.

References

1. **Aciduman, A., B., Arda, F., Özaktürk, Ü. Telatar.** What does Al-Qanun Fi Al-Tibb (The Canon of Medicine) say on head injuries? – *Neurosurgery Rev*., **32**, 2009, 255-263.
2. **Aciduman, A., D. Belen**. The Earliest document regarding the history of cranioplasty from the Ottoman era. – *Surgical Neurology*, **68**, 2007, 349-353.
3. **Acsádi, G., J. Nemeskéri.** *History of human life span and mortality.* Budapest, Akademiai Kiado, 1970, pp. 346.
4. **Alekseev, V.** *Osteometry. Methods of the anthropological investigation.* Moskow, Nauka, 1966, pp. 251. [In Russ.: Алексеев, В. Остеометрия, методика антропологических исследований. Москва, Наука]
5. **Alekseev, V., G. Debets.** *Craniometry, methods of the anthropological investigation.* Moskow, Nauka, 1964, pp. 128. [In Russ.: Г. Дебец. Краниометрия, методика антропологических исследований. Москва, Наука]
6. **Bass, W.** Human osteology: a laboratory and field manual of the human skeleton. University of Missury, 1971, p. 280.
7. **Boev, P**. On the historical trepanations in Bulgaria. - *Bulletin of the Institute of Morphology*, **3**, 1959, 197-231. [in Bulg. ***Боев, П. Върху историческите трепанации. – Известия на Института по Морфология***]
8. **Boev, P.** Trepanned skull from Sofia. – *Archaeologia*, **4,** 1961, 70-72. [in Bulg. ***Трепаниран череп от София. – Археология***].
9. **Boev, P.** *The race types from Balkan Peninsula, the East Aegean Islands and their significance for the origin of their population*. Sofia, Publishing House of Bulgarian Academy of Sciences, 1972, pp. 271. [In Germ.: Die Rassentypen der Balkanhalbinsel und der Ostgäischen Inselwert und deren Bedeutung für die Herkunft ihrer Bevölkerung]
10. **Capasso, L., G. di Totta.** Possible treatment for headaches in ancient times. – *International Journal of Osteoarchaeology*, **6**, 1996, 316-319.
11. **Dimitrov, D**. Protobulgarian necropolis N 2 by Devnya. - *Buletin of the National Museum, Varna,* **6** (21), 1970, 21-47. [in Bulg.: Димитров, Д. Ил. Старобългарски некропол № 2 при Девня. – ИНМ Варна].
12. **Dimopoulos, V., J. Robinson, K. Fountas.** The pearls and pitfalls of skull trephination as described in the hippocratic treatise "On Head Wounds". – *Journal of the History of the Neurosciences*, **17**, 2008, 2, 131-140.
13. **Erbengi, A.** History and development of neurosurgery in Anatolia (Part One). – *Turkish Neurosurgery*, **3**, 1993, 1-5.
14. **Georgieva P.,V. Russeva.** Artifacts from human skull - roundels and a skull cap from Kozareva Mogila, a Late Eneolithic site. – *Archaeologia Bulgarica*, XX, **2**, 2016, 1-28.
15. **Grigorov, V., V. Russeva, N. Atanassova.** Graves from the palace centre – east site: an attempt at ethnic cultural identification of burials intra muros in Pliska. – *Contributions to Bulgarian Archaeology,* **12,** 2022, 101-146.

16. Kühl, R. Skeletal remains from the prehistoric graves with cremation burial ritual and their potential statements, with references to specific issues in Schleswig-Holstein. – *Mitteilungen der Anthropologischen Gesellschaft in Wien* (MAGW), Band **115,** 1985, 113-137. [In Germ.: Skelettreste aus prähistorische Brandbestattungen und ihre Aussagemöglichkeiten, mit Hinweisen auf spezielle Fragestellungen in Schleswig-Holstein].
17. Maresh, M. Measurements from roentgenograms. In: *Human growth and development* (Ed. R.W. McCammon), Springfield IL, C.C. Thomas, 1970, pp. 157–200.
18. Martin, G. Was hippocrates a beginner at trepanning and where did he learn? – *Journal of Clinical Neuroscience*, **7**, 2000, 6, 500-502.
19. Martin, R., K. Saller. *The textbook of anthropology.* Stuttgart, Gustav Fischer, 1959 [in Germ.: Martin, R., Saller K. Lehrbuch der Anthropologie]
20. Mednikova, M. *Trepanations in the ancient world and head cult*. Alteya, Moscow 2004, pp. 208 [in Russ.: ***Медникова***, М. ***Трепанации*** в ***древнем мире*** и ***культ головы***]
21. Melamed, K. Necropolises. – In: *Durankulak*, 1 (Eds. K. Todorova et al.), Sofia, BAS, 1989, 113-147. (in Bulg. – Меламед, К. Некрополите. В: Тодорова, Х. и кол. Дуранкулак I.).
22. Naderi, S., A. Erbengi. History of neurosurgery and neurosurgical applications in Turkey. – *Surgical Neurology*, **64**, 2005, 115-122.
23. O'Donnabhein, B. Trepanations and Pseudotrepanations: Evidence of Cranial Surgery from Prehistoric and Early Historic Ireland. – In: T*repanation, discovery, history, theory* (Eds. R. Arnot, S. Finger) Swets & Zeitlinger, 2003, 79-94.
24. Panourias, I., P. Skiadas, D. Sakas, S. Marketos. Hippocrates: a pioneer in the treatment of head injuries. – *Neurosurgery*, **57**, 2005, 1, 181-189.
25. Roberts, C., J. McKinley. Review of trepanations in British antiquity focusing on funerary context to explain their occurrence – In: *Trepanation, discovery, history, theory* (Eds. R. Arnot, S. Finger), Swets & Zeitlinger, 2003, 54-78.
26. Rocca, J. Galen and the uses of trepanation. – In: *Trepanation, discovery, history, theory* (Eds. R. Arnot, S. Finger), Swets & Zeitlinger, 2003, 253-271.
27. Russeva, V. Anthropological aaterial from a pit complex from the iron age near Svilengrad. – In: *Rescue Archaeological Excavations on the way of the Railway Line Plovdiv-Svilengrad in 2005 year* (Eds. V. Nikolov, G. Nehrizov, Y. Tsvetkova) 2008, 556-568. [In Bulg. **Русева, В. Антропологичен материал от ямен комплекс от желязната епоха при Свиленград. В: ред. Николов, В., Г. Нехризов, Ю. Цветкова. Спасителни археологически разкопки по трасето на желзопътната линия Пловдив-Свиленград през 2005 г.**]
28. Russeva, V. Religion, magic or medicine? New finds of trepaned skulls from Southeastern Bulgaria, 11th-13th c. – *Archaeologica Bulgariica*, **XVII**, 2012, 77-95.
29. Russeva, V. Burried in the necropolis – anthropological evidences. – In:. *The Protobulgarian Necropolis in Balchick* (Eds. L. Doncheva-Petkova, K. Apostolov, V. Russeva) Sofia 2016, pp. 583. [in Bulg.: **Погребаните в некропола – антропологични данни. В: Дончева-Петкова, Л., Апостолов, К., Русева, В. Прабългарският некропол при Балчик**].
30. Russeva, V., Y. Meshekov, I. Borissova, V. Panchev. Defects on cranial bones from tomb №1, Sofia, Janko Sakazov Str. – *Acta Morphol. Anthropol.*, **29**, 3-4, 2022, 93-98.
31. Schwartz, J. H. *Skeleton keys: An introduction to human skeletal morphology, development and analysis)*. New York, Oxford Press, 1995, pp. 402.
32. Sternberg, L. Chosenness in the religion. – In: *ABC of the Ethnology* (Ed. L. Gheorghieva), 1927, 77-101. [In Bulg.: Щернберг, Л. Избранничеството в религията. В: Георгиева, Ив. АВС на етнологията].
33. Ubelaker, D. *Human skeletal remains: excavation, analysis, interpretation* (2nd Ed.), Washington DC, Taraxacum, 1989, pp. 172

34. Vaklinov, S. *Genesis of the Bulgarian culture VI-XI c*. Sofia, Nauka i Izkustvo, 1977, pp. 298. (In Bulg. – Ваклинов С. Формиране на старобългарската култура VI – XI век).
35. Walrath, D., P. Turner, J. Bruzek. Reliability test of the visual assessment of cranial traits for sex determination. – *Am. J. Phys. Anthropol.*, **125**, 2004, 132-137.
36. Weber, J., A. Czarnetzki, A. Spring. Neurosurgical diseases of the skulls from the Middle Ages – *German Medical Announcemen*t, **98**, 2001, A3196-A3201 [In Germ.: Neurochirurgische Erkrankungen des Schädels im frühen Mittelalter. Deutsches Ärzteblatt]
37. Yordanov, Y., N. Atanassova-Timeva, Y. Dimitrov. Anthropological study of two skeletons with trepanations from Pliska (the End of X-XI c.) – In: *From Regional to National* (Ed. H. Haritonov) Veliko Tarnovo, 2010, 43-60 [in Bulg.: ***Йорданов, Й., Атанасова-Тимева, Н., Димитров, Я. Антропологично изследване на два скелета с трепанации от Плиска. – От регионалното към националното***].
38. Yordanov, Y., B. Dimitrova. Data from the anthropological investigation of the buried in the medieval necropolis N 2 by the village Odartsi, Dobrich distr. – In:. *Odartsi – necropolises from XI c.* (Ed. L. Doncheva-Petkova), Sofia, "Prof. Marin Drinov Academic Publishing House", 2005, 415-460. [in Bulg. ***Йорданов, Й., Димитрова, Б.*** Данни от антропологичното проучване на погребаните в средновековния некропол № 2 при с. Одърци. В: Дончева-Петкова, Л. Одърци – некрополи от XI в.].
39. Zubov, A. *Odonthology, methods of the anthropological investigation*. Moskow, Nauka, 1968, pp. 198. [In Russian: Зубов А. Одонтология, методика антропологических исследований. Москва, Наука, 1968].

Institute of Experimental Morphology, Pathology and Anthropology with Museum
Bulgarian Anatomical Society

Acta Morphologica et Anthropologica, 30 (3-4)
Sofia ● 2023

Shape and Surface Structure of the Human Cerebellum: Variant Anatomy

Mykhailo Kalinichenko, Oleksandr Stepanenko*

Department of Histology, Cytology and Embryology, Kharkiv National Medical University, Kharkiv, Ukraine

*Corresponding author e-mail: mokalinichenko.po20@knmu.edu.ua

The aim of the study was to determine the characteristics of individual variability in the shape and external structure of the human cerebellum. Cadaveric material (cerebella and adjacent brainstems of 100 people) was studied. We proposed a comprehensive method for evaluating the cerebellar shape in the morphometry of anatomical specimens, which involves measuring linear dimensions (width, length, and height) and calculating relative parameters, which describe cerebellar shape by the ratio of one dimension to the other two: *relative width of the cerebellum* (rW), *relative length of the cerebellum* (rL), and *relative height of the cerebellum* (rH). The magnitude of the relative parameter determines its contribution to the shape and surface structure of the cerebellum. The combination of relative parameters ultimately defines the characteristics of the shape and surface structure of the cerebellum, which were described in this study.

Key words: human, anatomy, cerebellum, morphometry

Introduction

One of the manifestations of individual anatomical variability of an organ is the variability of its shape. Evaluating the ratio of linear dimensions of an organ is one of the ways to determine its shape [1, 3, 4]. Modern neurovisualization research methods, including magnetic resonance imaging, allow for *in vivo* identification of morphological features of the cerebellum. However, the information about the anatomical norm of the cerebellum, upon which the criteria for the standards of neurovisualization diagnostic methods are based, does not take into account the characteristics of its individual anatomical variability. *The purpose of this study* was to determine the characteristics of individual variability in the shape and surface structure of the human cerebellum.

Materials and Methods

Materials

The study was conducted on 100 samples. Each sample included cerebellum and an adjacent brainstem. They were obtained from adult human cadavers (67 male and 33 female) who died of causes unrelated to brain pathology at the age between 20 and 92.

Measuring the cerebellum

Cerebellar width (W), length (L) and height (H) were measured. The width was measured between the most distant points of the cerebellar hemispheres lying on the surface of the superior semilunar lobules (**Fig. 1**). The length was measured between the most distant points on the surface of the inferior semilunar lobule at the back and the quadrangular lobule at the front (**Fig. 2**). The height was measured between the uppermost point on the surface of the culmen of the vermis and the straight line connecting the lowermost points of the two biventer lobules (**Fig. 3**). If there were discrepancies in the length measurements between the right and left sides, the average value was taken.

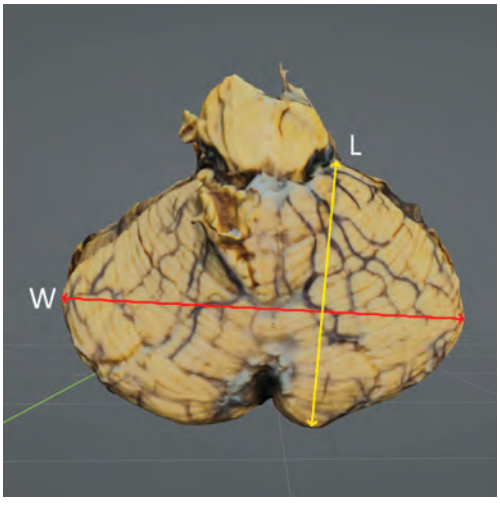

Fig. 1. Determination of the width and length of the cerebellum.

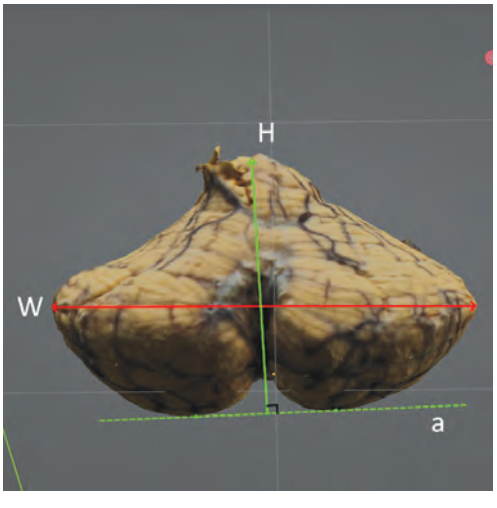

Fig. 2. Determination of the width and height of the cerebellum: a – a straight line connecting the lowermost points of the two biventer lobules.

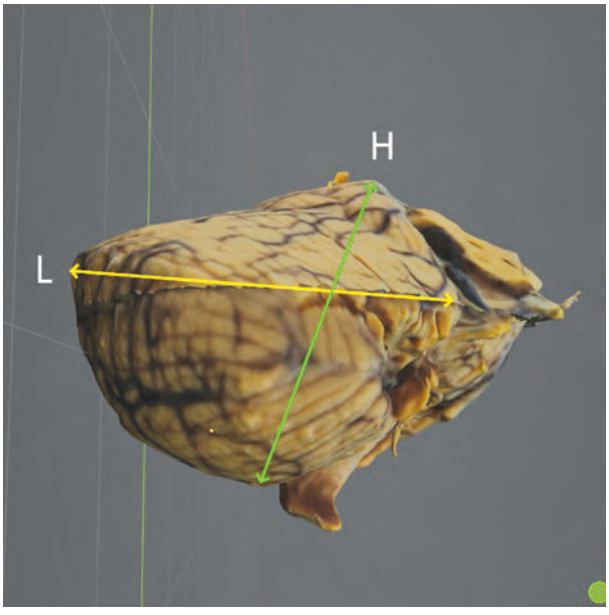

Fig. 3. Determination of the length and height of the cerebellum.

Method for determining the shape of the cerebellum

To describe cerebellar shape by the ratio of one parameter to the other two, *relative width of the cerebellum* (rW), *relative length of the cerebellum* (rL), and *relative height of the cerebellum* (rH) were proposed using the following formulas:

$$rW = W^2 / (L \times H) \quad (1)$$

$$rH = H^2 / (W \times L) \quad (2)$$

$$rL = L^2 / (H \times W) \quad (3)$$

A statistical analysis was conducted, including the calculation of the sample mean (M), standard deviation (S), coefficient of variation (Cv), and determination of the minimum and maximum values. Correlation analysis was also performed, with the calculation of the Pearson correlation coefficient (r). The values of cerebellar dimensions and their ratios were grouped based on the mean and standard deviation into three categories: small (from the minimum value to M–S), medium (M±S), and large (from M+S to the maximum value).

Results and Discussion

Variability in the linear dimensions of the cerebellum. **Table 1** presents the values for the width, length, and height of the cerebellum.

Table 1. Statistical evaluation of the distribution of cerebellar measurement values and relative parameters

Parameter	Test statistics					
	M	m	S	CV,%	min	max
A. Parameters						
W	104.4	0.5	5.5	5.3	90	117.3
L	60	0.3	3.4	5.7	51.4	67.7
H	50	0.4	4.3	8.6	40	62.5
B. Relative parameters						
rW	3.71	0.05	0.51	13.81	2.22	5.22
rL	0.7	0.01	0.08	11.65	0.52	0.9
rH	0.4	0.01	0.08	19.34	0.25	0.62

As evident from the data in **Table 1 (A)**, there is variability in the values of the linear dimensions of the cerebellum in the studied sample, but it is insignificant; the greatest variability is observed in height (Cv = 8.6%), which confirms previously obtained data [2].

Figures 4, 5 and 6 depict the distribution of values for paired linear dimensions of the cerebellum.

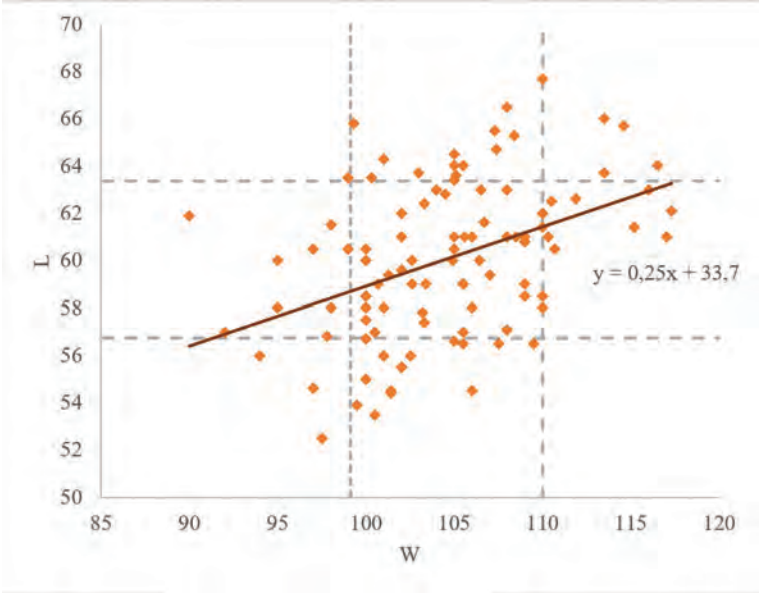

Fig. 4. Distribution of values for the width and length of the cerebellum. Note: Dashed lines correspond to the values of M–S and M+S (here and in **Figs. 5, 6**)

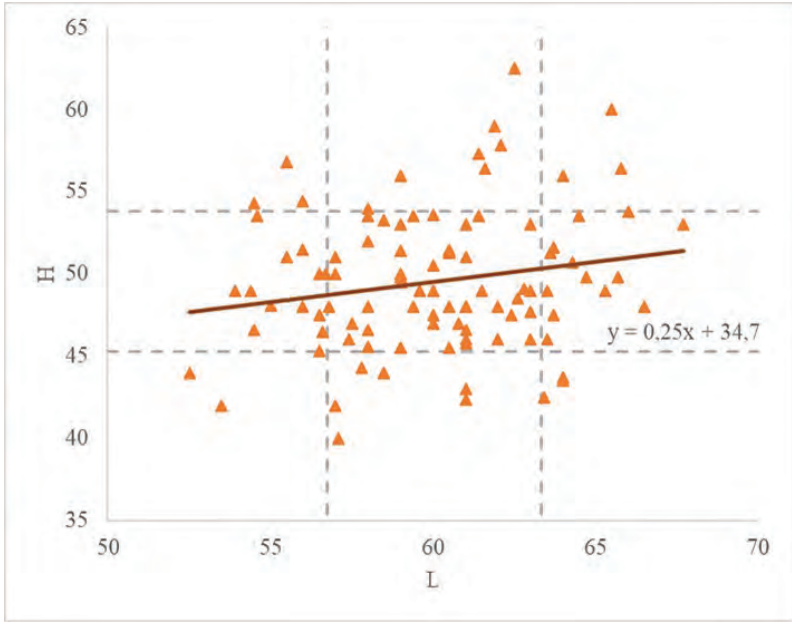

Fig. 5. Distribution of values for the length and height of the cerebellum

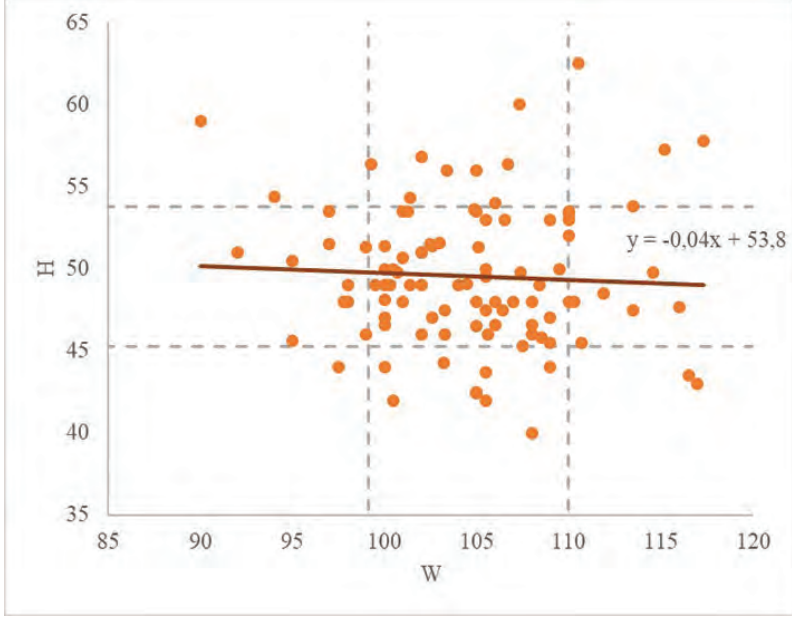

Fig. 6. Distribution of values for the width and height of the cerebellum

As evident from the data in **Figs. 4-6**, there appears to be a relative independence of variability of one linear dimension to the variability of the other two: correlation

analysis showed a weak and statistically insignificant linear relationship between the values of width and height ($r = 0.07$, $p>0.05$) as well as between the values of length and height ($r = 0.16$, $p>0.05$). There is, however, a moderate and statistically significant linear relationship between the values of width and length ($r = 0.44$, $p<0.01$). The presence of a statistically significant linear relationship between width and length values has been previously established [2].

Relative parameters of the cerebellum

The data of the relative parameters of the cerebellum are presented in **Table 1 (B)**. According to these data, the overall shape of the cerebellum can be characterized by the magnitude of the relative parameter. If the values of the investigated cerebellar parameters fall within the range of mean values, such a cerebellum is described as proportional, while extreme values indicate disproportionality:

- *relatively wide*, with a large value of rW (4.27 ÷ 5.22) or conversely, *relatively narrow*, with a small value of rW (2.22 ÷ 3.2);
- *relatively long*, with a large value of rL (0.78 ÷ 0.9) or conversely, *relatively short*, with a small value of rL (0.52 ÷ 0.62);
- *relatively high*, with a large value of rH (0.48 ÷ 0.63) or conversely, *relatively low*, with a small value of rH (0.25 ÷ 0.32).

The magnitude of the relative linear dimension determines its contribution to the shape and influence on the external structure of the cerebellum.

Therefore, cerebella that are *relatively wide* tend to have a more flattened shape, a greater separation between the hemispheres and tonsils, and broad posterior and anterior notches. In contrast, *relatively narrow* cerebella appear compressed from the sides, with a narrower posterior notch compared to cerebella of other shapes, resembling a slit. The inferior vermis may not be visible, or only a single part of it is noticeable. The tonsils are closely adjacent to each other.

Relatively long cerebella exhibit a deep anterior notch, and the course of their gyri resembles parabolas. Conversely, in *relatively short* cerebella, the vermis protrudes forward relative to the anterior edge of the hemispheres, thereby reducing the depth of the anterior notch.

The hemispheres of *relatively high* cerebella are massive and form a sharp peak. In contrast, *relatively low* cerebella appear flattened, with the vermis declive protruding above the superior surface of the hemispheres.

The complexity of the three-dimensional spatial organization of the cerebellum, on one hand, and the diversity of individual anatomical variability of the cerebellum, on the other hand (in this case, the variability in its linear dimensions, specifically the relative independence of variability of one linear dimension to the other two), lead to varying combinations of relative parameters.

The combination of relative width and relative length (horizontal projection):

Proportional cerebella have a rounded, slightly convex superior surface, and the culmen of the vermis is moderately elevated above it. The lateral contour formed by the surfaces of the superior semilunar lobules has a regular, rounded shape, and the posterior corners of the cerebellum are smoothed. The gyri resemble open arcs of concentric circles. The posterior notch of the cerebellum has a slit-like shape. Through the *cerebellar valley*, the inferior surface of the vermis is partially visible.

Relatively wide and *relatively short* cerebella have a lateral contour that, unlike proportional cerebella, is oval-shaped and stretched sideways. The hemispheres appear to be spread apart from the midline. As a result, the valley of such cerebella is wide, and the lower vermis is visible along its entire length. The lateral and posterior corners, as well as the anterior and posterior notches, are more distinctly defined.

Relatively narrow and *relatively long* cerebella appear as if "compressed" from the sides and stretched from front to back, giving their lateral contour an elliptical arc shape. The lateral corners are directed more forward than in proportional cerebella, and the posterior corners are sharp. The anterior notch is deeper than in cerebella of other shapes, while the posterior notch is narrower. Due to the relative increase in length, the course of the gyri resembles parabolas rather than concentric circles, as seen in proportional cerebella. The hemispheres are compressed by their medial surfaces, the border line between them becomes uneven, and only the vermis pyramid remains visible on the inferior surface. Unlike proportional cerebella, the tonsils are of unequal size and asymmetric in their positioning.

The combination of relative width and relative height (frontal projection):

Proportional cerebella have approximately flat surfaces. When viewed from behind, the cerebellum's contour resembles an isosceles triangle with a right or obtuse angle at the vertex. The posterior notch is narrow, but as it transitions to the inferior surface, the distance between the hemispheres increases, revealing the tonsils and the lower vermis.

Relatively wide and *relatively low* cerebella have a flat, slightly flattened superior surface, and the culmen of the vermis is not pronounced. The angle at which the superior surfaces of the hemispheres converge approaches to straight. The posterior notch is large, and the posterior and lower portions of the vermis are clearly visible. The inferior surface is flat, and the cerebellar valley is the least deep and widest among all cerebella.

Relatively narrow and *relatively high* cerebella have massive hemispheres, and the culmen of the vermis is prominently elevated. The angle formed by the hemispheres is the sharpest among such cerebella. The posterior notch appears as a narrow slit. On the inferior surface of the hemispheres, they are compressed, and the cerebellar valley is the deepest and narrowest among all cerebella. The lower vermis is either not visible, or only a single portion is visible. The tonsils can be symmetric or overlap each other.

The combination of relative length and relative height (sagittal projection):Proportional cerebella. The angle formed by the superior and inferior surfaces of the hemispheres is approximately 45 degrees. The course of the gyri on the superior and inferior semilunar lobules has a horizontal direction, and the gyri of the quadrangular lobule bend downward.

Relatively long and *relatively low* cerebella. The angle between the superior and inferior surfaces of the hemispheres is acute. The declive protrudes above the superior surface because the culmen is flatter than in proportional cerebella. The gyri gradually curve downward as they move away from the vermis.

Relatively short and *relatively high* cerebella have the greatest angle between the superior and inferior surfaces of the hemispheres, approaching a right angle. The vermis is positioned more vertically, so the declive is not visible behind the hemispheres. The gyri of the superior semilunar lobule run horizontally, those of the inferior semilunar lobule turn forward and upward, and those of the quadrangular lobule turn downward.

The distribution of values for all three relative parameters by the value of the feature is compared together in **Table 2**.

Table 2. Observed variants of the cerebellar shape (based on relative parameters)

Group	rW	rL	rH	Count
1	wide	long	low	2
2	wide	medium	medium	3
3	wide	medium	low	7
4	wide	short	medium	2
5	medium	long	medium	7
6	medium	long	low	4
7	medium	medium	high	3
8	medium	medium	medium	45
9	medium	medium	low	1
10	medium	short	high	4
11	medium	short	medium	9
12	narrow	long	medium	2
13	narrow	medium	high	4
14	narrow	medium	medium	5
15	narrow	short	high	2
Total				100

As evident from the data in **Table 2**, there is a variety of combinations of cerebellar shape parameters. 45 cerebella have average values for each of the three parameters (Group 8), 28 have average values for two out of the three parameters (Groups 2, 5, 7, 9, 11, 14). In 23 cerebella, only one parameter falls within the range of average values (Groups 3, 4, 6, 10, 12, 13), and there were also 4 non-proportional cerebella (Groups 1, 15).

The combination of relative parameters ultimately determines the characteristics of the cerebellar shape and its surface structure. For instance, relatively narrow cerebella with medium length (Groups 13, 14) have symmetrically located tonsils adjacent to each other, whereas relatively narrow and relatively long cerebella (Group 2) have tightly yet asymmetrically arranged tonsils overlapping like the branches of a purse. The relative length of the cerebellum affects the depth of the anterior notch, the relative width influences its width. The relative width affects the width of the cerebellar valley, and the relative height influences its depth, and so on.

Conclusions

The proposed comprehensive method for evaluating the cerebellar shape in the morphometry of anatomical specimens involves measuring linear dimensions (*width, length,* and *height*) and calculating relative parameters (*relative width, length*, and *height of the cerebellum*) using specific formulas.

The magnitude of the relative parameter determines its contribution to the shape and surface structure of the cerebellum. The combination of relative parameters ultimately defines the characteristics of the shape and surface structure of the cerebellum.

References

1. **Sazonova, O., O. Vovk, D. Hordiichuk, V. Ikramov, Y. Onashko.** Establishing the range of variability of the skull structures in adulthood. – *J. Educ. Health Sport,* **7**(12), 2017, 656-664.
2. **Stepanenko, A. Yu.** Variant anatomy and individual variation of human cerebellum macroanatomical indexes. – *MC3,* **47-48** (2-3), 2010, 81-87. [in Russian]
3. **Stepanenko, A. Yu.** Individual variation of the shape and appearance of human cerebellum. – *MC3,* **56** (3-4), 2012, 48-52. [in Russian]
4. **Zhang, Y., X. Wu.** Asymmetries of cerebellar lobe in the genus homo. – *Symmetry,* **13** (6), 2021, 988.

Institute of Experimental Morphology, Pathology and Anthropology with Museum
Bulgarian Anatomical Society

Acta Morphologica et Anthropologica, 30 (3-4)
Sofia ● 2023

Morphometric Study of Exophytic Growths of the Humerus and its Clinical Implications

Meera Jacob[1], Helga Sudiptha[2]*

[1] Department of Anatomy, Yenepoya Medical College, Mangalore, India
[2] Yenepoya Medical College, Mangalore, India

*Corresponding author e-mail: meerajacob@yenepoya.edu.in

Exophytic growths of humerus are rare anatomical variant which can be misdiagnosed as osteochondroma, benign lesion that occurs in the diaphysis of the bone. Case series: 100 adult humeri from osteological collection of department of Anatomy, Yenepoya Medical college, Mangalore, India were procured for the study and examined for any morphological variations. Two of 100 humeri presented with exophytic growths. One humerus presented with a bony projection from the anteromedial surface of the humerus about 6 cm above the medial epicondyle. Another humerus showed a lateral osteophytic growth. Both are rare anatomical variants. Knowledge of exophytic growths of bone is essential for clinicians because of its occasional presence for differential diagnosis and surgical management. Such anatomical variations can be a morphological indicator in the recognition of different races, as the incidence of such cases was reported more among Turkish population.

Key words: Humeri, exophytic growth, supracondylar process, variations

Introduction

Exophytic lesions are usually incidental finding that includes anatomical variations, arthritic changes or as sequelae of metabolic defects [10]. Exostosis is a benign growth of bone extending outwards from the cortical surface of the bone more commonly from the metaphyseal region of long bones. Most common type of exostosis includes osteochondroma which is differentiated histologically by the presence of cartilage. Osteochondroma is a benign bone tumour with an incidence of 1-2% [23)]. Exophytic growths of the immature skeleton generally affect the extremities of the long bones resulting in deformities. They usually occur singly, but a multiple form of presentation may be found. They are easily diagnosed as they have a very characteristic

appearance. When presented in axial skeleton, malignant transformation of the lesion can sometimes make it difficult to identify osteochondromas immediately by means of radiographic examination because of unusual site of presentation [25]. Other bone lesions that mimic osteochondroma can be of diagnostic and therapeutic challenge due to its clinical similarity and rarity of presentation [21]. Most of the diagnosis is made due to neurovascular compression symptoms. The progress of such exophytic growths is unpredictable with some remain throughout life without any complications, some disappear and few undergo malignant transformation. Such growths are mostly seen in bones with endochondral ossification [2, 22, 14] as bones of the shoulder, legs and pelvis. Benign exostosis is generally asymptomatic but when it is symptomatic the pain may be due to the adjacent structures being affected. Exostosis may limit the range of motion of the affected bones like flexion or rotation. Osteochondromas can interfere with the development of the skeletal system and may give rise to deformities of the limbs and thereby the consequences could be malalignment of the joints, bowing or adjacent bone dislocation. Other complications include fracture, osseous deformities, bursa formation neurological symptoms [4, 12]. Many conditions can mimic osteochondroma. Hence the differential diagnosis of osteochondroma include Subungual Exostosis (also referred to as Dupuytren exostosis), Dysplasia Epiphysealis Hemimelica (Trevor Disease), Turret Exostosis, Bizarre Parosteal Osteochondromatous Proliferation (Nora lesion), Parosteal osteosarcoma, Juxtacortical chondroma, Subperiosteal hematoma [3, 8, 16, 17].

The aim of the study was to identify any exophytic growths associated with humerus and to define morphometric parameters about that. In the present study we report 2 cases: a case of supracondylar process of humerus and an outgrowth from lateral surface of humeral diaphysis. Reporting of such exophytic variations can reduce misdiagnosis and improve symptoms with surgical excision.

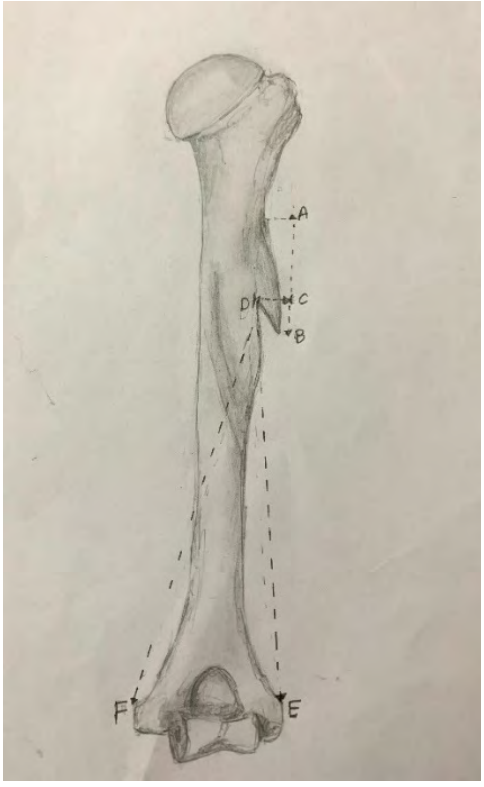

Fig. 1. Schematic representation of the first case. Distance AB shows the length of the spur. Distance CD shows the breadth at its base. DE is the distance of spur from lateral epicondyle of humerus and DF is the distance from medial epicondyle of humerus.

Material and Methods

Out of 100 humeri which was randomly procured from the osteological collection of Department of Anatomy, Mangalore, India, two humeri showed unusual bone projections with an incidence of 2%. Both bones belonged to the right side. The dimensions of bone growths were measured, tabulated and photographed. The following measurements like length of the spur, breadth at its base, the distance from nutrient foramen, the distance from the process to the medial and lateral epicondyle, distance from highest point on head of humerus and trochlea (**Fig. 1**) were measured with sliding calipers. The remaining parts of skeletons of these specimens were not available for the study.

Results

Case 1: During routine evaluation an unusual bony projection was observed from lateral surface of humerus. The tip of the process was sharp and the base where it is attached to humerus presented a foramen. There were no other signs of pathology observed along the entire bone. There were no signs of fracture healing or other deformities observed. The distance measured is tabulated in **Table 1**.

CASE1

CASE2

Fig. 2a. Right humerus with lateral exophytic growth (**2b**) Right humerus with supracondylar process

Case 2: The supracondylar process was directed laterally from the anteromedial surface of the distal part of humerus. The process was 2 cm long, 0.8 cm wide. Thickness was 1 mm and the process projected at an angle of 80 degree from the shaft. The rest of the humeral architecture appeared to be normal with no hyperplasia. Metric measurements related to the process measured is tabulated in **Table 1**.

Table 1. Dimensions of exophytic process of humerus

Parameter	**Case 1**	**Case2**
Length of the spur	2.4 cm	2 cm
Breadth at its base	0.8 cm	0.8 cm
Distance from lateral epicondyle of humerus	13 cm	6.3 cm
Distance from medial epicondyle of humerus	15 cm	5.4 cm
Distance from nutrient foramen	5.5 cm	5.9 cm
Distance from highest point of head of humerus	11.9cm	24.9 cm
Distance from trochlea	15 cm	5.5 cm

Discussion

Variations in skeletal data are vital in anthropology and important for radiologists, anaesthesiologists and surgeons for diagnosis and treatement [20]. Myositis ossificans includes all tissue reactions that occur due to trauma and result in bone or cartilage formation, it can be either extraosseus, periosteal and paraosteal [5]. Detailed understanding of evolution is necessary for proper classification. Haiet *et al* noted that such lesions usually develop in relation with large muscle masses. It follows injuries in which these masses get compressed against the bone and may lead to avulsion of tendons and fascia from their attachment and contributes to the etiology of such growths [7]. First case reported in this paper is unique as there was a process arising laterally from the upper diaphysis of humerus. No soft tissues were attached to dry bone and can be due to ossification of lateral intermuscular septum due to stress caused by nearby muscles [1]. The case presented goes with the factor that myositis ossificans developed after crush injury with tearing of periosteum. This can be correlated with Tackler's exostosis which has a constant location that is lateral aspect of humeral shaft [6]. Neurovascular structures like radial nerve and branches of brachial artery can be damaged due to this sharp bony projection. As there are no other cases reported of such exophytic growth, the aetiology and genetics of such variant is not clear. Second case reported was that of supracondylar process for which the reported incidence is very low – only 2%. The dimensions measured are compared with other studies and are shown in **Table 2**. The present study has higher values compared to other studies. This can be an associated factor in cornelia de lang syndrome occurring in every 10,000 births [18].

Table 2. Dimensions of supracondylar process of various studies

Authors	Length of the spine	Breadth of the spine at base	SCPME	SCPNF
Guptha R. K [6]	0.3 cms	1.1 cms	6.5 cms	-
Oluyemikayode et al [19]	1.6	-	5.3	5.5
Prabahitha et al [21]	1.1	1.5	6.5	4.4
Present study	2	0.8	5.4	5.9

Compression of median nerve can occur as it passes under the ligament of Struthers. Since ulnar nerve does not pass under the ligament of Struthers the nerve stretches posteriorly around the process in the few cases. Carpal tunnel syndrome-like symptoms, ulnar nerve symptoms, loss of sensation, and disappearance of the radial or ulnar artery pulse on extension and supination of the forearm are seen when a process arises proximal to the medial epicondyle [11]. Stress fractures that may occur as a result of such growths are very difficult to treat due to their close relation to nerves and vessels [15]. Vascular symptoms like ischemia and claudication and nervous symptoms like paraesthesia, weakness and muscle wasting can occur as part of such growths which are exaggerated by heavy manual operations [9]. So thorough knowledge of various anatomical variants can reduce the complications during surgery [18]. The distance of the process from lateral epicondyle was 6.3 cm and is more than the distance from the medial epicondyle and this point is very important in nail placement in orthopaedic surgeries as the best point being anteromedial point [26]. Exophytic growths can lead to misdiagnosis by radiologists as such growths mimic osteochondroma. Exophytic growths are directed towards the joint with a continuous cortex whereas osteochondromas are directed away from the joint [20, 24]. As recurrence is common after excision of such exophytic growths they have to be removed along with overlying periosteum [9]. The diagnosis proposed is palpation but difficult in patients with well-developed musculature, radiological imaging is confirmatory method supported by doppler evaluation [13].

Conclusion

Exostosis of bones can be considered as anatomical variant but such lesions can be misjudged as pathological bone lesion. Awareness of osteophytic growths is important in orthopaedics since it is very important in preoperative planning of distal humeral fractures, for surgeons in diagnosing and treating neurovascular compression syndromes and also for radiologists to avoid misdiagnosis.

References

1. Bhatnagar, S., J. Iwanaga, A. S. Dumont, R. S. Tubbs. Lateral Supracondylar Spur Process of the Humerus. – *Cureus*, **13**(2), 2021, 13514.

2. Castriota-Scandeberg, A., M. G. Bonetti, M. Cammisa, B. Dallapiccola. Spontaneous regression of exostoses: Two case reports. – *Pediatr. Radio*, **25**, 1995, 544-548.
3. Douis, H., A. Saifuddin. The imaging of cartilaginous bone tumours, Benign lesions. – *Skeletal Radiol.*, **41**(10), 2012, 1195-1212.
4. Garcia, R. A., C. Y. Inwards, K. K. Unni. Benign bone tumours - recent developments. – *Semin. Diagn. Pathol.*, **28**, 2011, 73-85.
5. Gilmer, W. S., L. D. Anderson. Reactions of soft somatic tissue which may progress to bone formation. – *Southern Med. J.*, **52**, 1959, 1432-1448.
6.Gupta, R. K., C. D. Mehta. A study of the incidence of supracondylar process of the humerus. – *J. Anat. Soc. India*, **57**, 2008, 111-115.
7. Hait, G., J. Boswick, N. Stone. Heterotopic bone formation secondary to trauma (myositis osificans traumatica). – *J. Trauma*, **10**, 1970, 405-411.
8. Hughes, P., D. Dow, L. Boyer, V. Morganti. Ossifying chronic subperiosteal haematoma of the iliac bone. – *J. Med. Imaging Radiat. Oncol.*, **63**(4), 2019, 479-480.
9. Ivins, G. K. Supracondylar process syndrome: A case report – *J. Hand Surg. Am.*, **21**, 1996, 279-281.
10. Mhuircheartaigh, J. N., Y.-C. Lin, J. S. Wu. Bone tumour mimickers: A pictorial essay – *Indian J. Radiol. and Imaging*, **24**(3), 2014, 225-236.
11. Kessel, L., M. Rang. Supracondylar spur of the humerus – *J. Bone Joint Surg. Br.*, **48**, 1966, 765-769.
12. Khare, G. N. An analysis of indications for surgical excision and complications in 116 consecutive cases of osteochondroma. – *Musculoskeletal Surg.*, **95**(2), 2011, 121-125.
13. Laha, R. K., M. Dujovny, S. C. DeCastro. Entrapment of median nerve by supracondylar process of the humerus: case report - *J. Neurosurg.*, **46**, 1977, 252-225.
14. Lange, R.H., T. A. Lange, B. K. Rao. Correlative radiographic, scintigraphic, and histological evaluation or exostosis – *J. Bone Jt. Surg.*, **66**, 1984, 1454-1459.
15. Martin-Schütz, G. O. A meta-analysis of the supracondylar process of the humerus with clinical and surgical applications to orthopaedics – *Int. J. Morphol.*, **37**, 2019, 43-48.
16. Mavrogenis, A. F., P. J. Papagelopoulos, P. N.Soucacos. Skeletal osteochondromas revisited. – *Orthopedics*, **31**(10), 2008, 1018-1028.
17. Murphey, M. D., M. R. Robbin, G. A. McRae, D. J. Flemming, H. T. Temple, M. J. Kransdorf. The many faces of osteosarcoma – *Radiographics*, **17**(5), 1997, 1205-1231.
18. Mutnuru, P. C., L. M. Perubhotla. Rare Mimickers of Exostosis: A Case Series – *J. Clin. Diagn. Res.*, **10**(7), 2016, 06-7.
19. Oluyemikayode, A., C. Okwuonuuche, A. Adesanyaolamide, B. Akinolaoluwole, D. A. Ofusori, V. O. Ukwenya, B. I. Odion. Supracondylar and infratubercular processes observed in the humeri of Nigerians. – *African J. Biotechnol.*, **6**, 2007, 2439-2441.
20. Peter, E. D., J. H. Mcmaster. Tackler's exostosis – *J. Sports Med.*, **3**(5), 1975, 238-242.
21. Prabahita, B., R. C. Pradipta, K. L. Talukdar. A study of supracondylar process of humerus – *J. Evol. Med. Dent. Sci.*, **1**(5), 2012, 822.
22. Resnick, D., G. D. Greenway. Tumours and tumour-like lesions of bone: Imaging and pathology of specific lesions. – In: *Bone and Joint Imaging, 2nd edn.*, Philadelphia, W. B. Saunders, 1996, 991-1063.
23. Resnick, D., M. Kyriakos, G. D. Greenway. Osteochondroma – In: *Diagnosis of bone and joint disorders. 3rd ed. vol. 5.*, Philadelphia, W. B. Saunders, 1995, 3725-3746.
24. Roopali, D. N., D. B. Nikumbh, M. A. Doshi, M. N Ugadhe. Morphometric study of the supracondylar process of the humerus with its clinical utility – *Int. J. Anat. Res.*, **4**(1), 2016, 1941-1944.
25. de Souza, A. M. G., R. Z. B. Júnior. Osteochondroma: ignore or investigate? – *Rev. Bras. Ortop.*, **49**(6), 2014, 555-564.
26. Thompson, J. K., J. D. Edwards. Supracondylar process of the humerus causing brachial artery compression and digital embolization in a fast-pitch softball player: A case report – *Vasc. Endovascular Surg.*, **39**(5), 2005, 445-448.

Institute of Experimental Morphology, Pathology and Anthropology with Museum
Bulgarian Anatomical Society

Acta Morphologica et Anthropologica, 30 (3-4)
Sofia ● 2023

Sinus Tarsi – The Eye of the Foot and its Anatomical Contradictions

Atanas Katsarov

Institute of Experimental Morphology, Pathology and Anthropology with Museum, Bulgarian Academy of Sciences, Sofia, Bulgaria

*Corresponding author e-mail: zanasko@gmail.com

The descriptive anatomy of the tarsal sinus, canal and ligaments has been a matter of debate until today because of many inconsistencies in the description and nomenclature of the sinus tarsi ligaments. It is generally believed that the subtalar ligamentous structures consist of the cervical ligament (CL), the interosseous talo-calcaneal ligament (ITCL), the anterior capsular ligament (ACaL), and 3 roots of the inferior extensor retinaculum (IER).The importance of intrinsic subtalar ligaments in relation to the subtalar joint stability is growing more and more for the last years.

Key words: sinus tarsi, tarsal sinus, subtalar, coxa pedis, talus, calcaneus, foot

As a part of the subtalar joint sinus tarsi is an anatomically determined cavity surrounded by the bony surfaces of the talus (proximal) and calcaneus (distal), dividing the subtalar joint into anterior and posterior sections [4].

Due to its anatomy, it is specifically depicted in imaging studies of the foot and is known as the 'eye of the foot' or 'bullet hole'. The scope of this article is firstly to discuss the variations in the ligamentous structures of the tarsal sinus of the foot, the functional relationships between them in the light of clinical practice and the different names under which they are found in the literature (**Fig. 1**).

The posterior subtalar joint or just subtalar joint is ovoid in shape and is formed between the relatively concave posterior facet of the talus and the convex posterior facet of the calcaneus, while the anterior subtalar joint includes the head of the talus, the middle and anterior facets of the calcaneus, and the navicular bone, i.e. is the talocalcaneonavicular joint. Together they form coxa pedis. The anterior and posterior departments are united in a single functional complex and therefore are often called the peritalar complex [24].

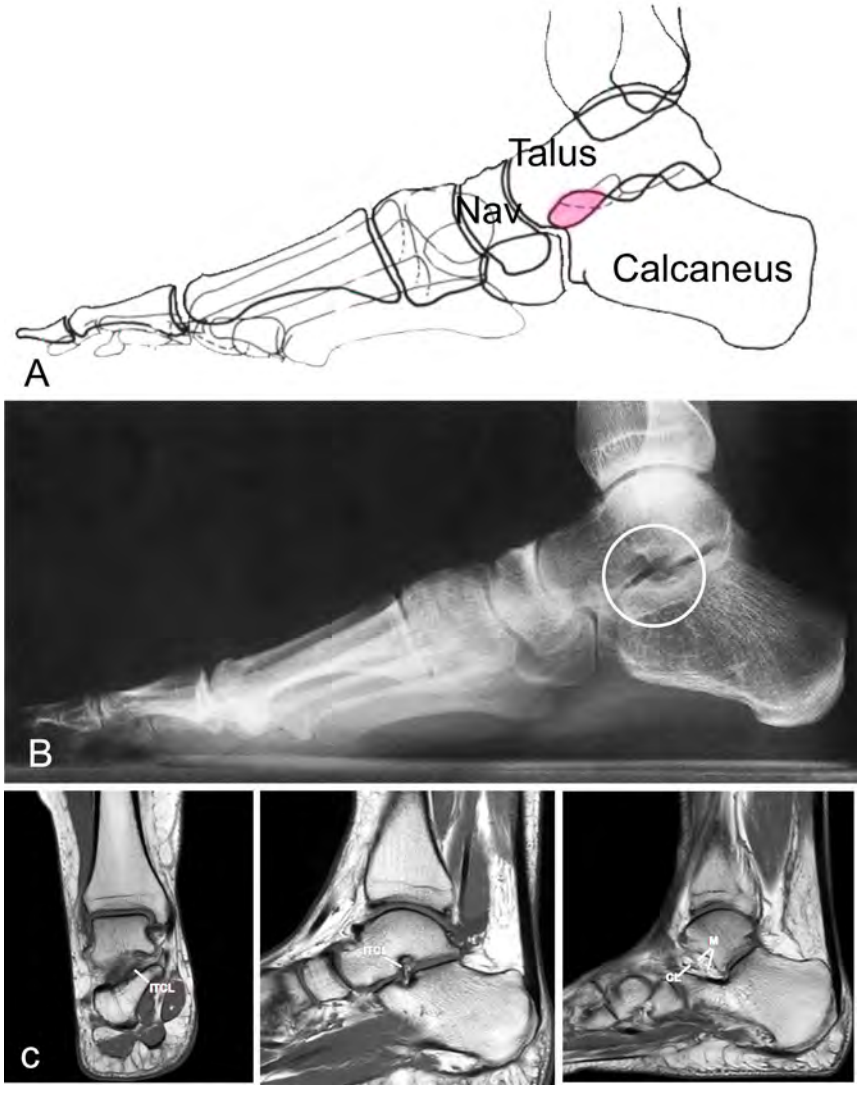

Fig. 1. Tarsal sinus (eye of the foot) A. Schematic presentation of the bones forming the subtalar joint and sinus tarsi, Nav – os naviculare.; B. X-ray imaging (lateral view) of the tarsal sinus. C. MRI of the subtalar joint, sinus tarsi and ligaments – ITCL – Interosseal talocalcaneal ligament, CL – Cervical ligament, M – Medial root of the inferior extensor retinaculum (IER)

The posterior subtalar joint has both intra-capsular and extra-capsular ligamentous supports. The intra-capsular ligamentous supports include the posterior talo-calcaneal ligament, lateral talo-calcaneal ligament and anterior capsular ligament of the posterior subtalar joint. The extra articular ligamentous supports include the calcaneo-fibular ligament, superficial deltoid ligament and the interosseous talo-

calcaneal and cervical ligaments [10]. The inferior extensor retinaculum also imparts stability to the posterior subtalar joint. One of the variabilities present medial talo-calcaneal ligament is extra-articular and provides ligamentous support to the posterior subtalar joint.

The longitudinal axis of the canal is deviated about 45 degrees from the calcaneus. The sinus tarsi space is filled with connective and fatty tissue that contribute to the stability and overall proprioception of the ankle and serves as a substrate for numerous mechanoreceptors and free nerve endings that, along with ligaments and muscles, provide nociceptive and proprioceptive information about foot and ankle movement [4,17,1].

The sinus has a conical shape and a wider part is located antero-laterally. In the direction from anterior-lateral to posterior-medial, the surface of the sinus narrows to an almost transverse cylindrical space, the so-called tarsal canal. It ends behind the level of the sustentaculum tali of the talus.

A number of variations in subtalar joint articular facet anatomy are known, including medial extension of the articular surfaces to involve the posterior margin of the sustentaculum and the antero-inferior margin of the posteromedial process of the talus [8] (**Fig. 2)**

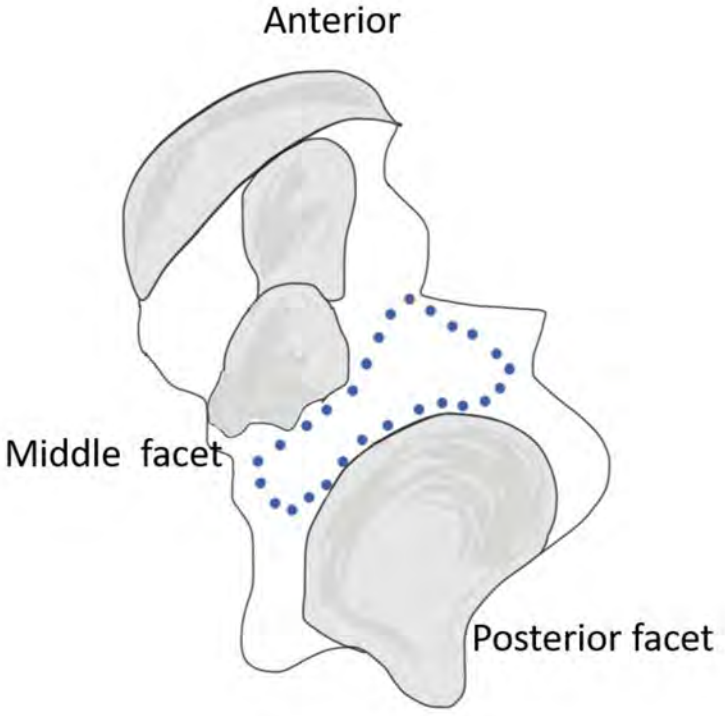

Fig. 2. Tarsal sinus and tarsal canal projection (cranial view) (From Irgit, K., Katsarov, A. Flexible Progressive Collapsing Foot Deformity Is There Any Role for Arthroereisis in the Adult Patient?, Foot and Ankle Clinics, 2021., With permission)

In addition to fatty and connective tissue, the sinus contains branches of the peroneal and posterior tibial arteries, which anastomose in the sinus and a branch of the superficial peroneal nerve – the cutaneous dorsolateral nerve [7].

Proprioceptive nerve endings are responsible for perceiving the spatial arrangement of both body parts and the whole body. As part of the sensorimotor system, they maintain the properly functioning position of the bones involved in the joints.

In addition to the structures listed, the tarsal canal contains the reinforced synovial capsule of the posterior subtalar joint and the talocalcaneoniavicular joint, as well as the following ligaments.

The most medial of them is the interossal talocalcaneal ligament (ITCL) or interossal ligament (IL), which can also be found in the literature as the talocalcaneal ligament or Ligament of the tarsal canal or Axial ligament or Cruciate ligament of the tarsus [23] or as "Hedge" ligament of Farabeuf [11] or Oblique astragalo-calcanean ligament [20] **(Fig. 3)**. The ITCL is a vertical ligament significantly thinner than the ATFL, CFL, and CL, with its attachments parallel to the tarsal canal [15]. Several anatomical variants are observed – band type, fan type, and multiple type [13].

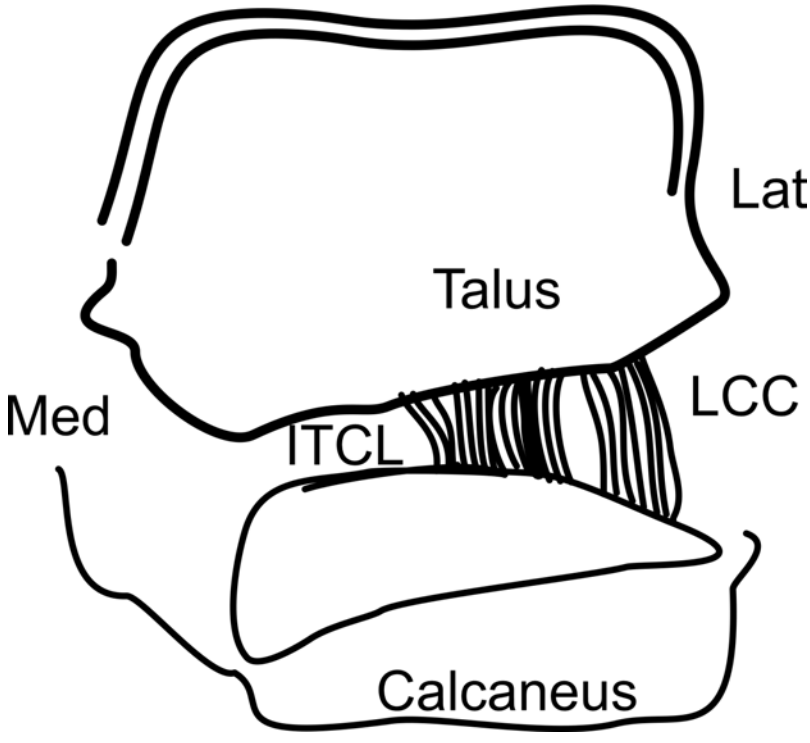

Fig. 3. Interosseous talocalcaneal ligament and lateral calcaneal component of the medial root (posterior view). Med – medial, Lat – lateral, ITCL – Interosseous talocalcaneal ligament, LCC – lateral calcaneal component of the medial root.

The ITCL together with the Anterior capsular ligament (AcaL) form the ITCL – AcaL complex, whose role is to maintain the apposition of the subtalar joint and perform eversion and inversion [2, 15]

The Cervical ligament (CL) **(Fig. 1)** known as Ligament of Fick [23] or Cervical talocalcaneal ligament [11] or External talocalcaneal ligament [20] or Oblique talocalcaneal ligament [16] or Anterolateral talo-calcaneal ligament [19]; Anterior capsular ligament known as Posterior capsular ligament [9] or Ligament of the anterior capsule of the posterior talocalcaneal joint [21] or Anterior talo-calcaneal ligament [16], is located in the sinus tarsi and is similar in size to the ATFL and CFL [18] . In the neutral position, the CL passes from the anterosuperior and medial aspect of the talus to the posteroinferior and lateral aspect of the calcaneus.

In inversion, CL is stretched in a vertical position, while in eversion CL is stretched in a horizontal position. Unlike the CFL, which is not stretched during fore-aft translation, the CL stays stretched. According to Yamaguchi et al, the CL is the fibrous part of the capsule of the talocalcaneonavicular joint [25].

The ACaL is a vertically located, rectangular bundle and corresponds to a thickened part of the anterior articular capsule of the posterior facet of the calcaneus [18, 24].

ACaL is often seen as ITCL or as a second band of ACaL. This is not clearly described in the literature and should be interpreted with caution [12]. ACaL insertion sites are located primarily in the sinus tarsi, but often extend into the tarsal canal. The ACaL and ITCL taken together have been called Farabeuf's "hedge" ligament because they are wide and short and lie in the same direction [11] (**Fig. 4**).

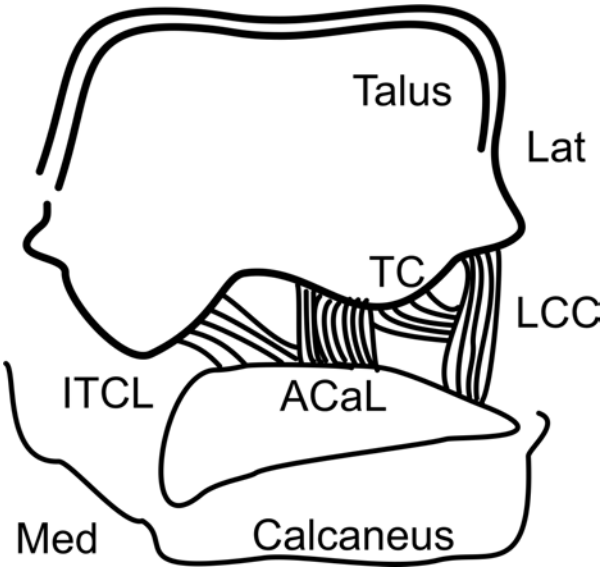

Fig. 4. Anterior capsular ligament and interosseous talocalcaneal ligament (posterior view). While the ACaL ran vertically, the ITCL ran obliquely. The ITCL had a large insertion area on the calcaneus. Med – medial, Lat – lateral, ITCL – Interosseous talocalcaneal ligament, LCC – lateral calcaneal component of the medial root, ACaL – anterior capsular ligament, TC – talar component.

Going deeper into the canal, it is found that the synovial tissues, including the inferior extensor retinaculum (IER) are those that divide the subtalar joint into two – the posterior talocalcaneal facet and the anteriorly fused anterior and middle talocalcaneal facets [25]

The extensor retinaculum (IER) covers 3 layers in depth, from back to front:

the anterior articular capsule of the posterior talocalcaneal joint, the interosseous talocalcaneal ligament (ITCL), and the medial insertion of the inferior extensor retinaculum (IER), as well as the posterior capsule of the talocalcaneavicular joint. The anterior capsule of the posterior talocalcaneal joint consists of fibrous and synovial tissues that intertwine with each other [25].

The roots of the inferior extensor retinaculum anchor the lateral stalk of the retinaculum to the calcaneus, limiting extensor tendon excursion and limiting ankle inversion.

The medial root of the inferior extensor retinaculum is located posterior and medial to the cervical ligament CL, attached to the calcaneus at the bottom of the medial sinus, often merging with the calcaneal attachment of the interosseous ligament [8].

Sarrafian noted that the medial root of the IER has 3 components (the medial calcaneal component, the talar component, and the lateral calcaneal component) [24].

Jotoku et al and Li et al. confirmed these findings and reported that the medial calcaneal component (MCC) and the talar component (TC) of the medial root displayed 3 distinct anatomical variations in their shape and attachments [3,9]. In Jotoku' study, the author described the blending of 1 type of MCC with the fibers of the ITCL to form a V-shaped structure in the tarsal sinus and canal. Based on this, he hypothesized that the MCC may transmit the force of the extensors to the ITCL. [3].

Unlike Jotoku et al, Li et al. found that the medial root of the IER diverged into 2 components rather than 3 [9].

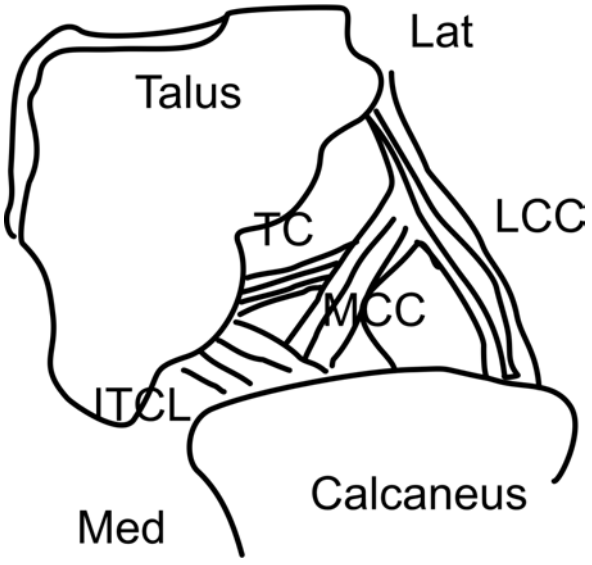

Fig. 5. Talar component of the medial root diverged from MCC (posterior view), Med – medial, Lat – lateral, ITCL – Interosseous talocalcaneal ligament, LCC – lateral calcaneal component of the medial root, TC – talar component, MCC – medial calcaneal component.

The intermediate root of the inferior extensor retinaculum also called the intermediary root, attaches to the calcaneus just behind the cervical ligament, passing anteriorly and superiorly over the medial edge of the extensor digitorum longus tendon [6].

The lateral root of the inferior extensor retinaculum was first described by Wood-Jones in 1944 as the “ligamentum frondiform”. Later, Cahill (1965) described its subtarsal location and divided the lateral root into three - lateral, intermediate, and medial [2].

This structure wraps around the lateral edge of the extensor digitorum tendon, fusing with the medial root to form a sling-like structure over the tendon. The lateral fibers extend posteriorly and laterally, attaching to the lateral cortex of the calcaneus or blending with the deep fascia [9].

Tarsal Canal Ligament is a short vertical ligament lying on the medial side of the tarsal canal just between the middle talocalcaneal facet and the lamina formed by the medial band of the medial root of the IER and the ITCL. Its presence in the population is about 60% [9].

The TCL forms a short, tight connection between the talus and the calcaneus. On its medial side is the sustentaculum tali, where some fibers of the TCL join those of the medial talocalcaneal ligament MTCL.

The middle subtalar joint is formed by the articular facet of sustentaculum tali of the calcaneus and the middle talar articular facet of the talus. The joint is next to the talo-navicular joint and could be found as the talo-navicular middle subtalar joint complex in the literature. Middle talar articular facet anatomy is relatively constant. Occasionally, the middle and anterior calcaneal and talar articular facets may be contiguous. The posterior capsule of the middle subtalar joint may be of variable thickness, occasionally being relatively thick, potentially mimicking a fibrous coalition or the interosseous talo-calcaneal ligament. The ITCL may be hypoplastic in the setting of a thick posterior capsule of the middle subtalar joint [10].

Anatomical knowledge of the tarsal canal and sinus is still unclear owing to the complexity of the ligamentous structures within them, particularly the relationship with the capsules of the subtalar joints [25].

Much of the ambiguity is due to the fact that in different studies, the authors use different and several names for individual ligaments and structures, as well as the very anatomical variation of the structures, their presence or absence in individual representatives of the human population.

The most important extrinsic ligaments are the CFL, which limits inversion, and deltoid ligament, which limits eversion. Some studies indicate that the anterior talofibular ligament (ATFL) has an indirect function in the stability of the subtalar joint [3].

Today, several recent publications support the hypothesis that the intrinsic subtalar ligaments play an important role in the stability of the subtalar joint [12]. It is believed that the ligament of the tarsal canal appears to maintain apposition of the talus and calcaneus in all positions.

References

1. **Akiyami, K., Y. Takakura, Y. Tomita Y, K. Sugimoto, Y. Tanaka, S. Tamai.** Neurohistology of the sinus tarsi and sinus tarsi syndrome. – *J. Orthop. Sci.*, **4**, 1999, 299-303.
2. **Cahill, D. R.** The anatomy and function of the contents of the human tarsal sinus and canal. – *Anat. Rec.*, **153**, 1965, 1-17.
3. **Jotoku, T, M. Kinoshita, R. Okuda, M. Abe**. Anatomy of ligamentous structures in the tarsal sinus and canal. – *Foot Ankle Int*., **27**(7), 2006, 533-538.
4. **Helgeson, K**. Examination and Intervention for Sinus Tarsi Syndrome. – *N. Am. J. Sports Phys. Ther.*, **4**(1), 2009, 29-37.
5. **Kelikian A. S., S. K. Sarrafian**. *Sarrafian's Anatomy of the Foot and Ankle: Descriptive, Topographical, Functional.* (Eds S. Kelikian) Philadelphia, Wolters Kluwer Health/ Lippincott Williams & Wilkins, 2011.
6. **Kjaersgaard-Andersen, P., J. O. Wethelund, P. Helmig, K. Søballe**. The stabilizing effect of the ligamentous structures in the sinus and canalis tarsi on movements in the hindfoot. An experimental study. – *Am. J. Sports Med.*, **16**(5), 1988, 512-516.
7. **Klein, M. A., A. M. Spreitzer**. MR imaging of the tarsal sinus and canal: normal anatomy, pathologic findings, and features of the sinus tarsi syndrome. – *Radiology*, **186**(1), 1993, 233-240.
8. **Lee, M. S., H. T. Harcke, S. J. Kumar, G. S. Bassett**. Subtalar joint coalition in children: new observations. – *Radiology*, **172**, 1989, 635-639.
9. **Li, S., Z-D. Hou, P. Zhang, H. Li, Z-H. Ding, Y-J. Liu**. Ligament structures in the tarsal sinus and canal. – *Foot Ankle Int.*, **34**(12), 2013, 1729-1736.
10. **Linklater, J., C. L. Hayter, D. V. Tse**. Anatomy of the subtalar joint and imaging of talo-calcaneal coalition – *Skeletal Radiol.*, **38**, 2009, 437-449.
11. **Mabit, C., M. P. Boncoeur-Martel, J. M. Chaudruc, D. Valleix, B. Descottes, M. Caix**. Anatomic and MRI study of the subtalar ligamentous support. – *Surg. Radiol. Anat.*, **19**(2), 1997, 111-117.
12. **Michels, F., E. Vereecke, G. Matricali**. Role of the intrinsic subtalar ligaments in subtalar instability and consequences for clinical practice. – *Front. Bioeng. Biotechnol.*, **11**, 2023, 1047134.
13. **Michels, F., G. Matricali, E. Vereecke, M. Dewilde, F. Vanrietvelde, F. Stockmans**. The intrinsic subtalar ligaments have a consistent presence, location and morphology. – *Foot Ankle Surg.*, **27**(1), 2021, 101-109.
14. **Michels, F., S. Ozeki, S. W. Kong, G. Matricali, G. Assessment of subtalar instability**. – In: *Lateral ankle instability. An international approach by the ankle instability group.* First ed. (Eds. H. Pereira, S. Guillo, M. Glazebrook, M. Takao, J. Calder, N. Van Dijk, J. Karlsson), Berlin, Springer, 2021, 63-77.
15. **Michels, F., O. Taylan, F. Stockmans, E. Vereecke, L. Scheys, G. Matricali**. The different subtalar ligaments show significant differences in theirmechanical properties. – *Foot Ankle Surg.*, **28**, 2022, 1014-1020.
16. **Mittlmeier, T., S. Rammelt**. Update on subtalar joint instability. – *Foot Ankle Clin.*, **23**, 2018, 397-413.
17. **Pisani, G., P. C. Pisani, E. Parino**. Sinus tarsi syndrome and subtalar joint instability. – *Clin. Pod. Med. Surg.*, **22**, 2005, 63-77.
18. **Sarrafian, S. Anatomy of the foot and ankle**. – In: *Descriptive, topographic, functional. 2nd Edn* (Eds: S. Sarrafian), Philadelphia, J. B. Lippincott, 1993, 113-217.
19. **Shellshear, J., N. Macintosh**. *Surveys of anatomical fields*. Sydney, Grahame Book Company, 1949.

20. Smith, E. B. Astragalo-Calcaneo-navicular joint. – *J. Anat. Physiol*., **30**(3), 1896, 390-412.
21. Stephens, M. M., G. J. Sammarco. The stabilizing role of the lateral ligament complex around the ankle and subtalar joints. – *Foot Ankle*, **13**(3), 1992, 130-136.
22. Tsao, L. Sinus Tarsi Syndrome. – MRI Web Clinic, 2020, Available at: https://radsource.us/sinus-tarsi-syndrome/**Viladot, A., J. C. Lorenzo, J. Salazar, A. Rodriguez**. The subtalar joint: Embryology and morphology. – *Foot Ankle*, **5**(1), 1984, 54-66.
23. Wood-Jones, F. The talocalcaneal articulation. – *Lancet*, **247**, 1944, 241-242.
24. Yamaguchi, R., A. Nimura, K. Amaha, K. Yamaguchi, Y. Segawa, A. Okawa, K. Akita. Anatomy of the Tarsal Canal and Sinus in Relation to the Subtalar Joint Capsule. – *Foot Ankle Int.*, **39**(11), 2018, 1360-1369.

Institute of Experimental Morphology, Pathology and Anthropology with Museum
Bulgarian Anatomical Society

Acta Morphologica et Anthropologica, 30 (3-4)
Sofia ● 2023

Review Articles

Lateralisation, Hubs and Cognition in the Mammalian and Avian Brain

Enrico Marani

Dept. Biomedical signals and systems, TechMed Centre, University Twente, Enschede, The Netherlands

*Corresponding author e-mail: e.marani@utwente.nl

This article concerns an analysis of the frequently uttered statement that due to similarities in avian and mammalian brain connectivity and development comparable cognitive capacities are present. Two citations are given: “It is in the circuitry of mammalian and avian brains, rather than in their cytoarchitecture, that a marked degree of similarity exists”; “Cognitive functions are similar in birds and mammals”. Subjects treated are physiognomy and phrenology, both exponents of form asymmetry, causing the awakening of functional asymmetry. Dax, Broca and their speech localisation in the human brain are dealt with. Lateralisation in mammals and birds, the importance of the corpus callosum, differences between cortex of mammals and pallium of birds are described. Claustrum’s relation with cognition involves claustrum connections, split brain in humans is compared to avian hemisphere structure together with development of the avian and mammalian claustrum. Avian neuroanatomy contradicts the claim of similarity of mammalian and avian cognition.

Keywords: mammalian & avian cognition, lateralisation, Claustrum, physiognomy, phrenology

Introduction

Physiognomy, a person’s facial features or expression, especially when regarded as indicative of character, came into vogue when portraits became realistic representations of body or face. A tribute to Bulgaria in this respect is the work of Zograf Vasilie [41]. Vasilie belongs to the first painters that produced Pre-Renaissance natural portraying and started off even earlier than Cimabue (1240-1302; first work, crucifix, 1268).

Vasilie's decorations of the Saint Nicola temple of 1259, Boyana, Bulgaria, are legendary (**Fig. 1**).

Giambattista Della Porta (1535–1615) wrote "De humana physiognomonia libri III" (on human physiognomy in three parts) in 1586 [42]. Although the Greek and Roman works already indicated the resemblance between human faces and animal ones, Della Porta's book stressed the similarity. Since characteristic properties are given to animals (e.g., the lion symbolizing force), the resemblance also indicated that these animal properties are present in the nature of man (**Fig. 1**). Johann Casper Lavater (1741–1801) claimed physiognomy to be a science. His four volumes called "Physiognomische Fragmente zur Beförderung der Menschenkenntnis und Menschenliebe" [27] (Essays on physiognomy designed to promote the knowledge and the love of mankind, 1775–1778) produced serious controversies in literary and scientific circles, e.g. Johan Wolfgang Goethe (1749–1832) and Friedrich Schiller (1759–1805), and later on Duchenne de Boulogne (1806–1875), due to his electro-physiological studies of human facial muscles. Nevertheless, the success of Lavater's physiognomy books was based on his claim that physiognomy scientifically studied the inner and outer selves. Arguments are a semiotic one "The relations of facial signs contain a meaning", the other, instinctively we all think at the first appearance of a person that we can deduce his nature: unconscious judgements or snap judgements (**Fig. 1**). Thus, founded on Renaissance ideas, form of the head and/or face was related to (psychological) functions, which created the ambiance for Franz Joseph Gall (1758-1828). His ideas were "based on his early observations about the skull sizes and facial features of his classmates" by "making a connection between one classmate's odd shaped skull and advanced language abilities" [56]. In 1818 Gall introduced phrenology, changes of the skull cap due to the underlying brain differences. You could define it as physiognomy by the skull cap alone (**Fig. 1**). Gall supposed that parts of the brain were specialized in steering special human functions. He proposed that in particular cases (e.g. musicians or scientists) these cortical areas could grow larger than other areas and as a consequence the skull at these places protruded. **Form** asymmetry of the brain was phrenology's base, but was grounded on conjectures. Physiognomy and phrenology failed gravely, e.g. Lombroso (1835–1909); (see 31 for an extended description). Nevertheless, Gall produced the base for modern neuroscience by distributing and popularizing the idea of functional localizations within the brain that was accepted and/or discussed by the scientific circles of the 19th century.

Still, inconsequentially form asymmetry has been used a fifty years ago. Just the reverse argumentation has been employed in e.g. dyslexia. Absence of asymmetry in the left and right planum temporale supports dyslexia [12, 13]. The more general Geschwind-Behan-Galaburda (GBG) model of cerebral lateralization (caused by testosterone) provides a "complex but testable theory of cerebral lateralization". "Evaluation of the model suggests that it is not well supported by empirical evidence and that in the case of several key theoretical areas, the evidence that does exist is inconsistent with the theory" [5]. Structural brain asymmetries are nowadays found in various species e.g. great apes and rat. One should note that anatomical asymmetries need not to be directly coupled to actual asymmetries in function and vice versa.

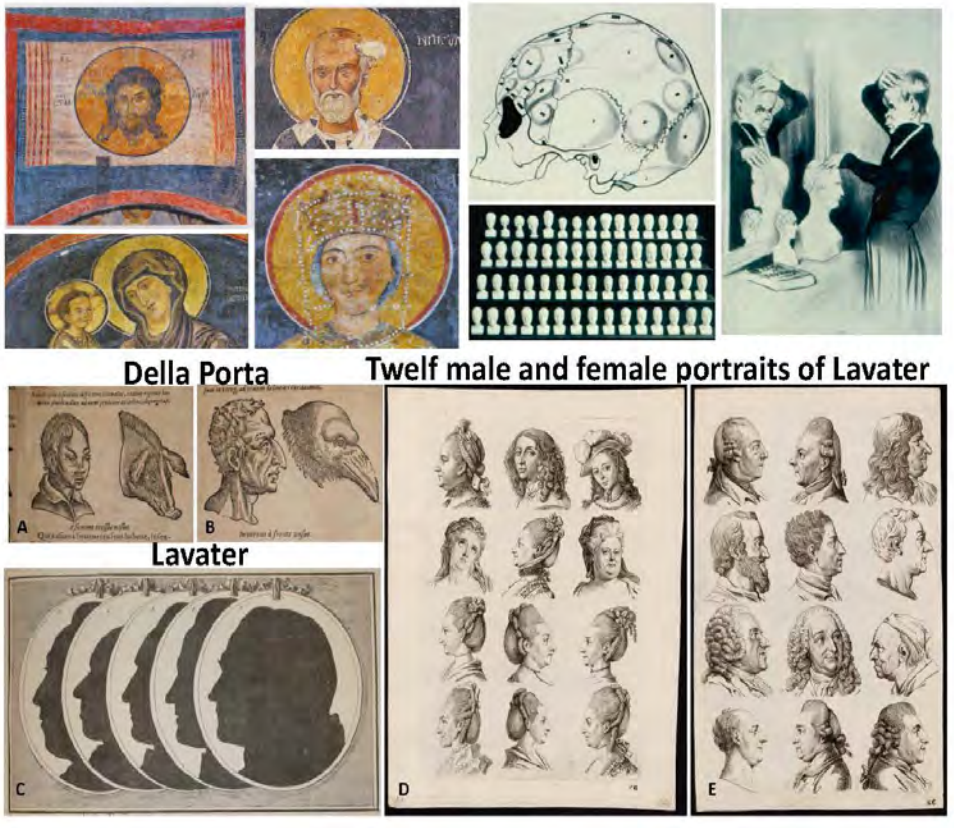

Fig. 1. Left upper part: Parts of the frescoes of the Boyana Church to demonstrate the Pre-Renaissance picturing of 1259. Left upper fresco is the Holy Mandylion (cloth upon which a miraculous image of Jesus's face is present); left lower figure contains the faces of the Holy Virgin and Child; upper right figure shows the face of St. Nicholas of Myra, and the lower right is the face of St. Ekaterina. Note the realistic portraying and facial expressions (oral permission Boyana church). Phrenology. Skull with extended bone areas related to specific brain areas and functions. Round game with all types of skulls for comparison and caricature of the phrenology application (courtesy Leiden Anatomical Museum) A to E: A and B are figures from Della Porta's work on physiognomy, indicating comparable face structures between man and animal. C, contains the silhouettes of faces made by Johann Casper Lavater: from left to right, 1 is the silhouette of Johan Martin Miller (poet, 1750–1814) described as: forehead and eye of a soft-feeling poet, weak lower lip and weak chin; 2, Asmus, pseudonym of Matthias Claudius (poet, 1740–1815): not weak, nor clever, honourable, credulous and direct, truth, man of feeling, modesty and tranquillity; 3, Friedrich Heinrich Jacobi: sharp angle of the forehead and the characteristic upper lip to chin indicates searching, wisdom and by its bent face weakness or poetry; 4 and 5 are compared: 4, critical mind, nose and forehead indicate poetic forces; 5, more active brain, nose indicates wisdom and is more beautiful, and mouth and chin relate to wisdom and tranquillity, modesty. D, Twelfth heads of unknown famous wives (men in E) of different nationalities and ages for Lavater. (Figures Della Porta and Lavater, courtesy Leiden University Library with permission)

Face recognition started with facial recognizable points, in which Anatomy was leading. From 1800 onwards, Anatomy and Physical Anthropology collected the measures of the skull and its parts, face, teeth, nose, ears and eyes. The quantitative results have been summarized in anatomical overviews (e.g. 3, 32, 51). These measures have been studied during development into adulthood and ageing. However, "Elastic bunch graph matching" uses Gabor wavelets that are marked here by circles on the face images (**Fig. 2**) and has been applied in geometric and photometric face recognition. Other methods are principal component analysis and linear discriminant analysis. The conclusion is that face recognition does not need any anatomical qualitative or quantitative information using these mathematical methods. You need, e.g., a series of Gabor nodes, simple reference points (tip of the nose, eyes), and you can place them anywhere on the face. Moreover, to get emotions present on the human face subtle changes have to be detected by finite element meshes or best feature detection [28, 55]. However, realistic contraction of facial muscles can also be studied with the VICON movement capture system (Oxford Metrics, UK). Using the VICON system, normal patterns for the movements of wrinkling the forehead and frowning, smiling and opening and closing the eyes are described [22]. Even facial emotions can be detected by a movement capture system: another view of physiognomy due to biometric artificial intelligence that recognizes instant emotions?

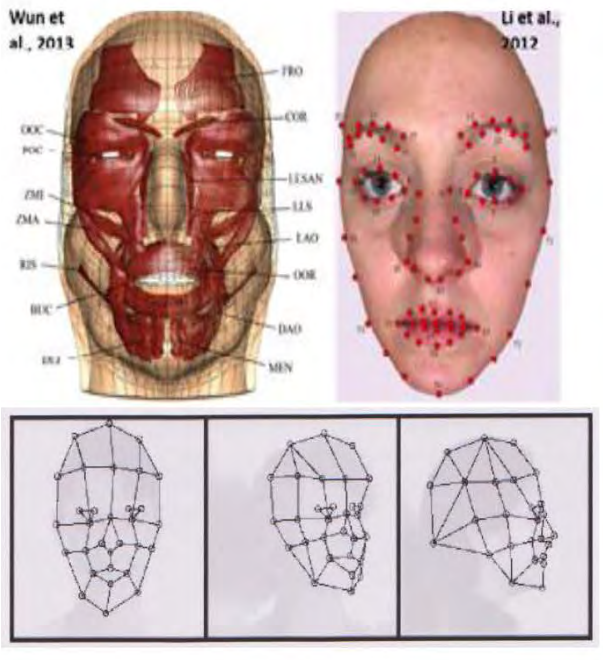

Fig. 2. During smiling subtle changes are also noted around the eyes, mouth, face edges and nose. Wearing spectacles disturbs even more the recognition of facial emotions. Therefore, a series of subtle changes has to be detected that needs registration of facial changes around eyes, mouth nose and circumference of the face. Techniques in producing a finite element mesh with the realistic face muscles projected in it (Wu et al. 2013, with permission) are studied [55]. The basic research on circumferential information versus local changes in the face is shown by Li et al. (2012, with permission)[28]. Lower figure: Facial recognizable points based on Anatomy and Gabor wavelets that placed over the face (figure is taken from the National Science and Technology Council (NSTC) subcommittee of Biometrics; [31].

Functional asymmetry of the human brain was found due to the study of brain damage. Aphasia was presented during a discourse at the medical society of Montpellier in France by Marc Dax (1770-1837) in 1836. Disability of speech has already been well known and the lecture of Dax was not unique. However, Dax noted that aphasia was exclusively coupled to the left hemisphere. "His paper was an unqualified flop. It aroused virtually no interest and was soon forgotten" [11]. The son Gustave Dax (1815-1893) published and extended his father's work. "*Observations tendant à prouver la coïncidence constante des dérangements de la parole avec une lésion de l'hémisphère gauche du cerveau*", *(Observations performed to prove the constance coincidence of word disturbances with a lesion of the brain left hemisphere)* was published in April 1865. The functional asymmetry of the brain got its establishment by Paul Broca (1824-1880). He indicated a special area in the sole left hemisphere responsible for speech: posterior inferior frontal gyrus (pars triangularis) now called Broca's area. Damage to this area produces aphasia. Broca himself did not recognize directly the importance of his findings in 1865 (*"Sur le siège de la faculté du langage articulé*."), but in fact he established the significance of the frontal left hemisphere in speech and consequently the functional lateralisation of the brain for speech [4]. By the way, Broca was greatly influenced by Gall's ideas, since Gall's functional brain localizations retained a certain reputation among scientists. Paul Broca's publication arrived one week after Gustave Dax's publication, not mentioning the Dax's works. Broca knew the work of Dax, because in 1863 he wrote: The hypotheses of Dax were valueless and without future in the eyes of history, because they were not published [15, 45]. Right hemisphere specialisations were also detected and concern orientation and awareness. Damages in the right hemisphere give hemispatial inattention, agnosias and also amusia, since e.g. singing is controlled by the right hemisphere. Although interest in cerebral dominance stayed present, its momentum occurred in 1960-1990. Mountcastle's (1962) "Interhemispheric relations and cerebral dominance" (John Hopkins Press) was followed by "Lateralization in the nervous system" produced by Harnard et al. (1977, Academic Press) and Glick's "Cerebral lateralisation in non-human species" (1985; Behavioral biology, Academic Press) to mention a few of the larger publications [18, 57, 58]. The popularization of the theme by "Left brain, right brain" of brought it to the attention of the layman [11].

Initial avian lateralisation studies

Cutting the left or right branch of the hypoglossal nerve, the tracheosyringeal nerve of the canary (*Serinus canaria*) does produce different results. Surgery of the right tracheosyringeal nerve does not change the song of the male canary as studied by sound spectrograms. However, surgery of the left tracheosyringeal nerve destructs the main repertoire of the song (**Fig. 3**). The song is replaced by silent gaps, clicking sounds or distorted modulations. "Such birds sing vigorously, as judged by their posture and motion, yet look like actors in a silent cinema film" [38]. The conclusion of these surgical results of 49 male canaries is that the left tracheosyringealis nerve, is dominant for song

control. Extra results show that this dominance is not related to auditory processing but is a muscle motor phenomenon. We owe to Nottebohm the establishment of asymmetry in bird's brains [38]. In the canary the left hemisphere is the location for both song and song learning (**Fig. 3**). Small and large lesions targeted to the nuclei involved in song production showed that in the canary the left hemispheric lesions disturbed song production heavily, while analogous lesions to the right hemisphere had clearly less effect on song production. The Zebra finch *(Taeniopygia guttata)* shows the reverse. In this bird species the right hypoglossus nerve is dominant for song control. Moreover, there is a difference between male and female, the male sings and the female is mostly silent as in the canary. The Zebra female hypoglossal nucleus volume is 63% of the male, the female neuron somata within this nucleus are 86% of the male and the female syrinx musculature weight is 51% of the male [53]. Females masculinized by hormones do start singing. The part of the hyperstriatum that respond to sounds and normally induces song in the males, can be stimulated with the consequence of song of the males, but not of the females. Although the same stimulation has been applied no response passes over the right tracheosynringeal nerve of the female [54].

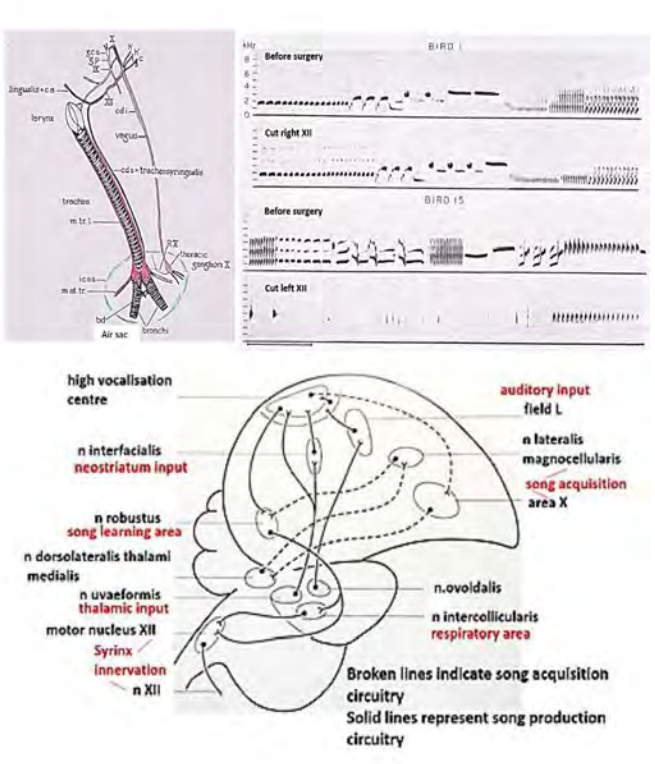

Fig. 3. Left upper part: topography of the left XII cranial nerve around trachea and syrinx: The sternotracheal muscle (m.st.tr) and the syrinx muscle mass (red). In green is the interclavicle air sac's position indicated (i.c.a.s.). Right: effects on song of the canary before and after surgery of the right and the left tracheosyringeal nerve (branch of the XII).Lower figure: Left hemisphere is dominant for song production and song learning in the canary adapted from [38]

Differences between mammalian and avian brain

Brain structure of birds differs from mammalian brain structure. A few examples are: The cortex structure is different. The avian pallium is based on nucleated clusters, while the mammalian cortex is known by its laminated neuron organisation (**Fig. 6**) [21, 25]. The storage of neurons in the avian forebrain is different, resulting in more neurons/volume [39]. The density of the avian neuron storage in the forebrain gives e.g. starling (483 million neurons) compared to rat (200 million), rook (1509 million) and marmoset (636 million neurons), all with the same brain mass. Birds contain on average twice more neurons per brain mass. The avian brain halves are restrictedly interrelated by its *commissura* anterior and a *commissura supraoptica* (**Fig. 4**), while the mammalian brain has an enormous interhemispheric connection, the corpus callosum. Specific areas of the bird pallium, e.g., nidopallium *caudolaterale*, have no connection with the hippocampus while several avian cortical areas do contain this memory construction inherently. Episodic memory, conscious memory of a previous experience, is more limited and processed in a different manner in birds when compared to mammals. "Food hoarding birds can remember what food they hide, where and when. Neuroanatomical and neurophysiological studies suggest that there may be a fundamental difference between episodic-like memory in birds and mammals. In contrast to the mammalian hippocampus, the avian hippocampus only receives visual and olfactory input; most high-order association areas in the avian brain involved in performing functions similar to those performed by neocortical association areas do not project to the hippocampus or structures providing it with direct input." [44].

All placental mammals do contain the corpus callosum, which constitutes the mutual functional hemispherical connections. Although the mammalian cortex is constructed layered, a module-like organization is present [50]. The modules are 200-300 um sectioned, explaining that corresponding cortical areas can be connected. The human corpus callosum contains over 200 million fibres (160 million [1]; 180 million [52]. Growth during childhood and adolescence shows callosal increase in thickness over the whole corpus, except the rostrum in women [29]. The resus monkey contains 56 million myelinated callosal fibres [26]. The diameter of the myelinated fibres counted can vary. In the rat brain diameters between 1 and 3 μm are noted [2]. One should note that beside myelinated fibres also unmyelinated ones are present, but hardly counted. Total commisurotomy of the human corpus callosum, known as split brain, has been studied by Sperry (1974). He concluded: "We can now demonstrate with appropriate tests a whole of distinct impairments that are most simply summarized by saying that the left and right hemispheres, following their disconnection, function independently in most conscious mental activities [48]. Each hemisphere, that is, has its own private sensations, perceptions, thoughts, and ideas all of which are cut off from the corresponding experiences in the opposite hemisphere. Each left and right hemisphere has its own private chain of memories and learning experiences that are inaccessible to recall by the other hemisphere. In many respects each disconnected hemisphere appears to have a separate "mind of its own".

The corpus callosum is absent in the avian brain (**Fig. 4**), meaning that interaction between both hemispheres is strongly reduced and is not comparable to the hemispherical interaction of mammals. Information towards avian hemispheres asks for relay groupings, of which 8 are discerened: Lateral and intermediate thalamofrontal, striotegmental, medial thalamo-frontal, medial strio-hypothalamic, quinto frontal, supraoptic and septo mesencephalic tract (**Fig. 4)** [10, 24, 40]. The functional lateralisation as common in the human brain is also present in the avian brain, but in its own hemispherical separated way. Lateralisation comprises several of the functional asymmetries in the avian brain, which clearly can differ in various bird species. Generally, the left hemisphere is dominant for mate recognition, category distinction, vocalisation, olfactory cues, while the right hemisphere knows dominance for spatial abilities, predator recognition, fear expression and aggression.

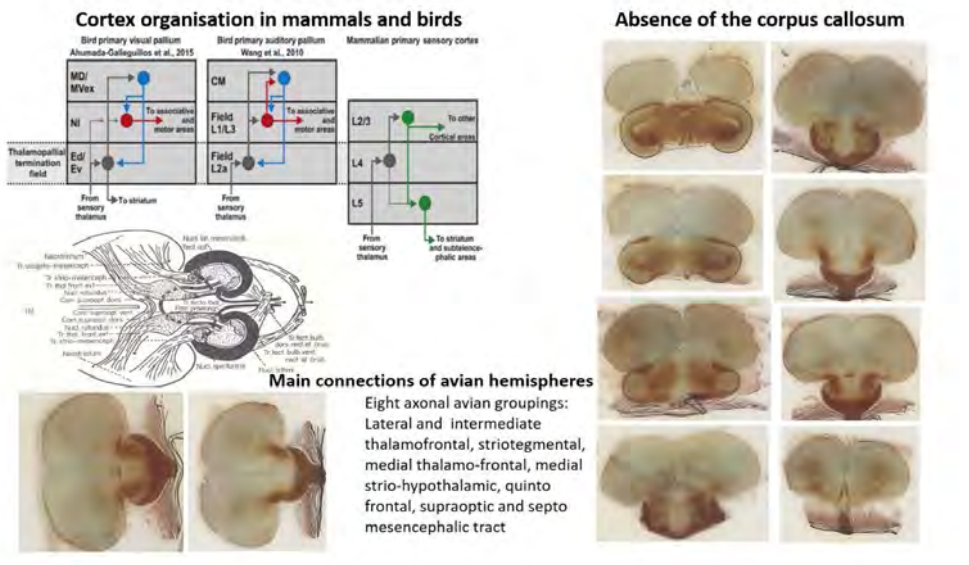

Fig. 4. Three aspects of the differences between mammalian and avian brains. Cortex organisation is altered in its laminar (mammals) and cluster-like (birds) construct (with permission) [17, 46]. Both avian hemispheres lack a “corpus callosum”, as demonstrated for the pigeon by silver colouration [35]. To serve information to these separated hemispheres several and unique axonal tracts are present [10, 24, 40].

Hubs

A hub is defined as a node occupying a central position in the overall organization of a network. Nodes are connected by edges considered as structural connections or functional relationships. The connections determine whether a node has a high

degree (lot of connections) or a low degree (less connections). Networks thus can contain several groups of nodes called modules. “A module includes a subset of nodes of the network that show a relatively high level of within-module connectivity and a relatively low level of intermodule connectivity. ‘Provincial hubs’ are high-degree nodes that primarily connect to nodes in the same module. “Connector hubs are high-degree nodes that show a diverse connectivity profile by connecting to several different modules within the network” [19]. The first “hub” diagram of the avian pallium has been composed by Stingelin [49]. He discerned 10 types of cells and four types of organisations that are present in the avian hemisphere pallium. Adding organisation-density values to the cell types (8 values discerned: 8 high and 1 low) a nexus diagram could be made. *Globus pallidus* (*paleostriatum primitivum*) came out highest, while the lateral striatum (*paleostriatum augmentatum*) belonged to the lowest qualified structures. Each pallial subparts contained its own node value see [40]. The connectivity matrix of the avian forebrain was studied by graph theory showed a connective core of hubs based on modular networks [46]. The nodes are characterized by an overload of connections that can be named according to their module organisation: prefrontal, premotor, septo-hippocampal, limbic-olfactory, viscero-limbic, tectofugal-visual and auditory module (**Fig. 5**).

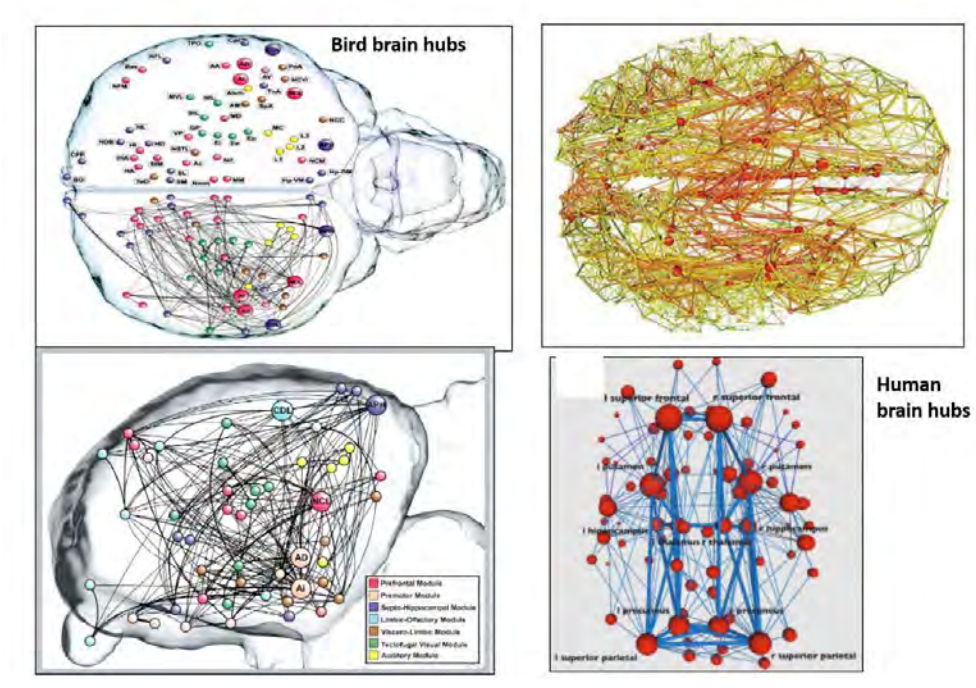

Fig. 5. Bird brain hubs are restricted to one hemisphere. Human brain hubs contact the hubs of the other hemisphere. Moreover the “intensity” of the connections over the corpus callosum belong to the strongests ones (thickness of the blue lines indicates the intensity of the interhemispherical connections) (with permission) [19, 46].

The spatial hemispherical distribution of the pigeon nodes does not contact the other hemisphere. Hubs regions need extra energy and are also called rich-club areas due to the possession of highly efficient neural information transfer in the brain's network. These rich-club hub areas in the human and mammalian brain indeed heavily contact the other hemispheres (**Fig. 5**) [19].

Cognition

Cognition is defined in the Oxford English Dictionary as "the action or faculty of knowing". The extended definition of cognition says: "the mental action or process of acquiring knowledge and understanding through thought, experience, and the senses. It encompasses many aspects of intellectual functions and processes such as attention, the formation of knowledge, memory and working memory, judgment and evaluation, reasoning and "computation", problem solving and decision making, comprehension and production of language". This extended definition of cognition does not make it easier to prove its existence in birds. Only restricted utterances of cognition can be studied in birds, even if we replace language for song. Animal cognition investigates in what way birds perceive, learn, store and use information, adding the warning for anthropomorphism (see Colbert-White and Kaufman, 2019 for anthropomorphic approaches) [8, 59]. In literature e.g. the corvid's repertoire of cognition embraces, among others, manufacture and use of tools, conspecifics support, spatial and long-term memory, and quickly recognize behavioural and numerical principles [6]. This crow cognition has been studied in relation to absolute numerosity, the abstract categorization of absolute numerical quantity [36].

The comparison between humans, monkeys and crows unmistakably shows that crows, although they have the capacity of "counting", act worse compared to humans and monkeys (**Fig. 6**). Absolute numerosity is considered an indication or measure of intelligence. Aesop's fable "The crow and the pitcher" tells of a thirsty crow dropping stones in a pitcher to raise the water level. The

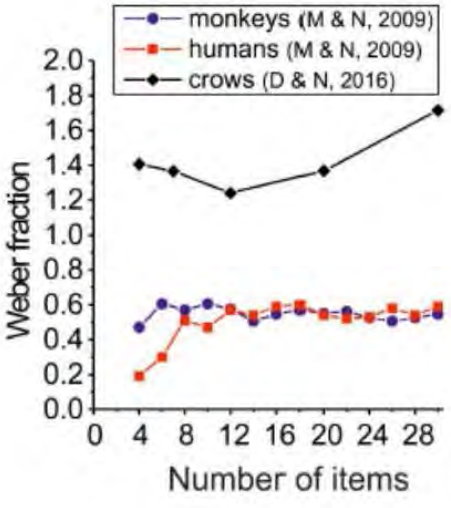

Fig. 6. The smaller the Weber fraction, the higher is the discrimination accuracy of animals in absolute numerosity judgements (humans, monkeys and crows are compared; Nieder, 2020 [36]; MN, Merten and Nieder, 2009, J Cogn Neurosci 21: 333-346; DN, Ditz and Nieder, 2016, Proc R Soc B 283: 20160083).

water level was initially too low to drink. These type of experiments, called "Aesopus" experiments, have been carried out frequently and all published experiments have been re-studied in a so-called meta-analysis [14]. "Does being sensitive to causal cues imply causal understanding? This question is important to evaluate experiments with 'arbitrary' tasks, but it is also relevant to animal cognition in general. We maintain that animals can use causal cues efficiently while lacking what we commonly label 'understanding'. This point is far from new, as the ethological and psychological literature contains many examples of what we may term cognitive blind sight, that is, behaviour that is suggestive of cognitive complexity yet emerges from a combination of genetic predispositions, general mechanisms such as stimulus generalization, and trial-and-error learning" and at the end of their paper: "We conclude that Aesop's fable experiments have not yet produced evidence of causal understanding" [14]. An undervalue of the innate identity of the bird's brain occurs due to the regular position taken that bird brains are evolutionary comparable to mammalian brains and that intelligence and cognition are based on the same archaic characteristics [7]. "Cortical cells and circuits are present in all amniotes but with different macro-architectures in birds versus mammals" [25].

Claustrum

The research importance of the mammalian claustrum started with the study of Francis Crick and Christof Koch (2005) "What is the function of the claustrum?" [9]. They involved the claustrum in consciousness, which encountered criticism later on [33]. Attention was supported by Yael Goll, Gal Atlan and Ami Citri (2015), while cognition was sustained by Nicola Clayton and Nathan Emery (2005) [7, 16]. This cognition model of the claustrum has been backed up by various research projects (see e.g. ten Cate and Healy, 2017, birds; Madden et al., 2022, mammals) [30, 59]. The claustrum has been divided into dorsal and ventral zones. The claustrum's dorsal quantitative cytoarchitectonic appearance has been studied in the Anatomical department of the Sofia University [20]. The study increased the previous three or four into eight types of neurons: large, medium-sized and small multipolar, bipolar and pyramidal-like neurons, and three types of aspiny neurons. The lower ventral zone is directed towards the amygdaloid region with supposed comparable amygdaloid characteristics. The human claustrum is regarded as a multi-modal information processing network [23, 37]. The claustrum exercises cognitive control, and its activation is: or at the beginning of a task or at changing the cognitive strategy or at setting a new goal. Gender differences and variances between left and right hemisphere have been reported. Claustrum's connections with the cortex bring cognitive task performances to the forefront in human research, especially its role in cognition control by its frontal cortex relations. Cortical-claustral contralateral projections dominate the amount of ipsilateral cortical-claustral projections in mammals. "Claustral connections enable interhemispheric transmission of certain types of modality-specific information to widely-separated cortical areas. By transmitting information from the frontal cortex

in one hemisphere to parietal and occipital regions in the other hemisphere, the claustrum provides an interhemispheric route that extends beyond the other callosal projections that interconnect corresponding sites in both hemispheres" [47]. Claustral function can be described as combining visual, tactile, auditory and emotional sensations both intra and interhemispherically. The claustrum contributes to memory storage, contiguity learning, suppression of natural urges, psychoses, recognition of fear and planning control. This is considered its integrative function between sensory and motor functions together with the reporting back to the mammalian involved cortex.

Constrained Spherical Deconvolution Tractography demonstrated the human interhemispheric and intrahemispheric connections of the claustrum (**Fig. 7)** [34]. Four types of bundles (anterior, posterior, superior, and lateral) could be discerned that connected the claustrum with the cortex. The anterior and posterior cortico-claustral bundles relayed the claustrum to prefrontal cortex and visual cortex. The superior tract involved the claustrum into sensory-motor areas, while the lateral pathway associated the claustrum with the auditory cortex. A claustral medial pathway, connecting the claustrum with the basal ganglia, is described, including caudate nucleus, putamen, and globus pallidus. "An interesting and exciting new finding is the demonstration of a bilateral connection between claustrum and contralateral cortical areas and an interclaustral communication with interconnection bundles interspersed within the bulk of the trunk of the corpus callosum" [34]. By transmitting information from the frontal cortex in one hemisphere to parietal and occipital regions in the other hemisphere, the claustrum provides an interhemispheric route that extends beyond the other callosal projections. All these interhemispheric connections are absent in birds.

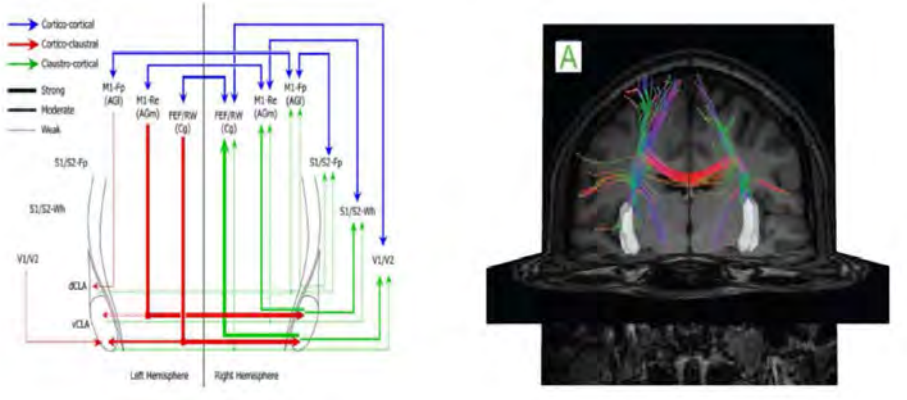

Fig. 7. Circuit diagram of interhemispheric sensimotor cortico-claustro-cortical circuits in rats [47]. Claustral connections enable intrahemispheric and important interhemispheric transmission of certain types of modality-specific information to widely-separated cortical areas. Tractograph figure: Claustra are in white, "The whole interhemispheric claustrum connectome is showed on this figure. Some fibers of the medial and lateral pathways are visible", (with permission) [34].

Development claustrum in reptiles, birds and mammals

The orphan nuclear receptor Nr4a2 characterizes the claustrum, even during development as does the mature expression of G protein gamma 2 subunit (Gng2) and parvalbumin (PV) immunoreactivity [33, 43]. While in mammals and reptiles the claustrum stays an independent leaflet, its organisation in birds is characterized by a connection between its dorsal endopiriform nucleus and the subplate layer. Insula-like neurons grow internally in reptiles and birds, while in mammals an exterior localisation path is followed. “Note that reptilian and avian cell masses are layered in an outside-in pattern, whereas mammalian counterparts become stratified in an inside-out pattern” [43]. The avian claustrum has evidently its own developmental topography that is different from mammals.

Conclusion

Despite the statement that due to similarities in avian brain connectivity and brain development comparable cognitive capacities are present in the mammalian and avian brain, the absence of a corpus callosum, the differences in cortical structure and hub organisation, the special separate claustrum topography, and the presence of an avian “split brain giving each hemisphere its own mind”, avian neuroanatomy challenges this claim.

References

1. Aboitiz, F., A. B. Scheibel, R. S. Fisher, E. Zaidel. Fiber composition of the human corpus callosum. – *Brain Research*, **598**, 1992, 143-153.

2. Barazany, D., P. J. Basser, Y. Assaf. In vivo measurement of axon diameter distribution in the corpus callosum of rat brain. – *Brain*, **132**, 2009, 1220.

3. Bookstein, F. L. *Morphometric Tools for Landmark Data: Geometry and Biology*, Cambridge, Cambridge University Press, 1992.

4. Broca, P. Sur le siège de la faculté du langage articulé. - *Bulletins et Mémoires de La Société d’Anthropologie de Paris*, **6**, 1865, 377-393.

5. Bryden, M. P., I. C. Mcmanus, M. B. Bulmanfleming. Evaluating the empirical support for the Geschwind-Lehan-Galaburda model of cerebral lateralization. – *Brain and Cognition*, **26**, 1994. 103-167.

6. Butler, A. B., R. M. J. Cotterill. Mammalian and avian neuroanatomy and the question of consciousness in birds. – *The Biological Bulletin*, **211**, 2006, 106-127.

7. Clayton, N. S., N. J. Emery. Avian models for human cognitive neuroscience: A proposal. – *Neuron*, **86**, 2015, 1330-1342.

8. Colbert-White, E. N., A. B. Kaufman. *Animal cognition 101*, Springer Publishing Company, 2019.

9. Crick, F. C., C. Koch. What is the function of the claustrum? – Philosophical Transactions of the Royal Society - *Biological Sciences*, **360**, 2005, 1271-1279.

10. Dubbeldam, J. L. The neural substrate for ‘learned’ and ‘nonlearned’ activities in birds: a discussion of the organization of bulbar reticular premotor systems with side-lights on the mammalian situation. – *Acta Anat. (Basel)*, **163**, 1998, 157-172.

11. Ettlinger, G. Left brain, right brain. – *The British Journal of Psychiatry*, **140**, 1982, 217-218
12. Galaburda, A. M. *Dyslexia and development: neuro-biological aspects of extra-ordinary brains*, Harvard University Press, 1993.
13. Galaburda, A. M., G. F. Sherman, G. D. Rosen, F. Aboitiz, N. Geschwind. Developmental dyslexia: four consecutive patients with cortical anomalies. - *Annals of Neurology*, **18**, 1985, 222-233.
14. Ghirlanda, S., J. Lind. 'Aesop's fable' experiments demonstrate trial-and-error learning in birds, but no causal understanding. – *Animal Behaviour*, 123, 2017, 239-247.
15. Giménez-Roldán, S. A critical review of Broca's contribution on aphasia: from priority to Leborgne the hatter. – *Neurosciences and History*, 5, 2017, 58-68.
16. Goll, Y., G. Atlan, A. Citri. Attention: the claustrum. – *Trends in Neurosciences*, **38**, 2015, 486-495,
17. Güntürkün, O., T. Bugnyar. Cognition without cortex. – *Trends in Cognitive Sciences*, **20**, 2016, 291-303.
18. Harnad, S. R. *Lateralization in the nervous system*, New York, Academic Press, 1977
19. Heuvel, M. P. van den, O. Sporns. Network hubs in the human brain. – *Trends in Cognitive Sciences*, 17, 2013, 683-696.
20. Hinova-Palova, D., G. Kotov, B. Landzhov, L. Edelstein, A. Iliev, S. Stanchev, G. P. Georgiev, V. Kirkov, T. Angelov, D. Nikolov, K. Fakih, A. Paloff. Cytoarchitecture of the dorsal claustrum of the cat: a quantitative Golgi study. – *Journal of Molecular Histology*, **50**, 2019, 435-457.
21. Jarvis, E., O. Güntürkün, L. Bruce, A. Csillag, H. Karten, W. Kuenzel, L. Medina, G. Paxinos, D. J. Perkel, T. Shimizu, G. Striedter, J. M. Wild, G. F. Ball, J. Dugas-Ford, S. E. Durand, G. E. Hough, S. Husband, L. Kubikova, D. W. Lee, C. V. Mello, A. Powers, C. Siang, T. V. Smulders, K. Wada, S. A. White, K. Yamamoto, J. Yu, A. Reiner, A. B. Butler. Avian brains and a new understanding of vertebrate brain evolution. – *Nature Reviews Neuroscience*, **6,** 2005, 151-159.
22. Jorge, J. J., P. R. Pialarissi, G. C. Borges, S. A. F. Squella, M. de F. de Gouveia, J. C. Saragiotto, V. R. Gonçalves. Objective computerized evaluation of normal patterns of facial muscles contraction. – *Brazilian Journal of Otorhinolaryngology*, **78**, 2012, 41-51.
23. Kanarev, M., N. Petrova1, A. Petrova, S. Sivkov. Functional aspects of the human claustrum – literary review**.** – *Acta Morphol. Anthropol.*, **29**, 2022, 195-197.
24. Kappers, C., G. Huber, E. Crosby. The Comparative anatomy of the nervous system of vertebrates, including man. – *JAMA*, **107**, 1936, 1833-1834.
25. Karten, H. J. Neocortical Evolution: Neuronal Circuits Arise Independently of Lamination. – *Current Biology*, 23, 2013, R12-R15.
26. Lamantia, A.-S., P. Rakic. Cytological and quantitative characteristics of four cerebral commissures in the rhesus monkey. – *The Journal of Comparative Neurology*, **291**, 1990, 520-537.
27. Lavater, J. C. *Physiognomische fragmente, zur beförderung der menschenkenntniß und menschenliebe.* Leipzig, Weidmann and Reich, 1776.
28. Li, X., Q. Ruan, Y. Ming. A remarkable standard for estimating the performance of 3D facial expression features. – *Neurocomputing*, **82**, 2012, 99-108.
29. Luders, E., P. M. Thompson, A. W. Toga. The Development of the Corpus Callosum in the Healthy Human Brain. – *The Journal of Neuroscience*, **30**, 2010,
30. Madden, M. B., B. W. Stewart, M. G. White, S. R. Krimmel, H. Qadir, F. S. Barrett, D. A. Seminowicz, B. N. Mathur. A role for the claustrum in cognitive control. – *Trends in Cognitive Sciences*, **26**, 2022, 1133-1152.
31. Marani, E., C. Heida. *Head and Neck*, Springer Cham, 2018.
32. Martin, R. *Lehrbuch Der Anthropologie Band I: In Systematischer Darstellung,* Stuttgart, Gustav Fischer Verlag, 1957.

33. **Mathur, B. N.** The claustrum in review. - *Frontiers in Systems Neuroscience*, **8**, 2014.
34. **Milardi, D., P. Bramanti, C. Milazzo, G. Finocchio, A. Arrigo, G. Santoro, F. Trimarchi, A. Quartarone, G. Anastasi, M. Gaeta.** Cortical and subcortical connections of the human claustrum revealed in vivo by constrained spherical deconvolution tractography. – *Cerebral Cortex*, **25**, 2015, 406–414.
35. **Nauta, W. J. H., P. A. Gygax.** Silver impregnation of degenerating axon terminals in the central nervous system: (1) Technic. (2) Chemical notes. - *Stain Technology*, **26**, 1951, 5–11.
36. **Nieder, A.** Absolute Numerosity Discrimination as a Case Study in Comparative Vertebrate Intelligence. - *Frontiers in Psychology*, **11**, 2020.
37. **Nikolenko, V. N., N. A. Rizaeva, N. M. Beeraka, M. V. Oganesyan, V. A. Kudryashova, A. A. Dubovets, I. D. Borminskaya, K. V. Bulygin, M. Y. Sinelnikov, G. Aliev.** The mystery of claustral neural circuits and recent updates on its role in neurodegenerative pathology. - *Behavioral and Brain Functions*, **17**, 2021.
38. **Nottebohm, F., T. M. Stokes, C. M. Leonard.** Central control of song in the canary, *Serinus canarius*. - *The Journal of Comparative Neurology*, **165**, 1976, 457–486.
39. **Olkowicz, S., M. Kocourek, R. K. Luèan, M. Porteš, W. T. Fitch, S. Herculano-Houzel, P. Nemec.** Birds have primate-like numbers of neurons in the forebrain. - *Proceedings of the National Academy of Sciences of the United States of America*, **113**, 2016, 7255–7260.
40. **Pearson, R.** *Avian brain*, 1st edition, Academic press, 1972.
41. **Popkonstantinov, K.** *Zograf Vasilie and The Boyana Church 750 Years Later*, Sofia, Unicart, 2009.
42. **Porta, G.** *De Humana Physiognomonia. Libri II*, Sorrento, Giuseppe Cacchi, 1586
43. **Puelles, L., A. Ayad, A. Alonso, J. E. Sandoval, M. Martínez-de-la-Torre, L. Medina, J. L. Ferran.** Selective early expression of the orphan nuclear receptor Nr4a2 identifies the claustrum homolog in the avian mesopallium: Impact on sauropsidian/mammalian pallium comparisons. – *Journal of Comparative Neurology*, **524**, 2016, 665–703.
44. **Rattenborg, N. C., D. Martinez-Gonzalez.** A bird-brain view of episodic memory. – *Behavioural Brain Research*, **222**, 2011, 236–245.
45. **Roe, D., S. Finger.** Gustave Dax and his fight for recognition: an overlooked chapter in the early history of cerebral dominance. - *Journal of the History of the Neurosciences*, **5**, 1996, 228–240.
46. **Shanahan, M., V. P. Bingman, T. Shimizu, M. Wild, O. Güntürkün.** Large-scale network organization in the avian forebrain: a connectivity matrix and theoretical analysis. - *Frontiers in Computational Neuroscience*, **7**, 2013.
47. **Smith, J. B., K. D. Alloway**. Interhemispheric claustral circuits coordinate sensory and motor cortical areas that regulate exploratory behaviors. - *Frontiers in Systems Neuroscience*, **8**, 2014.
48. ***Sperry, R. W.*** Lateral specialization in the surgically separated hemispheres, 1974.
49. **Stingelin, W.** *Vergleichend morphologische untersuchungen am vorderhirn der vögel auf cytologischer und cytoarchitektonischer grundlage*, Basel, Verlag Helbing & Lichtenhahn, 1958.
50. **Szentágothai, J.** The modular architectonic principle of neural centers. – *Reviews of Physiology, Biochemistry and Pharmacology*, **98**, 1983, 11–61.
51. **Titus, R. von L., W. Werner. Kopf: Teil A: Übergeordnete Systeme.** – Heidelberg, Springer Berlin, 1985.
52. **Tomasch, J.** Size, distribution, and number of fibres in the human *corpus callosum*. – *The Anatomical Record*, **119**, 1954, 119–135.
53. **Wade, J., L. Buhlman, D. Swender.** Post-hatching hormonal modulation of a sexually dimorphic neuromuscular system controlling song in zebra finches. - *Brain Research*, **929**, 2002, 191–201.

54. **Williams, H.** Sexual dimorphism of auditory activity in the zebra finch song system. – *Behavioural and Neural Biology*, **44**, 1985, 470–484.
55. **Wu, T., A. P. L. Hung, P. Hunter, K. Mithraratne.** Modelling facial expressions: A framework for simulating nonlinear soft tissue deformations using embedded 3D muscles. – *Finite Elements in Analysis and Design*, **76**, 2013, 63–70.
56. **Reader in the History of Aphasia: From Franz Gall to Norman Geschwind.** (Ed. Eling, P.), 1994
57. **Mountcasle, V.** Interhemispheric Relations and Cerebral Dominance. – *Bulletin of the Orton Society*, **14**, 1964.
58. **Glick, S.,** *Cerebral Lateralization in Nonhuman Species*, 1st Edition, Academic Press, 1985.
59. **Ten Cate, C., S. Healy (Eds.).** *Avian Cognition***.** - Cambridge, Cambridge University Press, 2017.

Institute of Experimental Morphology, Pathology and Anthropology with Museum
Bulgarian Anatomical Society

Acta Morphologica et Anthropologica, 30 (3-4)
Sofia ● 2023

National Anthropological Museum: A Review of Sixteen Years of Experience

Atanas Katsarov

Institute of Experimental Morphology, Pathology and Anthropology with Museum, Bulgarian Academy of Sciences, Sofia, Bulgaria

*Corresponding author e-mail: zanasko@gmail.com

The National Anthropological Museum (NAM) is largest bone archival repository in Bulgaria dedicated to preserving bone archival material and serving as a scientific, educational and cultural institution. It is a part of the Institute of Experimental Morphology, Pathology and Anthropology (IEMPAM) of Bulgarian Academy of Sciences (BAS). From its creation until now, the museum has been working for the popularization of anthropological knowledge and the affirmation of anthropology in Bulgaria, contributing to increasing interest in cultural-historical heritage and social memory. Established to promote and popularize anthropological research in Bulgaria, the museum has become a center for various anthropological, historical, archaeological and even culture events.

Key words: anthropology, education, National Anthropological Museum, IEMPAM

Introduction

As a unique museum in Bulgaria, NAM was established on March 21st, 2007, as a result of expansion of the traveling exposition of IEMPAM – "The Man in the Past". In addition to the large number of anthropological studies of Bulgarian population, the museum also provides knowledge about the people who inhabited the Bulgarian lands in the ancient times. Despite the fact that the results of these studies are known to a specialized circle of experts, during all 16 years of its existence, the NAM team and the management of IEMPAM made a considerable effort to popularize anthropological knowledge, which is evident from the overall work of the museum.

Scientific priorities of the National Anthropological Museum

The research activity of IEMPAM and NAM aims to establish both institutions as a scientific unit with complex innovative research on the problems of human and veterinary medicine, anthropology and national heritage [2]

The scientific priorities of IEMPAM and NAM is consistent with the guidelines outlined in the National Strategy for the Development of Scientific Research in the Republic of Bulgaria 2017-2030, "Strategy for the Development of the Bulgarian Academy of Sciences 2018-2030" and the priorities of the new EU Framework Program for scientific research and innovation 5 "Horizon Europe" (2021-2027) with priorities "Health", "Food, bioeconomy and natural resources", "Environment", "National identity", "Cultural and historical heritage".

At the level of its scientific production and popularization, IEMPAM, resp. NAM, are proving themselves as leading institutions in the field of morphology, pathology, anthropology and museum activity with a certain own place in the national and international research area.

Scientific contribution and activities of the National Anthropological Museum

The activity of NAM is popularized through media presentations, public lectures, participation of the team in various events, etc. The museum exposition is established in accordance with two main principles in museology: thematic and chronological [3]. The topic covering the anthropological characteristics of the population of the Republic of Bulgaria is directly related to the chronology, as many archaeological artifacts are added to the main exhibition material - human bone remains, discovered during the archaeological excavations of necropolises, sanctuaries, temples and settlements from the relevant historical periods, studied on the territory of Bulgaria at present [4].

The permanent exhibition of the museum presents cultural practices related to the way of burial during different historical periods, the healing and ritual effects that left traces on the human bone remains, as well as 3-dimensional reconstructions of the head on the skull, visualizing the people who inhabited our lands through different historical periods since ancient times to the present days. A special emphasis in the exhibition is various pathological changes found on the human bone remains. They reveal the prevalence and incidence of various diseases and are reliable and convincing source of what were the living conditions at that time.

In parallel with its permanent exhibition, the museum presents temporary thematic exhibitions, the purpose of which is to attract the public and popularize the anthropological knowledge. They are devoted to three main topics:

The first topic presents anthropology in Bulgaria – "The Monastery of Mostich" (2009), "Prominent Bulgarian Anthropologists – Kadanov and Balan" (2010), "Modern Anthropology" (2014).

The second major topic reveals the cultural practices related to death and the faith of man – "Funeral practices from Prehistory to the Middle Ages in our lands" (2016), "Kremikovtsi Monastery" "St. Vmchk Georgi Pobedonosets" – known, but also unknown" (2020), "Between the two worlds" (2022).

The third topic of the National Anthropological Museum's temporary exhibitions is the revelation of humanity embodied by medicine – "Diseases and Treatment

through the Ages" (2018), "Great Epidemics in History" (2020), "The Infirmary in Antiquity and the Middle Ages" (2021), Materia Medica (2023).

The temporary exhibitions are the object of great visitor interest, both in the museum and when traveling exposition is visiting other regional museums in Bulgaria. The museum also is a venue of two photography exhibitions – "Hello Africa" and "Underwater Addiction".

The annual events, which are organized in collaboration with scientists from the Department of Anthropology and Anatomy of IEMPAM – BAS, have become more popular and attractive during the last sixteen years. One of these events is the participation of NAM in the European Night of Museums, which originated in France. The diverse program and the presentation of interesting facts and events in the field of anthropology attracted the attention of an increasingly large audience. The established tradition of conducting anthropological measurements and interesting thematic lectures become an exciting event at the Night of the Museums, and the National Anthropological Museum has proved itself as an attractive place for visitors, e.g. students, scientists, citizens, etc. (**Fig. 1A, 1B**)

Fig. 1A.

The participation of NAM in the first edition of the "Salon of Museums" in the National Palace of Culture was also significant achievement of the Museum. The event was part of the official cultural program of the Bulgarian Presidency of the Council of the European Union and presented to a wide audience the data on the historical and cultural development and religious beliefs during the different eras, the types of people, the knowledge of diseases and injuries that have left traces on the bone remains in the museum's exposition, as well as medical and ritual effects on them.

The Museum team participate in various current archaeological, anthropological and archaeogenetic studies. New advanced methods for sexing skeletal remains, both cranial

Fig. 1B.

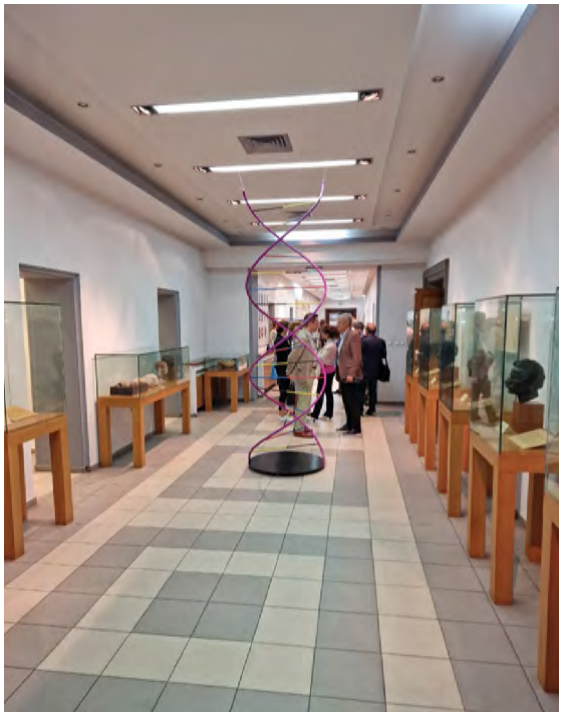

and postaxial, are being developed. Scientists from IEMPAM and NAM participate in rescue archaeological excavations of infrastructure sites of European, national and regional importance. Anthropological research is being carried out on human bone remains (movable cultural values) discovered during archaeological investigations at various places in the country. The research data enrich the idea of the paleodemographic development of the population in our lands. Models of ecological and social adaptation of the various human groups of the past are being developed, which allow the complex study of man with the constant interaction of his nature and culture.

One of the most actively developing activities of the museum are educational programs with children and students (**Fig. 2**). Since the beginning of 2017, the NAM team together with scientists and researchers from the Department of Anthropology and Anatomy at IEMPAM reate and implement educational programs in "Biology and Health Education" and "History and Civilization". They were structured in several modules – "The Way of Man (Anthropogenesis)", "The Human Body" and "Young Researcher", Laboratory "Face from the Past".

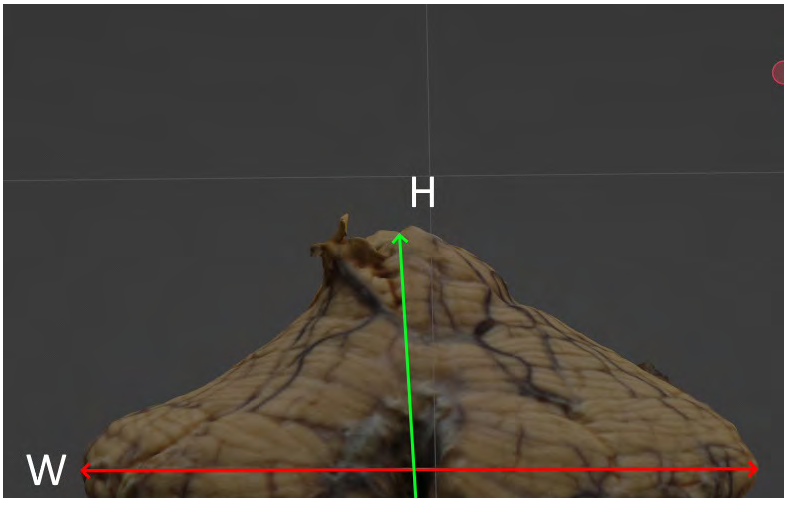

Fig. 2.

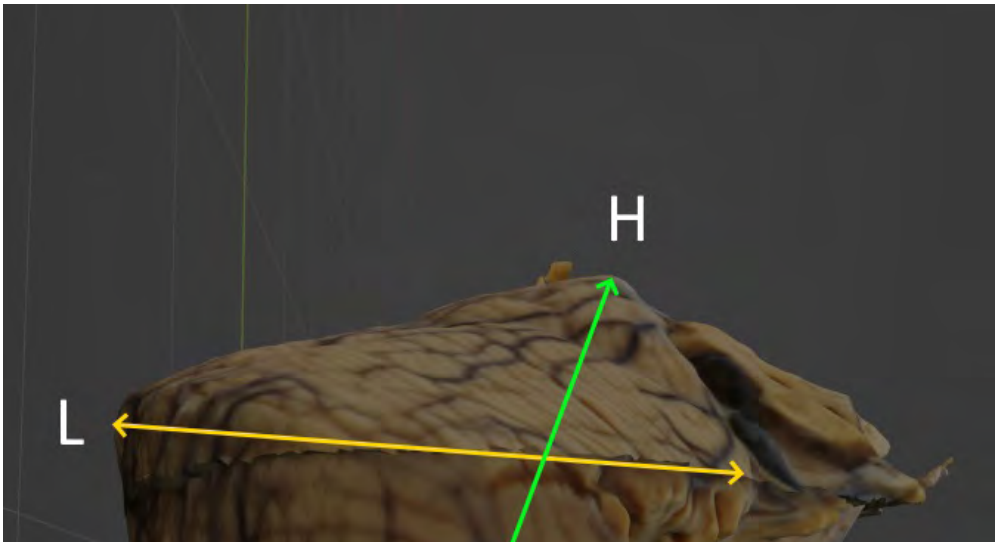

Fig. 3

In the first module "The Human Body", the program has been expanded with museum lessons aimed at introducing students of different age groups to the most complex functioning organism – the human body.

In the second module – "Young Researcher Laboratory", students from Sofia schools take on the role of investigators taking their own fingerprints, examine them and compare them, participate in various examinations and find the answers to the tasks themselves, such as: to determine the height of the medieval Bulgarian by measuring long bones, to examine the density of the bone under a microscope, etc.

In the third module "Face from the Past" students from Bulgaria, Poland, Italy, Portugal and Spain may attend a lecture "Everyday Life of the Anthropologist" that is presented in a hybrid form. The lecture is focused on the contribution of anthropology in elucidating the past of man and the field work of a specialist-anthropologist.

With the support of the Ministry of Education and Science, the museum conducts a summer anthropology school "Man and his Health", in which high school students, learn the secrets of anthropology by lectures and practical activities revealing the physical development of man and the conditions that influence him. By involving the participants in classes on anthropometry and anthroposcopy, body composition analysis using the bioimpedance method, laboratory analysis of food, etc. attention is also paid to socially significant phenomena related to human health. The implementation of the educational museum "My Body" provide new opportunities for the National Anthropological Museum in interactive learning in schools, with aim of upgrading the knowledge obtained at school. The program is designed for students from 5th to 11th grade.

The emphasis in conducting modules is on students acquiring knowledge of basic historical problems and processes for mastering skills that allow them to navigate the huge flow of information and necessary for them in the process of building their personal development. The inclusion of practical modules has proven

to be the winning model for attracting a teenage audience that wants not only to be informed and observe, but also to empathize and participate in the process of acquiring knowledge and skills.

Last but not least, the National Anthropological Museum is the venue of traditional National Conference with International Participation, Morphological Days, organized by IEMPAM and Bulgarian Anatomical Society (**Fig. 3**). The conference demonstrates that morphological science has spread beyond the classical macroscopic and microscopic morphology by developing multidisciplinary and interdisciplinary research with molecular and cellular biology, chemistry, computer sciences and modelling, archaeology and national identity [1].

Conclusion

From its creation (2007), NAM has gone through many obstacles, but we can say that our ambition to become recognizable to the general public is almost fulfilled. Efforts in this direction can be seen from the reviews in the internet, on the website of the museum, as well as on our pages in social networks and navigation applications.

One of the main museum contributions is the research on the bone remains found during numerous archaeological expeditions that provides new knowledge for scientific literature. On the basis of these scientific studies, NAM is unique institution for anthropological restoration and conservation, development of methods for preservation of museum artefacts, the creation of museum expositions, as well as other museum activities.

Over the years, through its good cooperation with various educational institutions (schools, universities), the National Anthropological Museum has become an educational center where the knowledge of history, biology and art is complemented with the new knowledge. NAM is the only museum institution in the country for anthropological studies of the past and the recent population of the Republic of Bulgaria. The museum presents bone artefacts from archaeological excavations, original plastic reconstructions of the head on the skull of great Bulgarians as well as thematic exhibitions from many regional history museums in the country. NAM provides exhibits to the National History Museum and regional museums useful for preserving and popularizing the national historical heritage and strengthening the museum's work.

References

1. **Atanassova, N.** Editorial: VIII National Conference with International Participation "Morphological Days", Sofia, 10-12 of June, 2022. – *Acta Morphol. Anthropol.*, **29**(3-4), 2022, 7-9.
2. Institute of experimental morphology, pathology and anthropology with museum, Bulgarian academy of sciences, 2023. Available at http://www.iempam.bas.bg/
3. **Nedkov, S.** Museum exhibitions. In: *Museums and museology*, Lik, 1998, 61-65. [In Bulgarian]
4. **Yordanov, Y., Br. Dimitrova.** Anthropological museum – concept, principles and implementation. In: *The modern museum – models for adaptation*, 2003, 85-90.

Institute of Experimental Morphology, Pathology and Anthropology with Museum
Bulgarian Anatomical Society

Acta Morphologica et Anthropologica, 30 (3-4)
Sofia ● 2023

IN MEMORIAM

Associated Professor Anastasiya Gelyazkova Nacheva, MD, PhD

On the 17 of August 2023 Associated Professor Anastasiya Nacheva passed away. Anastasiya Nacheva was born on the 25th of May 1940 in the town of Svilengrad in a pastor's family. She lived, studied and worked in the town of Svilengrad and in the city of Sofia.

Anastasiya Nacheva graduated Faculty of Dentistry at Higher Medical Institute in Sofia (1964). After graduating she worked in a rural health department. She was appointed an intern at the Department of Surgical Dentistry of the Higher Medical Institute in Sofia, and in 1972 she acquired a specialty in Surgical Dentistry. In November 1973, Anastasiya Nacheva was appointed as a researcher in the Department of Anthropology at the Institute of Morphology, Bulgarian Academy of Sciences. In 1986 she acquired PhD degree after defense of dissertation on "Differentiation in the anthropological characteristics of workers with different type of labor activity". In February 1982 Anastasiya Nacheva was promoted into Assistant Professor, later in 1990 to Associate Professor and then she joined the scientific council of IEMPAM–BAS. She was a member of the Bulgarian Anthropological Society, Bulgarian Anatomical Society and European Anthropological Association.

Anastasiya Nacheva's remarkable scientific activity was in different fields of physical anthropology: paleoanthropology, morphology, dentistry, ergonomics, auxology, physical development, medical and applied anthropology. She created original methods for the quantitative assessment of the manifestations of morpho-functional asymmetry in the human body. Her main fundamental and applied scientific achievements are:

– Determining the specifics of the age-sex differences in the anthropological characteristics of different groups of the Bulgarian population – children, adolescents and adults with an emphasis on the assessment of regularities in the processes of growth and physical development of Bulgarians living in the 20th and 21st Centuries;

– Follow up the secular trend in the physical development of the Bulgarian population in the 20th and 21st Centuries;

– Anthropometric characterization of the body composition and nutritional status of the individuals and determination of the boundaries between morbidity and health in these characteristics;

– Anthropological characterization and assessment of adaptive morpho-functional changes in different living conditions and different labor and physical activity;

Associated Professor Anastasiya Nacheva is a co-author of the 4 monographs in Bulgaria and 1 abroad, such as: „Anthropological-ergonomic characteristics of the Bulgarian population" (1985); "Anthropology of the Bulgarian Population at the End of the 20th Century" (2006); "Physical Development of Children and Youths in Bulgaria on the Borderline between 20th and 21st Century" (2012) and other. She is the author of more than 130 publications in Bulgaria and abroad; 8 Bulgarian government standards /BDS/ implemented in practice and 2 inventions of scientific equipment. She participated in the organization of many scientific events.

Associated Professor Anastasiya Nacheva was dedicated in teaching students from Sofia University "St. Kliment Ohridski" and National Sports Academy, Sofia. She was a mentor of many young anthropologists and supervisor of graduate and post-graduate students, supporting their scientific development and academic promotion.

She was a beloved teacher, a scientist with wide interests not only in the field of anthropology and biomedicine, but also in the field of history and archaeology, literature, art, music, etc.

We lost a great scientist with nice personality and humanism, Anastasiya Nacheva will leave for ever an everlasting bright mark among us with her erudition, strong spirit, active position, dedication and love for science!

Ivaila Yankova – Pandourska

Institute of Experimental Morphology, Pathology and Anthropology with Museum
Bulgarian Anatomical Society

Acta Morphologica et Anthropologica, 30 (3-4)
Sofia ● 2023

SUPPLEMENT – ABSTRACTS OF THE 26TH NATIONAL CONGRESS OF BULGARIAN ANATOMICAL SOCIETY, SOFIA, 29 SEPT. – 01 OCT. 2023

Morphological Alterations in Tumor and Normal Tissue after Microbeam Radiotherapy

V. Djonov

Institute of Anatomy, University of Bern, Bern, Switzerland

* E-mail: valentin.djonov@unibe.ch

Microbeam-Radiation-Therapy (MRT) is a type of spatially fractionated radiation therapy which modulates the radiation dose on a micrometre scale. This unique dose distribution makes MRT highly efficient even for the treatment of radioresistant tumours. Mice bearing B16-F10 melanoma, human glioblastoma xenografts, developing chick chorioallantois membrane (CAM) were exposed to MRT. Tumor progression and alterations have been documented by Magnetic Resonance Imaging (MRI), micro CT, histological, electron microscopy and molecular-biological analysis at multiple timepoints. In a murine B16-F10 melanoma model, temporally fractionated MRT completely ablated 50% of tumors and prevented organ metastases and local recurrences for 18 months after treatment. In a mouse glioblastoma model, MRT in combination with cisplatin reduced tumor volume 6-fold compared with cisplatin alone and 60-fold compared with untreated mice. The radiation biology underlying the "MRT effect" include novel radiobiological mechanisms: (1) Induction of selective vascular disruption of immature tumor vasculature or transient vascular permeability in a dose-dependent manner (2) Direct cellular damage in the microbeam path that elicits tissue-specific responses. (3) Induction of a unique, tumor-targeted immune response leading to local and systemic anti-tumor immune responses including infiltration of cytotoxic lymphocytes. Spatially fractionated MRT demonstrated one best treatment outcome ever achieved in preclinical models. MRT provides a novel mechanism for drug delivery by increasing vascular transpermeability while preserving vessel integrity and in addition is busting the anti-tumor immune response. These unique features support MRT as a novel therapeutic approach for the treatment of inoperable, radioresistant lesions.

Key words: cancer treatment, spatially fractionated radiotherapy, cell death, micro beams, vascular permeability

Making, defining, and Wiring Cerebellar Inhibitory Interneurons: More Data, More Questions

K. Schilling

Anatomisches Institut – Anatomie & Zellbiologie, Rheinische Friedrich-Wilhelms-Universität Bonn, Germany

* E-mail: karl.schilling@uni-bonn.de

The cerebellum, notably its cortex, is typically described as a highly stereotyped structure and primarily associated with motor control. Yet this view belies the intrinsic complexity of the cerebellum, and it may distract from the fact that our understanding of cerebellar histogenesis, cellular integration and how its circuitry mechanistically implements its diverse functions is still rather fragmentary. Here, I will focus on the characterization and development of cerebellar inhibitory interneurons. Results from different fields and obtained using various technologies over the past two converge to point out that these cells are quite more diverse than traditionally portrayed. As molecular targeting of these cells is still very limited, understanding of their functions or their functional distinction remains challenging. This is particularly true for inhibitory interneurons of the cerebellar nuclei. Indeed, it is not really clear whether interneurons in the classical sense of this expression do exist there, or whether at least some nuclear cells traditionally viewed as interneurons also send collaterals to the cerebellar cortex. I hope that the data summarized, however fragmentary, may stimulate interest and help focus research towards understanding the cerebellum.

Lateralisation, Hubs and Cognition in the Avian Brain

E. Marani

Department of Biomedical Signals & Systems, TechMed Centre, University Twente, Enschede, The Netherlands

* E-mail: enrico.marani@sfr.fr

It is analysed whether similarities in avian and mammalian/human brain development and connectivity result in comparable cognitive capacities as stated e.g. by Güntürkün et al. (2021) “Cognitive functions are similar in birds and mammals”. In the avian brain dominance exists for song and song development: in the left hemisphere in the canary and in the right hemisphere in the Zebra finch. Functional asymmetry of the human brain was clinically found for speech in the left hemisphere and orientation and awareness in the other half. Despite the presence of functional asymmetries in both, differences between mammalian and avian brain concern the cortex structure. The avian cortex contains clusters, while the mammalian cortex consists of laminae. The avian brain halves are restrictedly interrelated by small commissures (anterior and supraoptica), while the mammalian brain has an enormous interhemispheric connection, the corpus callosum. This corpus callosum is absent in the avian brain, meaning that each hemisphere has a separate “mind of its own”. The storage of neurons in the avian forebrain is different, resulting in more neurons/volume. Specific areas of the bird pallium have no connection with the hippocampus, e.g. nidopallium caudolaterale, but contain memory inherently. Hubs contain nodes that are characterized by an overload of connections that can be named according to their module organisation e.g. prefrontal,

premotor or auditory module. The spatial intrahemispherical distribution of the pigeon nodes does not contact the other hemisphere, which is at strong difference with the human brain. The claustrum is regarded as a multi-modal information processing network important in cognition. In humans cognition is codetermined by the callosal bilateral connection between claustrum and contralateral cortical areas and the callosal inter-claustral communication, which is absent in the avian brain. Moreover, the avian claustrum has its own development and topography that is different from mammals and reptiles. Therefore, avian neuroanatomy contradicts the claim of similarity of mammalian and avian cognition.

Güntürkün O, von Eugen K, Packheiser J, Pusch R (2021) Avian pallial circuits and cognition: A comparison to mammals. Curr Opinion Neurobiol 71:29–36

Carotid Bodies and Neuroepithelial Bodies: Polymodal Arterial and Airway Sensors

N. Lazarov

Department of Anatomy and Histology, Medical University of Sofia, Sofia, Bulgaria

* E-mail: nlazarov@medfac.mu-sofia.bg

Oxygen sensing is of paramount importance for the survival, adaptation and maintenance of homeostasis in living organisms. In humans, the carotid body (CB) is the main oxygen sensor in arterial blood while the innervated groups of neuroendocrine cells in the lung called neuroepithelial bodies (NEB) are considered the most important intrapulmonary oxygen sensors. However, recent evidence suggests that both structures are polymodal arterial and airway chemoreceptors, which respond to a variety of environmental stimuli. Indeed, the CB is purposefully situated at the carotid bifurcation and NEBs are typically positioned at branching points along the intrapulmonary pathways. This location is strategic for monitoring intraluminal blood and airway chemicals. They are analogous structures that do not share a common embryonic origin but have a similar structural plan that reflects their unique role as complex sensory receptors. The CB consists of clusters composed of two juxtaposed cell types, neuron-like glomus cells which are considered chemosensory cells and glial-like sustentacular cells which are regarded to be supporting cells and glomus cell precursors. In turn, NEBs are made up of clustered specialized epithelial cells in close association with secretory nonciliated club cells as a potential stem cell source. The receptor cells are dually innervated by both sensory and autonomic nerve fibers. Such an arrangement and innervation are ideally suited for both autocrine and paracrine regulation of cell function. In response to external stimuli, chemoreceptor cells release a broad range of neurotransmitters including peptides and amines which activate chemoafferent nerve endings and send signals to the central nervous system to correct the condition. Moreover, both CBs and NEBs exhibit remarkable structural and neurochemical plasticity, critical for their physiological adaptation to changing environmental and pathological conditions. Knowledge of the morphofunctional characteristics and neurochemical phenotypes of CBs and NEBs is becoming crucial for our better understanding of respiratory homeostasis and cardiovascular responses in health and disease.

Key words: carotid body; neuroepithelial bodies; oxygen sensing; polymodal sensing; structural and neurochemical plasticity

Acknowledgement: This study was funded by the European Union-NextGenerationEU, through the National Recovery and Resilience Plan of the Republic of Bulgaria, project No. BG-RRP-2.004-0004-C01.

Carotid Body Adaptation in a Hypertensive Environment

*D. Atanasova[1,*2], A. Ivanov[1,3], N. Lazarov[1,3]*

[1] *Institute of Neurobiology, Bulgarian Academy of Sciences, Sofia, Bulgaria*
[2] *Department of Anatomy, Faculty of Medicine, Trakia University, Stara Zagora, Bulgaria*
[3] *Department of Anatomy and Histology, Medical University of Sofia, Sofia, Bulgaria*

* E-mail: d.atanasova@inb.bas.bg; dimitrinka.atanasova-dimitrova@trakia-uni.bg

The carotid body (CB), a small structure located at the bifurcation of the common carotid artery, is involved in sensing peripheral chemoreception, which is believed to be a key factor in triggering a number of cardiovascular diseases. There is undisputed evidence in the literature explaining the cause of essential hypertension in a relationship involving both carotid body dysfunction and increased sympathetic innervation. To gain insight into the morphological and neurochemical nature of chemoreceptor glomus cells in hypertensive conditions, we have investigated by stereological methods and immunohistochemical techniques the structural organization, expression and neurochemical profile of certain neuroactive substances in spontaneously hypertensive rats (SHR) compared with age-matched normotensive Wistar rats (NWR). The structural adaptation of the hypertensive CB is associated with an almost two-fold increase in its total volume and the total number of glomus cells as well as in the total length of the capillary network in SHR compared to normotensive animals. In contrast, the globally average cross-sectional area of a capillary in the CB of NWR was 2.8-fold greater than the sectional area in age-matched SHR. Our immunohistochemical experiments demonstrated an increased content of catecholamines, serotonin, neurotrophic factors and their corresponding receptors in the CB of SHR, while the expression of gamma-aminobutyric acid, the density of substance P- and vasoactive intestinal peptide-containing fibers were reduced compared to NWR. It can be inferred that the increased levels of certain neuroactive substances and neurotrophic factors in hypertensive animals modulate chemoreceptor information processing, leading to dysfunction, hyperactivity, and increased blood pressure.

Key words: carotid body, hypertension, plasticity, neurotransmitters, sympathetic innervation

Acknowledgement: This research is financially supported by the European Union-NextGenerationEU, through the National Recovery and Resilience Plan of the Republic of Bulgaria, project No. BG-RRP-2.004-0004-C01 and by the Faculty of Medicine at Trakia University – Stara Zagora (Grant No. 5 /2022).

Neuroepithelial Bodies and Their Role in the Development and Regulation of Pulmonary Hypertension

N. Stamenov[1], D. Atanasova[2, 3], L. Jelev[1], A. Dandov[1], N. Lazarov[1, 2]*

[1] *Department of Anatomy and Histology, Medical University of Sofia, Bulgaria*
[2]*Institute of Neurobiology, Bulgarian Academy of Sciences, Sofia, Bulgaria*
[3]*Department of Anatomy, Faculty of Medicine, Trakia University, Stara Zagora, Bulgaria*

* E-mail: nstamenov@medfac.mu-sofia.bg

Neuroepithelial bodies (NEBs) are a key component of the normal mucosa of intrapulmonary airways. They have a wide array of functions including oxygen sensing, mechanoreception, immunological role and may be involved in the regeneration of normal lung cells. The so-called neuroepithelial body microenvironment (ME) includes their main cells, neuroendocrine cells and also supporting cells, i.e. club or Clara-like cells. The complex innervation of NEBs from both sensory and autonomic nerve fibers makes them even more important for the maintenance of lung homeostasis. For the purpose, NEBs possess a broad range of neurochemicals and they respond to all kind of stimuli including increased blood pressure by changes in this neurochemical profile. Our study focuses on the differences of the neurochemical expression of certain neurochemical substances by NEB in normotensive Wistar rats (NWR) and spontaneously hypertensive rats (SHR). We performed immunohistochemical staining for calcitonin gene-related peptide (CGRP), serotonin (5HT), substance P (SP), gamma-aminobutyric acid (GABA), neuropeptide Y (NPY) and compared their expression levels in both NWR and SHR. We found increased expression of CGRP, SP and GABA in the SHRs compared to the normotensive WR. Those three neurotransmitters may play an important role towards regulation of the blood pressure as they serve as potent vasodilators. Our results suggest that NEBs are very sensitive to changes in the pulmonary blood pressure and are involved in its regulation as well as the systemic blood pressure. The results for the other neuropeptides used in the current experiment were not conclusive and did not show major differences between the two breeds of rats. Further experiments will reveal the detailed mechanisms of their involvement in the maintenance of hypertension.

Key words: neuroepithelial bodies; hypertension; immunohistochemistry; normotensive Wistar rats; spontaneously hypertensive rats

Acknowledgement: This study was funded by the European Union-NextGenerationEU, through the National Recovery and Resilience Plan of the Republic of Bulgaria, project No. BG-RRP-2.004-0004-C01.

Abnormal Hemispheric Lateralization as a Marker for the Neurodevelopmental Origin of Schizophrenia

K. Akabalieva[1], A. Beshkov[2], V. Kotetarov[1], V. Akabaliev[2], S. Sivkov[3,4]*

[1]Department of Psychiatry, Medical University-Sofia, Sofia, Bulgaria
[2]Department of Psychiatry and Medical Psychology, Medical University-Plovdiv, Plovdiv, Bulgaria
[3]Department of Anatomy, Histology, and Embryology, Medical University-Plovdiv, Plovdiv, Bulgaria
[4]Research Institute at Medical University of Plovdiv, Plovdiv, Bulgaria

*E-mail: Stefan.Sivkov@mu-plovdiv.bg

Left-eyedness as a measure of altered hemispheric lateralization and minor physical anomalies appear potential criteria of prenatal neural maldevelopment. To assess the difference in left eye dominance and MPAs between schizophrenic and control subjects and determine the relations between these biological markers of neuronal dysontogenesis in schizophrenia. A case-control study, conducted 2014-2019. Three tests for eye dominance and seven MPAs of the Waldrop scale were used. The study included 180 participants (98 schizophrenic and 82 control) with a mean age of 34.45 years. The refusal rate of potential participants is below 5%, excluding

selectivity bias. Participants were consecutively admitted in-patients, meeting DSM-V criteria for schizophrenia. The control group included volunteers, without previous or present psychiatric disorder. Exclusion criteria for both groups were history of drug or alcohol abuse, neurological disorder, intellectual disability and ocular pathology. The mean left-eyedness is higher in schizophrenic vs. controls: Looking through a hole -.81 vs. .39,p<.001; Looking through a monocle –.78 vs. .39,p<.002; Porta test –.86 vs. .41,p<.002. Importantly, the mean sum of the eye set is more than twice big in schizophrenic vs. control subjects, with marked statistical significance – 2.45 vs. 1.20, p<.000. The Spearman's rank correlation matrix shows that positive correlations are highly predominant between left-eyedness and MPAs. On the continuum of neuroontogenetic disorders any single biological marker may indicate a probable neurodevelopmental disturbance. However, the higher rate of co-occurrence of two biological markers for dysontogenesis, left-eyedness and MPAs, in one subject becomes a stronger reliable index of underlying neurodevelopment disorder.

Keywords: brain, laterality, eyedness, neurodevelopment, schizophrenia

Is the PC12 Cell Line Suitable for Synaptogenesis?

A. Ivanov

Department of Anatomy, Histology, and Embryology, Medical University – Sofia, Sofia, Bulgaria

* E-mail: aivanov@medfac.mu-sofia.bg

In 1975 Tischler and Greene reported the culture of a norepinephrine-producing pheochromocytoma. In the presence of nanogram quantities of NGF, the cells produced processes, grew on collagen, and produced much more dopamine than norepinephrine. This work aimed to determine whether the PC12 cell line may be a suitable cell model for investigating the neuronal accumulation, storage, and release of synaptic vesicles. After treatment with NGF on Day 21 the naïve cells showed characteristics of neuronal differentiation on three levels – light microscopy, immunofluorescence, and electron microscopy levels. The NGF additive was a trigger mechanism for multiple extension growth from virtually every cell in the culture. The cells were visually connected by an extensive network of processes that look like neurites of neurons. The demonstration of pre-and postsynaptic proteins via immunofluorescence circumstantially showed that the PC12 cells synthesize proteins that are associated with synaptic vesicles and functional neuronal junctions. The electron microscopy images show membrane-bound vesicles scattered around the growth cones and varicosities of the cell neurites. The abundance of synaptic vesicles, large dense-core vesicles, and multivesicular bodies indicate that after NGF treatment the PC12 cells show morphological features of differentiated neurons. The PC12 cells turn out to be a potential cell line that under the right conditions may differentiate into cells forming synapses similar to what neurons do **in vivo**. By having neuronal cells, we may investigate morphological changes before the onset of synaptic dysfunction in future models of neurodegenerative diseases.

Key words: PC12, synaptogenesis, synaptic vesicles

Phenotype of Testicular Dysgenesis Syndrome (TDS) – Origin and Cellular Mechanisms

N. Atanassova

Institute of Experimental Morphology, Pathology and Anthropology with Museum, Bulgarian Academy of Sciences, Sofia, Bulgaria

* E-mail: ninaatanassova@yahoo.com

Disorders of human male reproductive health manifested at birth (cryptorchidism, hypospadias) or in young adulthood (low sperm count, testicular germ cell cancer) are remarkably common, and they are increasing in incidence. These disorders comprise testicular dysgenesis syndrome (TDS) with a common origin in fetal life related to subtle deficiencies in fetal androgen (testosterone) production. Androgen action during fetal life is important for later correct development of male reproductive organs and their final size. Androgen driven events preferably occurred in a narrow window called masculinization programing window (MPW) during fetal life. For understanding the mechanisms involved in TDS an experimental model for induction of TDS was developed in rat by gestational exposure to anti-androgenic compound dibutyl phthalate (DBP). In fetal testis TDS has a distinct morphology of interstitial cells expressing tubular Sertoli cell markers (AMH, GATA-4). Postnatally, dysgenetic areas are manifested by ectopic expression in seminiferous tubules of 3βHSD, a marker enzyme for steroidogenic interstitial Leydig cell. COUP-TFII (chicken ovalbumin upstream promoter transcription factor-II) was identified as a cellular biomarker for impaired development of fetal Leydig cell (LCs) after in utero exposure to DBP. Abnormal persistence of COUP-TFII in fetal LCs is responsible for their dysfunction (T production) within MPW, being important in determining the risk and severity of down-stream TDS disorders in later life. Molecular mechanism of action of DPB involved downregulation of key genes for steroidogenesis (StAR, Cyp11a, Cytp17a, 3βHSD) in LCs by epigenetic change (increased methylation/H3K27me3), resulting in compensated adult LC failure manifested by low testosterone and elevated luteinizing hormone levels.

Key words: testis, androgens, TDS, Leydig cells, male infertility

Morphometric Analysis of the Myenteric Plexus in the Colorectal Region of Mice-D-Galactose Ageing Model

N. Genov[*1], N. Tomov[2], N. Dimitrov[1], N. Lazarov[3,4], L. Petrov[5], E. Tsvetanova[3], D. Atanasova[1,3]*

[1]*Department of Anatomy, Faculty of Medicine, Trakia University, Stara Zagora, Bulgaria*
[2]*Institute of Anatomy, University of Bern, Bern, Switzerland*
[3]*Institute of Neurobiology, Bulgarian Academy of Sciences, Sofia, Bulgaria*
[4]*Department of Anatomy and Histology, Medical University of Sofia, Sofia, Bulgaria*
[5]*National Sports Academy "Vassil Levski", Sofia, Bulgaria*

* E-mail: nikolay.genov@trakia-uni.bg

Ageing-related diseases are of paramount importance as a socioeconomic factor in the postmodern society. Neuronal degeneration is a known phenomenon in ageing. The D-galactose

model of accelerated ageing is widely used in the field of age-associated neuronal cell death because of the oxidative stress it induces, which correlates to reduced cognitive performance and robustly detectable neuronal shrinkage in the CNS. The aim of this study is to demonstrate the morphological changes of neurons of the myenteric plexus that occur in mice treated with D-galactose. D-galactose was given per os with drinking water, resulting in an average dose of 500 mg/kg daily for six weeks. In the D-galactose accelerated ageing model, a significant size reduction of the neuronal perikarya of the myenteric plexus was observed all along the large intestine. The average soma area at the caecum in the control group was 305 μm^2, which was reduced by approximately 18% in the ageing model. In contrast, at the level of the distal colon in the D-galactose ageing model, the average area of the neuronal soma was 190 μm^2 a reduction of almost 40%. There is a significant reduction of the area of the neuronal bodies in the myenteric plexus among different parts of the rat large intestine in the accelerated ageing model.

Key words: colorectal region, neuronal perikarya, myenteric plexus, D-galactose-induced accelerated ageing model

Acknowledgement: This research is supported by the Bulgarian Ministry of Education and Science under the National Program "Young Scientists and Postdoctoral Students-2" and by the Bulgarian Ministry of Education and Science (Grant D01-17/30.11.2018 and agreements DO1-323/18.12.2019, DO1-358/17.12.2020, and DO1-278/03.12.2021) under the National Research Programme "Innovative Low-Toxic Bioactive Systems for Precision Medicine (BioActiveMed)" approved by DCM # 658/14.09.2018".

When Our Eyes Become Too Dry – Anatomical Insights into the Pathophysiology of Dry Eye Disease

F. Paulsen

Friedrich Alexander University Erlangen-Nürnberg, Institute of Functional and Clinical Anatomy, Erlangen, Germany

* E-mail: friedrich.paulsen@fau.de

Disturbances in the dynamic balance of the lacrimal functional unit (LFU) can lead to hyposecretion (aqueous-deficient dry eye, ADDE) or hyperevaporation (evaporative dry eye, EDE) of the tear film and thus to the development of dry eye disease. Worldwide, the prevalence of this widespread disease is between 5 - 50 % depending on age, gender and ethnic origin. Patients experience a high degree of suffering due to persistent burning and itching of the eyes with a foreign body sensation. If the disease is severe and advanced, more serious complications usually occur, such as visual impairment, inflammation and scarring, and even blindness. The evaporative form, often associated with meibomian gland dysfunction (MGD), is the most common cause of dry eye disease. Here, a deficiency of the outer lipid component of the tear film leads to excessive evaporation of the muco-aqueous component with instability of the tear film hyperosmolarity. Both parameters are considered central pathomechanisms of dry eye disease. The lipids are produced and secreted by the meibomian glands in the eyelids. So far known central causes of meibomian gland dysfunction are a deficiency of androgens (male sex hormones), hyperkeratinisation of the excretory ducts, disturbed signal transduction of a central receptor in lipid metabolism (peroxisome proliferative-activated receptor gamma, PPARγ) and inflammatory reactions. The talk will give an overview of the formation of tears and the tear film as well as the current state of knowledge on the widespread disease dry eye.

Expression of Annulus Fibrosus Collagen Type I and III in Adult Degenerative Scoliosis

B. Landzhov[*1], A. Iliev[1], S. Stanchev[1], N. Stamenov[1], L. Gaydarski[1], GP. Georgiev[2]*

[1] *Department of Anatomy, Histology and Embryology, Medical University of Sofia, Sofia, Bulgaria*
[2] *Department of Orthopaedics and Traumatology, University Hospital 'Queen Giovanna – ISUL', Medical University of Sofia, Sofia, Bulgaria*

* E-mail: blandzhov@medfac.mu-sofia.bg

Adult degenerative scoliosis is a type of adult scoliosis that develops after skeletal maturity in a previously normal spine. Often the degeneration of intervertebral discs (IVD) starts as a result of abnormal mechanical load. Adult degenerative scoliosis (ADS) is the asymmetry of intervertebral discs and facet joints leading to the progressive appearance of low back pain, leg pain, and leg weakness in the advanced stages of the disease. The aim of this study was to evaluate the changes in the expression of annulus fibrosus collagen type I and III in the human IVD of adults with degenerative scoliosis. Our immunohistochemical study was conducted over seven human IVD obtained from cadavers (between 50 and 72 years old) without spine pathology marked as healthy and eight IVD obtained intraoperatively from patients with scoliosis (between 53 and 68 years old). Samples were examined with monoclonal anti-mouse antibodies for collagen type I and collagen type III. The assessment of the content of collagen types I and III was performed using an immunohistochemical study. Both types of collages were observed in the annulus fibrosus of the IVD from the thoracolumbar region. The positive reaction for collagen type I was observed predominantly in samples from IVD without spine pathology. Immunostaining for collagen type I was moderate in disc specimens from patients with ADS. In all IVDs, the expression of collagen type III was moderate and mainly localized in the perilacunar space. In addition, a small number of cells were observed in the examined annulus fibrosus of scoliotic discs. Our study confirmed that the expression of collagen type I in the annulus fibrosus increased in ADS. The immunohistochemical expression of collagen type III is localized in perilacunal space and probably links the isogenous group with the interterritorial matrix. This study sheds more light on the degenerative changes in the IVD and helps to understand the degenerative process in ADS.

Key words: adult degenerative scoliosis, intervertebral discs, collagen type I and type III

Induction of Oxidative Stress in Rat Testicular Cell Populations in Relation to Leydig Cell Function under Condition of Experimental Hyperglycemia

R. Ivanov[*1], E. Pavlova[1], I. Vladov[1], E. Shopova[2], Y. Gluhcheva[1], E. Petrova[1], Y. Tabakov[1], P. Rashev[3], E. Lakova[4], N. Atanassova[1]*

[1] *Institute of Experimental Morphology, Pathology and Anthropology with Museum, Bulgarian Academy of Sciences, Sofia, Bulgaria*
[2] *Institute of Plant Physiology and Genetics, Bulgarian Academy of Sciences, Sofia, Bulgaria*

[3] *Institute of Biology and Immunology of Reproduction "Acad. Kiril Bratanov", Bulgarian Academy of Sciences, Sofia, Bulgaria*
[4] *Department of Pathophysiology, Medical University – Pleven, Pleven, Bulgaria*

* E-mail: rosen.ivanov@iempam.bas.bg

Diabetes mellitus (DM) comorbid with oxidative stress and inflammation may affect spermatogenesis and lead to infertility in man. We aimed to investigate the effects of prepubertally induced diabetes on Leydig cell population in tandem with inflammatory and oxidative stress biomarkers in rat testis and blood sera. DM was induced by single i.p. injection of streptozotocin on postnatal day 10 of male Wistar rats. Testicular and blood samples were taken on day 25 (puberty) and day 50 (adulthood). Morphometric, immunohistochemical, immunochemical (ELISA) and biochemical analyses were performed. In adult rats significantly increased glucose levels caused reduction of Leydig cell number corresponding to testosterone insufficiency (40% of control level). Spermatogenesis in adult animals was incomplete, marked by lack of the final stages of germ cell differentiation (elongated spermatids) visualized by specific marker testicular angiotensin converting enzyme. Morphological changes were manifested by reduction in testicular macro-parameters – absolute and relative (gonado-somatic index) testicular weight by 50% and 30% respectively. Experimentally induced diabetes increased protein expression of the pro-inflammatory tumor necrosis factor-α in both ages. Increased protein expression and concentration were also found in oxidative stress markers (3-nitrotyrosine and 4-hydroxy-2-nonenal) in testes and tissue homogenates. Diabetic condition in puberty and in adulthood possibly leads to faster depletion of the antioxidant capacity of cells, evidenced by elevated hydrogen peroxide levels and decreased catalase activity in sera. Prepubertal hyperglycemia induced inflammation and oxidative stress in the testis that are potential risk for reproductive disorders and infertility.

Key words: diabetes mellitus, oxidative stress, Leydig cell, spermatogenesis

Unusual Branching of the External Carotid Artery in a Human Cadaver: A Case Report

K. Stefanov[*1], *M. Dobrev*[1], *I. Bogeva-Tsolova*[1,2], *S. Trifonov*[1]

[1] *Department of Anatomy, Histology, Cytology and Biology, Faculty of Medicine, Medical University – Pleven, Pleven, Bulgaria*
[2] *Department os Surgery, Faculty of Medicine, Medical University – Pleven, Pleven, Bulgaria*

E-mail: stefantrifonov@outlook.com

Comprehensive understanding of the variations in the branching of the external carotid artery (ECA) is essential to minimize vascular complications during cranio-facial and neck surgical procedures. We demonstrate a rare case of unusual branching of ECAs in both carotid triangles and anomalous origin of the left ascending pharyngeal artery (APA). During routine dissection of embalmed female cadaver, the carotid triangles were carefully dissected, the origin of the caudal branches was detected, and the distance between the origin of each artery and the carotid bifurcation (CB) was measured by vernier caliper. The right and left common carotid arteries (CCA) bifurcated at the level of the upper border of the thyroid cartilage, which is the most typical level according to the literature reports. The right superior thyroid artery (STA) originated anterior to the CB, while the left STA originated from the anterior aspect of the left CCA. The right ECA trifurcated into linguofacial trunk (LFT), APA and distal ECA. The

reported incidence of common LFT is around 20%. On the left side, lingual artery and APA arose as a short common linguopharyngeal trunk (LPT). To our knowledge, this is the first report of a common LPT. The left facial and occipital arteries originated anteromedially and posteriorly at the same level. Variations in the branching pattern of ECA are relatively common. Increasing the knowledge of rare variations might help surgeons and interventional radiologists to avoid vascular complications during procedures on the neck and head.

Key words: external carotid artery, ascending pharyngeal artery, linguofacial trunk, superior thyroid artery, linguopharyngeal trunk

Distribution of Variations of Division of the Sciatic Nerve

A. Todorov[*1], M. Dobrev[1], T. Rashev[1], D. Marinova[1], I. Bogeva[1], M. Shoshkova[1], S. Trifonov[1]*

[1] *Department of Anatomy, Cytology, Histology and Biology, Medical University – Pleven, Pleven, Bulgaria*

* E-mail: alex_9020@abv.bg

Sciatic nerve (SN) is the thickest and longest nerve in the body, which leaves the pelvis by passing through the greater sciatic foramen. SN nerve further divides into two terminal branches – tibial (TN) and common peroneal (fibular) nerves (CPN). The point of division of the SN into the TN and the CPN is variable. The common site is at the junction of the middle and lower thirds of the thigh, near the apex of the popliteal fossa. Variations in the anatomical division of the sciatic nerve are not uncommon. During routine dissection course on lower limb we observed 22 extremities of formalin-fixed cadavers. SN usually divides in the upper angle of popliteal fossa to CPN and TN. In the current study, only 16 (73 %) of the SN confirmed to this standard description. High division of SN in the back of thigh was noted in 4 specimen (18 %) and higher division of SN in the pelvis was noted in 2 specimens (9 %). Variations in the anatomical division of the SN have clinical significance, because if this place of division varies from the pelvis to the popliteal fossa this may contribute to piriformis syndrome, sciatica, coccydynia, and muscle atrophy. Knowledge regarding such variations and differences in the course of SN is important in surgery and important for good clinical practice.

Keywords: sciatic nerve, division, variation

Variations of the Branches of Common Hepatic Artery – A Cadaver Case Report

*I. Bogeva-Tsolova[*1,2], K. Stefanov[1], M. Dobrev[1], S. Trifonov[1]*

[1] *Department of Anatomy, Histology, Cytology and Biology, Medical University – Pleven, Pleven, Bulgaria*
[2] *Department of Surgical Diseases, Medical University – Pleven, Pleven, Bulgaria*

* E-mail: irenbogeva@outlook.com

Knowledge of hepatic vascular anatomy is of great importance for the surgeon to perform abdominal intervention. It is known that changes, present at different stages of embryonic development, lead

to large variations in vasculature. The aim of our study is to show variating common hepatic artery in a cadaver study, where multiple variating vessels were found. This is a cadaveric study, performed during the education process at the Department of Anatomy, Histology, Cytology and Biology in Medical University – Pleven. The study we conducted showed unusual variation of the branches of the common hepatic artery. The celiac trunk is presented normally with its three main branches whereas 5 of the branches of the common hepatic artery in this case arise all together from the same segment, resembling a trunk. Observing and describing vascular variations in the body is the key to expend our surgical anatomy knowledge. Such rare branching of the common hepatic artery provides an opportunity to expand the scope of the vascular anatomy of the liver and this impacts the surgical planning and outcome.

Key words: common hepatic artery, celiac trunk, vascular anatomy

Integrating Medical Humanities and History of Medicine: Strategy for Existing Curriculum Implementation

R. Hage, A. Herry

Department of Medical Humanities and History of Medicine, St. George's University, School of Medicine, True Blue, Grenada

* E-mail: RHage@sgu.edu

Integrating Medical Humanities and History of Medicine (MHHM) into medical education enhances communication, empathy, and the physician-patient relationship. Incorporating MHHM as a standalone course in to an existing curriculum may not always be feasible. An alternative approach, presenting intermittent exposure to MHHM content throughout the basic science curriculum with special emphasis in the anatomy and histology courses, was devised to prime students early. The MHHM content was carefully selected to align with the original lecture topics, ensuring a smooth transition. MHHM faculty prepared two PowerPoint slides. Additional information and suggested approaches were provided to the lecturers, granting them flexibility in incorporating the MHHM material. An overview of how St. George's University has incorporated MHHM content in the gross human anatomy and histology course is demonstrated. Attendees learn how to identify lecture content that lends itself to adding MHHM information and to determine the optimal method of introducing two PowerPoint slides into existing lectures. The strategy of incorporating two slides with MHHM content into existing lectures offers a practical solution to integrate MHHM into medical education. What seemed to be a challenging task has shown to be rather simple. Feedback from students and faculty is presented.

Key words: humanities, history, medicine, curriculum,

Otto Lanz; an Uomo Universale and a Humanistic Physician?

R. Hage, S. Gluschitz

Department of Medical Humanities and History of Medicine, St. George's University, School of Medicine, True Blue, Grenada

*E-mail: RHage@sgu.edu

Medical Humanities, an interdisciplinary field encompassing the arts, social sciences, and humanities aims to stimulate qualities of self-efficacy, interpersonal skills, empathy, social and cultural awareness. This abstract explores the life of Otto Lanz (1865-1934), a surgeon, poet, playwright, art connoisseur, and traveler, to investigate whether his diverse interests and pursuits align with the concept of a humanistic physician. An extensive search in archives and libraries in various languages provided a profile of Otto Lanz. Born in Switzerland, Lanz received a culturally rich education before pursuing medical training throughout Europe. He established his medical practice in Bern and later held the Chair of Surgery at the University of Amsterdam. While Lanz's medical contributions, such as the Lanz point and Hautschlitz apparatus, were notable, his interests extended beyond the realm of medicine. Lanz's writings showcased his fluency in multiple languages, incorporating humor, reflections on art, and candid discussions of professional setbacks. Lanz's accomplishments reflect the ideals of a Renaissance man, whether he embodies the principles of a humanistic physician remains subjective. Contemporary descriptions of humanistic physicians emphasize self-reflection, patient connection, teaching, role modeling, and work-life balance. Although these attributes do not directly connect with the Renaissance, Lanz's life exemplifies the concept of a well-rounded individual. However, the extent to which he embodies the principles of humanistic care in his medical practice is subject to interpretation by modern colleagues and medical professionals.

Key words: humanities, history, art, humanistic

Functional and Structural Analyses to Assess Recovery after Facial Nerve Reconstruction Indicate that Injections of Neurotrophic Factors into Paralyzed Facial Muscles Promote Better Quality of Reinnervation and Motor Performance in Rats

S. Rink-Notzon[1], C. Hadjiparaskeva[2], J. Reuscher[2], L. Wollny[2], S. Pavlov[3], L. Sarikcioglu[4], M. Manthou[5], D. Angelov[2]*

[1] *Department of Prosthetic Dentistry, School of Dental and Oral Medicine, University of Cologne, Cologne, Germany*
[2] *Department of Anatomy I, University of Cologne, Cologne, Germany*
[3] *Department of Anatomy and Cell Biology, Medical University of Varna, Varna, Bulgaria*
[4] *Department of Anatomy, Akdeniz University, Antalya, Turkey*
[5] *Department of Histology and Embryology, Aristotle University, Thessaloniki, Greece*

* E-mail: angelov.anatomie@uni-koeln.de

Results from numerous animal experiments indicate that the major problems after peripheral nerve reconstruction are caused by the response of regenerating axons. First, results from pre- and postoperative retrograde neuronal labeling show that regrowing axons are misrouted and fail to rejoin their original nerve fascicles. Second, triple retrograde labeling reveals that each transected axon gives off up to 25 collateral branches within the nerve itself. Such excessive collateral branching leads to re-innervation of several muscle groups, often with antagonizing action, by one single motoneuron which is the reason for abnormally associated movements (synkinesis). Combined histo- and immunocytochemistry studies show a third problem, which

is the intramuscular sprouting of axons. Upon reaching a motor target, axons undergo an intensive intramuscular sprouting. The numerous axonal sprouts reinnervate simultaneously the neuromuscular junctions (NMJ) of many muscle fibers. Intramuscular sprouting has been regarded as an adaptive mechanism to compensate for reduced functional capacity. However, it has also a "maladaptive" side, characterized by the enlargement of the motor units and by the reinnervation of NMJ by more than one axon, a state known as "NMJ-polyinnervation". Since the first two components of misdirected reinnervation, the axonal navigation (pathfinding) and collateral branching at the lesion site can be hardly treated and prevented, we aimed our efforts at the third component, i.e. the polyinnervation of NMJ. Correlating recovery of facial-muscles function in rats (video-based motion analysis of vibrissal whisking) with histological observations, we found, that motor recovery after facial nerve injury is inversely proportional to the percentage of polyinnervated NMJ. Whereas it is established that the cellular correlate of NMJ-polyinnervation is the excessive sprouting of the terminal Schwann cells (TSC) – the molecular mechanisms that govern this excessive sprouting are poorly understood. Nowadays, it is only known that denervated muscles produce a mixture of short-range diffusible sprouting stimuli, some of which have been identified as trophic factors. Based on earlier own data that blind rats from the Sprague Dawley (SD)/RCS strain restore vibrissal whisking after facial nerve injury completely, we recently compared the expression (mRNA and protein) of brain derived neurotrophic factor (BDNF), fibroblast growth factor-2 (FGF2), insulin growth factors 1 and 2 (IGF1, IGF2) and nerve growth factor (NGF) between SD/RCS and SD-rats with normal vision but poor recovery of whisking function after facial nerve transection and suture. We found a complicated time course of expression with (1) a late rise in BDNF protein that followed earlier elevated gene expression, (2) an early increase in FGF2 and IGF2 protein after 2 days with sustained gene expression, (3) reduced IGF1 protein at 28 days coincident with decline of raised mRNA levels to baseline, and (4) reduced NGF protein between 2 and 14 days with maintained gene expression found in blind rats but not the rats with normal vision. In a logical continuation of these experiments, we investigated the effect of injections with different concentrations of trophic factors into the paralysed vibrissal muscles at different postoperative periods after facial (*r. buccalis*) nerve transection and suture (buccal-buccal anastomosis, BBA). We found that regardless of treatment, the range of vibrissal movements (amplitude) remained lower than in intact rats. Nevertheless, blockade of the post-injury-associated collateral axonal branching with BDNF and fostering of elongation in groups with high-dose FGF2 promoted better restoration of motor performance. We conclude that, after peripheral nerve injury and surgical repair, appropriate target reinnervation, and therefore function, can be restored by administering different trophic factors, which need to be applied over a specific time course and at specific concentrations.

Results from Anthropological Analysis of Bone Remains Excavated in 2021 during the Rescue Archaeological Surveys along the Route of „Hemus" Highway, Site 85-2 South, Village of Gradishte, Shumen District, Bulgaria

N. Atanassova

Institute of Experimental Morphology, Pathology and Anthropology with Museum, Bulgarian Academy of Sciences

* E-mail: naditimeva@gmail.com

In 2021, during the rescue archaeological excavations along the route of the „Hemus“ highway in site 85-2 South near the village of Gradishte, Shumen district (Bulgaria), 17 burial graves are discovered, studied and documented. The burial practice is inhumation. With the exception of grave No. 2, which is from the Late Chalcolithic, all other graves are preliminary dated in the 9th-10th c. AD. The present report includes the results of the anthropological analysis of the skeletons from graves No. 1÷17. In the age-sex identification of the individuals, established anthropological methods are applied. The reconstruction of stature and body mass in adults is carried out depending on the condition of the preserved long limb bones. The established pathological changes are identified according to the methods of Aufderheide, Rodriguez-Martin 1998; Ortner, Putschar 1981; Ortner 2003. In the Late Chalcolithic grave, a skeleton of a 6-7 years old child is found. On the skull of the child is established a trabecular form of *Cribra Orbitalia*. Children are found in 56% of the Medieval burials, incl. a fetus at 40 gestational week. In adults predominated males above 50 years. The occipital bones of two children showed *Serpens endocrania symetrica* – vascular impressions found on the endocranial surface. On the skeleton of an young male is observed a cervical rib attachment on the first right rib. In general, the analysis revealed a large number of cranial variations and paleopathological bone changes of the buried individuals.

Key words: late chalcolithic and medieval skeletons; anthropological analysis; paleopathological analysis; cribra orbitalia; serpens endocrania symmetrica

Observing 3D Bioprinted Constructs in Punch Skin Biopsy

I. Bogeva-Tsolova[1,2], M. Dobrev[1], G. Altankov[3]*

[1] Department of Anatomy, Histology, Cytology and Biology, Medical University – Pleven, Pleven, Bulgaria
[2] Department of Surgical Diseases, Medical University – Pleven, Pleven, Bulgaria
[3] Center of Competence Leonardo Da Vinci, Medical University – Pleven, Pleven, Bulgaria

* E-mail: irenbogeva@outlook.com

In recent years 3-dimensional bioprinting took quite a leap ahead creating tissues, produced in laboratory environment. The problem with bioprinted products occurs when it comes to their translation into the clinical practice and the survival rate once transferred. This is a study which focuses on the results of punch skin biopsy staining methods in order to observe epithelization after translation of 3D bioprinted tissue over to Wistar rats. The study we conducted showed full epithelization of a soft tissue defect, created on the dorsal region of Wistar rats after grafting a construct created from collagen, mesenchymal stem cells and a silicone scaffold, using 3D bioprinter. We used traditional staining techniques – hematoxylin and eosin, Van Gison and fluorescein which allowed to observe all skin layers with focus on the dermis and collagen fibers. The 3D bioprinted patches showed great endurance by the animal organism and no signs of rejection, infection or any other disturbances. In order to find a representative histological proof for the epithelization we found interesting variations in well known staining techniques.

Key words: bioprinting, staining, epithelization, fluorescein

Preoperative Planning for Complex Surgical Treatment of Acetabular Fractures with Patient-Specific 3D Printed Models

P. Valchanov, S. Ivanov

Department of Anatomy and Cell Biology, Medical University of Varna, Varna, Bulgaria

* E-mail: petar.valchanov@mu-varna.bg

Patient-specific 3D printed models in orthopedics and traumatology are a useful instrument in the planning of the surgical operation. They give a better insight regarding the injury patterns, surgical approaches, reduction techniques, and fracture fixation methods. The objective of this study is to evaluate the effectiveness the 3D printed models for optimal preoperative planning of the surgical treatment of complex acetabular fractures. Patients with complex acetabular fractures were assigned to two groups: Conventional group (n = 12) and 3D printed group (n = 10). Both groups included patients with complex acetabular fractures. Datasets from CT scanning were segmented and converted to STL format, with separated bones and fragments for 3D printing. Comparison between the two groups was performed regarding the quality of fracture reduction, functional assessment, operative time, blood loss, and number of intraoperative x-rays. A significant decrease in operative time, blood loss, and number of intraoperative x-rays was observed in the 3D printed group versus the conventional one ($p < 0.01$), with 80% of the patients in the former having good fracture reduction and 20% having fair reduction. In contrast, 50% of the patients in the onventional group had good reduction and 50% had fair reduction. The functional score at 18-month follow-up was better for patients in the 3D printed group.The 3D printing technique can be considered a highly efficient and patient-specific approach for management of complex acetabular fractures, helping to restore patient′s individual anatomy after surgery.

Three-dimensional layered anatomy of the cervical region. Photogrammetry study and practical application of the 3D database

T. Spiriev[1,2], J. Frederick Cornelius[3], A. Mitev [1], V. Stoykov[1], N. Dimitrov[1], V. Nakov[2], I. Maslarski[1]*

[1]Department of Anatomy and Histology, Pathology and Forensic Medicine, University Hospital Lozenetz, Medical Faculty, Sofia University, Sofia, Bulgaria
[2]Department of Neurosurgery, Acibadem City Clinic University Hospital Tokuda, Sofia, Bulgaria
[3] Department of Neurosurgery, University Hospital of Düsseldorf, Heinrich Heine University, Düsseldorf, Germany.

* Email: spiriev@gmail.com

Cervical region is characterized with complex layered anatomical structure comprising vital blood vessels, cranial nerves and organs. Usually, the study of this anatomy requires considering multiple sources to understand this anatomical region– textbooks, videos, dissection practice,

but this process remains difficult. Modern technology in the form of photorealistic three-dimensional (3D) models is another tool to help this process. The neck region was dissected in four fixed cadavers in two anatomical departments. Three of the specimens were color with color injected vessels. Stratigraphical dissections were done on the posterior, antero-lateral and anterior neck region. Every layer of the dissection was photogrammetrically scanned and presented as photorealistic 3D models. In total forty-four 3D models were created. Each model allowed the visualization of the associated anatomy in various visual angles, which might be beneficial for the study process. The models were annotated and uploaded to an online open-access platform allowing visualization in augmented and virtual reality environment. The resulting 3D models we implemented in the medical student's curriculum in the form of VR and AR classes with high positive feedback from the students.The technology of photorealistic 3D scanning allows for the creation of database of anatomical models useful in the teaching process and as a self-study method. Future analyses of the application and of this technology will show its benefits and potential drawbacks.

Key words: Anatomy, cervical region, 3D, virtual reality, augmented reality, scanning

Anxiety-Related Down-Regulation of Oxytocin Receptors in the Bed Nucleus of Stria Terminalis of Spontneously Hypertensive Rats

A. Gradev[1], L. Jelev[1], V. Iliev[1], P. Rashev[2], A. Dandov[1], N. Lazarov[1]*

[1] *Department of Anatomy, Histology and Embryology, Medical University of Sofia, Sofia, Bulgaria*
[2] *Institute of Biology and Immunology of Reproduction "Acad. Kiril Bratanov", Bulgarian Academy of Sciences, Sofia, Bulgaria*

* E-mail: a.gradev@medfac.mu-sofia.bg

In the last decades, the neuropeptide oxytocin (OXT) has attracted a great interest in behavioral neuroscience due to its effects on the different aspects of social and emotional behaviors. The bed nucleus of stria terminalis (BNST), a limbic forebrain structure, has been implicated in stress responses such as fear and anxiety but the specific factors that engage it remain elusive. There is recent evidence that the BNST neurons express high levels of oxytocin receptors (OXTR). To determine the anxiogenic effects of OXT in the BNST, we used spontaneously hypertensive rats (SHR), an established animal model of attention-deficit/hyperactivity disorder, also associated with reduced anxiety levels. We first attempted to identify by immunohistochemistry cells expressing OXTR in certain BNST subnuclei of SHR and then compared their expression levels with those in the corresponding BNST nuclei of normotensive Wistar rats (NWR). We found that the OXTR was expressed at lower levels in the oval and the medial-posteromedial nuclei of the BNST of SHR than in neurons of the same subnuclei in Wistar controls. The OXTR expression was reduced about 20% in hypertensive animals compared to controls, and this decrease was statistically significant. Our results suggest that innate lower anxiety levels of SHR are possibly due to the down-regulation of OXTR in BNST neurons, thus confirming the role of BNST oxytocin stimulated neurons in determining anxiety-like behavior. Overally, the SHR strain can be used in behavioral neuroscience as a valuable model of an impaired central oxytocin system and also in anxiety-related research involving BNST.

Key words: anxiety, bed nucleus of stria terminalis, oxytocin receptors, spontaneously hypertensive rats

Acknowledgements: This study was financially supported by the Medical Science Council at the Medical University of Sofia (Grant № Д-171/03.08.2023).

Expression of Neuropeptide-Y in Brattleboro and Wistar Pre- and Postpubertal Rats

A. Dandov[1], A. Gradev[1], P. Rashev[2], N. Lazarov[1,3], L. Jelev[1]*

[1] Department of Anatomy, Histology and Embryology, Medical University of Sofia, Sofia, Bulgaria
[2] Institute of Biology and Immunology of Reproduction "Acad. Kiril Bratanov", Bulgarian Academy of Sciences, Sofia, Bulgaria
[3]Institute of Neurobiology, Bulgarian Academy of Sciences, Sofia, Bulgaria

* E-mail: adandov@medfac.mu-sofia.bg

The bed nucleus of stria terminalis (BNST) is a limbic structure associated with the regulation of stress, hunger, aggression, and drug addiction. Recent studies have shown that neuropeptide-Y (NPY), a neuromodulator in the nervous system, relieves anxiety-like states and regulates hunger and appetite, and its expression is age- and gender-related. It has been revealed that NPY has higher levels in certain limbic structures in Brattleboro rats, a strain lacking vasopressin, and that it plays a certain role in the initiation of puberty. Thus, we set it as a task to follow the expression of NPY in prepubertal (20 days old) and postpubertal (60 days old) Brattleboro rats and compare it with those in Wistar rat controls. For our experiments, we applied immunohistochemistry for NPY using the avidin-biotin method. Our results showed that NPY was expressed in the neuronal bodies of certain areas of BNST in prepubertal Brattleboro rats, and its expression was better seen in females. On the other hand, a very weak expression was observed in prepubertal Wistar rats. In postpubertal Brattleboro rats, however, NPY expression in neuronal bodies of BNST disappeared. It was only detected in nerve fibers adjacent to the perikarya, the former possibly arriving from the hypothalamus. Such immunostaining was also seen in postpubertal Wistar controls. We can infer from our results that NPY does play a significant role during puberty in the Brattleboro strain and it is a matter of future studies to clarify exactly how it modulates anxiety and eating disorders during sexual maturation.

Key words: anxiety, bed nucleus of stria terminalis, Brattleboro rats, neuropeptide-Y, puberty

Acknowledgements: This study was financially supported by the Medical Science Council at the Medical University of Sofia (Grant № Д-171/03.08.2023).

En face Techniques for Observations of the Macrovascular Endothelium

L. Jelev

Department of Anatomy, Histology and Embryology, Medical University of Sofia, Sofia, Bulgaria

* E-mail: ljelev@medfac.mu-sofia.

To study the vascular endothelium from the surface (*en face*), a number of light and electron-microscopic methods have been used and special histological techniques developed for the past nearly 140 years. These methods and techniques allow examination on smaller or larger areas or even the entire endothelium of a vessel and differ in their ability to study particular characteristics of the endothelial cells. For the present work, of particular interest are the *en face* techniques for obtaining permanent preparations for long-lasting light-microscopic observations of the endothelium. Based on the thickness of the preparations produced these techniques are classified into three main groups: 1) techniques for "whole thickness" preparations, 2) techniques for "partial thickness" preparations and 3) techniques for producing endothelial cell monolayers or "Hautchen" preparations. The methodology and potential scientific application of the techniques in each one of the groups is described and they are thoroughly compared.

Key words: vascular endothelium, *en face* techniques, experimental research

Impact of Type 1 Diabetes Mellitus on the Somatotype of Adult Bulgarian Patients

A. Baltadjiev[1], M. Orbetzova[2], S. Sivkov[1], T. Petleshkova[1], Z. Harizanova[1], A. Fusova[1], M. Ilieva-Gerova[2]*

[1]Department of Anatomy, Histology, and Embryology, Faculty of Medicine, Medical University of Plovdiv, Plovdiv, Bulgaria
[2]Department of Endocrinology, Faculty of Medicine, Medical University of Plovdiv, Plovdiv, Bulgaria

* E-mail: atanas.baltadzhiev@mu-plovdiv.bg; dr_atanas@abv.bg

The aim of the study was to determine the somatotype of elderly Bulgarian patients with type 1 Diabetes mellitus. Sixty male and 60 female patients aged 20 to 40 years were involved in the study. A sample of healthy Bulgarian individuals in the same age range was used as a control group. The measurements were done by direct anthropometry. The Heath-Carter anthropometric method was used to rate the somatotype components of each participant. The somatotype of the female patients was mesomorphic endomorph (endo 5.37; meso 4.51; ecto 1.42). The endomorphic component was dominant, followed by the mesomorphic component and the ectomorphic component with the lowest rating. The somatotype of the control females was balanced endomorph (endo 3.74; meso 2.81; ecto 2.98). The endomorphic component was dominant, but the mesomorphic and ectomorphic components were equally presented. The values of endomorphic and mesomorphic components were significantly higher in the

female patients than in the healthy women. Both male patients and controls presented with endomorphic mesomorph somatotype: patients (endo 3.94; meso 4.66; ecto 2.37) and controls (endo 4.34; meso 5.19; ecto 2.22). The mesomorphic component was dominant, followed by the endomorphic component and the ectomorphic component was with the lowest rating. The mesomorphic component was significantly greater in the healthy males than in male patients. The somatotype of the Bulgarian female patients is mesomorphic endomorph, while of the healthy Bulgarian females is balanced endomorph. Both Bulgarian male patients and healthy males have endomorphic mesomorph somatotype.

Key words: anthropometry, body composition, Bulgarians, somatotype, type 1 Diabetes mellitus

Lectin Histochemistry of the Most Superficial Zone of the Normal Articular Cartilage during the Postnatal Reriod.

A. Fedotchenko

Zaporizhzhia State Medical and Pharmaceutical University, Zaporizhzia, Ukraine

* E-mail: afedotchenko@gmail.com

The existence of the most superficial zone (MSZ) of the articular cartilage (AC), is claimed by many authors. Its structure remains controversial. The hip joint of Wistar rats from birth till the 90th day was studied. Histologic sections were stained with hematoxylin and eosin (H&E) as well as lectins conjugated with horseradish peroxidase (HRP): peanut (PNA), soybean (SBA), Helix pomatia (HPA), wheat germ (WGA), Perca fluviatilis (PFA), Sambucus nigra (SNA), Lens culinaris (LCA), and Vicia sativa (VSA), analyzed by light microscopy and a semi-quantitative assessment. The MSZ was clearly distinct from the underlying AC as a layer with intense pink staining. Three sublayers could be seen in it: the outermost (closest to the articular surface) finest sublayer with a strong expression to all studied lectins; the middle (thickest) sublayer, containing cells (with affinity from weak (+) to moderate (++)) and extracellular matrix (expression from minimal (0/+) to weak (+)); the third (the innermost) sublayer as a continuous, relative thick lamina (with a strong expression, from +++ to ++++) that clearly delimited the MSZ from the underlying AC. The lectins affinity of the MSZ did not fluctuate significantly till the 90th day. The constant, strongly expressed double lectin-mediated barrier of the MSZ seems to emphasize its immunobiological protective importance for the AC.

Key words: articular cartilage, hip joint, lectins.

Glucagon- and Insulin Immunopositive Mast Cells in Porcine Gallbladder

I. Stefanov[1,4], S. Stefanov[2], M. Gulubova[3,4]*

[1] Department of Anantomy, Medical Faculty, Trakia University, Stara Zagora, Bulgaria
[2] Sixth year student at Medical Faculty, Trakia University, Stara Zagora, Bulgaria

[3] *Department of General and Clinical Pathology, Medical Faculty, Trakia University, Stara Zagora, Bulgaria*
[4] *Department of Anatomy, Histology and Embryology, Pathology, Medical Faculty, Prof. Dr. Asen Zlatarov University, Burgas, Bulgaria*

* E-mail: ivstefanov@abv.bg

It is well known that mast cells produce and release biologically active substances such as histamine, heparin, proteases, leukotrienes, cytokines, chemokines, and growth factors. However, their capacity to produce insulin and glucagon has not been established yet. We aimed to perform immunohistochemical study to determine the glucagon and insulin positive mast cell existence and distribution in the wall of porcine gallbladder. The collocalization of glucagon and insulin immunopositivity with metachromasy allowed us to detect the presence of glucagon and insulin positive mast cells in the bottom, body and neck of gallbladder in male pigs. In addition, an immunohistochemical detection of tryptase as a better marker for mast cells than toluidine blue dye was used to compare the number of mast cells to glucagon and insulin immunopositive cells. In all layers of gallbladder`s neck, the density of all types of mast cell was highest, followed by the body and bottom of gallbladder. The tryptase immunohistochemistry comparing to toluidine blue staining appeared to be more reliable technic for identifying all glu+ and ins+ mast cells. Glucagon- and insulin expression by mast cell granules allowed us to hypothesize a new unknown by now role of these cells regarding their participation in the regulation of the glucose homeostasis as well as the involvement of mast cells in the pathogenesis of diabetes mellitus. The presence of glucagon and insulin in mast cell granules may be due to the ability of mast cells to accumulate or to synthesize these hormones.

Key words: chromogranin A, gallbladder, glucagon, insulin, mast cells

Association Between Foot Arch Index and Other Morphometric Indices

D. Marinova, M. Angelova, V. Zhekova[1], S. Pavlov*

Department of Anatomy and Cell Biology, Medical University "Prof. Dr. P. Stoyanov"- Varna, Varna, Bulgaria

* E-mail: desislavamarinova81@gmail.com

The foot morphology is crucial for the normal functioning of the locomotor system. Abnormalities and deviations of its shape are associated with various conditions that interfere with and encumber daily life, work and sports activities. Our study is focused on the types of foot among the Bulgarian population. Footprints of randomly selected 150 Bulgarians aged 18 to 60 years were collected. We examined the morphological features of each foot by measuring the arch index, the Clarke angle and the Chippaux-Smirak index. The participants were grouped according to arch index values in three groups: with normal, with high, and with flat arched foot. Our results showed a greater incidence of high arched foot versus low arched foot (29% vs 11%). The study of the arch index once again confirmed the association of the Morton's toe foot with a high medial arch. BMI within the groups with different foot type was compared. In the group with high arched foot, BMI was lower than that in the other groups. However, further investigation of the possible relations between BMI and arch index found no significant correlation between them. We studied

the correlation between the used foot indices and found a particularly well-expressed one between the arch index and Chippaux-Smirak index. Our findings gave us reason to assume that the measurement of Chippaux-Smirak index can successfully replace the measurement of arch index, which would facilitate the assessment of foot type.

Key words: foot, foot indices, arch index

Asymmetry in Body Composition Variables of Youth Athletes

A. Dimitrova

Institute of Experimental Morphology, Pathology and Anthropology with Museum, Bulgarian Academy of Sciences, Sofia, Bulgaria

* E-mail: albena_84@abv.bg

Assessing bilateral differences in paired anthropometric features is an important methodological problem in sports anthropology. The present study includes 128 (59 rhythmic gymnasts, 58 tennis players, and 11 swimmers) adolescent female athletes. Body composition components were determined using multi-frequency bioelectrical impedance measurements (analyzer InBody 170). Statistical analysis is made by SPSS 16.00 for Windows. Asymmetry coefficients of muscle and fat mass accumulation in the upper (AA) and lower (AL) limbs were calculated by Nacheva` equation (1986). The percentiles method was applied to distribute the bilaterally studied anthropometric features according to the mean values of the units of asymmetry (UA). Wilkoxon-test is used to assess the statistically significant differences in paired variables ($p \leq 0.05$). Kruskal-Wallis test ($p \leq 0.05$) is applied to determine the differences in UA between three assessed athlete groups, depending on their age. The differences in body composition components between RG, TP, and SW are well expressed in all assessed age groups. The most considerable inter-group differences are observed in terms of the asymmetry coefficient in the lean body mass (LBM) and body fat mass (%, kg) of UL, which have signed the highest values in the tennis players group. Swimmers have significantly the lowest values of UA for all body segments. A close relation is found between asymmetry in body composition variables and the type of sports activity. Tennis was found as a sport with more pronounced inter-limbs asymmetry.

Key words: tennis players, rhythmic gymnasts, asymmetry, body composition, adolescent

Comparison of Inter-Incisive Index Between Bulgarians and Other Balkan Nations

V. Zaykova[*], *Z. Harizanova, A. Baltadjiev, F. Popova, N. Kadreva, Z. Todorova, M. Kanarev, K. Topalova, S. Sabri*

Department of Anatomy, Histology and Embryology, Faculty of Medicine, Medical University – Plovdiv, Bulgaria

* E-mail: Vyara.Zaykova@mu-plovdiv.bg

In recent years, aesthetic dentistry has become a major focus for the public. Facial attractiveness plays a key role on modern society and the creation of harmonious smile is a purpose for every dentist. The aim of this study was to define certain values of the inter-incisive index in Bulgarians, the sexual dimorphism and bilateral asymmetry and to verify differences of this index between Bulgarians and other Balkan populations. The present study included 121 males and 111 females of Bulgarian origin aged 20-40 years. Mesiodistal dimensions of maxillary central and lateral incisors were measured by Dentistry Sliding Vernier Caliper. We used the technique of direct anthropometry, modified by Prof. Y. Yordanov. We calculated the inter-incisive index as ratio of the mesiodistal dimension of maxillary lateral incisor to the mesiodistal dimension of the maxillary central incisor. The measurements were analyzed with SPSS 23. The level of statistical significance was set at $P< 0.05$. The inter-incisive index showed no statistically significant differences between left and right side of the dental arch in both sexes and between the sexes as well. This justifies the use of average values for the dimensions of left and right maxillary central and lateral incisors. On the other hand, we found statistically significant differences in MD values of incisors between Bulgarians and other Balkan nations. Inter-incisive index shows no sexual dimorphism and bilateral asymmetry in Bulgarians. This can be helpful in aesthetic dentistry, in prosthodontics and in orthodontic treatment planning.

Key words: incisors, proportions, hypodontia, prosthetics, orthodontics

Study on the digital transformation of Histology and Histopathology by Virtual Microscopy (VM) for an innovative medical school curriculum

Z. Harizanova, F. Popova, S. Novakov, Y. Koeva, N. Penkova, P. Atanasova*

Department of Anatomy, Histology and Embryology, Faculty of Medicine, Medical University – Plovdiv, Plovdiv, Bulgaria

* E-mail: zdravka.harizanova@mu-plovdiv.bg

Medical histology has been a basic science course in the medical school curriculum worldwide. A method such as light microscopy is dependent upon the availability of microscopy lab with rigid opening hours and a teacher. Virtual microscopy (VM) involves digitally photographing tissue sections on microscope slides and provides a physically distant opportunity for histology education. Its software reproduces a high-quality image with meticulous clarity and added features that allow students and teachers to highlight, annotate, and zoom. The aim of this project is the implementation of digital/virtual microscopy (VM)/ whole slide imaging (WSI) in undergraduate and postgraduate students' histology and histopathology education. Experts from Medical Universities of five countries participate in the project – Romania, Poland, Spain, Greece, and Bulgaria. 400 students will participate in a survey giving their opinion on the new method. 200 histology and histopathology slides will be scanned by the Romanian partners performed by Leica Aperio AT2 scanner. The result would be the creation of a large digital slides collection of normal and pathological human tissues and its implementation in a VM library platform in histology and histopathology. The possibility to combine and gather specimens from several universities would be useful both for teaching staff and undergraduate and postgraduate students. Virtual microscopy represents a modern tool, with increased quality

and utility in microscopy education. This project is the first of its kind in Bulgaria and would contribute a lot to the implementation of VM in histology and histopathology education.

Key words: virtual microscopy, light microscopy, histology, medical education

CT and 3D Anatomical Study of the Liver in the Chinchilla (Chinchilla lanigera)

Ö. *Dilek*[1], *R. Dimitrov*[2], *K. Stamatova-Yovcheva*[2*], *M. Ersen*[3], *D. Yovchev*[2], *E. Karakurum*[1]

[1]*Department of Anatomy, Faculty of Veterinary Medicine, Mehmet Akif Ersoy University, Burdur, Turkey*
[2]*Department of Veterinary Anatomy, Histology and Embryology, Faculty of Veterinary Medicine, Trakia University, Stara Zagora, Bulgaria*
[3]*Bucak State Hospital, Department of Radiology, Bucak/Burdur, Turkey*

* E-mail: kameliastamatovayovcheva@gmail.com

Single cases of neoplastic processes in the liver of chinchillas have been described. At the same time, the chinchilla is widely used as model for different scientific researches. The aim of the present study was to investigate CT and 3D imaging anatomical features of the chinchilla's liver. Twelve clinically healthy chinchillas (six males and six females) aged eighteen months were used. The animals were positioned in dorsal recumbency. As bone markers were used the vertebrae from Th8 to L2 and the sternum for transverse CT study. The vertebrae, the costal arch, the soft abdominal wall, the diaphragm, the stomach, and the right kidney were used as markers for CT coronal study. 3D reconstructions were made with the aid of a specific imaging program. On transverse and coronal CT images the chinchilla's liver was composed by liver by the left lateral lobe, middle lobe, right lobe and caudate lobe. The middle lobe was separated in left middle lobe and right middle lobe. The right lobe was presented by lateral and medial part. There was anatomical contact between the liver and the fundus and body of the stomach. The caudate process was in close contact with the right kidney. The gall bladder was elongated and ellipsoid. 3D reformat images confirmed the results, obtained by transverse and coronal CT study. The CT density of the liver in HU was 195.6±73.1. The presented CT and 3D reconstructed images are with high resolution. This data could be used as a morphological and imaging base.

Key words: chinchilla, liver, CT, 3D reconstruction

Effect of Aronia Supplementation on Aging Markers in the Testis

E. Daskalova[1*], *Y. Koeva*[1], *M. Pencheva*[2], *M.-F. Kitova*[3]

[1] *Department of Anatomy, Histology and Embryology, Medical Faculty, Medical University of Plovdiv, Plovdiv, Bulgaria*
[2] *Department of Medical Physics and Biophysics, Faculty of Pharmacy, Medical University of Plovdiv, Plovdiv, Bulgaria*

[3] *Medical Faculty, Medical University of Plovdiv, Plovdiv, Bulgaria*

E-mail: Elena.Daskalova@mu-plovdiv.bg

Spermatogenesis is a process that continues until the end of an individual's life, although with reduced activity with advancing age. Structural changes in the testicle are manifested by changes in the wall of the seminiferous tubules, a consequence of inflammatory, hormonal or external influences. The aim was to study the effect of Aronia on structural and functional changes in the testis in old rats, by measuring the intensity of expression of Neurotrophic tyrosine kinase receptor 3 (TrkC) and Neurotrophin 3 (NT-3) in Leydig cells and some morphological markers in testis. 18 male Wistar rats were divided into 3 experimental groups: young controls aged 2 months, old controls aged 27 months and 27 months old rats supplemented with chokeberry juice at a dose of 10 ml/kg for 3 months. The animals were bred and delivered from the Vivarium of the MU Plovdiv. The results showed significant differences between young and old animals in expression of the age-related changes that occurred. The morphometrically determined tubules structure data showed no significant differences between the three groups. However, the intensity of the immunoreaction for TrkC and NT-3 was demonstrably higher in the supplemented adult animals compared with the adult controls. These data indicate that supplementation with Aronia juice, thanks to its rich composition of antioxidant ingredients, slows down aging processes in the testis and preserves the functional activity of Leydig cells. Aronia supplementation can be recommended as a natural tool for healthy aging.

Key words: black chokeberry (Aronia melanocarpa), antioxidant activity, functional foods, spermatogenesis, aging

Markers of Oxidative Stress in the Testis are Affected by Aronia Melanocarpa

E. Daskalova[1], Y. Koeva[1], M. Pencheva[2], M.-F. Kitova[3]*

[1] *Department of Anatomy, Histology and Embryology, Medical Faculty, Medical University of Plovdiv, Plovdiv, Bulgaria*
[2] *Department of Medical Physics and Biophysics, Faculty of Pharmacy, Medical University of Plovdiv, Plovdiv, Bulgaria*
[3] *Medical Faculty, Medical University of Plovdiv, Plovdiv, Bulgaria*

* E-mail: Elena.Daskalova@mu-plovdiv.bg

Inflammation, oxidation, and apoptosis are events considered as predictors of pathogenesis and the development of age-related diseases observed in aged testes. Pro-oxidant and a pro-inflammatory microenvironment are characteristic of aged testes. One of the major reason for diminished semen quality seems to involve the accumulation of reactive oxygen species that accompanies aging. Use of natural compounds with known antioxidant and anti-inflammatory properties have a beneficial effect on the inflammatory and oxidative status of the aged testis. The aim of the present study was to determine the effect of supplementation with antioxidant rich Aronia melanocarpa on markers of oxidative stress in rat testis. 18 male Wistar rats were divided into 3 experimental groups: young controls aged 2 months, old controls aged 27 months and 27 months old rats supplemented with Aronia juice at a dose of 10 ml/kg for 3 months. Suplemented with Aronia group showed increased immunoexpression of NOS1, NOS3 and

MAS1 receptor both in the seminiferous tubules (spermatogenic epithelium, peritibular myofobroblasts) and in the blood vessels wall in comparison to the young and old control groups of rats. Higher expression of NOS1, NOS3, and MAS1 in the testes suggests that animals receiving Aronia have an increased antioxidant capacity. This can provide improved spermatogenic- and steroidogenic functional activity resulting in reduced age dependent testicular disfunction, better spermatogenesis, and preserved androgen production.

Key words: aging testis, oxidative stress, antioxidant activity, black chokeberry (Aronia melanocarpa)

Gastric Mucosal Mast Cell Activity in Children on Longitudinal Enteral Feeding with Percutaneous Endoscopic Gastrostomy, PEG

N. Penkova[1], P. Atanasova[1], I. Yankov[2], V. Yankova[3], P. Hrischev[4]*

[1]. Department of Anatomy, Histology and Embryology, Faculty of Medicine, Medical University of Plovdiv, Plovdiv, Bulgaria
[2]. Department of Pediatrics and Medical Genetics, Faculty of Medicine, Medical University of Plovdiv, Plovdiv, Bulgaria
[3]. Faculty of Medicine, Medical University of Plovdiv, Plovdiv, Bulgaria
[4]. Department of Physiology, Faculty of Medicine, Medical University of Plovdiv, Plovdiv, Bulgaria

* E-mail: nadja_penkova@abv.bg

Longitudinal enteral feeding via percutaneous endoscopic gastrostomy, (PEG) challenges the gastric mucosa. It is carried out in conditions of disturbed physiology - all stages of the digestive process until the food enters the stomach are absent. There is a risk of infection of the gastrointestinal tract (GIT), allergens. The aim of our study is to make a morphological and morphometric analysis of the gastric mucosa of children with longitudinal enteral feeding through PEG with an emphasis on the inflammatory component. The biopsy samples from the stomach of 37 children without GIT disease at age 0-18 years (20 of them are on oral feeding - controls and 17 on enteral feeding duration of 24–48 month through PEG) are examined with light-microscopy and morphometric analysis. We find the scanty amount of loose connective tissue in the lamina propria of children with PEG. The glands are next to each other with slightly hyperemic capillaries between them. The total cell count and the number of parietal cells in the fundic glands of children with PEG is double that the controls. In isolated cases is noticeable an increased number of mast cells some of them degranulate. The predominance of the glandular component over the connective tissue component in the gastric mucosa of children with PEG is probably an adaptation mechanism of the body for maximum absorption of nutrients from the enteral diet. Regarding increased mast cell activity further studies are needed to clarify whether this finding is related to the PEG or to the child‘s underlying disease.

Key words: enteral nutrition, paediatrics, percutaneous gastrostomy, tissue morphometry, mast cell

Morphological Study on the Acute and Subacute Toxic Effects of Tanacetum Parthenium Essential oil After Treatment of Experimental Animals

N. Penkova[1], P. Atanassova[1], L. Peychev[2], P. Hrischev[3]*

[1] Department of Anatomy, Histology and Embryology, Medical Faculty, Medical University of Plovdiv, Plovdiv, Bulgaria
[2] Department of Pharmacology and clinical pharmacology, Medical Faculty, Medical University of Plovdiv, Plovdiv, Bulgaria
[3] Department of Physiology, Medical Faculty, Medical University of Plovdiv, Plovdiv, Bulgaria

* E-mail: nadja_penkova@abv.bg

Tanacetum parthenium (T. Parthenium) is a perennial herbaceous plant of the Asteraceae family reaching. It is native to Europe, specifically the Balkan Peninsula, Asia but cultivation has spread it around the world. T. parthenium had an important role in the traditional medicine. The plant has been used to treat arthritis, asthma, constipation, dermatitis, earache, fever, headache, inflammatory conditions, toothache, etc.. The aim of our study is to determine the toxicity of Tanacetum parthenium essential oil in Wistar rats to detect possible pathological changes in different organs of treated animals. 24 Wister rets were used. 8 treated with Tanacetum parthenium essential oil (EO), 8 – a control group. Using the method proposed by Litchfield and Wilcoxon, the average lethal dose (LD50) of the EO on Wistar rats was determined for two routes of administration: oral and intraperitoneal. The subacute toxicity of the EO was also tested by oral administration of a daily dose of 1.0 g/kg b.w. for 28 days. The control group received saline and olive oil 1ml/kg b.w.. Haematological examination showed no toxicity. Blood and biochemical parameters are within the reference values. Histological examination of the internal organs establishes a normal structure without pathological changes. Histological and haematological studies doesn't show an evidence of toxic effects of Tanacetum parthenium essential oil and it is safe for use in doses below 1 g/kg b.w. for a period not exceeding one month. The wide distribution of this herb in Bulgaria can be used to create a new medicinal products and food supplements.

Key words: Tanacetum parthenium, essential oil, toxicity, biochemistry, histology

Risks in Cyber Environment

J. Aleksovski[1], N. Pirovski[2], I. Georgieva[3]*

[1] Student, Faculty of Medicine, Trakia University, Stara Zagora, Bulgaria
[2] Department of Anatomy, Faculty of Medicine, Trakia University, Stara Zagora, Bulgaria
[3] Philosophy of Science Department, Institute of Philosophy and Sociology, Bulgarian Academy of Sciences, Sofia, Bulgaria

* E-mail: yovanche.aleksovski.18@trakia-uni.bg

Cyber environment is a new type of interaction media. This implies a modification of existing risks and a new type of risks, covered by an instrument for risk evaluation. Existing risk

evaluation instruments, psychology risk questionnaires and cyber risks categories. Instrument for cyber risk evaluation with **a** specific modifications of the existing physical and psychological risks and the new type- cyber risks. Cyber environment is new, but very common and powerful. This creates an opportunity for improved functionality, but also for increased risk. The risk of using a cyber-environment is not limited to the field of information. It is a complex, personal, bio-psycho-social risk with daily and mass exposure and diverse consequences. Its assessment is difficult and currently inadequate in the direction of underestimation.

Key words: risk, cyber, psychology, philosophy of medicine

Acknowledgment: 1. Project of the Medical Faculty of Trakia University №16/2022 Visualization of formal complexes in Wushu through graphic figures of their steps. 2. Contemporary Issues and Discussions in the Philosophy and Sociology of Medicine (2021-2024). Institute of Philosophy and Sociology. Bulgarian Academy of Sciences. Department Philosophy of Science. Project manager: Assoc. Prof. Julia Vasseva-Dikova

Osteogenesis in Rat. Factors Influencing Osteogenesis

N. Kadreva, N. Penkova, P. Atanasova*

Department of Anatomy, Histology and Embryology, Faculty of Medicine, Medical University of Plovdiv, Plovdiv, Bulgaria

* E-mail: n.kadreva09@gmail.com

The process of bone formation is called osteogenesis or ossification. Osteogenesis is a core component of the skeletal system and depends on the well-coordinated and developed proliferation and differentiation of osteogenic cells. Multiple signaling pathways, transcriptional factors, environmental, systemic conditions and many more tightly regulate the process of osteogenesis. Any abnormities in bone formation could cause severe disorders. Bone regeneration, a complex and well-orchestrated physiological process of osteogenesis, remains a medical challenge in the field of orthopedics and maxillofacial surgery as well as tissue engineering approaches promoting regeneration by targeting osteogenesis. The current developments in the research in this field still aim to understand the complexity of the process of osteogenesis and its influencing factors. The current report will examine osteogenesis and development of bone in rats and review some of the factors pointed above that are under current research and show the most common and well described influence on the process and the cells. Over the last 20 years there has been an immense rise in the number of publications on the osteogenic potential of different influencing factors and the review will provide statistical significance a novel classification and latest data on the issue. In terms of influencing factors we point the ones that have inducing or suppressing effect on the process and mainly on the differentiating cells - Mesenchymal stem cells – MSC(s), Osteoblasts, Osteoclasts and Osteocytes. We can classify those factors that commit to differentiation at multiple levels, tuned with the involvement of biochemical pathways, transcriptional and growth factors, signaling molecules, pharmacological substances, hormones and nutrients and newly researched systemic or microenvironmental conditions.

Key words: osteogenesis, influencing factor, bone regeneration

Congenital Neural Tube Defects and the Meaning of their Prophylaxis

P-P. Petrov[1], E. Daskalova[1], T. Kitova[1], M. Zdravcheva[2], S. Kostova[2], S. Todorova [2]*

[1] Department of Anatomy, Histology and Embryology, Faculty of Medicine, Medical University of Plovdiv, Plovdiv, Bulgaria
[2]. Students, Faculty of Medicine, Medical University of Plovdiv, Plovdiv, Bulgaria

* E-mail:dr.petar.preslav@gmail.com

Neural tube defects (NTDs) are the most common birth defects that cause perinatal and infant mortality, lifelong disability, high medical care costs, and psychological trauma for affected families. The global prevalence of DNT is 2 per 1,000 births, with a disproportionately high incidence in developing countries. Risk factors for the occurrence of sporadic DNT include the nutritional status of the mother, pre-pregnancy diabetes, use of antiepileptic drugs and a previous pregnancy affected by DNT. Fetuses result from medically terminated pregnancies, intrauterine deaths, spontaneous abortions, and neonatal deaths after authorization for autopsy and genetic testing. The types of DNT and the embryonic mechanisms for their occurrence, the possibilities for their prenatal diagnosis and their prevention are discussed. The study is based on inter-university research projects: Fetal and placental pathology (project no. HO/DP – 03/15). Fetal morphology, development of the fetal brain, physiology and pathology of the nervous system (project no. P-8514). Exencephaly, anencephaly and cranial meningoencephalocele were examined from cephalic DNTs, and rachischisis and myelomeningocele from spinal ones. The necessary system for research and evaluation of implemented health programs and public health policy necessary to prevent the occurrence of STDs and their adverse outcomes is discussed. Public health policy is needed to implement specialized programs to prevent the occurrence of DNT and involve multidisciplinary teams that provide care to individuals with DNT to enable prevention and improve care and rehabilitation for affected children.

Key words: neural tube, psychological trauma, risk factors

Ostarine (SARM) and Endurance Training Affect Glycogen Content in Rat Liver, Heart and Skeletal Muscle

F. Gerginska[1], S. Delchev[1], V. Vasilev[2], K. Georgieva[2], N. Boyadjiev[2], M. Denev[3], M. Komrakova[4]*

[1] Department of Anatomy, Histology and Embryology, Faculty of Medicine, Medical University of Plovdiv, Plovdiv, Bulgaria;
[2] Department of Physiology, Faculty of Medicine, Medical University of Plovdiv, Plovdiv, Bulgaria;
[3] Student, Faculty of Medicine, Medical University of Plovdiv, Plovdiv, Bulgaria;
[4] Department of Trauma Surgery, Orthopaedics and Plastic Surgery, University Medical Center Goettingen, Goettingen, Germany

E-mail: Fanka.Gerginska@mu-plovdiv.bg

A number of diseases are accompanied by a decrease in muscle mass and physical function. Non-steroidal selective androgen receptor modulators (SARMs) have potent anabolic and androgen-

reducing effects. The information about the effect of SARMs on glucose metabolism and glycogen content in target organs with long-term use and in combination with exercise is insufficient. Male Wistar rats were divided into two groups - endurance trained and non-trained. Half of the trained and non-trained rats received SARM (Ostarine) for 8 weeks. PAS staining for glycogen in liver, heart, soleus and EDL was applied, followed by morphometric and statistical analysis. The trained rats had higher soleus weight and higher glycogen content in liver, heart and skeletal muscles compared to non-trained. SARM administration increased soleus glycogen in trained animals. Rats given Ostarine had significantly lower blood glucose than those treated with vehicle. Non-steroidal SARMs have weak or absent androgenic effects and similar or even better anabolic effects compared to testosterone. The reduction in blood glucose we found confirms the results of other authors. Ostarine increases the glycogen content in the examined muscles in trained rats, which proves the involvement of androgens in glycogen metabolism. These changes are mainly expressed in soleus, who actively participates in endurance training. This fact emphasizes the stimulating effect of SARMs in the adaptation to submaximal training. SARMs enhance the effect of endurance training on glycogen content in type I-predominant muscle fibers, which may improve the physical performance.

Key words: endurance training, glycogen, Ostarine, selective androgen receptor modulators (SARMs), rats

Mast Cells in Rat Pulmonary Pleura

I. Ivanova[1], I. Stefanov[1,2], V. Pilicheva[1]*

[1] Department of Anatomy, Medical Faculty, Trakia University, Stara Zagora, Bulgaria
[2] Department of Anatomy, Histology and Embryology, Pathology, Medical Faculty, Prof. Dr. Asen Zlatarov University, Burgas, Bulgaria

* E-mail: ivelina.ivanova@trakia-uni.bg

Mature and immature Wistar rats have been widely used to study the role of metachromatic and tryptase positive mast cells in pathological conditions of the lung, particularly the lung pleura. However, the knowledge of age-related features in the distribution of different phenotypes of mast cells in the lung pleura of healthy rats is scarce. We aimed to perform immunohistochemical study to determine the metachromatic, tryptase and ghrelin positive mast cells in pulmonary pleura of male rats at different ages. The collocalization of tryptase and ghrelin immunoreactivity with metachromasy allowed us to estimate the number of tryptase, ghrelin positive and metachromatic mast cells in lung pleura of male Wistar rats at different ages. We revealed that the amount of toluidine blue positive mast cells in the lung pleura was significantly less than that of triptase and ghrelin positive mast cells. The number of triptase and ghrelin positive mast cells showed similar values. In the comparative study on serial sections, we observed that some MCTr and GhrC did not show metachromasia. In the subserous layer of the pleura, the percentage of MCTr and GhrC with manifested metachromasia varies in different age groups: 58-59% in 1-year-old, 42% in 3-month-old and 20% in 20-day-old animals. The similar number of tryptase and ghrelin positive mast cells defines mast cells as a main source of ghrelin in pleura. Mast cell tryptase is a known smooth muscle mitogen participating in mast cell-mediated remodeling of the pleural vasculature but mast cell ghrelin may regulate contractility of vascular smooth muscle cells. It was found that immunohistochemical identification of mast cells by demonstration of tryptase in the rat lung is more reliable than toluidine blue staining. Mast cells are the main source of ghrelin in pleura.

Key words: mast cells, ghrelin, tryptase, pleura, rat

Variation of the Temporal Branches of the Facial Nerve Depending on the Branching Pattern

A. Babuci[1], I. Catereniuc[1], Z. Zorina[1], A. Sivreva[2]*

[1] Department of Anatomy and Clinical anatomy, Nicolae Testemitanu State University of Medicine and Pharmacy, Chisinau, Moldova
[2] Department of Medical psychology, social activities and foreign languages, Faculty of Medicine, Trakia University, Stara Zagora, Bulgaria

* E-mail: angela.babuci@usmf.md, t_o_n_y79@abv.bg

The temporal branches of the facial nerve are very susceptible to iatrogenic injures in plastic and reconstructive surgery of the upper third of the facial region. The aim of the study was to determine the distribution of the temporal branches depending on the facial nerve branching pattern. The research was conducted on 75 formalized hemiheads of adult cadavers (59 males and 16 females), at the Department of anatomy and clinical anatomy of „*Nicolae Testemitanu*" University. By ANOVA one-way test were established the intragroup and intergroup variations of the temporal branches depending on the facial nerve branching type. The number of the temporal branches varied from 1 to 4 branches: 1 branch (17.4%), 2 branches (49.3%), 3 branches (20%), 4 branches (13.3%). In males were determined 1-4 temporal branches and in females 1-3 branches. Depending on the branching pattern the mean number of the temporal branches was: Type I – 2.1±1.00 (95% CI 1.5-2.6); Type II – 2.3±0.65 (95% CI 1.9-2.7); Type III – 2.0±0.68 (95% CI 1.6-2.4); Type IV – 2.3±0.90 (95% CI 1.7-2.8); Type V – 2.0±0.82 (95% CI 1.2-2.8); Type VI – 2.8±1.12 (95% CI 2.2-3.4); Type NI (all the bizare branching patterns) – 2.7±1.03 (95% CI 1.8-3.5), p=0.263. The distribution of the temporal branches of the facial nerve was variable depending on the branching pattern. The highest mean value of the temporal branches was characteristic for Type VI and the lowest one for Type II and Type V.

Key words: temporal branches, facial nerve, branching pattern

Variational Morphology of the Pancreas Based on Imaging Study

Z. Zorina[1], I. Catereniuc[1], A. Babuci[1], A. Sivreva[2]*

[1] Department of Anatomy and Clinical anatomy, Nicolae Testemitanu State University of Medicine and Pharmacy, Chisinau, Moldova
[2] Department of Medical Psychology, Social Activities and Foreign Languages, Faculty of Medicine, Trakia University, Stara Zagora, Bulgaria

* E-mail: zinovia.zorina@usmf.md, t_o_n_y79@abv.bg

The pancreas is frequently subjected to surgical interventions and knowledge about its anatomo-topographical peculiarities and variability is of high clinical significance. The purpose of the study was to establish the anatomical variation of the pancreas based on imaging methods. The study was carried out on 35 patients, hospitalized with acute pancreatitis in the Clinical Republican Hospital „Timofei Mosneaga". The computed tomography and cholangiopancreatography images were taken, on the base of which the morphological structure of the pancreas, the

presence and course of the pancreatic ducts, and the type of their fusion with the common bile duct were studied. Using computed tomography, the structural variants of the pancreas were identified in 28.6% of cases: lobulated pancreas – in 11.4%, diffuse pancreatic steatosis – in 8.6%, hypoplasia of the pancreas – in 5.7% and accessory pancreatic lobule, located above neck of the pancreas, with the opening of its duct into the Wirsung duct was revealed in 2.9%. By cholangiopancreatography, variants of the course and fusion of the pancreatic ducts were identified in 14.3% of cases: sigmoid course of the Wirsung duct – in 8.6%, loop-shaped course of the Wirsung duct – in 5.7%, fusion of the Wirsung and Santorini ducts – in 2.9%, and the sigmoid-shaped Santorini duct – in 2.9%. The modern imaging methods are the most informative in identifying the anatomical variants of the pancreas, which detection is important for the efficiency of the therapeutic management of patients with clinical symptoms of acute pancreatitis.

Key words: pancreas, anatomical variants, imaging

The Role of Vascular Endothelial Growth Factor in Myocardial Aging

A. Iliev[1], G. Kotov[2], N. Stamenov[1], B. Landzhov[1], V. Kirkov[3], L. Gaydarski[1], S. Stanchev[1]*

[1] Department of Anatomy, Histology and Embryology, Medical University of Sofia, Sofia, Bulgaria
[2] Clinic of Rheumatology, University Hospital 'St. Ivan Rilski', Department of Rheumatology, Medical University of Sofia, Sofiaq Bulgaria
[3] Department of Health Policy and Management, Faculty of Public Health 'Prof. Dr Tzekomir Vodenicharov', Medical University of Sofia, Sofia, Bulgaria

* E-mail: dralexiliev@abv.bg

Vascular endothelial growth factor (VEGF) is a key signalling protein in angiogenesis. Despite the significant number of studies over the last few decades, its precise role in the complex regulatory mechanisms of cardiac homeostasis is yet to be fully elucidated. Recent advances show that VEGF expression within the heart changes with age which leads to alterations in the microvasculature and associated remodelling processes in the myocardium. The aim of the present research was to study the changes in VEGF expression in myocardial aging. In the present study, we used two age groups of Wistar rats – 6- and 12-month-old; n=6. VEGF expression was visualised through immunohistochemical and immunofluorescent methods and was assessed semi-quantitatively. In 6-month-old, as well as in 12-month-old animals, VEGF expression within the myocardium showed a specific pattern and a difference in the intensity of immunoreactivity was noted. Our semi-quantitative data revealed an increase in VEGF expression in Wistar rats both in the left and in the right ventricle between 6- and 12-month-old animals. Considering the fact that no obvious pathology was seen in the experimental animals, the results in the model studied herein strongly suggest that aging is the major factor causing these changes. The results of the present study point out to the altered expression of VEGF as a possible key mechanism of microvasculature remodelling as myocardial aging advances.

Key words: vascular endothelial growth factor (VEGF), myocardium, aging

Histological Study on Rare Accessory Bone in the Elbow Region

S. Stanchev[1], L. Gaydarski[1], A. Iliev[1], M. Krupev[2], G. Kotov[3], B. Landzhov[1]*

[1] *Department of Anatomy, Histology and Embryology, Medical University of Sofia, Sofia, Bulgaria*
[2] *Clinic of Imaging Diagnostics, University Hospital 'Alexandrovska', Department of Imaging Diagnostics, Medical University of Sofia, Sofia, Bulgaria*
[3] *Clinic of Rheumatology, University Hospital 'St. Ivan Rilski', Department of Rheumatology, Medical University of Sofia, Sofia, Bulgaria*

E-mail: stanchev_1989@abv.bg

Accessory bones in the elbow region are rarely observed. Although they have been previously described, limited data have been reported on their histological characteristics. The aim of the present study was to provide a detailed light microscopic description of an accessory bone in the posterior elbow region, proximal ulna and the surrounding soft tissues. During a routine anatomical dissection of the right elbow joint of a male formol-carbol fixed cadaver an accessory bone was found. The bone and the related neighbouring structures were histologically examined with azocarmine-aniline blue. Our results indicated the accessory bone was connected to the proximal ulna by a well-developed syndesmosis composed of dense regular connective tissue. Moreover, the zones of insertion of the described syndesmosis showed the typical morphological characteristics of enthesis. Several hypotheses have been suggested for the development of accessory bones in the posterior elbow region. The present study supports the congenital origin of the described bone. The current work has an important clinical and scientific significance as it revealed the presence of histologically proven syndesmosis between an accessory bone and the proximal ulna.

Key words: accessory bone, syndesmosis, elbow joint

Association of the Leptin Receptor Q223R (rs1137101) Polymorphism and Obesity in a Cohort of the North Bulgaria Population

T. Rashev[1], V. Nankov[2], D. Marinova[1], M. Dobrev[1], S. Trifonov[1]*

[1] *Department of Anatomy, Histology, Cytology and Biology, Faculty of Medicine, Medical University of Pleven, Pleven, Bulgaria*
[2] *Scientific Research Laboratory, Medical University of Pleven, Pleven, Bulgaria*

* E-mail: t_rashev@mail.bg

Q223R polymorphism occurs as a result of a non-conservative A to G substitution at codon 223 resulting in a glutamine to arginine amino acid change. Numerous studies in various populations have replicated the association between Q223R SNPs and obesity with the variant G allele. The aims of the current study it to investigate probable association between the *LEPR* Q223R polymorphism in the leptin receptor gene and obesity in a cohort from Northern Bulgaria. The

study comprised of 157 subjects recruited by random sampling from hospitals in northern Bulgaria. Overweight and obesity were defined as a BMI ≥ 25 kg/m^2 and BMI ≥ 30kg/m^2 respectively, based on criteria of the World Health Organization. Genomic DNA was isolated from peripheral blood leucocytes using column-based DNA extraction (ThermoScientific, USA). Genotyping of LEPR Q223R was carried out using PCR-RFLP assay. The present study included 157 individuals. All participants were divided into two groups: target (obese) and control (non-obese). The target group consisted of 82 subjects (52.6%) and the control group comprised of 74 individuals (44.7%). The frequencies of the A and G alleles were: 0.45 and 0.55 in the obese group and 0.49 and 0.51 in the non-obese group, respectively. No significant differences in the distribution of genotype frequencies were observed between the two groups. In conclusion, this study showed that the *LEPR* Q223R polymorphism in North Bulgarian subjects was not associated with obesity.

Key words: LEPR gene, obesity, body mass index, genotype frequencies

Immunohistochemical Assessment of Vascular Endothelial Growth Factor's Expression in the Myocardium of Spontaneously Hypertensive Rats

L. Gaydarski[1], I. Angushev[1], A. Iliev[1], S. Stanchev[1], G. Kotov[2], N. Stamenov[1], B. Landzhov[1]*

[1] Department of Anatomy, Histology and Embryology, Medical University of Sofia, Bulgaria
[2] Clinic of Rheumatology, University Hospital 'St. Ivan Rilski', Department of Rheumatology, Medical University of Sofia, Bulgaria

* E-mail: lgaidarsky@gmail.com

Vascular endothelial growth factor (VEGF) is an essential for angiogenesis. In humans, five variations of VEGF were reported. High blood pressure is the primary risk factor for cardiovascular disease. However, the etiology and complex pathogenesis of arterial hypertension remain elusive. Existing literature suggests a potential role of VEGF in the compensatory mechanisms of hypertension. Therefore, the present study aims to assess the immunoreactivity of VEGF in the hypertensive myocardium and compare it normotensive controls in order to provide insights into the involvement of VEGF in the pathogenesis of hypertension. We employed 6-month-old spontaneously hypertensive rats as an animal model to simulate arterial hypertension and 6-mont-old normotensive Wister rats as a control. To detect the presence of VEGF, immunohistochemical and immunofluorescent staining were used. Subsequently, a semi-quantitative analysis was conducted to evaluate the expression of VEGF. VEGF immunoreactivity was detected in the predominantly in the cytoplasm of cardiomyocytes in both ventricles. Interestingly, VEGF expression was strongest in the right ventricle of spontaneously hypertensive rats. Additionally, the hypertensive group exhibited significantly higher levels of VEGF expression in both ventricles compared to the controls. The elevated expression of VEGF implies compensatory upregulation of angiogenesis as a desperate attempt of the heart to cope with the increased overload. Our study demonstrates significant elevation of VEGF expression in both ventricles of hypertensive animals, compared to the control group. Thus indicating a potential key role in the pathogenesis of hypertension.

Key words: VEGF; myocardium; hypertension

Some results for anti-GD1a antibodies as a biomarker of neuronal changes in different diseases

V. Kolyovska[1], S. Ivanova[2], D. Drenska[3], D. Maslarov[3,4]*

[1] *Institute of Experimental Morphology, Pathology and Anthropology with Museum, Bulgarian Academy of Sciences, Sofia, Bulgaria*
[2] *University Hospital for Neurology and Psychiatry "St. Naum", Sofia, Bulgaria*
[3] *University First MHAT-Sofia, "St. John Krastitel", Neurology Clinic, Sofia, Bulgaria*
[4] *Medical University of Sofia, Medical College "Y. Filaretova", Sofia, Bulgaria*

* E-mail: verakol@abv.bg

Evidence has been obtained to support the view that gangliosides are involved in the pathogenesis of multiple sclerosis (MS) and its experimental model, chronic relapsing experimental allergic encephalomyelitis (CREAE). GD1a ganglioside is one of the major neuronal gangliosides. It was detected in the spinal cord of Lewis rats with CREAE before the onset of clinical signs and during the first clinical episode. Elevation of serum GD1a gangliosides during the first attacks of the disease has been suggested to be an indicator of neuronal destruction. The aim of the present study is to determine to what extent the value of the anti-GD1a antibody titer can be considered a biomarker for changes in neurons and the need to introduce into clinical practice screening for the levels of GD1a ganglioside in the blood of the healthy population as a marker of neuronal damage in the brain. This will allow early detection of diseases and effective timely treatment. We work with sera from patient with multiple sclerosis, vascular cognitive dementia and elderly people over 90. The blood was taken before any medical intervention. The titer is determined by the enzyme-linked immunosorbent assay (ELISA) technique. A high titer of anti-GD1a antibodies is present only in patients with MS, at the time of an attack. The study was conducted in triplicate. The positive titer of anti-GD1a antibodies can be considered as possible biomarkers only in MS patients in a severe attack. A low titer indicate no neuronal changes.

Key words: anti-GD1a ganglioside antibodies, neurochanges, multiple sclerosis, vascular cognitive dementia, elderly

Assessment of Sex Differences in Size and Shape of Human Mandible Using Geometric Morphometrics

D. Toneva[1], S. Nikolova[1], N. Fileva[2], D. Zlatareva[2]*

[1] *Department of Anthropology and Anatomy, Institute of Experimental Morphology, Pathology and Anthropology with Museum, Bulgarian Academy of Sciences, Sofia, Bulgaria*
[2] *Department of Diagnostic Imaging, Faculty of Medicine, Medical University of Sofia, Sofia, Bulgaria*

* E-mail: ditoneva@abv.bg

The accuracy and effectiveness of methods for sex estimation depends on the level of sexual dimorphism manifested by human bones. There are various methods for examination of the sex differences in size and shape of the bones. The present study uses a geometric morphometric approach to investigate sexual dimorphism in size and shape of the mandible. Computed

tomography images of 190 adult Bulgarians (98 males and 92 females) were used for generation of surface models of the skulls of individuals. The three-dimensional coordinates of 45 landmarks located on the mandible were acquired. The raw landmark coordinates were superimposed by generalized Procrustes analysis. The statistical significance of sex differences in size (centroid size) and shape (shape variables) of the mandible was evaluated. Multivariate regression, principal component analysis, and discriminant analysis were applied in the study. The accuracy of sex classification was calculated by leave-one-out cross-validation. The size of the mandible showed significant differences between males and females. Significant sex differences were also found in the shape variables including the allometric component. The classification accuracy achieved by the centroid size was 87%. The shape variables provided lower accuracy, which differed considerably depending on the type of shape variables used in the analysis (Procrustes coordinates: 78%; regression residuals: 53%). Male and female mandibles differ significantly in size and shape. Size classifies the mandibles with higher accuracy than shape.

Key words: mandible, sexual dimorphism, geometric morphometrics, computed tomography

Acknowledgement: The study was funded by the Bulgarian National Science Fund, Grant **КП**-06-**Н**51/4–11.11.2021.

Impact of Supernumerary Calvarial Bones on the Neurocranium Morphology: A Comparative Geometric Morphometric Study

S. Nikolova, D. Toneva*

Department of Anthropology and Anatomy, Institute of Experimental Morphology, Pathology and Anthropology with Museum, Bulgarian Academy of Sciences, Sofia, Bulgaria

* E-mail: sil_nikolova@abv.bg

Supernumerary bones in the cranial vault arise during embryogenesis as a result of non-fusion between the normal ossification centers or emerging of additional centers in the cranial sutures and fontanelles. This study aims to assess the impact of metopism and supernumerary bones in the occipital region on the cranial morphology. A series of 245 male crania of adult individuals was investigated. They were divided into four series according to the presence or absence of metopism and supernumerary bones in the occipital region: control (n = 115); metopic crania (n = 32); crania with supernumerary bones in the occipital region (n = 67); and metopic crania with supernumerary bones in the occipital region (n = 31). Polygonal 3D models were generated and 3D coordinates of 35 landmarks of the neurocranium were collected on these models. Size and shape of the assembled landmark configurations were compared using geometric morphometric analyses. Significant intergroup size differences were found in the frontal and occipital bone configurations. All configurations showed significant intergroup shape differences except the occipital one. The supernumerary bones in the occipital region are not associated with significant changes of the cranial morphology, but they are related to an intensification of the typical of metopism modification of the neurocranium shape and size.

Key words: metopism, neurocranium, supernumerary calvarial bones, anatomic variations

Acknowledgement: The study was funded by the Bulgarian National Science Fund, Grant КП-06-Н51/4–11.11.2021.

Zn(II)/Au(I) and Zn(II)/Ag(I) Complexes with Schiff Bases- A New Approach in Treatment of Human Glioblastoma Multiforme Cells

L. Dyakova[1], A. Abudalleh[2], T. Zhivkova[2], G. Marinescu[3], D.-C.-Culita[3], T. Mocanu[3], R. Alexandrova[2]*

[1] *Institute of Neurobiology, Bulgarian Academy of Sciences, Sofia, Bulgaria;*
[2] *Institute of Experimental Morphology, Pathology and Anthropology with Museum, Bulgarian Academy of Sciences, Sofia, Bulgaria;*
[3] *Institute of Physical Chemistry "Ilie Murgulescu", Romanian Academy, Bucharest, Romania*

* E-mail: sigma13@abv.bg

The control of glioblastoma multiforme is one of the big challenges in current oncology practice. (Multiple) drug resistance of glioblastoma cells, their escape from the immune response, tumor heterogeneity, limited access of drugs to the tumor due to the blood-brain barrierand high invasiveness of the tumor make treatment of this neoplasia very hard and slow. The aim of our study is to investigate the influence of newly synthesized complexes of Zn (II), Zn (II)/Au(I) and Zn(II)/Ag (I) with Schiff bases (derivatives of 2,6-diformyl cresol (diald) - Aepy, Ampy and Dmen,in 8MGBA human glioblastoma multiforme cells. Cytotoxic/antitumor activity of the compounds was evaluated by: i) short-term (24-72h) experiments –using MTT test, neutral red cytotoxicity assay, crystal violet staining technique, double staining with acridine orange and propidium iodide and ii) long-term experiments (37 days) – by 3Dcolony-forming method. The compounds investigated decrease in time-and concentration-dependant manner viability and proliferation of treated glioblastoma cells. Metal complexes are more effective compared to their ligands alone. They induce cytopathological changes and inhibit the 3D growth of tumor cells in a semi-solid medium. The higher cytotoxic/antitumor activity exhibit ZndmenAu and ZndmenAg. The results obtained show the promising antitumor activity of the compounds investigated. More experiments are needed to clarify their mechanism of action.

Key words: glioblastoma multiforme, cytotoxic/antitumor activity, cell line, metal complexes

Acknowledgements: Grant№ КП-06-М61/3 from 13.12.2022, National Science Fund, Bulgarian Ministry of Education and Science, bilateral project between Bulgarian Academy of Sciences and Romanian Academy.

In vitro and *in vivo* Anticancer Activity of Ethanol Extract of *Epilobium Parviflorum* Schreb on Ehrlich Carcinoma Tumor Model

I. Sulikovska[1], K. Todorova[1], I. Ivanov[2], D. Tasheva[3], I. Iliev[1], A. Vasileva[2], M. Dimitrova[1]*

[1] *Institute of Experimental Morphology, Pathology and Anthropology with Museum, Bulgarian Academy of Sciences, Sofia, Bulgaria*
[2] *Medical University of Sofia, Sofia, Bulgaria*

[3] *Sofia University "St. Kl. Ohridski", Sofia, Bulgaria*

* E-mail: inna_sulikovska@ukr.net

Epilobium parviflorum Schreb (EPE) is a flowering plant widely applied in traditional medicine for treatment of different diseases including cancer. The present study aims to assess the antitumor potential of 80% ethanol extract by using both *in vitro* and *in vivo* tumor models. Anticancer activity was investigated on a mouse model of solid and ascites forms of Ehrlich's breast cancer and 5-fluorouracil (5-FU) was used for comparison as a standard chemotherapy medication. The changes in hematological, biochemical biomarkers and histopathological features were analyzed. The *in vitro* activity of EPE was evaluated by the MTT test using Ehrlich's Ascites Carcinoma (EAC) cell lines. The morphological changes induced by the extract in both models were analyzed by light and/or fluorescent microscopy. The results of *in vitro* studies indicated that the EPE induced significant antiproliferative and apoptogenic effects in the EAC cells. *In vivo* studies showed that EPE treated mice had better clinical and histopathological status compared to untreated ones. The plant extract can be used as an auxiliary implement for alleviating the symptoms in breast cancer.

Key words: Ehrlich Carcinoma tumor model, antitumor activity, ethanol extract of *E. parviflorum* Schreb

Acknowledgements: This work is financially supported by the National Science Fund of the Bulgarian Ministry of Education and Science, Grant Nr KP-06-N31/1.

Study of the facial proportions in Young Bulgarians by 3D Laser Scanning

T. Petleshkova[1], S. Sivkov[1], A. Baltadjiev[1], A. Fasova[1], H. Manev[2], R. Raycheva[3], P. Timonov[4]*

[1] Department of Anatomy, Histology and Embryology, Faculty of Medicine, Medical University of Plovdiv, Plovdiv, Bulgaria
[2] Department of Medical Physics and Biophysics, Faculty of Pharmacy, Medical University of Plovdiv, Plovdiv, Bulgaria
[3] Department of Social Medicine and Public Health, Faculty of Public Health, Medical University of Plovdiv, Plovdiv, Bulgaria
[4] Department of Forensic Medicine and Deontology, Faculty of Medicine, Medical University of Plovdiv, Plovdiv, Bulgaria

* E-mail: Tsvetanka.Petleshkova@mu-plovdiv.bg

The knowledge of the variations in facial proportions in different populations may find applications in plastic and maxillofacial surgery. The aim of the study was to examine facial proportions in young Bulgarians. The study included clinically healthy individuals of Bulgarian origin (46 men and 49 women), aged between 21 and 30 years. Three-dimensional images were obtained from each subject using a hand-held laser scanner (FastSCAN Cobra, Polhemus Inc., Colchester VT). On each of the obtained images, a set of anthropometric landmarks was placed: nasion (n), stomion (sto), frontotemporale (ft_r, ft_l) and zygion (zy_r, zy_l). From the landmarks, the physiognomic upper facial height (n-sto), bizygomatic breadth (zy_r-zy_l) and smallest forehead breadth (ft_r-ft_l) were measured and averaged for sex. The measurements were used to calculate the Physiognomic upper facial index and Jugofrontal index. The results obtained show that in the

jugofrontal index most of studied men and women fall into the category medium 50% and 51%, respectively. In the category narrow, the percentage of women and men was 32.7% and 28.3%. The highest percentage of men and women in the physiognomic upper facial index fall into the category mesen, 43.5% and 44.9%. In the categories lepten and euryen, the percentage of men was 26.1% and 19.6% and women was 30.6% and 18.4%. For this two indices, no statistically significant gender differences were found in the percentage distribution by categories ($p>0.05$). The highest percentage of studied men and women fall into the categories medium and mesen in the two studied indices.

Key words: 3D laser scanning, facial proportions, Bulgarians

Somatotype of Bulgarian Young Adults

I. Vladimirov[*], *R. Stoev*

Institute of Experimental Morphology, Patology and Anthropology with Museum of BAS, Sofia, Bulgaria

* E-mail: garet_1991@abv.bg; rastesto@abv.bg

An important element of physical development of man is the constitutional type – somatotype. That is why it is object of many studies. Because of complex reasons mass anthropometric studies in Bulgaria are rare in last years and serveys in university students are used to characterize the physical development of young adults. During the period 2016-2023, ananthropometric study was carried out on 190 Bulgarian young adults, students in different universities in Sofia, 75 males and 115 females. The mean age of these students is 21 years for males and 20 years for females. Standard anthropometric measurements and somatotypological characterization after Heath-Carter are applied. The mean height of the investigated students is 177,6 cm in males and 163,1 cm in females. Their weight is 79,2 and 58,5 kg respectively, their Body Mass Index 25,0 and 22,0. Their average somatotype is 3,7: 5,4: 2,1 in males and 4,2: 4,2: 2,5 in females. It is interesting that their somatotype is practically the same as that of the students at the NSA nearly 50 years ago, studied by Maria Toteva. Close are also the somatotypes of students of sports in Warsaw, Turkey and Split, especially in females. Despite the general opinion about the immobilization and obesity of the Bulgarian youth in recent years, we do not find such. The probable reason is the spread of sports activities and more rational nutrition today.

Key words: young adults, somatotype, body height, body mass, body mass index

Exposure to Cobalt Chloride Affects Mouse Testis via Altered Iron Metabolism

E. Pavlova[*], *Y. Gluhcheva, V. Mihaylova*[2], *E. Petrova*[1], *I. Vladov*[1], *N. Atanassova*

[1] *Institute of Experimental Morphology, Pathology and Anthropology with Museum, Bulgarian Academy of Sciences, Sofia, Bulgaria*
[2] *Faculty of Chemistry and Pharmacy, Sofia University "St. Kliment Ohridski", Sofia, Bulgaria*

* E-mail: e_bankova@yahoo.com

Cobalt (Co) exposure is known to interfere with iron (Fe) metabolism. Our aim was to study the effect of chronic cobalt chloride administration on spermatogenesis in tandem with changes in iron homeostasis in adult mice. Pregnant mice were exposed to 75 mg or 125 mg /kg b.w. $CoCl_2 \times 6H_2O$ with drinking water for 3 days before delivery. Treatment continued until postnatal day 90 of the pups. Control animals obtained tap water. Testes of control and Co-treated mice were processed for immunohistochemical and inductively coupled plasma mass spectrometry analyses. Sperm count was performed. Chronic $CoCl_2$ administration resulted in significant Co accumulation and increase of Fe content in the testis that was 2.7-fold higher after treatment with low dose compared to high dose. Significant dose-dependent reduction in testicular index after Co administration was established. Seminiferous tubules diameter was obviously reduced associated with lack of lumen formation. Disorganization of the seminiferous epithelium was accompanied with sloughed off immature germ cells into the lumen and multinuclear germ cells. These findings correspond to significant reduction of sperm count by 2.15-fold for low dose and 3.35-fold for high dose. Stage specific expression of androgen receptor protein in Sertoli cells was not seen after Co exposure. Reduced expression of transferrin receptor-1 protein and increased hepcidin immunoreactivity was also found. Ferroportin expression was not affected by Co administration. Data suggest that cobalt exerts its toxicity on testis possibly through altered iron homeostasis.

Key words: cobalt, testis, iron regulation, androgen receptor

Morphometric Analyses of the Left Atrium

Y. Stoyanov[1], N. Genov[1], N. Dimitrov[1], I. Stefanov[1], D. Atanasova[1,2], I. Ivanova[1], S. Hamza[1], A. Georgieva[1], N. Pirovski[1], V. Pilicheva[1], I. Valkova[1], N. Malcheva[1]*

[1]*Department of Anatomy, Faculty of Medicine, Trakia University, Stara Zagora, Bulgaria*
[2] *Institute of Neurobiology, Bulgarian Academy of Sciences, Sofia, Bulgaria*

* E-mail: yordan.stoyanov@trakia-uni.bg

The left atrium has a thin wall the thickness of which could vary significantly. In normal population four pulmonary veins having four independent ostia drain into that chamber. Anatomical variations and branching patters of the pulmonary veins ostia are not typical but are reported by various studies. The circumferential pulmonary vein line is the circular connection between the ostia at each side and is reported to be thicker on the left side. In addition its anatomical characteristics are vital for pulmonary vein isolation (PVI) during the treatment of atrial fibrillation. The aim of this study is to conduct morphometric analyses on these structures on the formalin-fixed hearts used at our Department of Anatomy. The results of our research showed that 35% of the examined hearts were presenting anatomical variations in the pulmonary venous ostia (PVO). Around 28% showed more than 2 ostia at the right side. On the contrary only 14% of left pulmonary veins showed variation from the anatomical model. The mean value of the thickness of the left atrium was bigger in the hearts without anomaly: 2.67mm, but wasn't showing statically significant difference. In contrast pulmonary vein thickness (PVT) of the ostia (Mean= 1.746 mm) and the circumferential pulmonary vein thickness (Mean=1.736 mm) were showing statically significant thickening in the left side in comparison with the right. PVO variations were presented into one third of the examined hearts. The left pulmonary veins ostia were significantly thicker compared to the right.

Key words: branching pattern, pulmonary veins, left atrium, morphometry

Morphological Changes in Aging Testis in Melatonin Deficiency Conditions

A. Petrova[1], D. Barbutska[1], Y. Koeva[1], K. Georgieva[2], Y. Tchekalarova[3], G. Nanov[4]*

[1] *Department of Anatomy, Histology and Embryology, Medical University of Plovdiv, Plovdiv, Bulgaria*
[2] *Department of Physiology, Medical University of Plovdiv, Plovdiv, Bulgaria*
[3] *Institute of Neurobiology, Bulgarian Academy of Sciences, Sofia, Bulgaria*
[4] *Student in Medicine, Faculty of Medicine, Medical University of Plovdiv,Plovdiv, Bulgaria*

* E-mail: Anelia.Petrova@mu-plovdiv.bg

In a wide range of research, it has been established that melatonin influences the male hypothalamic-pituitary-gonadal axis, and has a direct effect on the testicular parenchyma through its receptors. Melatonin affacts the testicular Leydig cells (LCs) and functions as a local modulator of steroidogenesis. Moreover, the involvement of melatonin in the processes of maturation and differentiation is discussed in relation to the spermatogenic epithelium. To investigate the potential role of melatonin in terms of testicular function in a melatonin deficiency model of rats of different ages. Male Wistar rats of three age subgroups: 5 months, (sexually mature); 16 months, (adults) and 20 months old (old) were divided into two groups: animals with removed pineal glands, using the Hoffman-Reiter technique (PIN), and a control group (SHAM). Hematoxylin and eosin and Azan (Heidenhaim) staining of paraffin sections of testicular fragments were used to evaluate the morphological changes. By using hematoxylin-eosin staining of testicular fragments of 16- and 20- months old animals with removed pineal glands we found hypertrophy and hyperplasia of LCs in an enlarged testicular interstitium, whereas in the lumen of the seminiferous tubules we established spermatogenic arrest, with almost complete absence of spermatozoa. The Azan staining revealed a folded basal lamina of the seminiferous tubules, with predominant sclerotic changes, especially in the PIN group**.** The results obtained are further evidence of the role of melatonin in the processes of spermatogenesis and steroidogenesis in the male reproductive system.

Key words: Leydig cells, melatonin, steroidogenesis

Fetal MRI and its Meaning for Prenatal Diagnosis of Neural Tube Defects

A. Petrova[1], M. Kanarev[1] M., Shishmanova-Doseva[2], A. Georgiev[3], E. Uchikova[4], K. Kilova[5], A. Tenev[6], T. Kitova[1]*

[1] *Department of Anatomy, Histology and Embryolog, Medical university of Plovdiv, Plovdiv, Bulgaria*
[2] *Department of Pharmacology, Toxicology and Pharmacotherapy, Medical University of Plovdiv, Plovdiv, Bulgaria*
[3] *Department of Diagnostic Imaging, Medical University of Plovdiv, Plovdiv, Bulgaria*
[4] *Department of Obstetrics and Gynaecology, Medical University of Plovdiv, Plovdiv, Bulgaria*
[5] *Department of Medical Informatics, Biostatistics and E-learning, Medical University of Plovdiv, Plovdiv, Bulgaria*
[6] *Student in Medicine, Faculty of Medicine, Medical University of Plovdiv, Plovdiv, Bulgaria*

* E-mail: Anelia.Petrova@mu-plovdiv.bg

The neural tube defects are a heterogeneous group of congenital abnormalities of the central nervous system that occure due to a failed closure of the neural tube. Despite the improvement of the ultrasound methodology, the prenatal examination often provides uncertain findings and the neural tube defects remain a diagnostic challenge. Fetal magnetic resonance is an additional imaging technique that provides clarification of questionable ultrasound data and detection of associated abnormalities not visible by sonographic examination. The aim of the present study was to evaluate the role and significance of fetal magnetic resonance imaging for the prenatal diagnosis of neural tube defects. The magnetic resonance findings of two pregnant women are presented, in which the prenatal ultrasound examination established evidence of malformative syndromes. The study was conducted at the Translational Neuroscience Research Institute at Medical University of Plovdiv, through a translational neuroimaging with a functional 3 Tesla nuclear magnetic resonance. The investigations confirmed the presence of neural tube defects: occipital encephalocele in one, hydrocephalus, Arnold-Chiari type II syndrome and lumbar myelomeningocele in the other. In cases in which the prenatal ultrasound diagnosis suspects an existing central nervous malformation, the magnetic resonance imaging is a recommended method that provides medical professionals and parents with the necessary information to determine the outcome of the pregnancy.

Key words: fetal magnetic resonance imaging, malformative syndromes, neural tube defects

Cavum Vergae and Cavum Septi Pellucidi Cyst–Anatomical Variation, a Case Aeport

M. Kanarev[1], A. Petrova[1], N. Petrova[1], F. Popova[1], Z. Harizanova[1], St. Sivkov[1], T. Lolovski[2]*

[1] Department of Anatomy, Histology, and Embryology, Medical University of Plovdiv, Plovdiv, Bulgaria
[2] Student in Medicine, Faculty of Medicine, Medical University of Plovdiv, Plovdiv, Bulgaria

* E-mail: Marin.Kanarev@mu-plovdiv.bg

Cavum vergae and cavum septi pellucidi are congenital anatomical variations which are common in infancy but usually do not persist until adulthood. If this rarely occurs it is usually asymptomatic. When the condition is pronounced and the variation is of a large size and a diameter of more than a centimeter it can be classified as a cyst. The latter presents as a cystic lesion located in the midline below the body and splenium of corpus callosum above the fornix. If it is large enough in size it can lead to obstructive hydrocephalus. When this occurs, it should be treated radically. The aim of the present case report is to illustrate that anatomical variations are present as asymptomatic cases and can be accidently detected. The accidental magnetic resonance findings of a 29-year-old male subject with an asymptomatic cavum vergae cyst are presented. The study was conducted at the Translational Neuroscience Research Institute at Medical University of Plovdiv, through a translational neuroimaging with a functional 3 Tesla nuclear magnetic resonance. The MRI study was conducted as part of a Doctoral and postdoctoral project No ДПДП-7/2022 at Medical University of Plovdiv. The investigations confirmed the presence of a cavum vergae variation which as long as asymptomatic should not be treated, rather only monitored. MRI is a convenient method for establishing the parameters of CNS variations and malformations.

Key words: cavum vergae, cavum septum pellucidum, cavum vergae cyst, magnetic resonance imaging

Estimation of Humeral and Femoral Length Using Proximal Dimensions in Bulgarian Population

*A. Fasova[*1], P. Timonov[2], A. Baltadjiev[1], T. Petleshkova[1]*

[1] *Department of Anatomy, Histology and Embryology, Medical Universtiy of Plovdiv, Plovdiv, Bulgaria*
[2] *Department of Forensic medicine and Deontology, Medical University of Plovdiv, Plovdiv, Bulgaria*

* E-mail: Antoaneta.Fasova@mu-plovdiv.bg

The role of skeleton is invaluable in determining age, height, sex, race and presence of disease. Reconstruction of length of the long bones is an important part of identification procedure which is related to height estimation. Numerous standards for sex and height determination of bones from different populations have been proposed for forensic and archaeological practice. Due to the presence of racial, population and evolutionary differences, no universal method has yet been created. The current study introduces a method of estimating the length of humerus and femur from proximal dimensions of the bones specific to the Bulgarian population. 139 adult humeri with known age and sex were studied. The proximal anthropometric features include circumference, transverse, and vertical diameters of the head of bones. Simple linear regressions were obtained to define the length. For males, regression formulae, which included head circumference, provided the best fit of the data, resulting in the highest correlation. For females, the vertical diameter of the head showed the best correlation with maximum length. The regression formula suggested that the proximal end is the best estimator of length. The derived formulae are population and sex specific.

Key words: humerus, femur, forensic practice, length estimation

Sectional Area Differences of the Myenteric Ganglia in the Rat Colorectal Region

N. Genov[1], N. Tomov[2], N. Dimitrov[1], N. Lazarov[3,4], D. Atanasova[1,3]*

[1] *Department of Anatomy, Faculty of Medicine, Trakia University, Stara Zagora, Bulgaria*
[2] *Institute of Anatomy, University of Bern, Bern, Switzerland*
[3] *Institute of Neurobiology, Bulgarian Academy of Sciences, Sofia, Bulgaria*
[4] *Department of Anatomy and Histology, Medical University of Sofia, Sofia, Bulgaria*

* E-mail: nikolay.genov@trakia-uni.bg

The myenteric (Auerbach) plexus lying between the longitudinal and circular layers of the muscularis externa in the intestinal tract consists of ganglia interconnected by nerve fibers. The myenteric plexus, which receives innervation from the autonomic nervous system, is primarily responsible for the peristaltic movement of the intestines. This study has been conducted to determine the sectional area differences in the ganglia and their constituent neuronal perikarya

in the myenteric plexus at the levels of the proximal colon, distal colon and rectum in the rat. The results of the morphometric analyzes pointed out a similarity between the sectional area of myenteric ganglia in all three examined regions. More than 30% at the level of the distal colon and more than 20% of the ganglia in the rectum have cross-sectional area ranging from 500 μm^2 to 1500 μm^2. Conversely, at the level of the proximal colon more than 40% of the ganglia had sectional area sizes in the range of 1000 μm^2 to 2000 μm^2. Differences in the size of the neuronal perikarya have been observed as well. Smaller neuronal bodies with a mean value of 50 μm^2 were frequently observed in the proximal colon and the rectum while almost 40% of the neuronal perikarya had an average value of 100 μm^2 at the level of the distal colon. Differences in the sizes of myenteric ganglia and neuronal perikarya are observed in different regions of the large intestine, which determines the presence of regional features and is probably related to certain peculiarities in motility.

Key words: colon, morphometry, myenteric plexus, rectum, rat

Acknowledgement: This research is supported by the Bulgarian Ministry of Education and Science under the National Program "Young Scientists and Postdoctoral Students-2".

Investigations on Cytotoxic and Antiviral Effects of 1,8-Naphthalimide Derivatives

R. Alexandrova[1], H. Hristov[1], A. Abudalleh[1], L. Dyakova[2], D. Staneva[3], M. Georgieva[4], G. Miloshev[4], A. Said[5], I. Grabchev[6]*

[1] *Institute of Experimental Morphology, Pathology and Anthropology with Museum, Bulgarian Academy of Sciences, Sofia, Bulgaria*
[2] *Institute of Neurobiology, Bulgarian Academy of Sciences, Sofia, Bulgaria;*
[3] *University of Chemical Technology and Metallurgy, Sofia, Bulgaria*
[4] *Institute of Molecular Biology, Bulgarian academy of Sciences, Sofia, Bulgaria*
[5] *Department of Chemistry, Faculty of Science, Assiut University, Assiut, Egypt*
[6] *Sofia University "St. Kliment Ohridski", Faculty of Medicine, Sofia, Bulgaria*

* E-mail: rialexandrova@hotmail.com

The aim of our study was to evaluate the cytotoxicity, genotoxicity and mitotchondrial toxicity of first generation polypropylene imine dendrimer modified with 1,8-naphthalimide and chitosan modified with 4-amino-1,8-naphthalimide. The following cell lines were used as model systems: MDA-MB-231 (human triple negative breast cancer), MCF-7 (human luminal type A breast cancer), HeLa (human cervical carcinoma) and Lep-3 (non-tumor human embryonic cells). The effect of the compounds on cell viability and proliferation was studied by: i) short-term experiments for 24-72h, performed with monolayer – 2D cell cultures, carried out by MTT test, neutral red uptake assay, crystal violet staining and double staining with acridine orange and propidium iodide); ii) long term experiments – the influence of 1,8-naphthalimide derivatives on viability and 3D growth of cancer cells was assessed during 26-28 days by 3D colony-forming technique. Their genotoxicity was investigated by comet assay. FACS analysis was applied to determine the ability of the compounds to inhibit the mitochondrial membrane potential ($\Delta\Psi m$) in the treated cells. The results obtained revealed that modified chitosan has more pronounced cytotoxic activity than the first generation polypropylene imine dendrimer modified with 1,8-naphthalimide and non-modified chitosan. Non-tumor Lep-3 human cells are less sensitive to the cytotoxic effect of the compounds examined as compared to human breast

cancer and cervical carcinoma cell lines. All examined compounds induce double-strand DNA breaks but only modified chitosan (applied at a concentration of 600 μg/ml for 72h) inhibit the mitochondrial membrane potential in the treated HeLa cells.

Key words: cancer cells, 1,8-naphthalimide derivatives, cytotoxicity, genotoxicity, mitochondrial toxicity

Renal Inflammation Following Chronic Administration of Cobalt Chloride

Y. Tabakov[1], R. Ivanov[1], E. Pavlova[1], E. Petrova[1], A. Tinkov[2,3], O. Ajsuvakova[2,3], A. Skalny[4], Y. Gluhcheva[1]*

[1] *Institute of Experimental Morphology, Pathology and Anthropology with Museum, Bulgarian Academy of Sciences, Sofia, Bulgaria*
[2] *Yaroslavl State University, Yaroslavl, Russia*
[3] *IM Sechenov First Moscow State Medical University, Moscow, Russia*
[4] *Federal Research Centre of Biological Systems and Agro-technologies of the Russian Academy of Sciences, Orenburg, Russia*

* E-mail: yavor.tabakov@iempam.bas.bg

Cobalt (Co) is an essential trace element that can cause severe health effects upon occupational or environmental exposure. Cobalt chloride ($CoCl_2$) has been used in the research of kidney diseases, due to its ability to induce hypoxia. To assess the alterations in mouse kidney following chronic exposure to $CoCl_2$. Pregnant ICR mice were subjected to $CoCl_2x6H_2O$ at a daily dose of 125 mg/kg body weight 2–3 days prior delivery and treatment continued up until day 90 after birth. The compound was administered via drinking tap water. Age-matched mice obtaining regular tap water were used as a control group. Pups were sacrificed, kidneys were excised and processed for histological and immunohistochemical analyses. Myeloperoxidase (MPO) was studied as a marker of inflammation. Cobalt content was measured using inductively coupled plasma mass spectrometry (ICP-MS). Kidney organ weight index (KI) was reduced following chronic $CoCl_2$ administration compared to the controls. Renal Co content was significantly elevated (12.9-fold) compared to the age-matched controls indicating that the kidney is one of the main targets of Co exposure. Pathohistological analysis showed numerous leukocyte infiltrates, altered glomeruli structure and tubular necrosis which may be the cause for the reduced KI. MPO was well expressed in the renal tubules, glomerular membrane and in the vascular endothelial cells of Co-exposed mice suggesting a possible $CoCl_2$-induced oxidative stress as well. The study shows that chronic $CoCl_2$ supplementation induces renal inflammation which may lead to kidney dysfunction and organ damage.

Key words: cobalt chloride, chronic exposure, kidney, inflammation, MPO

Expression of the Transcription Factor ZBTB20 in the Subventricular Zone of Adult Macaque Monkey under Physiological and Ischemic Conditions

L. Veleva [1], D. Stoyanov [1], M. Ivanov [1,2], A. Mladenov [1], S. Pavlov [1], AB Tonchev [1, 2]*

[1] *Department of Anatomy and Cell Biology, Faculty of Medicine, Medical University of Varna, Varna, Bulgaria*
[2] *Research Institute, Medical University of Varna, Varna, Bulgaria*

* E-mail: dimo.stoyanov@mu-varna.bg

The subventricular zone (SVZ) is a major neurogenic area in the adult mammalian brain. The mRNA of the transcription factor ZBTB20, important for neurodevelopment, is known to be present in the monkey anterior SVZ (SVZa). This prompted us to study the expression pattern of ZBTB20 in the SVZa and rostral migratory stream (RMS) of non-human primates and the expression changes in a primate model of cerebral ischemia, a strong activator of neuronal progenitors. Adult macaque monkeys underwent either sham surgery or transient global cerebral ischemia. Sections were processed for fluorescent immunohistochemistry. Cell counting was done using ImageJ, statistical analysis was performed in R. ISH images from the database *Monkey Niche* were analyzed using cellDetekt. Here we demonstrate the diverse immunophenotype of ZBTB20+ cells in the adult primate SVZa and RMS, accounting for nearly all DCX+ and GFAP+ cells and the majority of the Ki67+ cells, representing neural stem cells, neuroblasts and transit-amplifying progenitors, respectively. Our data reveal noticeable enhancement of ZBTB20 mRNA expression and higher co-expression of the ZBTB20 protein with DCX and Ki67 following transient global ischemia. Our results suggest a role for ZBTB20 in regulating the activity of neural stem cells and progenitors. This may have implications for stroke treatment and brain tumour biology. The expression of ZBTB20 in all stages of adult neurogenesis suggests that it could regulate the proliferation of neural progenitors in the primate SVZa. Moreover, ZBTB20 may be implicated in the postischemic activation of adult neurogenesis.

Key words: ZBTB20; non-human primate; subventricular zone; neural progenitor

Zbtb20 is Required for Cortical Interneuron Development

D. Stoyanov[1], M. Ivanov[1], S. Pavlov[1], I. Manoylov[3], J. Tchekalarova[3], A. Tchorbanov[3], A. Stoykova[2], A. Tonchev[1]*

[1] *Department of Anatomy and Cell Biology, Faculty of Medicine, Medical University of Varna, Varna, Bulgaria*
[2] *Max Planck Institute for Multidisciplinary Sciences, Göttingen, Germany*
[3] *Bulgarian Academy of Science, Sofia, Bulgaria*

* E-mail: dimo.stoyanov@mu-varna.bg

Zbtb20 is a transcription factor, involved in hippocampal patterning, cortical layering, and olfactory bulb development. Its function in the context of cortical interneuron (CINs) development is unexplored. Brain sections from wild type (WT)/Zbtb20$^{-/-}$ mice were stained

by means of immunofluorescence or in situ hybridisation. BrdU labelling was done to quantify proliferation and birth date. Images were analysed in ImageJ, statistical analysis was done in R. Zbtb20 is expressed in CINs stem cells, found in the VZ of the developing ventral forebrain. Postnatally, Zbtb20$^{-/-}$ mice show sharp reduction of PV^{+} but not SST^{+} CINs, both derived from the MGE. CGE-CINs, expressing Prox1, are also reduced. Ventral forebrain gene patterning is preserved. No premature stem cell differentiation was observed. BrdU labelling revealed lower proliferation in the E12.5 -> E13.5 MGE. BrdU birth dating showed that E12.5 born CINs are fewer in Zbtb20$^{-/-}$ mice. Analysing the upper (UL) and lower layers (LL) separately showed that at E12.5 -> P8 mutants generate fewer LL CINs compared to the WT. Conversely, E16.5 -> P12 mutant animals make more LL CINs than the control, at the expense of UL CINs. Interneurons hold great therapeutic promise. Studying the genetic regulation of their development may allow for more precise stem cell manipulation and their therapeutic application. Zbtb20 is expressed in the germinative zones of CINs. Zbtb20$^{-/-}$ mice show reduction of specific types of CINs. Developing mutant animals have proliferative deficits and delay in the switch from LL to UL CINs production.

Key words: Zbtb20; cortical interneurons; development

Acupuncture Channels and Visible Meridian Phenomena

N. Dimitrov[1], N. Malcheva[1], N. Genov[1], S. Hamza[1], D. Atanasova[1,2]*

[1] Department of Anatomy, Faculty of Medicine, Trakia University, Stara Zagora, Bulgaria
[2] Department of Synaptic Signalling and Communications, Institute of Neurobiology, Bulgarian Academy of Sciences, Sofia, Bulgaria

* E-mail: nikolay.dimitrov@trakia-uni.bg

Acupuncture channels (meridians) are structures on the human body described by traditional Chinese medicine. The meridian phenomena are observed along the course of channels following acupuncture. Their visible manifestations include alterations in the colour of the skin - white lines and red lines, concurring with the channels. The present work aims to demonstrate visible meridian phenomena manifested in human skin and to correlate them to described acupuncture channels. Patients with various diseases on whom acupuncture was applied were observed and photographed. The human skin with visible meridian phenomena manifested was photographed using standard photographic equipment and a mobile camera. We observed that the human skin reacted during acupuncture. In most patients, we observed differently manifested hyperemia around the needles. Hyperemia around the needles usually disappears after 20 minutes, but it lasts longer in some patients. Only a few patients have visible meridian phenomena on the skin observed during acupuncture. Usually, the channels are activated after several times stimulation with acupuncture needles or at the end of the treatment course. White lines remained visible for a shorter period (5 - 15 min) and were observed more often in patients. Red lines have been marked longer (up to one hour after needle removal) in several patients. The observed white and red lines coincided with described acupuncture channels. The observed visible meridian phenomena coincide with described acupuncture channels.

Key words: acupuncture, visible meridian phenomena, acupuncture channels

Acupuncture Needle Tract in Human

N. Dimitrov[1], B. Panova[2], N. Malcheva[1], N. Pirovski[1], I. Ivanova[1], S. Hamza[1], I. Valkova[1], D. Atanasova[1,3]*

[1] Department of Anatomy, Faculty of Medicine, Trakia University, Stara Zagora, Bulgaria
[2] PZU Fizio –Medika, Strumica, Northern Macedonia
[3] Department of Synaptic Signalling and Communications, Institute of Neurobiology, Bulgarian Academy of Sciences, Sofia, Bulgaria

* E-mail: nikolay.dimitrov@trakia-uni.bg

Acupuncture on the human body and tongue is part of Traditional Chinese Medicine. The present study aims to demonstrate the needle tract in the human body and tongue formed during acupuncture. We used the method for needle tract visualization developed by us to demonstrate the needle tract. The moment of intervention to the needles remains "frozen in time" and reveals the tissues in a circumstance, maximally close to the condition during the acupuncture. This method was applied to samples on human cadavers. We could visualize the needle tract in a transverse and longitudinal direction in the human body's tissues and the tongue. The size of the observed needle tract corresponds to the size of used the acupuncture needles. The tissues in the vicinity of the needle tract have been saved, which allows their morphological examination. The needle tract was observed in different tissues like the epidermis, dermis, subcutis and striated muscle tissue. Morphological changes in the cells and tissues are kept near the needle tract. Acupuncture needles during acupuncture form visible needle tracts in the human body and tongue, which can be measured and analyzed.

Key words: needle tract, acupuncture, human, tongue

Assessment of the Basic Body Composition Components in Young Bulgarian Adults in Dependence of Their Nutritional Status Type

Z. Mitova[1], S. Mladenova[2], E. Andreenko[3]*

[1] Institute of Experimental Morphology, Pathology and Anthropology with Museum, Bulgarian Academy of Sciences., Sofia, Bulgaria
[2] Plovdiv University "Paisii Hilendarski"- Branch Smolyan, Department of Natural-Mathematical and Economical Sciences, Smolyan, Bulgaria
[3] Department of Human Anatomy and Physiology, Biological faculty, Plovdiv University "Paisii Hilendarski", Plovdiv, Bulgaria

* E-mail: zorkamitova@gmail.com

This study presents the results of a bioimpedance analysis *(BIA)* on the body composition of representative samples of Bulgarian men and women (students at the University of Sofia, the University of Plovdiv, and its Smolyan Branch). The study is cross-sectional and was conducted in the period 2015-2022. All the subjects examined were measured by height, body weight, waist, and hip circumferences by means of standard anthropometry. In addition, the body mass index *($BMI=weight_{(kg)}/height_{(m)}^{2}$)* was calculated. Underweight, normal, and overweight (incl. obesity)

were defined according to the cut-off points of BMI by *Cole et al. (2000, 2007)*. The evaluation of body composition was carried out by means of the bioelectrical impedance analyzer of body composition *ABC-01 "Medass"*. Of each person, the individual values of resistance, reactance, impedance, and phase angle at a signal frequency of 50 *kHz* were measured, which are the basis for the evaluation of body composition. It was characterized by the absolute and relative values of its components such as body fat mass, fat-free mass, skeletal-muscle mass, body cell mass, and total body water. Descriptive statistics for calculating mean values and standard deviations of the indicators were used. The data was processed through the software packages *STATISTICA 10.0* and *SPSS 16.0*. Results show that all indices examined have higher values in men with the exception of active resistance, reactance, impedance, and fat mass, which have higher in women. Relationships were established between the type of nutritional status and some of the physiometric indicators.

Key words: bioelectrical impedance analysis, body composition, nutritional status type, young adults men and women, students

Testing of Primers and Optimization of PCR for the Detection of Alternatively Spliced Variants of Mouse ChAT mRNA

D. Marinova[*]*, T. Rashev, S. Trifonov*

Department of Anatomy, Histology, Cytology and Biology, Faculty of Medicine, Medical University Pleven, Pleven, Bulgaria

* E-mail: drdesko@gmail.com

Acetylcholine as neurotransmitter plays important functions in the central as well as in the peripheral nervous system. Its biosynthesis is catalyzed by choline acetyltransferase (ChAT). In the mouse, the gene has three 5'-noncoding (R, N and M) and 14 coding exons, from which seven mRNA isoforms (M, N1, N2, R1, R2, R3 and R4) are transcribed. They differ in the 5'-noncoding ends and encode the same protein (common ChAT). Additional isoform that lacks coding exons from 5 to 8 that encodes a smaller protein (peripheral ChAT). Forward and reverse primers targeting M, R3, N1, N2, cChAT and pChAT isoforms were designed. The optimal PCR conditions (primer concentration and annealing temperature) and specificity of the primers were tested in a series of reactions using specially designed templates. The PCR mix (20µl) contained 0,01pmol/ml template, 0.25µM forward and reverse primers, 10µl Luna Universal qPCR Master Mix (BioLabs). The appropriate annealing tº, which yields sufficient specificity for each tested primer pair was as follows: M–65ºC; N1–63ºC; N2–65ºC; R3–60ºC; cChAT–63ºC and pChAT–65ºC. Specially designed gBlock DNA fragments (IDT) or plasmids containing isoform-specific nucleotide sequences were used as templates. The following PCR protocol was applied: 40 cycles at 95°C for 15 sec; 60ºC, 63ºC or 65ºC (primer pair specific) for 10 sec; 60ºC for 30 sec. Primers specific for several ChAT mRNA isoforms were successfully designed and tested. These primers can be used to detect the desired variants in biological samples.

Key words: choline acetyltransferase, primer, polymerase chain reaction, alternatively spliced variants

Immunophenotype of Apelin Receptor Expressing Cells in the Adult Human Subventricular Zone

A. Mladenov[1], M. Ivanov[1,2], L. Veleva[1], D. Stoyanov[1], S. Pavlov[1], A. Tonchev [1,2]*

[1] Department of Anatomy and Cell Biology, Faculty of Medicine, Medical University, Varna, Bulgaria
[2] Research Institute, Medical University, Varna, Bulgaria

* E-mail: andonmladenov5@gmail.com

Adult neurogenesis is the process of generating new functional neurons from pluripotent neuronal stem cells, located in two "canonical" areas: the subventricular zone (SVZ) and the hippocampal subgranular zone. In this ongoing study, we are trying to elucidate the functions of the Apelinergic system, comprising the apelin receptor (APLNR) and its ligands, in the human SVZ, composed of an ependymal layer, a gap zone and an astrocytic ribbon. Fluorescent immunohistochemistry was performed on coronal sections of the SVZ from 3 human brain tissue samples without evidence of neuropathology and neuropsychiatric patient history. Manual cell counting in selected Regions of Interest along the dorso-ventral axis of the SVZ was done using ImageJ. Statistical analysis was completed in R. We found that the APLNR is present in all layers and diverse cell types of the SVZ in the adult human brain, including proliferating cells. While in the gap zone the predominant cell populations, expressing APLNR, are microglia and neuroblasts or immature neurons, in the astrocytic ribbon, the majority of APLNR+ cells represent astrocytes and most probably TAPs. Therefore, our future research will be aimed at phenotyping the SVZ cell populations after ischemic injury and at exploring the effects of the Apelingergic system in neurospheres, organotypic cultures, as well as human and chimpanzee brain organoids. Here we confirm the expression of APLNR in the adult human SVZ and demonstrate the variety of the associated cell types ranging from astrocytes and neural stem cells to neuroblasts.

Key words: adult neurogenesis; subventricular zone; Apelinergic system

eNOS and nNOS Expression in the Wistar and SHR Rat Kidney after Selective Blockade of Endothelin-B Receptors

V. Iliev[1], L. Jelev[1], A. Gradev[1], L. Malinova[1], P. Markova[2], R. Girchev[2]*

[1] Department of Anatomy, Histology and Embryology, Medical University of Sofia, Bulgaria
[2] Department of Physiology and Pathophysiology, Medical University of Sofia, Bulgaria

* E-mail: v.iliev@medfac.mu-sofia.bg

Endothelin-1 (ET-1) is the most potent vasoconstrictor peptide known to date, acting through two type receptors: ETA and ETB. The aim of the current study was to investigate the role of endothelin B receptor subtype in regulation of neuronal (nNOS) and endothelial (eNOS) nitric oxide synthase expression in kidney of normotensive Wistar (W) and spontaneously hypertensive rats (SHR). Experimental animals (12-14 weeks old) were distributed in 4 experimental groups, each consisting of 6 animals: control groups W and SHR and experimental group Wistar and SHR with selective ETB receptors blockade with BQ788 (1mg/kg/min for 1 hour). The expression of nNOS and eNOS in the kidney tissue was determined immunohistochemically on paraffin

embedded tissue slices. In control condition we established higher expression of nNOS in medullar blood vessels in SHR in comparison to normotensive rats. The selective blockade of ETB receptors induced different expression of NOS isoforms in the kidney of normotensive and spontaneously hypertensive rats. In Wistar rats eNOS expressed predominantly in the cortex tubules and blood vessels but in SHR in the medullar blood vessels and tubules and. In addition, in SHR we found enhanced expression of nNOS in the medullar blood vessels after BQ788 application. Some of the effects of ET-1 are associated with the interaction with nitric oxide synthase and production of NO. Our result shown that ET-1, by ETB receptors affect the eNOS and nNOS expression in specific area of kidney in normotensive and spontaneously hypertensive rats.

Key words: Endothelin-B receptor, eNOS, nNOS, kidney, SHR

3D Printing, Histological and Radiological Analysis of Nanosilicate-Polysaccharide Composite Hydrogel as a Tissue-Equivalent Material for Complex Biological Physical Phantom

P. Valchanov, N. Dukov, S. Pavlov, A. Kotny*

Department of Anatomy and Cell Biology, Medical University of Varna, Varna, Bulgaria

* E-mail: petar.valchanov@mu-varna.bg

The nanosilicate-polysaccharide composite hydrogels are a well-studied class of materials in regenerative medicine that combine good 3D printability, staining, and biological properties, which makes them an excellent candidate material for complex bone scaffolds. The aim of this study is to develop a hydrogel, suitable for 3D printing that has biological and radiological properties similar to those of the natural bone, and to develop protocols for their histological and radiological analysis. We synthesized a hydrogel, based on alginate, methylcellulose and laponite and 3D-printed it into a series of complex bioscaffolds. The scaffolds were scanned with CT and CBCT scanners and exported as DICOM datasets. Then they were cut into histological slides and stained with standard histological protocols. From the DICOM datasets the average value of the voxels in HU was calculated and compared with the densities of the natural spongious bone. On the histological sections, we tested different approaches to reduce the background hydrogel staining, which would make the cytological and histological analysis possible. The results confirmed that an alginate/methylcellulose/ laponite based composite hydrogel can be used for 3D printing of complex three-dimensional scaffolds simulating biological and radiological properties of the spongious bone with high fidelity. The development of multipurpose biological physical phantom, mimicking the bone tissue, opens a new avenue for the design of high fidelity dynamic models of the normal and pathological bone.

Purinergic Nerve Structures in the Rat Colorectral Region

T. Kirov[1], D. Atanasova[2, 3], L. Malinova[1], N. Lazarov[1, 2]*

[1] Department of Anatomy and Histology, Medical University of Sofia, Sofia, Bulgaria
[2] Institute of Neurobiology, Bulgarian Academy of Sciences, Sofia, Bulgaria
[3] Department of Anatomy, Faculty of Medicine, Trakia University, Stara Zagora, Bulgaria

* E-mail: tkirov@medfac.mu-sofia.bg

The enteric nervous system with its constituent submucosal and myenteric plexuses has been extensively studied for several decades now. Despite being an essential component of its non-adrenergic, non-cholinergic transmission, purinergic nerve structures remain neglected. Hence, determining the role ATP plays in the regulation of motility and secretion is essential for the proper understanding of enteric neuronal circuitry and various pathophysiological mechanisms. In the current study, the presence, distribution and staining intensity of the ATP-immunoreactive myenteric nerve structures in the colorectal region of the adult rat have been investigated by means of immunohistochemistry at the light microscopical level. Following ATP immunostaining, the myenteric ganglia were easily distinguished, even though no positive neuronal bodies were registered. Both the ganglia and their constituent neurons were markedly outlined by the surrounding immunopositive beaded nerve fiber bundles. ATPergic neuronal structures were readily observed both in the space between the muscle layers and inside them. The immunostained bundles were arranged parallel to the muscle cells. We encountered no statistically significant differences in the staining intensity of the positive nerve fibers. Taken together with previous morphological and pharmacological research the results of this study suggest that the ATP-mediated neurotransmission is of physiological and likely of pathological significance for the colorectal region, which requires further work in future studies.

Key words: ATP, colorectal, rat, myenteric plexus

„Tubarial (salivary) Glands“ – Do They Exist? Preliminary Results

B. Blagova[*], *L. Malinova*

Department of Anatomy, Histology, and Embryology, Medical University of Sofia, Sofia, Bulgaria

* E-mail: b.blagova@medfac.mu-sofia.bg

In 2020 Valstar et al. reported an accidentally discovered on PSMA PET/CT „new organ at risk“ located above the *torus tubarius*. The authors named it „tubarial (salivary) glands“. The discovery of a „new“ body structure in the 21st century was certainly generating scientific interest and controversy. The proposed study aimed to verify the presence of these structures in humans. Tissue blocks sized ca. 3 *x* 3 *x* 3 cm were obtained from the *torus tubarius* of three cadavers and examined by hematoxylin and eosin (H & E), periodic acid Schiff (PAS), and Alcian blue staining. The dissected area showed submucosal large aggregates of predominantly mucous gland tissue demonstrated by the PAS and Alcian blue staining, a low number of serous acini, myoepithelial cells, and draining ducts. An „organ“ is defined as an anatomical region with a specific shape and structure, consisting of more than one type of tissue that performs specific tasks. It can be argued that the „tubarial glands“ do not have a capsule as opposed to the major salivary glands, however, the sublingual glands also have an unencapsulated part that consists of 8 – 30 minor mixed glands. The discovery of the „tubarial glands“ sparked scientific interest which opened the door to further digging into the thrust area with more evidence from different studies. More research is needed to resolve the controversies about the „tubarial (salivary) glands“ and to formulate a consensus and establish their place in anatomy and clinical practice.

Key words: fourth pair major salivary glands, new organ, tubarial (salivary) glands

A Brief History of the Anatomy Department at the Faculty of Medicine – Stara Zagora

D. Sivrev[*]

Department of Anatomy, Faculty of Medicine, Trakia University, Stara Zagora, Bulgaria

* E-mail: dsivrev@abv.bg

On April 8, 1982, the Higher Medical Institute and Department of Anatomy, Histology and Embryology, was opened in the city of Stara Zagora. Its founder and first Head of Department is Prof. Christo Nikolov Chouchkov, MD, PhD, DSc - one of the founders of the University. Prof. Chouchkov was the Head of the Departmen from 1982 to 2000, and the main scientific priority during this period was the study of the structure of the nervous system by tracing, cyto- and histochemical methods, cell cultures and cultivation of epithelium and nerve cells, plastination of organs and anatomical objects for the needs of the education process. In 2000, Prof. Nikolay Lazarov, PhD, DSc was appointed the Head of the Department of Anatomy. He also held the position of Vice-Dean for Research from 2000 to 2003. In May 2007 Assoc. Prof. Irina Stoyanova, MD, PhD temporarily held the position of Head of Department until December. After her departure to Netherlands the temporary Head of the Department is Prof. Maya Gulubova, MD, PhD. After winning a competition in January 2008, Prof. Dimitar Sivrev, MD, PhD is a Head of the Department of Anatomy, a position he held until 2020. Assoc. Prof. Nikolay Dimitrov, MD, PhD since 2020 has been elected Head of the Department of Anatomy at the Medical Faculty of the Trakia University. Assistant-Professors in this period was: Dr Detelin Sokolov, Dr Stefan Stratiev, Dr Hristo Terziev, Dr Marin Marinov, Dr Peter Penkov, Dr Deniza Penkova, Dr Konstantin Trenchev, Dr Pejo Mutavchiev, Dr Roumen Angelov, Dr Jordan Stoyanov, Dr Antoaneta Georgieva, Dr Ivelina Ivanova, Dr Sevinch Hamza, Dr Irena Valkova, Dr Nikolay Genov, Dr Nedelina Malcheva, Dr Vanesa Pilicheva, Dr Ralitsa Plamenova. The scientific work of the Department of Anatomy are presented in more than 200 complete articles in national and foreign periodicals. The lecturers have participated in over 120 scientific symposia, conferences, congresses and other scientific events in Bulgaria and abroad. More than 20 textbooks and manuals and several monographs have been published in the Department of Anatomy.

Key words: department, anatomy, head, professor, history

Endothelin Receptors in Testicular Tissue Homogenate of Normotensive and Spontaneously Hypertensive Rats after Unilateral Testicular Torsion

M. Kozhuharov[1*], *V. Iliev*[2], *A. Ivanov*[2], *A. Gradev*[2], *Z. Sabit*[3], *L. Jelev*[2], *P. Markova*[1, 3]

[1] *Department of Anatomy and Physiology, SWU "Neofit Rilski" – Blagoevgrad, Blagoevgrad, Bulgaria*
[2] *Department of Anatomy, Histology, and Embryology, Medical University of Sofia, Sofia, Bulgaria*
[3] *Department of Physiology and Pathophysiology, Medical University of Sofia, Sofia, Bulgaria*

* E-mail: kozhuharov@swu.bg

A potential role of the endothelium in male idiopathic infertility has been suggested. The endothelium plays an essential role in maintaining the balance between the vasodilator and vasoconstrictor effects of the substances produced in it, which is of fundamental importance for the reproductive function. Endothelin-1, produced by endothelium, is a substance with a powerful vasoconstrictor effect, achieved by activation of 2 type of receptors: ETA and ETB. Research studies have found reduced sexual behavior and impaired spermatogenesis in a rat model of hypertension, as well as abnormal sperm morphology in hypertensive men, indicating a possible link between male infertility and hypertension. The current study investigated the changes of ETA, ETB receptors in testicular tissue of normotensive Wistar rats (WR, n=5) and spontaneously hypertensive rats (SHR. n=5) after unilateral testicular torsion. In testicular tissues homogenate ETA and ETB receptors were quantified by ELISA method (Fine Biotech Co, Ltd). We established decreased the ETB receptor quantity in SHR testicular tissue in comparison to normotensive rats, $p<0.05$. The unilateral torsion increased ET-A and ET-B quantity in both Wistar rats and SHR, $p<0.05$, however affects in different manner endothelin receptor subtype in contralateral testis: in Wistar rats incresed quantity of ET-A whereas in SHR, ETB receptor subtype. The results obtained in the present study indicate the involvement of different mechanisms in the response of the testicular endothelial system to unilateral testicular torsion. In hypertension, ET-B receptor-mediated pathways play a dominant role, while in normotension, mechanisms mediated by the ET-A receptor subclass are important.

Key words: male infertility, spontaneously hypertensive rats, endothelin receptors

Acknowledgement: This work was supported by a scientific project financed by SWU Neofit Rilski, Blagoevgrad, Contract No. RP – B2/23.

Application of Three-Dimensional (3D) Printing in the Preoperative Study and Planning for Neurosurgery

T. Bogdanov[1], D. Ferdinandov[2], T. Hikov[1]*

[1] 3DLab, Department Medical Physics and Biophysics, Medical Faculty, Medical University of Sofia, Sofia, Bulgaria
[2] Neurosurgery clinics, Saint Ivan of Rila University Hospital, Sofia, Bulgaria

* E-mail: tbogdanov@medfac.mu-sofia.bg

The utilization of three-dimensional (3D) printing in neurosurgery preoperative study and planning has revolutionized the field. This abstract explores the multifaceted application of 3D printing technology, enabling the creation of patient-specific anatomical models, surgical guides, and implants. These personalized 3D-printed models enhance surgical precision, reduce operative time, and improve patient outcomes. Additionally, they serve as invaluable tools for education and communication among surgical teams. The integration of 3D printing in neurosurgery underscores its potential in optimizing surgical approaches, minimizing risks, and ultimately advancing the field by providing neurosurgeons with a tangible and accurate representation of each patient's unique anatomy. We employed InVesalius 3D software for medical image segmentation and reconstruction in this study. Patient-specific 3D models were then printed using Fused Deposition Modeling (FDM) printers. These versatile devices ensured the precise replication of anatomical structures from standard medical imaging data. In cases of brachycephaly, the 3D models obtained serve as essential tools for doctors during case study and preoperative planning. These models provide a tangible and detailed visualization of the

patient's cranial deformity, facilitating in-depth analysis, personalized treatment strategies, and improved surgical planning to achieve optimal outcomes in the correction of brachycephalic conditions. In summary, 3D printing, utilizing InVesalius 3D software and FDM printers, offers a revolutionary approach to neurosurgery, with significant potential in brachycephaly cases. These patient-specific models enhance diagnosis, treatment planning, and surgical precision, promising improved outcomes and personalized care in the field of neurosurgery.

Key words: three-dimensional (3D) printing, neurosurgery, InVesalius 3D software

Author Guidelines

Acta Morphologica et Anthropologica is an open access peer review journal published by Bulgarian Academy of Sciences, Prof. Marin Drinov Publishing House.
Corporate contributors are Bulgarian Academy of Sciences, Institute of Experimental Morphology, Pathology and Anthropology with Museum and Bulgarian Anatomical Society.

Acta Morphologica et Anthropologica is published in English, 4 issues per year.

The journal accepts manuscripts in the following **fields**: experimental morphology, cell biology and pathology, anatomy and anthropology.

Publication types: original articles, short communications, case reports, reviews, Editorial, letters to the Editors.

Acta Morphologica et Anthropologica is the continuation of Acta cytobiologica et morphologica

The **aim** of the Journal is to disseminate current interdisciplinary biomedical research and to provide a forum for sharing new scientific knowledge and methodology. The general editorial policy is to optimize the process of issuing and distribution of *Acta Morphologica et Anthropologica* in line with modern standards for scientific periodicals focusing on content, form, and function.

Scope – experimental morphology, cell biology and pathology (neurobiology, immunobiology, tumor biology, environmental biology, reproductive biology, etc.), new methods, anatomy and pathological anatomy, anthropology and paleoanthropology, medical anthropology and physical development.

Acta Morphologica et Anthropologica is published twice a year as one volume with 4 issues. For the first two issues (1-2) the deadline for manuscript submission is March 15th and for the next two issues (3-4), the deadline is September 15th. Electronic version for issues 1-2 is uploaded on the website till June 30th and for issues 3-4 – till December 30th.

Contact details and submission

Manuscript submission is electronical only. The manuscripts should be sent to: ama.journal@iempam.bas.bg with a copy to the Managing Editor: yordanka.gluhcheva@iempam.bas.bg or ygluhcheva@hotmail.com

All correspondence, including notification for Editor's decision, requests for revision, is sent by e-mail.

Article structure

Manuscripts should be in English with total length not exceeding 10 standard pages, line-spacing 1.5, justified with 2.5 cm margins. The authors are advised to use Microsoft Word 97-2003, Times New Roman, 12 pt throughout the text. Pages should be numbered at the bottom right corner of the page.

The article should be arranged under the following headings: Introduction, Material and Methods, Results, Discussion, Conclusion, Acknowledgements and References.

Title page – includes:

- **Title** – concise and informative;
- **Author(s)' names and affiliations** – indicate the given name(s) and family name(s) of all authors. Present the authors' affiliation addresses below the names. Indicate all affiliations with a lower-case superscript after the author's name and in front of the appropriate address. Provide the full postal address information for each affiliation, including the country name.
- **Corresponding author** – clearly indicate who will handle the correspondence for refereeing, publication and post-publication. An e-mail should be provided.
- **Abstract** – state briefly the aim of the work, the principal results and major conclusions and should not exceed 150 words. References and uncommon, or non-standard abbreviations should be avoided.
- **Key words** – provide up to 5 key words. Avoid general, plural and multiple concepts. The key words will be used for indexing purposes.

Introduction – state the objectives of the work and provide an adequate background, avoiding a detailed literature survey or summary of the results.

Material and Methods – provide sufficient detail to allow the work to be reproduced. Methods already published should be indicated as a reference: only relevant modifications should be described.

Results – results should be clear and concise.

Discussion – should explore the significance of the results in the work, not repeat them. A combined *Results and Discussion* section is often appropriate. Avoid extensive citation and discussion of published literature.

Conclusions – the main conclusions of the study should be presented in a short section.

Acknowledgements – list here those individuals who provided help during the research and the funding sources.

Units – please use the International System of Units (SI).

Math formulae – please submit math equations as editable text, not as images.

Electronic artwork – number the tables and illustrations according to their sequence in the text. Provide captions for them on a separate page at the end of the manuscript. The proper place of each figure in the text should be indicated in the left margin of the corresponding page. **All illustrations (photos, graphs and diagrams)** should be referred to as "figures" and given in abbreviation "Fig.", and numbered in Arabic numerals in order of its mentioning in the manuscript. They should be provided in grayscale as JPEG or TIFF format, minimum 300 dpi. The illustrations should be submitted as separate files.

References – they should be listed in alphabetical order, indicated in the text by giving the corresponding numbers in parentheses. The "References" should be typed on a separate sheet. The names of authors should be arranged alphabetically according to family names. In the reference list titles of works, published in languages other than English, should be translated, original language must be indicated at the end of reference (e.g., [in Bulgarian]). Articles should include the name(s) of author(s), followed by the full title of the article or book cited, the standard abbreviation of the journal (according to British Union Catalogue), the volume

number, the year of publication and the pages cited, for books – the city of publication and publisher. In case of more than one author, the initials of the second, third, etc. authors precede their family names. Ideally, the names of all authors should be provided, but the usage of "et al" after the fifth author in long author lists will also be accepted.

For articles: **Davidoff, M. S., R. Middendorff, G. Enikolopov, D. Riethmacher, A. F. Holstein, D. Muller**. Progenitor cells of the testosterone-producing Leydig cells revealed. – *J. Cell Biol.*, **167**, 2004, 935-944.

Book article or chapter: **Rodriguez, C. M., J. L. Kirby, B. T. Hinton. The development of the epididymis.** – In: *The Epididymis - from molecules to clinical practice* (Eds. B. Robaire, B. T. Hinton), New York, Kluwer Academic Plenum Publisher, 2002, 251-269.

Electronic books: **Gray, H.** *Anatomy of the human body* (Ed. W.H.Lewis), 20th edition, NY, 2000. Available at http://www.Bartleby.com

PhD thesis: **Padberg, G**. Facioscapulohumeral diseases. *PhD thesis*, Leiden University, 1982, 130 p.

Website: National survey schoolchildren report. National Centre of Public Health and Analyses, 2014. Available at http://ncphp.government.bg/files

Page charges
Manuscript publication is free of charges.

Ethics in publishing
Before sending the manuscript the authors must make sure that it meets the Ethical guidelines for journal publication of Acta Morphologica et Anthropologica.

Human and animal rights

If the work involves the use of human subjects, the authors should ensure that work has been carried out in accordance with *The Code of Ethics of the World Medical Association* (Declaration of Helsinski). The authors should include a statement in the manuscript that informed consent was obtained for experimentation with human subjects. The privacy rights of human subjects must always be observed.
All animal experiments should comply with the *ARRIVE guidelines* and should be carried out in accordance with the U.K. Animals (Scientific procedures) Act, 1986 and the associated guidelines *EU Directive 2010/63/EU* for animal experiments, or the National Institutes of Health guide for the care and use of Laboratory animals (NIH Publications No. 8023, revised 1978) and the authors should clearly indicate in the manuscript that such guidelines have been followed.

Submission Details

Acta morphologica et anthropologica is published twice a year as one volume with 4 issues. For the first two issues (1-2) the deadline for manuscript submission is March 15th and for the next two issues (3-4), the deadline is September 15th. Electronic version for issues 1-2 is uploaded on the website till June 30th and for issues 3-4 – till December 30th.

Manuscript submission is electronical only.

The manuscripts should be sent to: ama.journal@iempam.bas.bg with a copy to the Managing Editor: yordanka.gluhcheva@iempam.bas.bg or ygluhcheva@hotmail.com

All correspondence, including notification for Editor's decision, requests for revision, is sent by e-mail.

Submission declaration

Submission of the manuscript implies that the work described has not been published previously, is not considered under publication elsewhere, that its publication is approved by all authors, and that if accepted, it will not be published elsewhere in the same form, in English or in any other language, including electronically, without the informed consent of the copyright-holder.

Contributors

The statement that all authors approve the final article should be included in the disclosure.

Copyright

http://www.iempam.bas.bg/journals/acta/Author%20Copyright%20Agreement_last.pdf

Upon acceptance of an article, the authors will be asked to complete a "**Copyright Transfer Agreemen**t".
http://www.iempam.bas.bg/journals/acta/Copyright_Transfer_Agreement_Form_AMA.doc

Peer review

Once a manuscript is submitted, the Managing Editor (or the Editor-in-Chief) briefly checks the manuscript for conformance with the journal's Focus, Scope, Policies and style requirements and decide whether it is potentially suitable for publication and can be processed for review, or rejected immediately, or returned to the author for improvement and re-submission.
Manuscripts are peer-reviewed by the Editors, Editorial Board members, and/or external experts before final decisions regarding publication are made. The entire editorial workflow is performed in the following steps:

1. The submitted manuscript is checked in the editorial office whether it is suitable to go through the normal peer review process.
2. If deemed suitable, the manuscript is sent to 2 reviewers for peer-review. The choice of reviewers depends on the subject of the manuscript, the areas of expertise of the reviewers, and their availability.
3. Each reviewer will have 2 weeks to provide evaluation of the manuscript. The Editor may recommend publication, request minor, moderate or major revision, or provide a written critique of why the manuscript should not be published (rejected).
4. In case only one reviewer suggests rejection of the manuscript, the latter is subjected to additional evaluation by a third reviewer.
5. The manuscript will be published in a revised form provided that the authors successfully answer the critics received. The Editor-in-Chief is the final authority on all editorial decisions.

Open Access

This journal provides immediate open access to its content on the principle that making research freely available to the public supports a greater global exchange of knowledge.

After acceptance

Proof correction

The corresponding author will receive proofs by e-mail in PDF format and will be requested to return it with any corrections within two weeks.

ISSN 1311-8773 (print)
ISSN 2535-0811 (online)